



HAL
open science

Analysis and modeling of the physiological bases of floral induction and fruit production irregularity. Application to apple tree genotypes with contrasted architectures

Fares Belhassine

► To cite this version:

Fares Belhassine. Analysis and modeling of the physiological bases of floral induction and fruit production irregularity. Application to apple tree genotypes with contrasted architectures. Agricultural sciences. Montpellier SupAgro, 2020. English. NNT : 2020NSAM0009 . tel-04069678

HAL Id: tel-04069678

<https://theses.hal.science/tel-04069678>

Submitted on 14 Apr 2023

HAL is a multi-disciplinary open access archive for the deposit and dissemination of scientific research documents, whether they are published or not. The documents may come from teaching and research institutions in France or abroad, or from public or private research centers.

L'archive ouverte pluridisciplinaire **HAL**, est destinée au dépôt et à la diffusion de documents scientifiques de niveau recherche, publiés ou non, émanant des établissements d'enseignement et de recherche français ou étrangers, des laboratoires publics ou privés.

THÈSE POUR OBTENIR LE GRADE DE DOCTEUR DE MONTPELLIER SUPAGRO

En [BIDAP – Biologie Intégrative, Diversité et Amélioration des Plantes]

École doctorale [GAIA – Biodiversité, Agriculture, Alimentation, Environnement, Terre, Eau]
Portée par

Unité de recherche [AGAP – Amélioration Génétique et Adaptation des Plantes méditerranéennes et tropicales]

**Analyse et modélisation des bases physiologiques de
l'induction florale et de l'irrégularité de production en
fruits. Application à des génotypes de pommier
d'architectures contrastées.**

Présentée par [Fares Belhassine]

Le [04 juin 2020]

Sous la direction de [Evelyne Costes]

Et le Co-encadrement de [Benoît Pallas] et de [Damien Fumey]

Devant le jury composé de

[Jim Hanan, Dr, Université du Queensland]

[Nathalie Ollat, Dr, INRAE Bordeaux]

[Laurent Torregrossa, Pr, Montpellier SupAgro]

[Gerhard Buck-Sorlin, Pr, Agro Campus Ouest]

[Jessica Bertheloot, Dr, INRAE Angers]

[Frédéric Normand, Dr, CIRAD La Réunion]

[Evelyne Costes, Dr, INRAE Montpellier]

[Rapporteur]

[Rapporteur]

[Examineur]

[Examineur]

[Examineur]

[Invité]

[Directrice de thèse]



**UNIVERSITÉ
DE MONTPELLIER**



Remerciements

En m'ayant donné l'occasion d'effectuer des recherches, cette thèse a été une expérience extraordinaire. Je souhaite remercier ici toutes les personnes qui ont contribué directement ou indirectement à sa réalisation.

Tout d'abord, je tiens à remercier les membres de mon jury de soutenance de thèse d'avoir accepté de lire et d'évaluer ce travail et d'y avoir apporté leur regard critique.

Je voudrais exprimer ma sincère gratitude à Evelyne Costes pour avoir dirigé cette thèse, pour sa patience et sa disponibilité et pour tout le soutien et les encouragements qu'elle m'a apportés tant sur le plan scientifique que personnel.

Un grand merci également à Benoit Pallas pour sa motivation et sa grande implication dans l'encadrement de ce travail. Son aide inestimable durant un peu plus que trois ans a fait de ce travail ce qu'il est aujourd'hui, et pour cela je lui suis infiniment reconnaissant.

Merci à Damien Fumey pour son rôle d'encadrement et pour m'avoir intégré à différentes occasions à la vie d'entreprise. Je remercie également Jérôme Chopard pour son aide lors du développement du modèle. Merci aux membres d'ITK qui m'ont aménagé une place dans leurs locaux quand je passais à Cap Alpha et que j'ai surtout connu lors des événements organisés qui m'ont permis de sortir de ma routine. J'apprécie particulièrement leurs efforts pour apporter de la joie au travail. Je suis également reconnaissant à Eric Jallas, président de l'entreprise, pour avoir accepté de financer en partie cette thèse.

Je tiens à remercier les membres de mes comités de thèses : Christophe Pradal, Delphine Luquet, Dominique This, Fabrice Foucher, Jérôme Ngao et Thierry Simonneau. Merci pour les échanges qu'on a eus au cours de ces trois années et pour vos remarques et conseils pertinents qui ont permis de mieux cadrer ce travail.

Je remercie également tous les membres d'AFEF qui ont partagé cette aventure avec moi au quotidien. J'ai trouvé en vous des qualités humaines qui ont beaucoup facilité mon adaptation et mon intégration parmi vous. Merci pour avoir veillé à ma bonne santé physique et morale ainsi que pour votre intérêt et implication dans mon travail. Je vous remercie aussi de m'avoir soutenu pendant les moments difficiles.

Je souhaiterais exprimer toute ma gratitude à Sylvie pour le soutien et la délicatesse qu'elle a toujours montré. Merci Sylvie pour la période où on a partagé le même bureau, merci pour ton expérience, ton savoir-faire et ton efficacité. Une grande partie de mes résultats repose sur les longues journées que tu as passées au laboratoire et sur le terrain. Pour tout cela, je te remercie.

Je remercie Sébastien pour les longues journées passées à décrire les arbres et à les digitaliser. Je remercie également tous ceux qui m'ont aidé aux lourdes acquisitions des données.

Maintenant, il y a ces gens dont l'influence directe ne peut pas être mesurée, mais dont je ne pourrais manquer de mentionner le rôle essentiel. Quiconque a dû lutter contre les hauts et les bas d'une thèse connaît l'importance des amis et de leur soutien. Je m'abstiendrai de la lourde tâche consistant à énumérer leurs noms ici, ils se reconnaîtront. Je leur suis simplement reconnaissant pour les voyages, la musique, les pauses café et les sorties. Et bien sûr, pour l'équilibre qu'ils ont apporté entre vie professionnelle et vie privée, merci à tous.

Mes remerciements vont aussi à mes neveux qui ont dû, en leurs bas âges, tolérer mon absence et auxquels j'espère avoir montré l'importance de la persévérance.

Je suis reconnaissant à mes sœurs pour s'être impliquées de toutes les manières possibles pour que je garde le moral nécessaire pour que je finisse cette expérience. Leur amour m'accompagne partout où je vais.

Un immense remerciement va à mes parents sans qui je ne serais pas devenu ce que je suis aujourd'hui. Je les remercie de m'avoir donné le goût et la chance d'accomplir toutes ces années d'études et de nous avoir toujours encouragés, mes sœurs et moi, à aller au bout de nos projets. J'espère pouvoir leur rendre un jour les sacrifices qu'ils ont fait pour nous.

Je remercie ma mère pour sa force, sa patience et son amour inconditionnel. Sans sa bienveillance, il n'aurait pas été imaginable que j'arrive au bout du chemin.

Je voudrais rendre hommage à mon père, parti peu de temps avant de voir l'accomplissement de ce travail. En nourrissant ma curiosité scientifique dès le plus jeune âge, mon père a joué le plus grand rôle dans l'élaboration de la personne que je suis devenue. Pour cela, et pour tant d'autres choses que je porte toujours avec moi, je lui serais toujours reconnaissant.

Enfin, je voudrais dédier cette thèse à ma mère et à la mémoire de mon père.

Table of contents

I.	Introduction	1
II.	Literature review	3
1.	Floral induction	4
1.1.	General considerations	4
1.2.	Floral induction in the model plant <i>Arabidopsis thaliana</i>	4
1.3.	Irregularity in perennials	6
1.4.	Agronomic consequences and horticultural practices to manage irregular bearing	6
2.	Case of study: the apple tree	7
2.1.	Economic importance	7
2.2.	Apple origin	7
2.3.	Biology of apple tree	8
2.4.	Architecture characteristics of apple tree	9
2.5.	Factors affecting floral induction and biennial bearing in apple tree	12
2.6.	Molecular and genetic regulation of flowering in apple tree	14
3.	Modeling approaches of developmental processes in functional structural plant models	14
3.1.	General consideration	14
3.2.	Available modelling languages and platforms	15
3.3.	Description and acquisition of plant architecture	16
3.4.	Modeling plant architecture	18
3.5.	Modelling light interception and photosynthesis	20
3.6.	Modelling carbon allocation	20
3.7.	Retroaction between carbon allocation, trophic competition and plant development	22
3.8.	Modeling hormone transports in plant and their consequences on plant development	22
3.9.	Representing genotypic diversity in models	24
III.	Impact of within-tree organ distances on floral induction and fruit growth in apple tree: implication of carbohydrate and gibberellin organ contents	26
	https://doi.org/10.3389/fpls.2019.01233	26
1.	Résumé	27
2.	Abstract	28
3.	Introduction	29
4.	Material and methods	30
4.1.	Plant material and growing conditions	30
4.2.	Varying source-sink relationships by leaf and fruit removal treatments	31

4.3. Development and growth variables: floral SAM proportion and mean fruit weight at harvest	32
4.4. Responses of leaf photosynthesis and starch content	32
4.5. GA concentrations in SAM	32
4.6. Statistical analyses	33
5. Results	33
5.1. Tree fruiting status between treatments	33
5.2. Floral induction in SAM occurs after treatment onset	34
5.3. FI proportion is affected by leaf and fruit presence and by their distance to the SAM.....	35
5.4. Mean fruit weight is affected by distances between leaves and fruit	36
5.5. Relationships between FI and mean fruit weight variability and carbon availability	39
5.6. GA9 (precursor of active form) and GA1 (active form) decrease in fruit presence	40
6. Discussion	42
6.1. Relative roles of carbohydrates and GA in flower induction	42
6.2. Response of floral induction and fruit growth to changing source-sink distances.....	42
7. Conclusion	44
8. Supplementary Material.....	45
IV. Modelling transport of inhibiting and activating signals and their combined effects on floral induction: application to apple tree	51
1. Résumé	52
2. Abstract	53
3. Introduction	54
4. Material and methods.....	55
4.1. Model overview	55
4.2. Inhibiting and activating signal amounts and transport.....	55
4.3. Computation of floral induction probability	57
4.4. Model behavior assessment on simple structures.....	57
4.5. Description of the experimental dataset	58
4.6. Input architectures	58
4.7. Estimation of parameter values and model assessment.....	58
5. Results	59
5.1. Model behavior and sensitivity to model parameters	59
5.2. Model calibration and associated parameters values.....	63
5.3. Signal combined effect and model validation.....	65

6. Discussion	67
6.1. A model-based approach for quantifying the respective roles of leaves and fruit on FI....	67
6.2. Parameter estimation leads to new assumptions on the physiological process involved in the within-tree variability in floral induction.....	67
7. Conclusion	69
8. Supplementary Material.....	70
V. Analyses of the impact of carbon balance, hormonal concentrations and architecture on floral induction in genotypes issued from an apple tree core collection reveals complex genotypic-based regulations.	77
1. Résumé	78
2. Abstract	79
3. Introduction	80
4. Material and methods.....	81
4.1. Plant material and growing conditions.....	81
4.2. Architectural description	82
4.3. Yield component and tree crop load management by fruit removal	83
4.4. Leaf photosynthesis and organ concentration in non-structural carbohydrates (NSC)	83
4.5. Hormone concentrations in SAM	83
4.6. Determination of FI proportions and BBI	84
4.7. Statistical analyses.....	84
5. Results	84
5.1. Dynamics of tree architectures and flowering.....	84
5.2. Classification of genotypes based on architectural and production traits.....	88
5.3. Leaf photosynthesis and leaf, stem and SAM starch concentration.....	94
5.4. Leaf, stem and SAM sorbitol concentration	96
5.5. Correlations between NSC organ concentrations and photosynthesis	97
5.6. Correlations between photosynthesis, TCSA and crop load.....	98
5.7. Carbon metabolism in the different classes of tree architectures	99
5.8. Genotypic variability in SAM hormone concentrations	101
5.9. SAM hormones concentration in the different classes of tree architectures	102
5.10. Correlations between NSC organ concentrations and hormone concentration in SAM	102
5.11. Correlations between physiology-related variables and architectural traits	103
5.12. Correlations between physiology-related variables, number of floral GU and floral induction	105

6. Discussion	108
6.1. Genotypic variability in tree architecture	108
6.2. Genotypic variability in crop loads, carbohydrate metabolism and relationship with architecture.....	109
6.3. Genotypic variability in hormones and relationship to tree architecture.....	110
6.4. Relationship between floral induction, physiology traits and architecture	111
7. Conclusion	112
8. Supplementary Material.....	113
VI. General discussion	116
1. Analysis of inhibiting and activating signals effect on floral induction through an experimental approach.....	117
1.1. Main physiological mechanisms analyzed in this study.	117
1.2. Analysis of the main determinants of genotypic variability in floral induction.....	119
2. Modeling of FI variability and its determinisms	120
2.1. Added value of the modeling approach and limitation.....	120
2.2. Perspectives to account for genotypic variability in the model for simulating floral induction variability.....	122
VII. Résumé général	123
1. Contexte général.....	124
2. Objectifs.....	125
3. Démarche expérimentale.....	125
4. Démarche de modélisation	126
5. Principaux résultats.....	127
6. Conclusions et perspectives	128
VIII. References.....	130

I. Introduction

In polycarpic plants, flowering and reproduction can occur at different ages or developmental stages of the plant during their lifespan. In most of temperate trees, flowering takes place every year, but with large fluctuation or irregularity in its intensity depending on years. One of the most known phenomena associated with such a kind of variability is the biennial bearing pattern, which is characterized by the alternation of a year of intense reproduction followed by a year with low or no reproduction (Monselise and Goldschmidt, 1982). This phenomenon is observed particularly in perennials and has crucial economic issues in plants with agronomic importance. Fruit trees are prone to alternate or irregular bearing, which generates economic issues due to its influence on fruit yield and quality, gaps in profits between years and costs of orchard management to control this phenomenon. Biennial bearing also causes issues on fruit quality, may provoke wood crack damages and increase sensitivity to diseases. Processes related to biennial bearing have been studied for many years with the aim to attenuate flowering alternation. Previous observations have highlighted that biennial bearing is linked to fluctuations in floral induction (FI) that in turn provoke fluctuations in flowering intensity and fruit production. In fruit trees, FI usually occurs the year before flowering (Abbott, 1969), meaning that the potential number of fruits growing on a tree is determined by endogenous and exogenous conditions occurring the year before. Floral induction is determined by morphological and physiological changes that are supposed to occur under the control of internal and external signals and that lead to the transition of meristems from vegetative to reproductive state.

In fruit trees, two main hypotheses have been proposed to explain fluctuations in FI among years. The first hypothesis regards the competition for carbohydrates that occurs in years of high production between the growing organs (fruit and shoot) and the meristems to be induced (Palmer *et al.*, 1991; Wunsche *et al.*, 2000). This competition is likely to deprive meristems of assimilates, originating from leaf photosynthesis, which are supposed to be essential for FI transition, thus leading to low flowering and fruiting in the next year. The second hypothesis suggests that fruit produce substances, likely gibberellins produced by seeds in the case of apple tree, which are inhibiting floral induction in the nearby meristems (Chan and Cain, 1967). Some studies have focused on fruit trees productivity by characterizing carbon balance, water budget and the effects of biotic and abiotic stresses. However, it is not clear so far if these factors affect directly FI or other yield components (fruit set, fruit mass). Tree architecture has also been shown to be important for fruit production regularity by means of the spatial distribution of flower buds within the tree and flowering recurrence over years. Indeed, in tree architecture, not all meristems are flowering in a given year. On apple trees, it has been shown that depending on the variety, meristems are more or less synchronized and variety regularity is related to differences in their topological organization and branching (Costes *et al.*, 2003; Durand *et al.*, 2013).

Recently, studies have been performed to analyze the potential link between the genotypic variability in bearing pattern and carbon metabolism or carbon balance. (Pallas *et al.*, 2018). The authors conclude that FI variability among cultivars was not directly associated with contrasted photosynthesis activity or carbon availability in the plant, thus questioning the implication of carbon source/sink relationship in the determination of FI. New hypotheses about implication of hormones such as GA and architectural variability between organs in FI determination emerged from this study and from detecting quantitative traits loci (QTLs ; Guitton *et al.*, 2012). Nevertheless, no experimental works has been carried out to test such hypotheses.

This PhD, which focuses on apple tree as a case study, relies on the assumption that FI in fruit tree depends on both the tree architecture defined by the spatial organization of the different organs (fruit, leaves and meristems) and on signal exchanges(hormonal, carbon) between them. Moreover, this work was seeking to elucidate further if the genotypic variability in the regularity over years of floral induction may result from the variability in the tree architecture and/or in physiological processes.

The general strategy of this thesis relied on the complementarity between experimental and modelling approaches to explain within tree and between years floral induction variability on the one hand and its genotypic variability on the other hand. Experiments on the spatial, temporal and genotypic variability of

floral induction were conducted to allow the study of interactions between structural and functional variables that were assumed to be related to floral induction. The results obtained from these experiments were used to develop a modelling approach in which FI in meristems was assumed to be under the control of both inhibiting signals and activating signals moving within the structure and acting on meristems to determine FI.

On this basis, this thesis included three objectives. A first objective was to decipher the relative importance of the different signals assumed to be responsible for alternate bearing in apple tree and to quantify the impact of their distances to shoot apical meristems (SAM) on floral induction. For this, the number of organs assumed to be activating or inhibiting, i.e. leaves and fruit respectively, was manipulated at different scales in tree organization, shoot, branch and half tree. The second objective was to develop a generic model allowing the computation of activating and inhibiting signal quantities at different distances in complex tree structures and to test its capability to simulate the within-tree variability in meristem FI observed experimentally. The third objective was to study the genotypic variability in floral induction through the exploration of architectural and functional variables among six different apple cultivars, contrasted in terms of architecture and bearing patterns.

The thesis consists of five chapters. The first chapter is a literature review that introduces the basic concepts and the state of the art dealing with the subject of study, namely floral induction and tree architecture and the modelling approaches existing in the field of functional structural plant model (FSPM). The second chapter describes experimental results obtained on the impact of leaf and fruit presence and their distances to meristems on floral induction and fruit growth, obtained. It corresponds to a scientific paper already published in *Frontiers in Plant Science*, entitled “Impact of within-tree organ distances on floral induction and fruit growth in apple tree: implication of carbohydrate and gibberellin organ contents” (Belhassine *et al*, 2019). The third chapter presents the modelling approach used to simulate within-tree variability of floral induction depending on activating and inhibiting organs and their distances to the meristems where the signals are integrated. The model aims to quantify and analyze the impact of architectural traits on signals transport and floral induction proportions, at different scales of tree organization (shoot, branch and half tree). This chapter is also written in a scientific paper format. This paper has been submitted to the *Scientific Reports* journal and its title is “Modelling transport of inhibiting and activating signals and their combined effects on floral induction in meristems: application to apple tree”. The fourth chapter presents the study of architectural and functional differences among six apple cultivars and their correlation to the genotypic differences in FI and production regularity. These results highlight the existence of a large genotypic variability in carbon metabolism and hormonal characteristic and suggest that FI variability is under the complex control of architectural and probably hormonal balance in trees. Finally, the last chapter presents a general discussion of the approach followed to study alternate bearing and FI and the main results obtained on the three objectives. Moreover, new perspectives are proposed based on the findings resulting from this work.

II. Literature review

1. Floral induction

1.1. General considerations

Plants go through different developmental phases during their life cycles. Flowering is the biological process that ensures reproduction and durability of the species through the production of fruits and seeds dispersal. It represents an important step in a plant cycle that reflects reproductive success of plants in response to seasonal changes (Bäurle and Dean, 2006). During the juvenile stage, plants do not react to floral-inductive signals either environmental or endogenous and thus not able to develop flowering. The duration of the juvenile stage varies among species. In annuals, this juvenile phase can only last several weeks or months, whereas, in perennial crops juvenility can last several years (Ha, 2014). After this juvenile stage, the transition to flowering occurs and at the reproductive adult phase begins when plants are receptive to these floral inductive signals (Bäurle and Dean, 2006). During the adult phase, plants can regulate their flowering time synchronously with other individuals within the same species and/or with presence of pollinators to ensure reproductive success. Moreover, for many species, flowering must occur in weather/climatic conditions appropriate for reproductive development to follow (Kim *et al.*, 2009).

Floral induction (FI) is a key step in the flowering process that generates morphogenetic transition in shoot apical meristems (SAM) from the vegetative to the differentiated floral state (Bangerth, 2009). FI is supposed to be controlled by both internal and external factors (Hanke *et al.*, 2007). FI has been widely studied for decades in the model plant *Arabidopsis* because it has been the first plant with an entire sequenced genome, is easily transformable with a short life cycle that produces many seeds (Meinke *et al.*, 1998) and can be easily grown in growth chamber under controlled conditions.

Moreover, focusing on the mechanisms involved in *Arabidopsis thaliana* is of major interest since some of the key regulators of floral induction are assumed to be conserved and to share similar functions in both perennials and annual species (Samach and Smith, 2013).

1.2. Floral induction in the model plant *Arabidopsis thaliana*

In the model plant *Arabidopsis thaliana* (*At*), four flowering pathways have been described (Figure 1), including photoperiod, vernalization, gibberellin-induced, and autonomous pathways (Sung and Amasino, 2004; Bäurle and Dean, 2006; Lee and Lee, 2010). There is a common set of genes, partly related to gibberellins, that define the internal/autonomous signaling pathways in flowering among plant species (Putterill *et al.*, 2004), while photoperiod and vernalization are considered as the main external/environmental factors influencing FI (Mouradov *et al.*, 2002; Searle and Coupland, 2004; Corbesier and Coupland, 2006; Jung and Müller, 2009; Kim *et al.*, 2009).

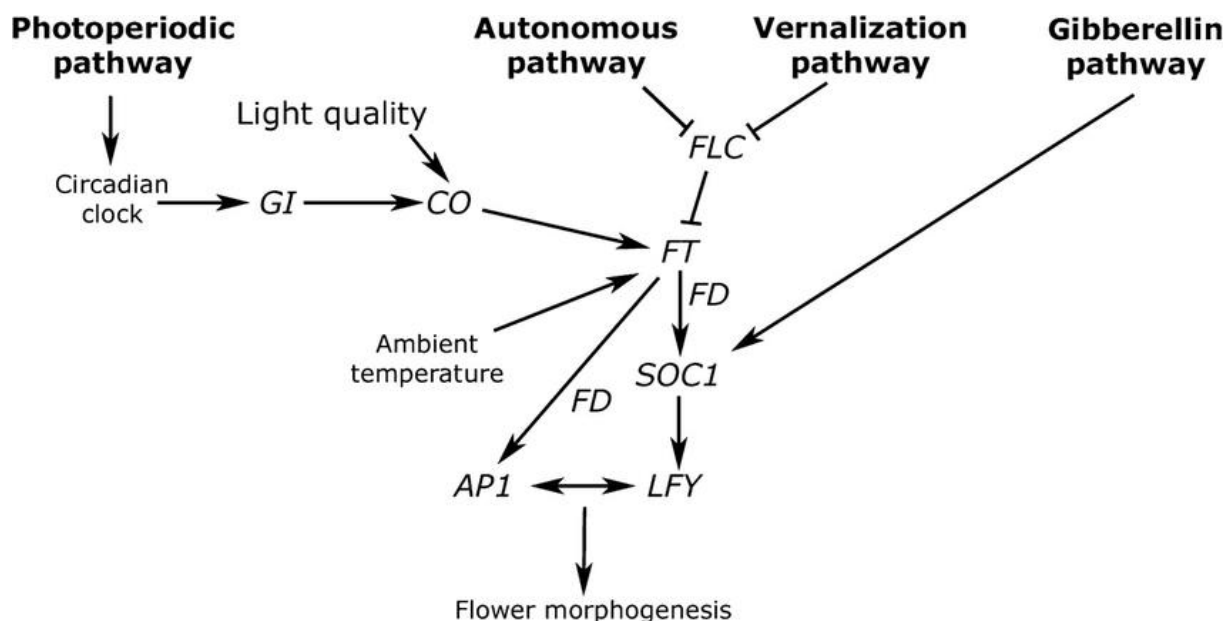


Figure 1. Simple model of the four pathways controlling flowering time in *Arabidopsis thaliana*. The photoperiod pathway promotes flowering specifically under long days. The transcription of the *GI* (*GIGANTEA*) and *CO* (*CONSTANS*) genes is regulated by the circadian clock, whereas light quality regulates *CO* protein abundance. The autonomous pathway negatively regulates the abundance of the mRNA of the floral repressor *FLC* (*FLOWERING LOCUS C*). *FLC* mRNA abundance is also repressed by vernalization independently of the autonomous pathway. Finally, gibberellin promotes flowering of *Arabidopsis*, particularly under short days. All four pathways appear to converge on the transcriptional regulation of the floral integrator genes *FT* (*FLOWERING LOCUS T*) and *SOC1* (*SUPPRESSOR OF OVEREXPRESSION OF CO 1*) which promote expression of *AP1* (*APETALA1*) and *LFY* (*LEAFY*), genes required to confer floral identity on developing floral primordia. Figure from Corbesier and Coupland (2006).

Photoperiod (day length) is one of the most important environmental factors that affect FI in *At*. Results obtained in *At* indicate that day-length, through light perception and the circadian clock, regulates *CONSTANS* (*CO*) inducing the production of *FLOWERING LOCUS T* (*FT*) gene expression (Hayama and Coupland, 2004). In that system light is perceived by photoreceptors, phytochromes and cryptochromes located in leaves (Mouradov *et al.*, 2002). Genes involved in light perception such as *PHYTOCHROME A* to *E* (*PHYA* to *PHYE*), *CRYPTOCHROME 1* and *2* (*CRY1* and *CRY2*) regulate and stabilize *CO* expression depending if light perception occurs under either long or short days (Goto *et al.*, 1991; Johnson *et al.*, 1994; Mouradov *et al.*, 2002; Valverde *et al.*, 2004).

Vernalization corresponds to a long exposure to low ambient temperature needed to induce flowering (Simpson and Dean, 2002; Boss, 2004). Vernalization leads to the expression of *VERNALIZATION 1* and *2* (*VRN1* and *VRN2*) and *VERNALIZATION INSENSITIVE 3* (*VIN3*) genes (Chandler *et al.*, 1996; Koornneef *et al.*, 1998; Sung and Amasino, 2004). These genes promote flowering by repressing *FLOWERING LOCUS C* (*FLC*), known as a flowering repressor. Vernalization pathway also involves, *FRIGIDA* (*FRI*) that acts to increase *FLC* expression level (Michaels and Amasino, 2000).

The autonomous pathway refers to different genes that act on flowering time without any implication of light or low temperature (Martinez-Zapater and Somerville, 1990; Srikanth and Schmid, 2011).

In the last pathway (GA pathway), GA signaling acts through *GIBBERELLIC ACID INSENSITIVE* (*GAI*), *REPRESSOR OF GA1-3* (*RGA*) and *RGA-LIKE 1* (*RGL1*) genes and GA biosynthesis genes (*GA1*, *GA4* and *GA5*) (Olszewski *et al.*, 2002) and have been shown to promote flowering in *At* (Wilson *et al.*, 1992). In *At*, gibberellins activate floral integrators genes such as *SUPPRESSOR OF OVEREXPRESSION OF CONSTANS 1* (*SOC1*), *LEAFY* (*LFY*), and *FLOWERING LOCUS T* (*FT*) in the inflorescence and floral meristems, and in leaves,

respectively (Mutasa-Göttgens and Hedden, 2009). However, the autonomous pathway may assist the photoperiodic and GA pathways through its action upon floral repressor FLC (Reeves and Coupland, 2001). This implies different genes that participate in regulating the expression of (FLC), such as LUMINIDEPENDENS (LD), FCA, FY, FPA, FVE, FLOWERING LOCUS D and K (FLD and FLK) (Michaels and Amasino, 1999).

The four flowering pathways converge to act on common target genes that regulate floral initiation genes (Simpson and Dean, 2002). Three genes, FLOWERING LOCUS T (*FT*), *SUPPRESSOR OF OVEREXPRESSION OF CO 1* (*SOC1*) and *LEAFY* (*LFY*), have been identified as flowering integrators. *FT* and *SOC1* are negatively regulated by FLC which integrates the autonomous and vernalization pathways (Lee *et al.*, 2000; Onouchi *et al.*, 2000). *SOC1* expression is also regulated by the GA pathway whereas *FT* expression is not, suggesting that *FT* and *SOC1* act differently in the integration of flowering pathways (Borner *et al.*, 2000; Moon *et al.*, 2003). *LFY* is an integrator regulated by both the photoperiod and GA pathways (Blazquez and Weigel, 2000). *FT* is considered as the florigen that triggers FI in SAM (Corbesier and Coupland, 2006). *FT*-homologous genes, whose proteins appear to fulfill the role of florigen, have been found in several other species such as rice (Izawa *et al.* 2002, Tamaki *et al.* 2007), cucurbits (Lin *et al.*, 2007), tomato (Lifschitz and Eshed 2006, Lifschitz *et al.* 2014) and the apple tree (Kotoda *et al.*, 2010).

1.3. Irregularity in perennials

FI is the main process determining flowering or fruiting intensity in perennials. Irregular FI is observed in different economically important fruit trees, with influences on fruit quantity and quality. Irregular bearing is a typical production mode observed in different fruit tree species that consists in an irregular fruit production over successive years. Alternate bearing or biennial bearing is a particular form of irregular bearing, for which the fruiting pattern is biannual (Hoad, 1984). This bearing pattern is characterized by years of high production ("ON" years) followed by years of low production ("OFF" years). "ON" years correspond to years with very significant fructification, caused by abundant flowering and little fruit drop and "OFF" years are marked by a lack of flowers or high fruit drop, and therefore a low fruiting (Monselise and Goldschmidt, 1982). Forest trees also display irregular bearing. In this case, flowering synchronicity among individuals in a given year is called "masting". Masting is defined as a cyclic process consisting in a variable and synchronized group reproduction behavior observed in non-cultivated perennial populations across wide geographic areas that massively produce fruits in a particular year, then low yield is observed for the next years (Koenig and Knops, 2005; Smith and Samach, 2013a)

Biennial bearing has been observed in many temperate and tropical perennial species, such as, olive trees (Lavee, 2007), pistachio (Rosenstock *et al.*, 2010), avocado (Lovatt, 2010), citrus fruits (Muñoz-Fambuena *et al.*, 2012), and apple trees (Guitton *et al.*, 2012). The most common assumption on irregular bearing is that sexual reproduction is expensive, trees need one to several years to refill the resources needed for reproduction and is referred to as the "costs of reproduction" (Bell, 1980). Costs of reproduction correspond to the investments in reproduction at cycle n , that is to say the resources that the individual allocates for its reproduction (flowering and fruit growth) and the consequences, in terms of vegetative growth and reproduction, in the $n + 1$ cycle. These investments can be identified through the consideration of physiological costs, like carbon utilization and through the number of buds turning into inflorescence (Obeso, 2002).

1.4. Agronomic consequences and horticultural practices to manage irregular bearing

Irregular bearing is particularly an issue for fruit production due to the significant reduction of yield in OFF years and low quality in ON years. Fruit quality in an 'ON' year is often lower than that of a regular bearing cultivar and the reduced fruit size during 'ON' years can decrease the marketable value of the production. Excessive crop load during 'ON' years can also provoke wood rupture and branch damages (Jonkers, 1979). Furthermore, irregular trees are more sensitive to frost damage and to pest and disease attack than regular cultivars because of depletion of carbohydrates reserves during 'ON' years (Jonkers, 1979).

Stabilizing yields of economically interesting fruits trees and annual income for growers is thus a challenge in horticulture. Flower and fruit thinning, pruning, girdling and using plant growth regulators are among

interventions helping to attenuate the biennial production cycle (Goldschmidt, 2018). Fruit load could be reduced by limiting flower number and fruit set or increasing fruit drop. Thinning can be performed either manually, mechanically or chemically (Dennis, 2000). Severe pruning during the spring of 'ON' years and light pruning the 'OFF' years help to regulate fruit load over years (Jonkers, 1979). Plant growth regulators (gibberellins, cytokinins, auxins, abscisic acid, ethylene) moderate yield fluctuations by repressing vegetative growth and by inhibiting or increasing the rate of flower initiation (Dennis, 2000; Bangerth, 2009).

Nevertheless, even if many agronomic practices exist it is far from to be straightforward to reach and find optimal fruit set target that do not tax the tree to the point that triggers alternation (Smith and Samach, 2013a).

Specific rootstock vigor can also reduce alternate bearing patterns in apples by limiting architecture development and thus the potential number of flowering buds. M9 rootstock is known to reduce shoot length and node number more than M106 and M793 rootstocks (Van Hooijdonk *et al.*, 2010). These rootstocks reduce growth by limiting hydraulic conductivity and through complex movements of abscisic acid, auxin and cytokinins (Tworkoski and Fazio, 2015). However, the effect of rootstock depends on the grafted cultivar. For 'Golden Delicious' and 'Granny Smith' cultivars, the incidence of biennial bearing increased as rootstock vigor increased, whereas with 'Redchief Delicious', a spur type cultivar, biennial bearing declined as rootstock vigor increased (Barritt *et al.*, 1997).

Although it appears that horticultural solutions can mitigate the problem by reducing fruit load, horticultural practices such as chemical flower and fruit thinning have a negative effect on the environment as well as on consumer health and increase the costs of orchard management. Scientific research is thus necessary to further study physiological processes involved in FI in order to adapt agronomic practices or find cultivars displaying a natural regular bearing pattern.

2. Case of study: the apple tree

2.1. Economic importance

Apples represent the main fruit crop of temperate regions of the world. Apple tree is the third most cultivated tree fruit in the world after citrus and bananas, with a worldwide production of about 83 million tons in 2017. Half of the apple production comes from China, while France hold the ninth rank in the world and the third in the European Union with a production of 1.7 million tons in 2017. Apple is the most produced fruit (more than half of the overall fruit production) and the most consumed fruit in France (FAOSTATS, 2019).

2.2. Apple origin

The domesticated apple (*Malus x domestica* Borkh) is a species of the genus *Malus* of the sub family Maloideae of the family Rosaceae. Apple tree has 17 pairs of chromosomes while other fruit species of the family Rosaceae such as peach, strawberry or rose have only between 7 and 9 chromosomes. Genome sequencing of the domesticated apple showed that this increase in the number of chromosomes in the apple tree is due to a genome-wide duplication in the Pyreae tribe 50 million years ago (Velasco *et al.*, 2010). Phylogenetic reconstruction of Pyreae and the genus *Malus*, relative to major Rosaceae taxa, identified the progenitor of the cultivated apple as *M. sieversii* (Velasco *et al.*, 2010). Later studies suggest that *Malus x domestica* Borkh has been domesticated from *M. sieversii* in the Tian Shan Mountains for 4000–10.000 years, and dispersed from Central Asia to West Europe along the Silk Road, allowing hybridization and introgression of wild crabapples from Siberia (*M. baccata* (L.) Borkh.), Caucasus (*M. orientalis* Uglitz.), and Europe (*M. sylvestris* Mill.) (Cornille *et al.*, 2014). In a recent review, it is mentioned that the increase in fruit size and changes in morphology during evolution in the wild Rosaceae resulted from hybridization events and evolved as a seed-dispersal adaptation recruiting megafaunal mammals like bear, deer and humans (Spengler, 2019).

2.3. Biology of apple tree

Apple tree is a perennial deciduous plant with allogamous reproduction, presenting a pollinic auto-incompatibility of gametophytic type, which requires the presence of another variety to ensure cross-fertilization. Apple cultivars are highly heterozygotic due to this auto-incompatibility (Chevreau *et al.*, 1985). When it develops from seeds, the tree goes through two phases: the juvenile phase represents the period at which the tree remains vegetative and cannot enter production under inductive environmental conditions and the adult phase where the tree is able to produce fruit (Crabbé, 1987; Pratt, 1990). Depending on the cultivar, the juvenile phase can last from six to twelve years for apple (Visser, 1964). As for most of the fruit trees, apple trees reproduction results from vegetative reproduction through grafting. In this case, grafts taken from an adult stock are physiologically mature, as soon as they are grafted on a rootstock. In that case, the time of first fruit set of the tree is fast and does not exceed 2 or 3 years. Using dwarfing rootstock can even more reduce juvenility and lead to earlier flowering (Visser, 1964, 1965).

As for other fruit trees grown in temperate conditions, the annual growth cycle of the tree is adjusted according to the seasonal environmental conditions (Figure 2). Winter buds enter in dormancy under the effect of cold temperatures and short photoperiod (Heide and Prestrud, 2005). Dormancy is a phase of development that allows trees to survive unfavorable conditions during the winter (Faust, 1994). Depending on the genotype and environmental conditions, dormancy release and bud break will occur at different dates in the next spring, due to different chilling and heat requirements (Legave *et al.*, 2013). Indeed endo-dormancy ending in winter conditions (low temperatures) and is replaced by eco-dormancy, which ends in favorable climatic conditions (increase in temperature). The buds will then resume their physiological activity, generating an increase in cell division and vegetative and floral development resumption (Horvath *et al.*, 2003). After anthesis, fruit set and growth take place along with vegetative growth, until the end of the cycle at fall, characterized by leaf senescence, reserve accumulations in woody compartments and the next entry into dormancy. In apple tree, FI occurs at end spring of a year in buds that will develop during the spring of next year. FI results from the differentiation of shoot apical meristems into flower bud.

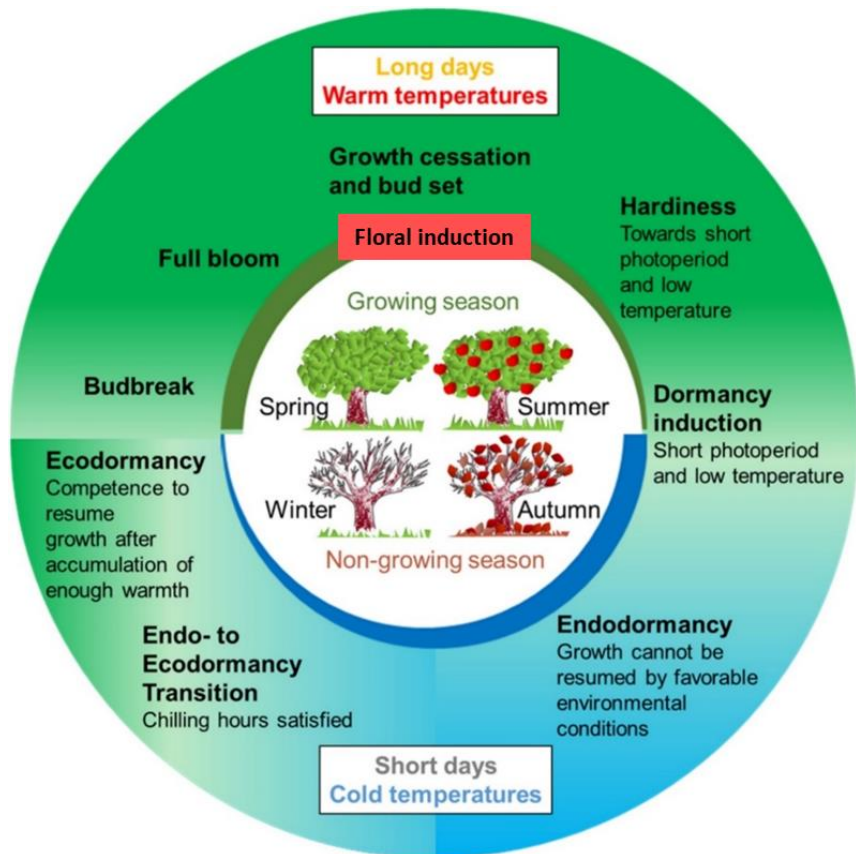


Figure 2. Representation of 1-year life cycle of a temperate fruit tree. Trees grow actively during the growing season, typically in spring and early summer. At the end of summer and beginning of autumn, they initiate growth cessation, presumably in response to short days. Toward autumn, trees increase their resistance to cold (hardiness) and buds enter in dormancy during autumn. Chilling temperatures during the winter periods triggers dormancy release. Then, ecodormant buds can respond to warm temperatures in the spring to promote budbreak, which is followed by active growth at the end of the spring and in the summer. Figure from Falavigna *et al.* (2019).

Organ growth follows seasonal patterns and depends on competition for resources with other tree components. In the early growth stages, young organs growth is insured by starch reserves of the tree (Hansen, 1971). Starch is hydrolyzed to soluble sugars that are transported through xylem to the growing parts (Bonhomme *et al.*, 2010). At one-third to one-half of their final area, leaves become autonomous, producing most of the carbohydrates they need. Leaves can export assimilates in different proportions depending on their growth stage and position along the shoot (Watson and Casper, 1984). Fruit growth in apple tree is usually dependent for local assimilates coming from close leaves (Hansen, 1969). Seasonal patterns in reserve storage are also observed. Low sugar and starch contents are found in the branches at the time of active growth and higher starch accumulation in branches is observed in autumn after harvest.

2.4. Architecture characteristics of apple tree

The architecture of a plant corresponds to organs organization in space and time that results from growth and branching processes modulated by exogenous conditions of the environment (Barthélémey and Caraglio, 2007). The branching, according to Hallé *et al.* observations (1978), can be characterized by the mode (monopodial, when the terminal bud continues to grow as a central leader shoot and the lateral buds remain latent versus sympodial, when the terminal bud ceases to grow and axillary buds become new leader shoots) and position (acrotonic, when long shoots are located in the top versus basitonic, when long shoots are located in the basal part of the bearing shoot). Branches display two growth types: sylleptic branches come from axillary meristems of an initial branch within any arrest between meristem initiation and their growth. Proleptic branches develop from axillary meristems forced to rest by winter cold. These

meristems produce buds that will not evolve immediately. The distribution of leaves along an axis that results from meristem activity is called phyllotaxy. A growth direction associated to phyllotaxy allows to distinguish plagiotropic axes, characterized by a horizontal to oblique growth direction (with planar phyllotaxies) from orthotropic axes, characterized by a vertical growth direction (with spiral phyllotaxy) (Costes *et al.*, 2006).

The apple tree is characterized by rhythmic growth and branching. Rhythmic growth is imposed by winter dormancy. Summer growth arrest can also be observed depending on the age of the tree (Costes and Guédon, 2012). Indeed, in young trees polycyclism usually occurs. In that case, two or more growth units (produced without growth interruption) can be distinguished in the same growing season. Meristems produce leaves according to an alternate spiral phyllotaxy with angles varying from $3/8$ to $4/5$ (Abbott, 1984). All axes follow an orthotropic orientation. In apple tree, it is possible to trace the development history of a branch following the traces of vegetative or floral development thanks to the presence of scars at the bud formation locations. “Inflated” scar (called “bourse”) will represent a morphological indicator of the presence of an inflorescence in a given year. In apple, two types of buds are observed: vegetative buds (producing leaves only) are distinguished from mixed buds (called floral buds) composed of a leafy basal part followed by a floral distal part (Abott, 1984). The growth of vegetative buds is monopodial ending with a dormant bud when growth cessation occurs. The growth of floral buds is also monopodial ending with the differentiation of the apical meristem into a flower bud, composed of preformed leaves, corresponding to the primordial leaves contained initially in the bud, surmounted by an inflorescence and called bourse. After the inflorescence, sympodial growth resumes in the same growing season from one or two meristems located in axillary position in the inflorescence. The shoot originated from these axillary buds is usually called “bourse shoot”.

Shoots of apple tree are polymorphic and three main categories are observed (Figure 3). Short shoots (brachyblasts) composed of preformed metamers with non elongated internodes only, long shoots (auxiblasts) composed of a preformed part and a neo-formed part with elongated internodes and medium shoots (mesoblasts) which are an intermediate form between the first two (Costes *et al.*, 2006). The terminal buds of short shoots (spurs) are more prone to death, called ‘extinction’, and this phenomenon has been demonstrated to be cultivar dependent (Lauri *et al.*, 1995).

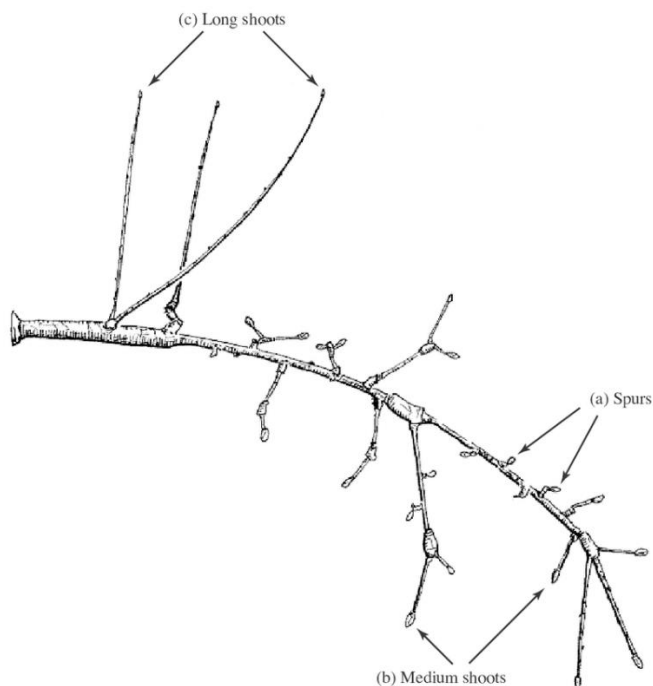


Figure 3. Example of shoot types in an apple branch. (a) Spurs, (b) medium shoots, and (c) long shoots (from Costes *et al.*, 2006. Original drawing from J. M. Lespinasse)

Regarding branching, metamer position on a shoot and the type of shoots itself also affect the axillary development and the distribution of vegetative, floral and extinct buds (Lauri and Terouanne, 1998). For instance, the study of axillary development patterns of long shoots showed that monopodial shoots tended to have more inflorescence buds than sympodial shoots, which had more extinction (Lauri and Terouanne, 1998).

Spatial variability of growth and development has been observed in apple and is caused by different distribution of vegetative and reproductive buds within the tree. Apple tree architecture has been categorized depending on cultivars into four classes (Figure 4) based on the angle of insertion of branches on the trunk, the distribution of branches (from basitony to acrotony), the type of branches bearing fruit and the distribution of fruit on the branches (Lespinasse, 1992; Lauri *et al.*, 1995). Type I presents a columnar shape (reduced internode length) with many short terminal branches that produce flowers (spurs), emerging from the main trunk. Type IV has vigorous growth, with flowering occurring at the tips of long branches located on the upper part of the tree. Type II and III are intermediate architectures, bearing fruit from spurs for Type II and on medium and long branches close to the trunk for Type III. As type III and IV apples set fruit on the ends of their branches, shoots tend to grow downwards driven by fruit weight. This architecture variability seems to be also associated with bearing pattern variability. Indeed, apple cultivars from type I and II categories are classified as alternating cultivars and cultivars from type III and IV are classified as regular.

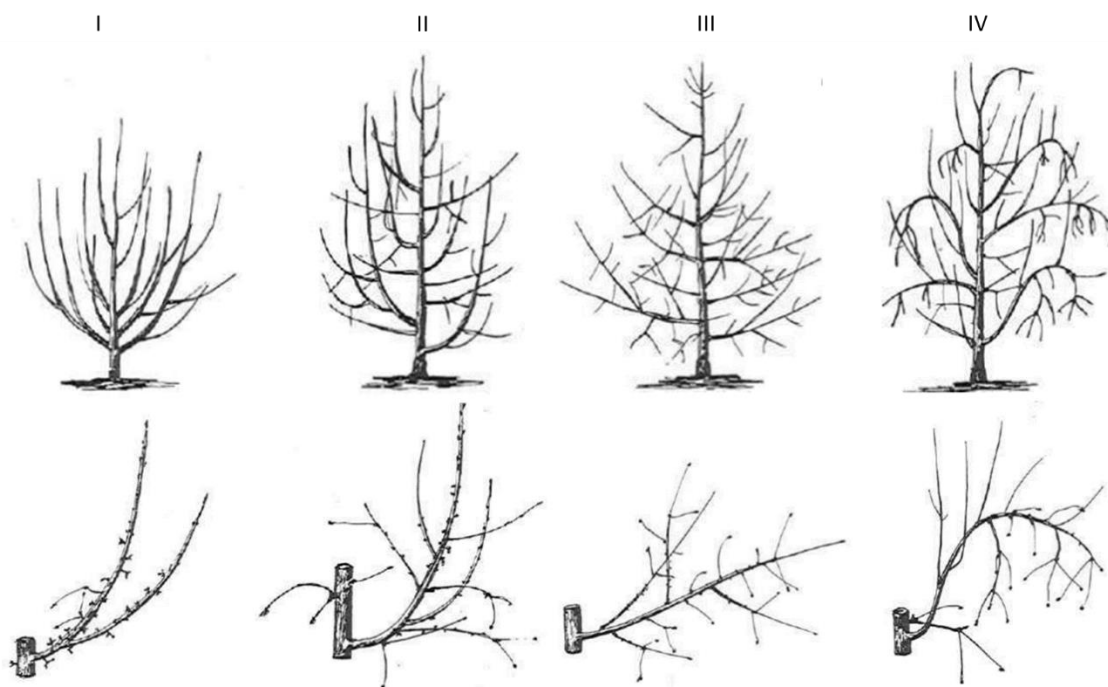


Figure 4. The four ideotypes of apple trees. Figure from Lespinasse and Delort (1986).

The architectural variability in apple tree has been studied for cultivars of type II, III and IV using Markovian models for branching and succession segmentation. Costes and Guédon (2002) analyzed branching on 1-year-old apple cultivars with diverse branching and fruiting habits. These models (hidden semi Markov) describe the successions, lengths and composition of the different branching zones along the shoots (Figure 5). Based on this modeling approach, cultivars have been characterized according to different sylleptic and proleptic branching patterns and shoot types (floral or long, medium and small vegetative). This method was also used to analyze succession and showed that successions of vegetative (long, medium and short) and floral growth units have specific locations in trees and that growth unit type depends on the type of its parent growth unit (Costes and Guédon, 2012). Branching patterns of different growth unit types (short,

medium, long) have also been analyzed by Renton *et al.* (2006). This study shows that a high degree of similarity between each growth unit type. In addition, the model indicates that branching patterns tend to become simpler when reducing the length of GU by moving from the center to the periphery of the trees. Other recent studies investigated the genotypic basis of traits related to plant architecture in bi-parental populations. These studies have indicated that most of the traits related to organ dimension (diameter or internode lengths) or branching (sylleptic or proleptic branching intensity) are highly heritable and under polygenic control of several QTLs (Segura *et al.*, 2008).

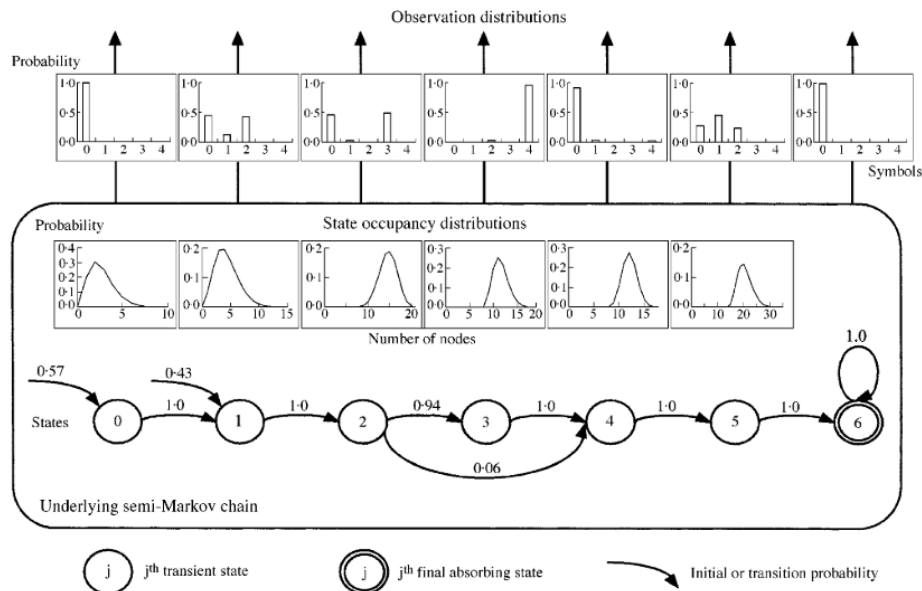


Figure 5. Modelling branching on 1-year-old trunks of 'Reinette Blanche du Canada' using a hidden semi-Markov chain. Each state, corresponding to a branching zone, is represented by a circle. Transient states are edged by a single line while the final state is edged by a double line. The possible transitions between states are represented by arcs with the attached probabilities noted nearby (for legibility, only transitions with probabilities exceeding 0.02 are shown). Thick arcs entering states indicate initial states. The attached initial probabilities are noted nearby. The occupancy distributions are shown above the corresponding states, as are the possible lateral types observed in each state. Each lateral type is represented by a symbol: 0, latent bud; 1, proleptic spur; 2, proleptic long shoot; 3, bourse; 4, sylleptic shoot. Figure from Costes and Guédon (2002).

2.5. Factors affecting floral induction and biennial bearing in apple tree

In apple trees, a negative correlation between crop load in a year and flowering in the next year is generally observed (Jonkers, 1979). Heavy fruit loads accentuate biennial behavior by reducing flower production. Reducing the fruit load can increase flower production and this effect was reduced when fruit removal in the year before flowering was delayed (Harley *et al.*, 1942) suggesting a specific period during fruit growth for which FI occurs. This period of FI was assumed to occur between 30 and 70 days after full bloom (DAFB) (Foster *et al.*, 2003; Haberman *et al.*, 2016).

Large genotypic variability in biennial bearing pattern has been observed in commercial cultivars, in bi-parental population and in collections of varieties. Several indicators were used to estimate and compare the intensity of biennial bearing among cultivars. Among them, the biennial bearing index (BBI) estimates the intensity of deviation in yield during successive years (Wilcox, 1944). Genotypes whose production oscillates much around the general yield trend are alternating trees and characterized by a high BBI value. On the other hand, genotypes whose production is very close to the yield trend with small variations are classified as regular and are characterized by a low BBI value (Durand *et al.*, 2013). The autocorrelation of residuals index refers to the correlation coefficient between consecutive residuals between the values of the observed flower or fruit number and its general trend over years (Durand *et al.*, 2013). This indicator is used to determine if high BBI values are associated with a biennial or simply irregular bearing pattern.

Durand *et al.* (2013) have also proposed an entropy index, which represents the synchronization of flowering or fruiting fates among the buds of a tree for each year. This last indicator is used to determine the level of flowering synchronicity between buds over consecutive years (Lauri *et al.*, 1995). In other words, this indicator is useful to know if a genotype with a regular bearing pattern has a tendency to have all its buds floral induced each year or if the regular bearing pattern is the result of alternation between shoots or branches (around 50% of buds induced each year) (Figure6).

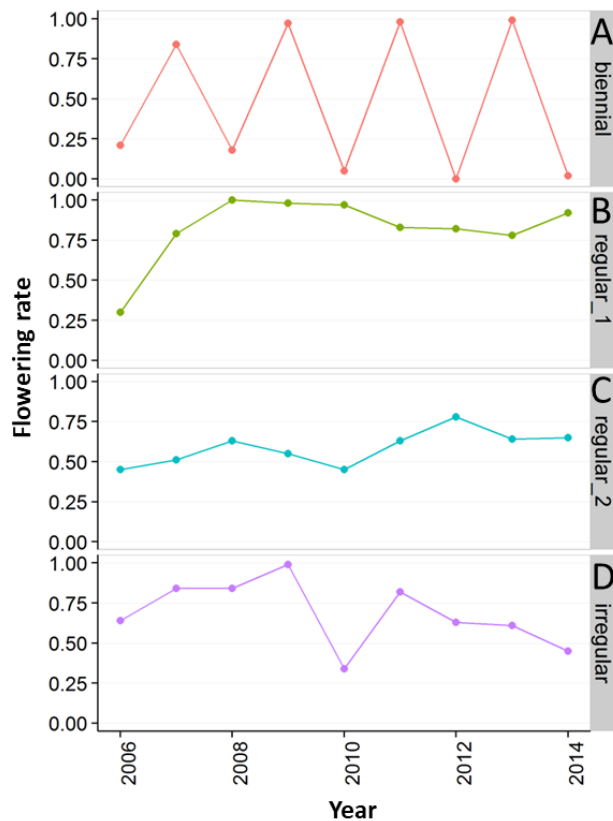


Figure 6. Bearing patterns of four genotypes from a cross between the INRA hybrid X3263 and the cultivar 'Belrène. (A) Biennial genotype, (B) Regular genotype with 100% of buds induced each year, (C) Regular genotype with around 50% of buds induced each year and (D) Irregular genotype. Figure adapted from Durand *et al.*, (2013).

Both competition for carbohydrates between fruit and vegetative growth and hormone production by fruit were suspected to affect FI. The possibility that fruits can remove from meristems carbohydrates necessary for flower initiation was advanced a long time ago, assuming that growing fruits are powerful sinks for the carbohydrates (Hansen, 1969) necessary for meristems to initiate flower buds (Sachs, 1977). Moreover, overloaded trees increased hormone production in the seeds, mainly GA that could inhibit the flower bud differentiation in the current year (Monselise and Goldschmidt, 1982). More precisely, GA4, an active GA form that has been shown to target key flowering genes in SAM in *Arabidopsis* (Eriksson *et al.*, 2006) has also been reported to be transported from fruit to bourse SAM (Ramírez *et al.*, 2004).

Light intensity also affects FI. Low light intensity, due to clouds or shading, can lead to decreased flowering in apple trees (Jackson *et al.*, 1977). Shading experiments showed that up to 30% shading, flowering of spurs was not affected but was totally inhibited when shading increased to 70% (Cain, 1971). Although variations in light intensity may quantitatively affect floral initiation, it is considered a secondary factor, related to the production of assimilates (Wilkie *et al.*, 2008).

In apple tree FI have been observed to be associated to the architectural properties at different levels (branches, shoots). At the branch level, high extinction rates, which reduce the branching density between

two consecutive years, may increase the flowering capacity of the remaining shoots. Authors hypothesized that this higher FI is associated with the lower branching density which improves the local light condition and thus brings into question the effect of environment on FI. Moreover, the length of the bourse shoot was shown to be positively related to the probability of return of flowering (Nielsen and Dennis, 2000). Shoot length can affect FI by increasing number of leaves and by increasing distances between SAM and fruit, considered as source of inhibition.

2.6. Molecular and genetic regulation of flowering in apple tree

Due to a whole genome duplication event (Velasco *et al.*, 2010), apple has duplicated gene copies for each known flowering gene in *Arabidopsis*. Two copies, *MdCOL1* and *MdCOL2*, encoding *CONSTANS-LIKE (COL)* proteins were isolated from cultivar 'Fuji' and their expression patterns suggest that these genes play an important role in reproductive organ development (Jeong *et al.*, 1999). Two orthologues of the *LFY* homologous genes (*AFL1* and *AFL2*) were isolated from cultivar 'Jonathan' (Kotoda *et al.*, 2000). Finally, two apple homologs of the *Arabidopsis FT* and two *TFL1* encoding genes have also been isolated for apple (Mimida *et al.*, 2009; Kotoda *et al.*, 2010).

Investigations on the genetic determinants of alternate bearing in apple were performed using trees issued from the bi-parental cross between 'Starkrimson', a strong biennial bearer, and 'Granny Smith', a regular bearer (Guitton *et al.*, 2012; Durand *et al.*, 2013, 2017). The number of inflorescences and yield-related traits exhibited the highest genotypic effect (Guitton *et al.*, 2012). Around 50 % of the phenotypic variability for biennial bearing was explained by quantitative trait loci (QTLs) on linkage groups LG4, LG8, and LG10 (Guitton *et al.*, 2011). These QTLs were collocated with floral integrator genes, meristem identity genes and gibberellin and auxin oxidase genes. QTLs for branching intensity were co-located with QTLs for biennial bearing, flower and fruit production on LG1, LG4 and LG13. A QTL for mean internode length of proleptic axillary shoots was co-located with a biennial bearing QTL on LG4 (Guitton *et al.*, 2012)

A study of RNA transcript expression between heavy fruiting (ON) and non-fruiting (OFF) adult apple trees aimed to identify candidate genes and processes involved in FI (Guitton *et al.*, 2016). Their results suggest that different flowering pathways may be involved in the control of FI in mature apple trees. The authors showed that genes sensitive to changes in nutritional and redox status could be involved as part of the autonomic pathway. They also suggested that genes associated with GA metabolism, circadian clock, and ambient temperature could be involved. The main hypothesis that emerged from their results is that the unfavorable redox effect and the nutritional state of the buds can induce a hormonal response that can in turn activate key regulators of SAM fate.

3. Modeling approaches of developmental processes in functional structural plant models

3.1. General consideration

Models describe complex systems by synthesizing knowledge. They can be used as predictive tools by simulating the impact of exogenous variables or can be used to test hypotheses to understand the implication of underlying processes on whole system behavior or some emergent properties (Marcelis *et al.*, 1998). In the domain of plant science, a model can be based on statistics applied to a set of experimental data (empirical modeling approach) or on biophysical laws aiming to reproduce the main processes involved in plant functioning (mechanistic approach). Models in plant science and more particularly in agronomy usually aim to simulate yield components variation as a decision support tools for practical management decisions in the short-term (e.g. watering scenario) or longer terms (e.g. planting density). For modeling plant development and functioning, models can be classified depending on whether they only focus on the processes such as radiation use/interception efficiency (process-based models, PBMs) or simulate the complex effects/feedback between physiological processes and architecture (functional structural plant models, FSPMs). PBMs usually describe plant development according to light interception, conversion of light into biomass and allocation of carbon and nitrogen allocation (Sievänen *et al.*, 2000) at the scale of individual plants (Heuvelink, 1995; Marcelis *et al.*, 1998) or populations (Battaglia and Sands, 1998; Pretzsch *et al.*, 2008). These models are widely used in agriculture and are able to predict

the production of crops and trees by taking into account abiotic factors like temperature, light, water or nutrients. For example, in fruit trees, the MaluSim model is used as a tool to help optimizing fruit thinning procedures by simulating natural apple fruit growth and abscission under different climatic variations (Lakso *et al.*, 1991). Usually, plant representation in that type of model is quite simplistic. Plants or crops are represented as a set of compartments (fruit, leaves, stems) without accounting for the topological connections between organs and plant geometry (Vos *et al.*, 2007).

FSPMs are models that take into account effects or interactions between physiological functions of organs during development of plant (Hanan and Prusinkiewicz, 2008). Leaf photosynthesis, transpiration, carbon allocation or hormonal fluxes are among the most important functions that can be simulated in FSPM. To reach this modeling objective, these models offer more detailed architectural representations of the plant than PBMs (Vos *et al.*, 2007). FSPMs have been applied to many species, annuals such as rice (Luquet *et al.*, 2006), wheat (Barillot *et al.*, 2019), tomato (Dong *et al.*, 2008) for instance and perennials such as rose (Buck-Sorlin *et al.*, 2011), kiwi (Cieslak *et al.*, 2011), peach (Allen *et al.*, 2005) and apple (Costes *et al.*, 2008). FSPMs are suitable for analyzing problems in which the spatial structure of the system is an essential factor contributing to the explanation of the behavior of the system of study (Vos *et al.*, 2007). For example, representing architecture is essential when dealing with light interception in apple trees. Such an impact of architectural traits has been tested with sensitivity approach and reveal the major impact of architectural traits like leaf area, internode length, branching intensity on light interception estimated through STAR values (Han *et al.*, 2012; da Silva *et al.*, 2014). In addition, representing plant architecture can be also crucial when dealing with endogenous processes (hormonal fluxes, carbon allocation) that can locally modify organ or meristems morphogenesis (e.g. Prusinkiewicz *et al.* 2009 for the simulation of apical dominance by auxin fluxes or Buck-Sorlin *et al.* 2007 for Barley morphogenesis depending on GA and light perception by phytochromes).

Boundaries between PBM and FSPM are not precisely established and intentions of coupling them have already been proposed by researchers (DeReffye *et al.* 2009) in a way to improve yield prediction. The GreenLab model (Yan *et al.* 2004) provides an example of such ambiguous boundaries. In GreenLab, as for other PBMs, the biomass emanates from a common pool and is directly related to the leaf area index and light use efficiency. Biomass allocation occurs between organs depending on sink strength, only without any description of the carbon transport within the structure. On the other hand, as is the case for FSPMs, it simulates the dynamics of the architecture evolution and organs appearance and growth according to environmental conditions based on the concept of physiological age to simulate growth variability between the different types of organs.

3.2. Available modelling languages and platforms

FSPMs rely on mathematical formalisms that describe plant architectural development. These formalisms have been described in different programming data structures such as strings of plant modules in L-Systems (Lindenmayer, 1968), multi-scale representations (MTG) (Godin and Caraglio, 1998) and graphs (XL-graphs) (Hemmerling *et al.* 2008). L-systems (Lindenmayer, 1968) consist of a set of rules running through strings. Additionally, a geometric interpretation was included through turtle geometry to model plant structures from the L-systems. The turtle can be defined as a 3-dimensional Cartesian coordinate system that can be moved and turned, assigning a specific location and orientation within every time step (Prusinkiewicz *et al.*, 1993). From several years, L-Systems have been complemented to introduce development rules not depending only on predetermined ontogeny but also on endogenous “signals” (Cieslak *et al.*, 2011) moving within the structure (based on the concept of context sensitive L-Systems) or exogenous conditions (Da Silva *et al.*, 2011).

MTGs allow the topological description of a plant and can contain features of organ properties. The multiscale nature of MTGs lies in possible different choices of decomposition of the plant into larger or smaller components (Godin, 2003). This formalism was firstly develop to provide an innovative way to describe and analyze plant architecture based on observations or measurements (Costes *et al.*, 1998) but it

is used nowadays as the basis for simulating physiological processes (e.g. water relationships within the plant and transpiration (Albasha *et al.*, 2019) or fungal epidemic development, Garin *et al.*, 2014).

An alternative approach towards the development of plant models was the establishment of “Relational growth grammar” (RGG), accompanied by a corresponding programming language, the XL language (eXtended L-system language) (Buck-Sorlin *et al.*, 2005). The XL-language is an extension of the Java programming language incorporating the graph- or rule-based features necessary in L-systems (Kniemeyer, 2008).

Different software and platforms for FSP modeling purpose in plant biology are available and most of the softwares are usually associated with a modeling language. These platforms contain many libraries used to simulate some plant growth or functional processes such as light interception, photosynthesis, or Markovian models from simulating developmental processes. L-Studio is the oldest platform. L-Studio is based on L-systems and supports the L+C language, which is the C++ language, extended to interpret L-systems. GroIMP (Growth Grammar-related Interactive Modelling Platform) is based on relative growth grammars (RGG) and uses the XL-language. Other examples are the open-source platform OpenAlea (Pradal *et al.*, 2008). OpenAlea relies on Python and uses a visual programming interface (VisuAla) and tools dedicated to plant modelling. It makes use of the MTG formalism to describe and simulate plant architecture but have also the possibility to integrate L-Systems through L-Py, which is a new implementation of the L-System formalism in Python (Boudon *et al.*, 2014). This platform also integrates tools for visualization or modeling (PlantGL, Pradal *et al.*, 2009), or dedicated models or modules for simulating light interception (Caribu for instance, Chelle *et al.*, 2004) or photosynthesis (RATP model, Sinoquet *et al.*, 2001). AMAPStudio (Griffon and de Coligny, 2014) could be also considered as a modeling platform, which integrates methods for architecture exploration based on the MTG formalism.

3.3. Description and acquisition of plant architecture

Plant structure may be described through several representations considering its topology and geometry (Le Roux *et al.*, 2001). Topology describes the physical connections between plant organs (mainly branching, succession) while geometry deals with their dimensions, including shape, size and orientation, and their location in a 3D coordinate system. For plant representations, the structure can be decomposed into inter-connected units described at different scales. The elementary plant unit, called metamer, consists of an internode, a node, a leaf and possibly flowers or fruits, and represents the smallest scale of organization of plant architecture according to White (1979). A succession of metamers without interruption of growth constitutes a growth unit (GU) and a set of growth units forms an axis, and all the axes form the tree (Costes *et al.*, 2006). Godin and Caraglio (1998) proposed a formalism for the description of plant topology. The representation of plant architecture at different scales (metamers, axis, branch, tree...) gives rise to the Multiscale Tree Graph (MTG) developed for topological analysis and presented before (Figure 7).

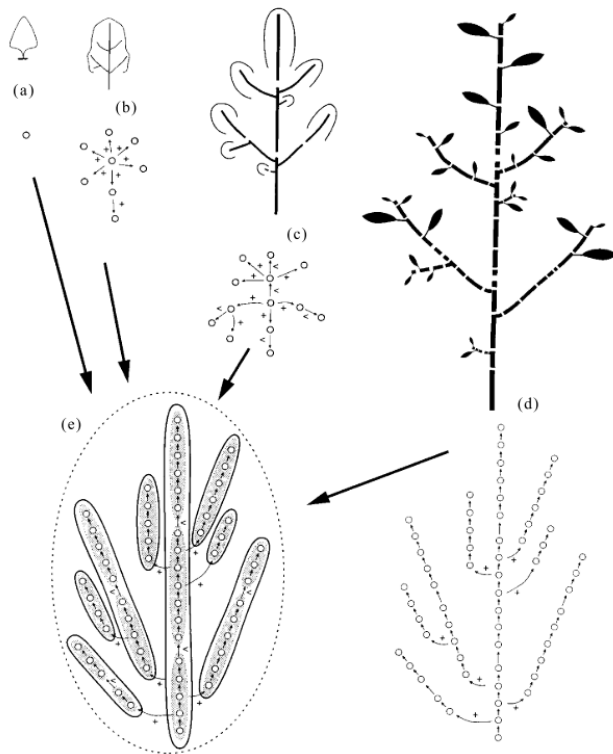


Figure 7. A tree at different scales of perception (a) Tree scale, (b) axis scale, (c) growth unit scale, (d) internode scale, (e) corresponding multiscale tree graph. Figure from Godin and Caraglio (1998).

Usually in the MTG formalism, axis of order 1 is the trunk, axes of order 2 are the branches connected to the trunk, axes of order 3 are the growth units and axes of order 4 are the internodes. The trunk and branches set during the previous years are represented as segments and annual growing shoots can be composed of one or several growth units (polycyclic). An axis is then a combination of segments (GUs older than one year) and growth units. For each scale, the topology relationship between organ can be described through succession or branching relationships between components (Godin *et al.*, 1999). Besides topology, quantification of organ shapes and orientations is essential from an architectural and functional point of view. MTGs can include geometrical characteristics for each element as additional features, i.e. their shape, dimensions and angles (Godin and Caraglio, 1998; Godin *et al.*, 1999). The space coordinates of these elements can be measured with 3D reconstruction techniques.

Different methods and tools have been developed to measure the spatial orientation and shape of plant organs, either with simple equipment such as rulers and protractors (Takenaka *et al.*, 1998) or obtained from digitizers that record directly the 3D points of interest, which can be directly added to MTG structures (Sinoquet *et al.*, 1997). Among the existing methods of structure reconstruction, digitizing relies on using a 3D-digitiser (Polhemus) that consists of an electronic unit, a receiver, a transmitter that generates a low frequency magnetic field and a power supply. The data acquisition starts by recording the base of the trunk as the first point (order 1) and from this order start the decomposition to branching point (order n) themselves decomposed to other segments (order n+1) and so on until the complete description of all the tree components. During this step, Cartesian coordinates (x, y, and z) and Euler orientation angles (azimuth, elevation, and roll) of the receiver are determined (Sinoquet *et al.*, 1997). The main limitations of the 3D-digitiser is that other magnetic sources or large metallic objects can interfere with its magnetic field and have to be removed from the active volume around the transmitter. In addition, this method can be time consuming and is difficult to apply to large plants. However, simplification on the number of digitized points can reduce the measurement time.

A more recent method for architecture data acquisition is terrestrial laser scanning (TLiDAR). TLiDAR has been shown to acquire accurate information rapidly on objects related to plant topology and organ geometry in a three-dimensional (3D) space (Côté *et al.*, 2009; Lecigne *et al.*, 2018). In apple trees, initial work has been performed to develop a high-throughput methodology to extract architectural traits on large population of individuals (Coupel-Ledru *et al.*, 2019). Although such methods are relevant to extract whole tree architectural features (volume, light interception, STAR) they seem difficult to use to extract the fine topological reconstruction needed for running most of FSPMs.

3.4. Modeling plant architecture

The use of the architecture description methods and formalisms under the corresponding modeling environments enable simulating in-silico 3D representations of plants. These representations can be used as a support to study the relationships between plant structure and function. When plant architecture is described at a given time models are static and when they include an evolution with time they are called dynamic (Prusinkiewicz, 2004) and allow simulating the development of architecture over time with different time steps (Figure 8). Static models can be based directly on 3D measurements or can use other sub-models to represent complete 3D structure from incomplete or local measurements of plants. In that case, empirical models based on allometric relationships are used to infer specific architectural variables at different scales of plant organization (e.g. Perez *et al.*, 2016).

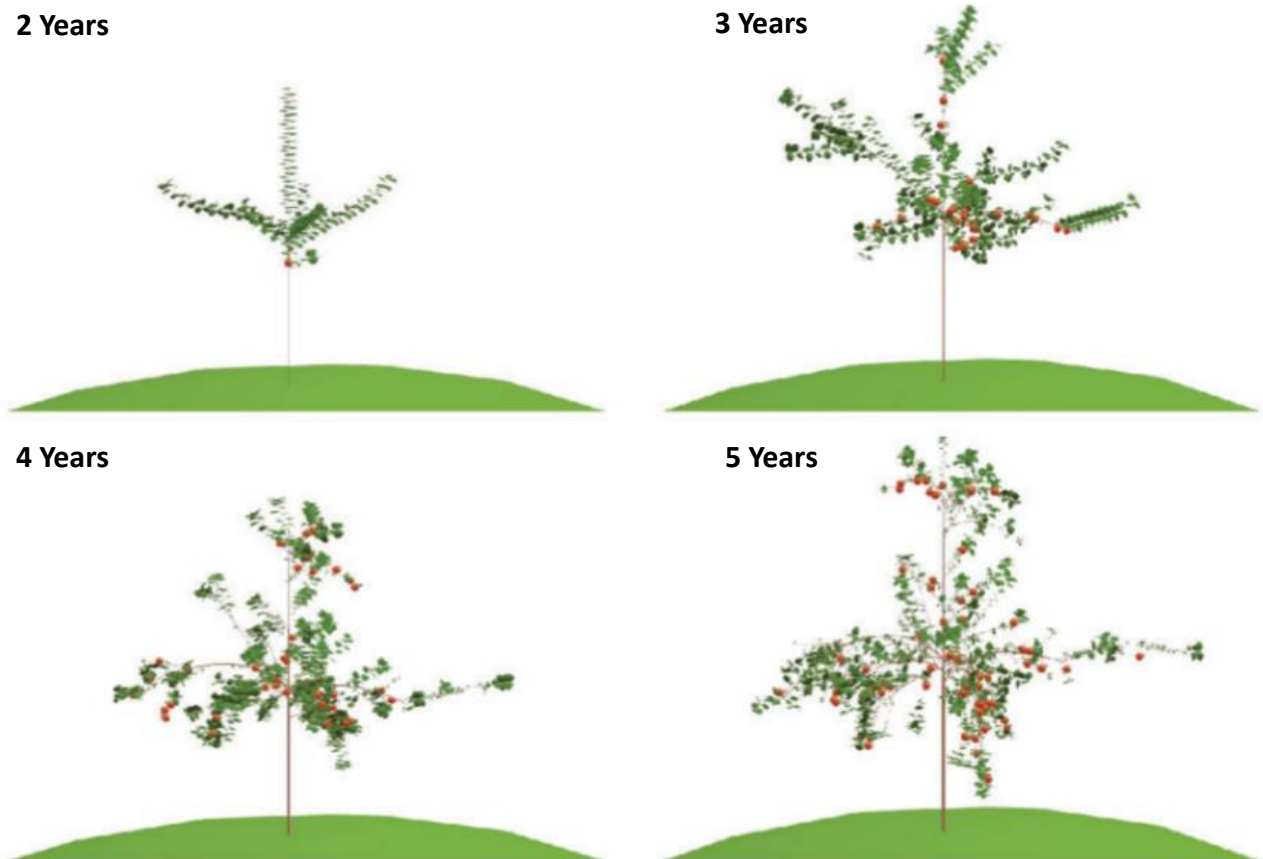


Figure 8. Year-to-year changes of a typical Fuji apple tree simulated using default values of model parameters. The tree is visualized each year from the second to fifth year of growth, just before harvest time. Figure adapted from Costes *et al.* (2008).

In apple, an FSPM model was built around ten years ago (MAppleT) with the aim of simulating growth and architecture from planting. This model simulates apple tree architecture evolution over the time by combining stochastic models to simulate plant topology and a bio-mechanistic model for geometry (Costes *et al.*, 2008). A first-order Markov chain with four state (short, medium, long and floral GUs) models the

within and between years succession of GUs along axes (Figure 9). A hidden semi-Markov model jointly models shoot length within each category and its branching structure. The branching model takes into account the transition probabilities between zone, the occupancy distributions of each zone in order to model the lengths of branching zones and observation distributions, to model the branching type composition within each branching zone. The shape of the axis scale was calculated at the metamer with a biomechanical model that takes into account dynamics of primary, secondary and fruit growth between successive years. The shape of the axis depends on gravity and a combined effect of phototropism and negative gravitropism (orthotropic force). In MappleT, starting dates of processes like primary and secondary growth were defined as specific dates in a year. Specific chronology was also defined for individual organs at the metamer scale, based on observations. In each GU category, new metamers are produced with a plastochron of three days. Metamer elongation was set to ten days. Leaves reach their maturity after twelve days of growth, flowers last for ten days and, if they become fruit, the fruit lasts until harvest (approximately 150 days) (Costes *et al.*, 2008). This model proves its ability to represent apple tree architecture for the Fuji Cultivar and was used in subsequent studies as a basis to evaluate the sensitivity of light interception to architectural parameters (Da Silva *et al.* 2014) or for simulating biomass allocation between organs (Pallas *et al.* 2016). Nevertheless, even though very informative this model is only based on empirical data and does not integrate most of the climatic factors (water stress for instance) or endogeneous processes (hormonal fluxes) that can modulate plant development over years.

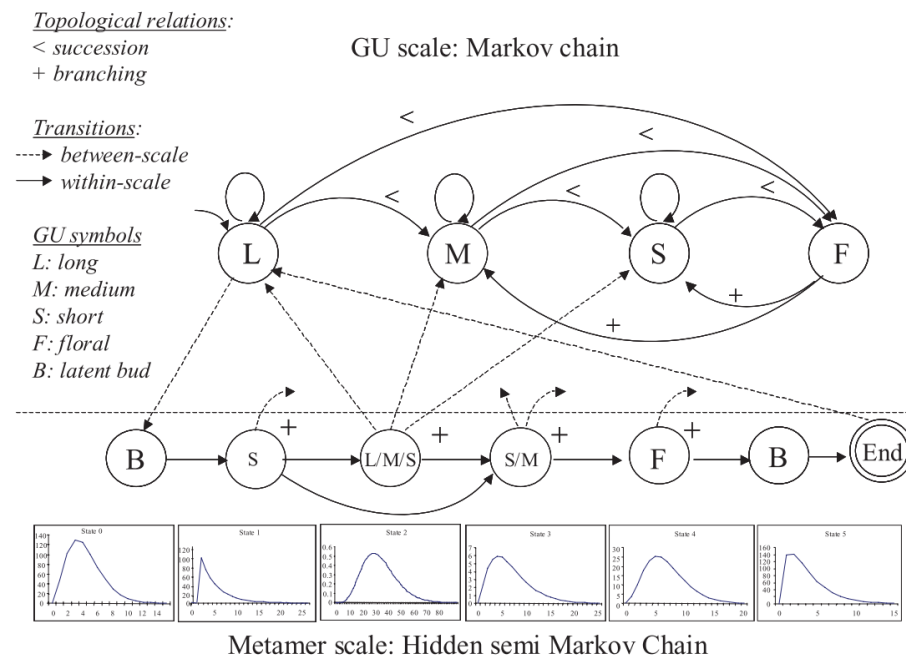


Figure 9. Hierarchical stochastic model representing tree topology. Successions and branching between entities are represented by '<' and '+', respectively. At the growth unit (GU) scale, the succession of GUs along an axis is modelled by a 4-state Markov chain. The four 'macro-states' are long (L), medium (M), short (S) and flowering (F) GU. The long and medium macro-states activate Hidden semi Markov Chains (HSMCs) with between-scale transitions (dotted arrows). The figure shows only the activation from the long GU macro-state. HSMCs model the GU branching structure at the metamer scale, as a succession of zones with a specific composition of axillary Gus (for instance a mixture of long, medium and short axillary GUs is observed in state 2). The HSMC ends with an artificial final state which gives control back to the pending macro-state. Likewise, for each axillary position, between-scale transitions give the control back to the macro-state model corresponding to the type of axillary GU generated by the HSMC (the figure illustrates only these transitions from HSMC state 2). Figure from Costes *et al* (2008).

3.5. Modelling light interception and photosynthesis

Plant architecture has an influence on light interception, as leaf distribution within the plant and leaf area density control the quantity of light intercepted (Duursma *et al.*, 2012). Leaf distribution, which depends on shoot number and internode length, and leaf insertion angles on shoots can modulate leaf aggregation, self-shading and consequently light interception (Dauzat *et al.*, 2008; Parveaud *et al.*, 2008).

To simulate light interception on 3D mockups, different methods are commonly used for estimating the radiative balance of plant or canopy elements ranging from simple projections of plant elements in different directions, radiosity or ray tracing (Monte Carlo Ray Tracing). The radiosity method is based on mutual light exchange factors between all the canopy components (Chelle and Andrieu, 1999). The interception properties can be deduced from the observed leaf area of a given direction, corresponding to the intercepted radiation in that direction (Adam *et al.*, 2004). Ray tracing models stochastically simulate light rays coming from light sources and rays that are scattered within the canopy to estimate the absorbed irradiance of individual leaves (Buck-Sorlin *et al.*, 2011; Cieslak *et al.*, 2011). These approaches make it possible to calculate the light intercepted by a canopy represented by a set of triangles. Other approaches calculate the light interception on representations at different scales as a set of voxel elements and using projections of plant elements in different directions (turtle model) for diffuse light and projection according to solar position in the sky for direct light. In this case, the calculation of the light interception is made with a hypothesis of homogeneity within each element (turbid medium). Organ spatial distribution is then reduced to a density of leaves with a distribution of leaf angles (Sinoquet *et al.*, 1991).

Photosynthesis at the leaf scale can be simulated by different types of models either quite empirical (for instance: non-rectangular hyperbola model (Prioul and Chartier, 1977) or by more mechanistic models such as the biochemical model proposed by Farquhar *et al.* (1980). In the photosynthetic biochemical model, leaf photosynthesis can be limited either by the activity of Rubisco or by the electron flow in the Calvin cycle (Balandier *et al.*, 2000; Adam *et al.*, 2004). The effect of leaf nitrogen content, leaf temperature, and internal CO₂ concentration, can also be included in biochemical photosynthesis models (Sinoquet *et al.*, 2001).

Photosynthetic activity is strongly associated with the resistance of stomata for CO₂ influx. Therefore, these models are coupled with stomatal conductance model (Jarvis, 1976; Ball *et al.*, 1987) accounting for the effects of various climatic conditions (VPD, temperature, light intensity).

The RATP model (Sinoquet *et al.*, 2001) allows simulating leaf photosynthesis and transpiration by considering plants as a set of voxels. It integrates the Farquhar model to compute potential photosynthesis, the Jarvis model for computing stomatal conductance and an energy balance for simulating leaf temperature and its retroaction effect on photosynthesis and stomatal conductance.

3.6. Modelling carbon allocation

Carbon allocation throughout the plant has been considered by Lacoite (2000), as mass-flow allocation, assumed in Münch theory. Assimilates are actively loaded into the phloem sieve tubes in sources and unloaded in sinks, generating an osmotic pressure gradient that drives the mass flow within the phloem tubes (Lacoite 2000, Ryan and Asao, 2014). Carbon translocation is a simple passive gradient process which is driven by active loading and unloading of the phloem (Deleuze and Houllier, 1997).

Some models that mock mechanistically this mass flow and the relationships between xylemian and phloemian tissues (Minchin and Lacoite, 2005; Thorpe *et al.*, 2011). Nevertheless, this approach requires complex calibration and has been only calibrated so far on simple plant architectures without any branching [two sources, three sinks (Thorpe *et al.*, 2011). In these models, assimilates quantities assigned to the growth can be controlled by the lighting conditions and the quantity of leaves in the tree (Perttunen *et al.*, 1998) or by the effect of cultural practices like thinning and pruning (Lescourret *et al.*, 2011).

Three main classes of simplified models have been proposed for simulation of carbohydrate/assimilate allocation (Lacoite, 2000). Empirical models are models where allocation is not driven by mechanisms but

by simplified allocation rules which are estimated from experiments (i) by weighting organs at different time-steps, (ii) labelling carbon flux from source sink or (iii) by estimating the growth rates of the different sinks. For instance, the model ECOPHYS (Rauscher *et al.*, 1990) is based on allocation rules directly derived from C labelling experiments. The main limitations of this type of models is that the allocation coefficients are valid only over a limited range of environmental conditions namely those on which measurements were performed (Lacointe, 2000). Growth-rules models are empirical models that can incorporate allocation rules such as the pipe model for cambial growth where there is a functional balance between the growth of roots and aerial parts. Transport-resistance models are more mechanistic models and describe assimilate movements as a diffusive process driven by concentration gradients across resistive pathways (Balandier *et al.*, 2000; Allen *et al.*, 2005; Cieslak *et al.*, 2011). Carbon allocation to each organ thus results from the distance to the producing source of carbon, to the resistance within the phloem pathways and from the capacity of the organ to extract assimilate (Allen *et al.*, 2005; Génard *et al.*, 2008). Carbon demand can also be calculated at the organ scale and allocated according to processes priorities (maintenance before growth) and organs (shoot growth before fruit growth) (Lescourret *et al.*, 2011).

The last class of models are “source-sink” models. In these models, assimilate fluxes and allocation are assumed to depend on sink strength or demand, defined as the respective ability of the different sinks to import available assimilates from the sources. Sink demand refers to the carbon needed by sinks to ensure their full growth. Carbon movements from sources to sinks may assume that distance between sources and sink does not matter and that each sink has an equal access to a common assimilate pool (e.g. Yan *et al.* 2004, Luquet *et al.* 2006). It can also include an effect of distance in the equation driving source-sink allocation (Balandier *et al.* 2000, Lescourret *et al.* 2011, Pallas *et al.* 2016). Models assuming a common assimilate pool assumption have been mainly used for small annual plants (Heuvelink, 1995; Luquet *et al.*, 2006). Models integrating a “distance” have mainly been used on more complex plants such as fruit trees. In such models the effect of distance can be modulated by a resistance or friction parameter that is usually estimated using model fitting procedures (Lescourret *et al.* 2011) as the best value for representing organ weight variability within the trees. When source-sink models integrate distance effect, they are close to the transport-resistance models. However, they do not account for the number and types of organs separating each source and sink but their distance only. Furthermore, the different models used for simulating carbon can consider different scales of plant organization as the elementary units exchanging carbon. Such scales range from the individual metamer (DeJong and Grossman, 1994; Allen *et al.*, 2005), growth unit (Balandier *et al.*, 2000), fruiting unit (Lescourret *et al.*, 2011) to branches and complete plants (Lakso and Johnson, 1990, Kang *et al.*, 2008).

More recently in apple tree, a carbon allocation model has been developed (Reyes *et al.*, 2019). In this model, the formalism used for simulated carbon allocation was directly adapted from the SIMWAL model. In this model, carbon allocated to a sink (F_{ij} , eq.1) depends on the carbon available in the supply (ACP_i) and the sink carbon demand ($Demand_j$) and is inversely related to the distance ($dist$) between source and sink and to a sap friction parameter (h).

$$F_{ij} = \frac{Demand_j \times f(dist_{ij,h}) \times ACP_i}{\sum_{k=1}^n Demand_k \times f(dist_{ik,h})} \text{ (eq. 1)}$$

The originality of this model is due to the multi-scale approach used to allow computing biomass allocation at different user defined scales of plant organization (branch, axis, GU, metamers). To reach this objective the model makes use of the multi-scale structures provided in the MTG formalism within the OpenAlea platform.

The model was able to represent the effects of competition for carbon assimilates on fruit growth variability. The model also reveals the major influence of the considered plant scale to get an adequate estimation with the best estimation observed when allocation was performed at the metamer scale. This result reveals the lack of homogeneity in organ mass within each specific entity while such hypotheses are used in some models such as Qualitree.

3.7. Retroaction between carbon allocation, trophic competition and plant development

In addition to a set of environmental factors (temperature, soil water content, relative air humidity) which can have a direct impact on plant development and growth, plant morphogenesis is strongly dependent on the competition between growing organs for photo-assimilates and reserves. Such competition can give rise to the concept of trophic competition for carbon whose intensity can drive a large part of plant phenotypic plasticity. In FSPM the intensity of trophic competition is usually computed as the ratio between source activity (determined by photosynthetic activity and eventually reserve mobilization) and sink demand depending on sink number and age or developmental stage (e.g. Luquet *et al.*, 2006, Yan *et al.*, 2004).

In some models carbon supply can be simulated as a common pool by using a function derived from the Beer-Lambert law formalisms at the scale of the whole plant, while demand is considered simulated at the level of each organ and then grouped together to provide the demand for the whole plant (Luquet *et al.*, 2006). The comparison of supply and demand balance at the plant level makes it possible to compute a whole plant state variable (the index of trophic competition) that can in turn affect several developmental processes. Affected developmental processes can be the tillering in ECOMERISTEM model (Luquet *et al.*, 2006) or the rhythm of appearance of the organs, the probabilities of branching or the fruit set in GREENLAB (Kang *et al.*, 2008; Mathieu *et al.*, 2008). In both models, development is considered as a global reaction without taking account of spatialization.

The ability of a meristem to modulate its development according to the carbon status of the plant has been confirmed by a number of experimental results showing the implication of genes for sugar signaling in the regulation of meristem activity (Gibson, 2005; Ji *et al.*, 2005).

Nevertheless, other studies pointed out the necessity to account for the spatial variability in this feedback loop between trophic competition and development. For instance, Pallas *et al.* (2008) showed that trophic competition affects the rate of secondary axis developmental but also that this effect is stronger for the secondary axis closed to the bunches. Such results underline the necessity to account for the spatial variability in within tree trophic competition when dealing with its effect on developmental processes. In apple trees, large within tree variability in developmental processes including flowering exists suggesting local regulation of the source-sink relationships. First experimental studies have been performed to analyze the scale of plant development at which growth and development processes are regulated (Pallas *et al.*, 2018). This study show that axis growth and flowering seem under the influence of local trophic competition at shoot or branch scale, but no modeling work has been carried out to analyze further or simulate these processes is known. Previous works on apple tree (Pallas *et al.*, 2016; Reyes *et al.*, 2019) developed source-sink models on apple trees to simulate organ growth (shoot and fruit) but these models runs on empirical structures or on a structure with a pre-determined growth calendar and did not integrate any feedback on development in the current growing season or over years.

3.8. Modeling hormone transports in plant and their consequences on plant development

Hormone or signal fluxes within plants have also been modelled, especially for the simulation of basipetal auxin transport and its impact on bud growth (Prusinkiewicz *et al.*, 2009; Renton *et al.*, 2012).

Auxin flux was modeled by Prusinkiewicz *et al.* (2009) using the L-System formalism. This model takes into account the effects of plants mutants for branching and dwarfism and decapitation manipulations to explain active auxin transport by the canalization hypothesis and branching habits. The rate of active transport driven by PIN proteins in the cell membrane directs polar auxin transport between different metamers. This model explains that the apical dominance and bud activation observed in Arabidopsis depends on the auxin transport along the stems and the competition of different auxin sources. Active and passive transport models have also been proposed for auxin transport at longer distances in pea by using L-systems (Renton *et al.*, 2012). The first simple model integrates a segmented based compartment where stems are composed of inter-connected compartments and auxin is transported basipetally in shoots by an active transport mechanism. The second model simulates a mechanistic intracell transport. In this model, within

the cell, auxin is assumed to move passively by diffusion. At the boundaries of the cell, auxin is carried by an active transporter (PIN) to get exported.

In apple tree and in the case of the within-tree FI determination, a model has been proposed to determine SAM flowering fate depending on ratios of promoting or inhibiting hormones (Pellerin *et al.*, 2012). In the model, tree architecture is simplified and described with simple fractals (Figure 10). SAMs are assigned randomly on a tree structure on branches of different lengths.

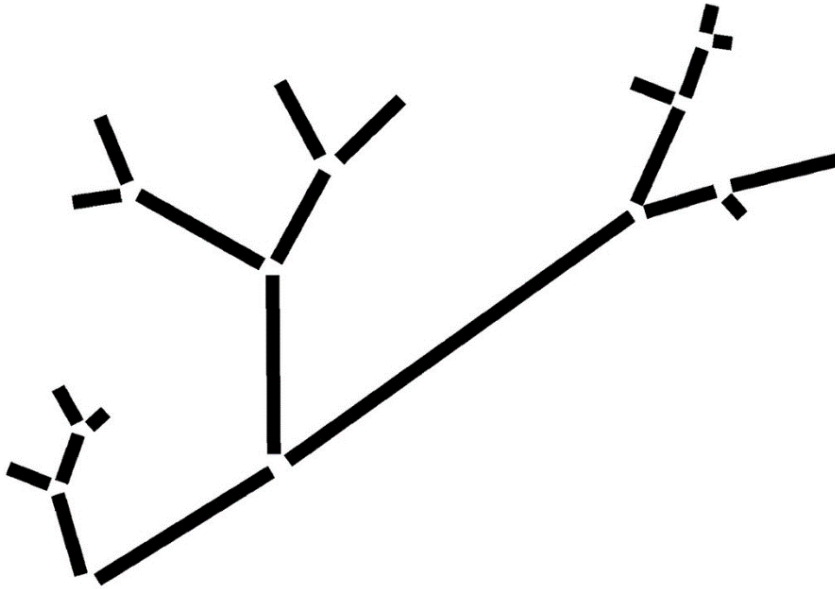


Figure 10. A simulated branch assembled with 22 growth units, used in Pellerin model. Figure from Pellerin *et al.* (2012).

Seeds and leaves are sources inhibiting and promoting hormones exported to SAMs. The model simulates SAM fate (flowering or not) depending on its spatial position within the structure. Depending on distance and resistance parameters, hormone concentration decreases as they spread from their source. SAM fate is determined depending on the amount of hormones/signals reaching it (inhibiting and activation) and on a critical value parameter below which FI is inhibited. Another generic model for inhibiting signal flux in basipetal and acropetal directions has been developed based on the L-system formalism (Figure 11) (Pallas, *et al.* 2016). Signal flux and partitioning have been simulated on simplified branching structures and on tree structures generated by the MappleT model. In the model, fruit are considered as sources of inhibiting signal that is transported both in basipetal and acropetal directions. The model assumes a passive diffusion of the signal with a resistance parameter to modulate the effect of distances between sink and sources. First simulations with this model shows its ability to simulate FI variability resulting from shoot length and type, for reproducing the impact of crop load on FI and different bearing pattern (regular, biennial) that could be associated with genotypic variability.

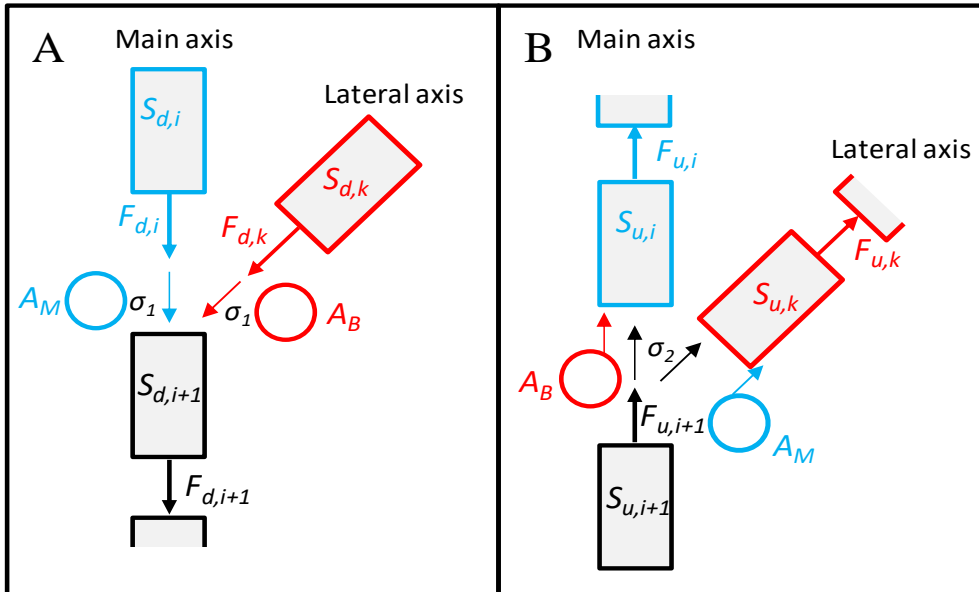


Figure 11. Compartment structure of the signal transport model for the simulation of basipetal (A) and acropetal (B) fluxes. F_d and F_u represent the basipetal and acropetal fluxes, respectively and S_d and S_u represent the amount of inhibitory signal in each metamer coming from basipetal and acropetal fluxes, respectively. A_M and A_B are the amounts of basipetal inhibitory signal that are “stored” at the branching point during the simulation of basipetal flux and reallocated during the simulation of the acropetal flux. σ_1 is the proportion of inhibitory basipetal signal that is “stored” at the branching point and σ_2 is used to split the acropetal flux between the main and lateral axes. Figure from Pallas *et al* (2016).

3.9. Representing genotypic diversity in models

Genotypic variability in crop model or FSPM are represented through a set of parameter values, which change value depending on genotypes. In crop models, these parameters are usually associated with phenology, allocation, leaf area expansion, light interception use efficiency and/or traits capturing responses to environmental factors (water stress, temperature...) (Brisson *et al.*, 2003; Hammer *et al.*, 2010; Tardieu, 2010; Casadebaig *et al.*, 2011). Integrating genotypic variability in FSPM has been less frequently performed mainly due to the complexity of evaluating model parameters such as architectural features on a large set of individuals. In apple tree and more precisely in the MAppleT model, some genotypic variability has been implemented in the model related to architectural traits such as internode length, branching intensity, individual leaf area or by using different trunk sequences associated with the observed variability in bi-parental population. In that context, Da Silva *et al.* (2014) explored the effects of this architectural traits on light interception estimated through STAR (silhouette to leaf area ratio) through a sensitivity analysis of the model (Willaume *et al.*, 2004; da Silva *et al.*, 2014)

Values of genotypic parameters are generally directly derived from experimental results. Parameters can be estimated directly from architectural (digitizing, Massonnet *et al.* 2007, T-Lidar, Coupel-Ledru *et al.* 2019 for FSPM in apple trees) and from morphological measurements (Segura *et al.*, 2008). For several years, high-throughput phenotyping platforms have made it possible to quantify the genetic variability and values of model parameters more associated with the response of plants to environmental stresses. These plant phenotyping platforms allow the measurement of plant traits in controlled conditions to analyze mainly drought and high temperature effects on a wide variety of species (corn, wheat, vine, apple tree and sorghum) (<http://www6.montpellier.inra.fr/lepse/M3P>). For example, the PhenoArch platform has been used to characterize the genotypic variability of architectural and functional traits in a collection of individuals in apple trees (Lopez *et al.* 2015).

In a model, genotypic parameters can be directly associated to phenotypic values or to genetic polymorphisms associated with the variability in the parameter. One of the first pioneer studies was performed by Chenu *et al.* (2009) on maize who integrate quantitative trait loci controlling leaf and silk elongation into a crop model to simulate crop growth, water use, and grain yield in different and contrasted weather conditions. More recently, in apple tree, an approach combining the MappleT model with genetic determination of architectural parameters aimed at modeling apple tree architecture of 1-year old apple trees belonging to a bi-parental population (Migault *et al.*, 2017). This approach consisted in integrating genetic polymorphism markers (SNPs) of some parameters (internode length, branching probability over time, individual leaf area) to simulate integrative traits such as total leaf area or trunk length.

Other parameters cannot be measured directly (hidden parameters) and are thus estimated indirectly by model inversion, i.e. by fitting the model to a target files of observed values. Such model inversion procedures have been performed in many studies by the GreenLab model or model derived from GreenLab (Mathieu *et al.*, 2009) which combine model parametrization procedures. This optimization tool used Generalized Least Square Method (GLSM) (Guo *et al.*, 2006) to determine hidden parameters such as organ sink strength or parameters related to the sensitivity of organogenesis processes to trophic competition (Pallas *et al.*, 2011). Such an approach appeared of major interest to extract physiological knowledge (heuristic approach) by using the model to quantify complex mechanisms and complex interactions that cannot be directly derived from experimental results, only.

III. Impact of within-tree organ distances on floral induction and fruit growth in apple tree: implication of carbohydrate and gibberellin organ contents.

This chapter corresponds to a scientific paper already published in Frontiers in Plant Science.

<https://doi.org/10.3389/fpls.2019.01233>

1. Résumé

Chez les plantes, la croissance des organes et le développement de la plante résulte de régulations complexes entre l'ensemble des organes. Nous avons cherché à étudier la distance à laquelle opère les interactions entre organes sur l'induction florale et la croissance des fruits ainsi que la contribution relative de la variation intra-arbre du contenu en carbohydrates et en hormones sur la variabilité intra-arbre de ces processus, dans le cas d'un arbre fruitier. Des manipulations du nombre de feuilles et de fruits ont été effectuées sur deux années sur la variété de pommier « Golden delicious », à l'échelle des pousses ou des branches ou sur un côté des arbres en forme de Y. Pour chaque traitement, la proportion d'induction florale et le poids moyen des fruits ont été enregistrés. La teneur en gibbérellines dans les méristèmes apicaux des pousses, la photosynthèse et les concentrations de carbohydrates non structuraux dans les organes ont été mesurées. L'induction florale était favorisée par la présence de feuilles et l'absence de fruits, mais n'était pas associée au contenu en carbohydrates non structuraux dans les méristèmes. Cela suggère une action combinée de signaux activateurs et inhibiteurs provenant des feuilles et des fruits, et impliquant des gibbérellines. Toutefois, ces signaux n'agissent qu'à courte distance, car la présence de feuilles et/ou de fruits à de longues distances n'a pas eu d'effet sur l'induction florale. À l'inverse, la croissance des fruits a été affectée par la présence de feuilles, même sur de longues distances lorsque les demandes de puits étaient déséquilibrées au sein de l'arbre, suggérant un transport à longue distance des carbohydrates. Nous avons ainsi clarifié l'effet des distances entre les organes, et donc en partie leur degré d'autonomie sur l'induction florale et la croissance des fruits.

2. Abstract

In plants, organs are inter-dependent for growth and development. Here, we aimed to investigate the distance at which interaction between organs operates and the relative contribution of within-tree variation in carbohydrate and hormonal contents on floral induction and fruit growth, in a fruit tree case study. Manipulations of leaf and fruit numbers were performed in two years on 'Golden delicious' apple trees, at the shoot or branch scale or one side of Y-shape trees. For each treatment, floral induction proportion and mean fruit weight were recorded. Gibberellins content in shoot apical meristems, photosynthesis, and non-structural carbohydrate concentrations in organs were measured. Floral induction was promoted by leaf presence and fruit absence but was not associated with non-structural carbohydrate content in meristems. This suggests a combined action of promoting and inhibiting signals originating from leaves and fruit and involving gibberellins. Nevertheless, these signals act at short distance only since leaf or fruit presence at long distances had no effect on floral induction. Conversely, fruit growth was affected by leaf presence even at long distances when sink demands were imbalanced within the tree, suggesting long distance transport of carbohydrates. We thus clarified the inter-dependence and distance effect among organs, therefore their degree of autonomy that appeared dependent on the process considered, floral induction or fruit growth.

3. Introduction

In plants, the determination of organ nature, their development and growth are considered as interdependent. For instance, the position at which flowers develop is linked to the number of nodes developed from the seed (Sachs, 1999). Architectural analyses have revealed a highly structured organization in a wide range of plants, with particular types of organs observed at particular positions and at particular times during ontogenesis (Barthélémy and Caraglio, 2007). This has been demonstrated for instance for the position of reproductive organs in *Quercus ilex* or *Pinus halepensis* (Barthélémy and Caraglio, 2007) or for flower buds along axes in different *Rosaceae* species (Costes *et al.*, 2014a). The interdependence and differential development of organs within plants are assumed to depend on water, carbohydrates, hormones, mineral nutrients, etc. that are transported within the plants. Both the availability of these resources and the total number of competing organs define a developmental and growth context for each organ depending on its position during plant life span. Among these shared resources, carbohydrates have been particularly studied as they are considered as a main limiting factor for organ growth (Grossman and DeJong, 1995) and as a regulator of the transition between vegetative and reproductive phase in plant life (Rolland *et al.*, 2006). In the particular case of fruit trees, the number, position of fruits, as well as their weight at harvest are dependent on the capability of a given meristem to be floral, then of this flower to fruit set, and finally of a fruit to capture resources for its growth.

In fruit trees, the capability of a shoot apical meristems (SAM) to be floral induced is strongly affected by the presence of fruit during the growing season. A first hypothesis explaining floral induction (FI) inhibition in conditions of high crop load is associated with a competition for carbohydrates between meristems and fruit (Monselise and Goldschmidt, 1982). Besides this “carbon” hypothesis, Chan and Cain (1967) have demonstrated that FI is inhibited by seed development through hormones. This hypothesis was confirmed by experiments on seedless apple and pear cultivars suggesting that seeds may inhibit FI, probably by gibberellins (Dennis and Neilsen, 1999). Gibberellins (GA) are considered among the pathways involved in floral induction control in *Arabidopsis thaliana* (Jung *et al.*, 2017). However, their effect is currently considered as inverse in *Arabidopsis thaliana* and in perennial woody plants. Indeed, GA promotes the transition from vegetative to reproductive development of buds in *Arabidopsis* (Wilson *et al.*, 1992), while it is assumed to inhibit FI in fruit trees such as mango (Nakagawa *et al.*, 2012) and apple (Wilkie *et al.*, 2008). GA₁₂ has been observed as the transported GA form moving within the plant through the vascular system in *Arabidopsis* (Regnault *et al.*, 2015). In the apple tree, GA₄ has been assumed to move from fruit to SAM in apple tree (Ramírez *et al.*, 2004). The involvement of GA in FI control was further confirmed by differential expressions of genes involved in the GA biosynthesis pathway (GA_{20ox} and GA_{2ox}) in SAM of apple trees with heavy or low crop loads (Guitton *et al.*, 2016). This study also suggested a context of carbohydrate starvation, in SAM of trees in high cropping conditions. Therefore, the co-involvement of carbohydrate and hormones in FI control appears as an assumption to further investigate. It implies the involvement of several processes: photosynthesis by leaves, transport from leaves to sinks, including SAM, but also the presence of GA in SAM likely the active forms GA₄ and GA₁ (Ramírez *et al.*, 2004). Moreover, leaves may have a dual role in FI control since, in addition to be source of carbohydrates, they are also producing FLOWERING LOCUS T (FT) protein, which is transported to the SAM to activate floral induction in many species, including fruit species (Hanke *et al.*, 2007). Nevertheless, it is currently still unclear at which distance the different “signals” originating from fruit and leaves act on FI in SAM.

Regarding carbohydrates, partitioning from sources to sinks is considered as a function of source supply, sink demand and distances between them (Lacointe, 2000). Nevertheless, in fruit trees there is no clear consensus about the impact of distances between sources and sink on carbohydrate allocation and on their consequences on the existing organ growth variability within the trees. Depending on their strength, i.e. the ability of an organ to import assimilate, sinks can use carbohydrates from nearby or distant sources. Carbohydrates can move at short distances, i.e. from non-fruiting to fruiting shoots (Walcroft *et al.*, 2004; Pallas *et al.*, 2018) to sustain fruit growth or at longer distances, i.e. between branches (Palmer *et al.*, 1991, Hansen 1997). Conversely, authors have suggested that branches can be considered as autonomous (Sprugel *et al.*, 1991). For instance, in shading experiments on walnut, sunlit branches have been observed

to grow faster than shaded ones without any allocation of carbon to distant sinks (Lacointe *et al.*, 2004), thus emphasizing the sink strength limitation to long distance transport. This limitation of long-distance carbon transport has potential impacts on developmental and growth processes. For instance, part-tree thinning of flower cluster has been shown to enhance branch vegetative growth and floral induction in the thinned tree sides (Palmer *et al.*, 1991; Grossman and Dejong, 1998). Similarly, shoot growth and to some extent starch accumulation in woody organs are impacted by fruit proximity (Berman and Dejong, 2003; Castillo-Llanque and Rapoport, 2011). Moreover, carbon transport and allocation change during a season. Indeed, carbon labelling experiments have shown that carbon is allocated from reserves to support new shoot growth in spring (Kandiah, 1979a). At fall, carbon accumulate in leaves moves at long distances to roots to contribute to root growth and storage, before being reallocated to new growth in the next year (Hansen, 1967; Kandiah, 1979b).

In plant, carbon allocation between organs is commonly analyzed through the variations in organ biomass and non-structural carbohydrate (NSC) content. Among the different NSC forms in apple tree, starch, sorbitol and sucrose are the carbohydrates directly derived from the photosynthetic activity, with sorbitol and sucrose being the mobile forms for carbohydrate transport (Escobar-Gutiérrez 1996, Teo *et al.*, 2006). Sorbitol and sucrose are transferred through the phloem to the sinks where they are converted into glucose and fructose (Teo *et al.*, 2006). Starch is commonly stored in reserve organs during the vegetative season. This NSC form is accumulated in reserve organs, where it can be mobilized for regrowth in spring or to buffer source-sink imbalances during the growing season (Sala *et al.*, 2012). Moreover, starch concentration, is directly associated to the ratio between source activity and sink demand (Naschitz *et al.*, 2010; Sala *et al.*, 2012).

In this study, we assumed that distances among organs and availability of resources are involved in both organ development (here floral induction) and growth (here considered as mean fruit weight). Our aim was to investigate the relative contribution of tree carbon balance, source-sink distances and GA availability in SAM on the FI and fruit growth. For this, we manipulated within-tree source-sink relationships during two years on 'Golden delicious' apple cultivar. We set trees in either high (ON trees) or low (OFF trees) crop loads, reducing by half the number of leaves (sources for both carbohydrates and florigen) or fruit (sources of gibberellins and sinks for carbohydrates). These manipulations were performed at different scales in the trees (shoots, branches and one side of the Y-shape trees) in order to clarify the effect of distances between sources and sinks. Moreover, we considered the within-tree variations in carbon acquisition (leaf photosynthetic activity) and accumulation (NSC concentration) and the gibberellins content in SAM to explore their respective involvement on FI. This study provides (i) new evidence of the likely co-involvement of gibberellins from fruits and signals originated from leaves other than carbohydrates in FI control and (ii) new elements on the debate on organ autonomy with respect to carbohydrate transport in trees.

4. Material and methods

4.1. Plant material and growing conditions

The experiment was carried out from 2016 to 2018 on 10-year-old apple trees (cv. 'Golden Delicious'). The orchard was located at the SudExpé experimental station in Marsillargues, in the south of France (43°66'N 4°18'E). Trees were initially planted in 1998 with 'Tentation' cultivar grafted on 'Pajam2' rootstock and then top grafted with 'Golden delicious' in 2005. The orchard was composed of four rows of 75 trees, each tree composed either of one vertical axis or of two main axes (Y-shape trees) arising five centimeters above the grafting point. Pruning and thinning were applied according to commercial practices before the beginning of the experiment in 2016. During the experimental period, all the trees were irrigated and fertilized to avoid any water or mineral deficiency.

4.2. Varying source-sink relationships by leaf and fruit removal treatments

In spring 2016, around 65 trees in the orchard were set in OFF conditions by removing all the flowers after full bloom (Supplementary Material Table S1). No thinning was performed on the same number of trees, in which complete fruit removal was performed in 2015 to get high crop load in 2016. These trees were then considered as ON trees. In the following year (2017), the cropping status was reversed. In this year, all the flowers of OFF trees were removed just after full bloom to ensure a crop load equal to zero. To determine the period of FI in our conditions, a specific experiment was carried out. Assuming that the period of irreversible inhibition of FI was between 30 and 70 days after full bloom (DAFB) (Foster *et al.*, 2003, Haberman *et al.*, 2016), young fruit were completely removed on a selection of ON trees, at successive dates during this period. Fruit removal was performed at six dates (one tree per date): 30, 36, 42, 50, 56 and 70 DAFB in 2016 and at four dates in 2017 (37, 43, 50, and 58 DAFB).

On the two tree subsets in either ON or OFF conditions, 11 different treatments were set up (three trees per treatment) in springs 2016 and 2017 (Supplementary Material Table S1). In order to modify fruit and leaves number, half of the leaves or half of the fruit were removed on the trees. Moreover, leaves and fruit were removed in different parts of the trees in order to modify the distances between the remaining leaves and fruit. Leaves and fruit were removed on either half of the shoots, half of the branches or one side of the Y-shape trees (Figure 1). A different set of trees were used in each year for the leaves and fruit removal treatments. New leaves that appeared after the first defoliation in spring were frequently removed throughout the growing season on the trees subjected to leaf removal. Trees not subjected to leaf or fruit removal either on ON and OFF crop load, were considered as controls.

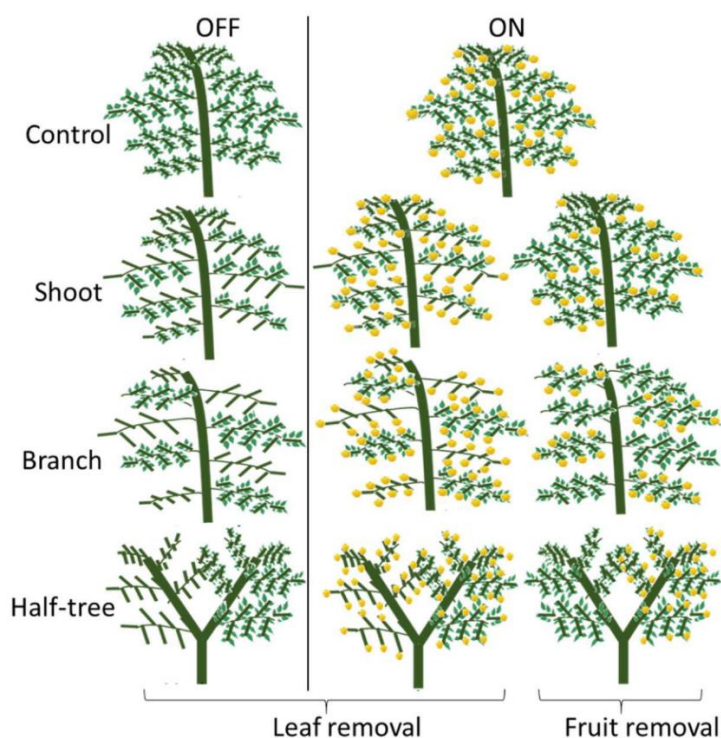


Figure 1. Schematic representation of the leaf and fruit removal treatments.

Crop load was estimated in each year by dividing the harvested fruit number per tree by its trunk cross sectional area (e.g. Francesconi *et al.*, 1996). Trunk cross sectional area (TCSA) was estimated each year in autumn after measurements and computed assuming a cylinder shape by measuring in spring the trunk circumference at 10 cm above the grafting zone. For Y-shape trees, crop load was computed for both sides of the tree separately, considering them as mono-axial trees. The tree crop load of Y-Shape trees was then determined, considering this treatment as a combination of two mono-axial trees, by the mean crop load of the two sides of the trees. Crop load in fruit number per TCSA was not computed for leaf removal treatments because it does not account for the impact of such manipulations on tree source-sink ratio.

Another set of trees (called additional trees, Supplementary Material Table S1), in either ON or OFF conditions and not subjected to leaf or fruit removal was used to build a reference relationship between tree crop load, and mean fruit weight. 69, 103 and 65 trees of the field were considered in 2015, 2016 and 2017 to build this relationship. This reference relationship was then used to evaluate if the impact of local fruit removal treatment was similar to what expected for trees with similar crop load but not subjected to such kind of treatments.

4.3. Development and growth variables: floral SAM proportion and mean fruit weight at harvest

The treatment effect on FI proportion in SAM was estimated at full bloom in the spring following treatment in 2017 and 2018 on all the trees including the additional trees and those subjected to sequential thinning in spring. FI proportion was estimated as the ratio of the total number of reproductive buds to the total number of growing buds. This proportion was estimated on six randomly distributed first-order branches per tree in each treatment, considering the leaf or fruit removal conditions (foliated/defoliated, fruiting/non-fruiting, 3 branches per condition). Unfortunately, no data were recorded for the trees subjected to fruit removal at the shoot scale in 2016.

At harvest, in early September of each year, fruit were collected on each treatment. Fruit were sorted by different parts of each tree considering whether they were subjected or not to leaf or fruit removal. All the fruit were collected on each tree except for the treatment performed at the shoot scale for which fruit were collected on two branches per tree, only. Then, each set of fruit was weighted, and the mean fruit weight was estimated as the ratio of the total fruit weight to the number of fruit.

4.4. Responses of leaf photosynthesis and starch content

Leaf photosynthesis and NSC contents were measured on August 2017 (from 119 to 145 DAFB) on fully expanded leaves belonging to short or medium shoots (shorter than 20cm, Costes *et al.*, 2003) and fully exposed to sunlight. Measurements were performed on ON and OFF trees and on foliated parts of the trees with leaf removal treatments and on both fruiting and non-fruiting parts of the trees with fruit removal treatments. Three measurements were performed for each tree and condition (fruit or leaf presence/absence). Measurements were done between 8 and 12 am, with an infra-red gas analyzer (LI-6400, LICOR, Lincoln, Nebraska, USA) under controlled conditions within the measurement chamber known to be non-limiting for photosynthesis (Massonnet *et al.*, 2007) (photosynthetic photon flux density = 1800 $\mu\text{mol}^{-2}\text{s}^{-1}$, relative humidity = RH = 70%, CO₂ = 400ppm, T = 25°C).

After each photosynthesis measurement, the leaf, the entire annual shoot (called stem) on which the leaf was located, the SAM of this shoot and a 5 cm section of the one-year-old wood supporting it were sampled for measuring their NSC content. Three replicates of all these organs were sampled on each tree and for each condition (fruit or leaf presence/absence). Samples were placed immediately in liquid nitrogen and stored at -20°C for about one week. Then, they were freeze-dried and grinded to fine powders using a ball grinder. Starch concentrations were then determined for all the organs. In SAM, glucose, fructose, sorbitol and sucrose concentrations were also evaluated. All these analyses were performed following the protocol described in Pallas *et al.* (2018).

4.5. GA concentrations in SAM

GA content measurements were performed on SAM collected on 31 May 2017 (58 DAFB), i.e. at the expected date of FI in short shoots (Foster *et al.*, 2003). SAM were sampled on short to medium shoots that had recently stopped growing and did not form protecting scars yet. SAM were collected on ON and OFF control trees, on trees subjected to fruit or leaf removal on half of the branches and on trees subjected to fruit removal on one side of Y-shape trees. Nine SAM were collected on each part of the trees (foliated/defoliated, fruiting/non-fruiting) and were gathered together for each tree. All samples were conserved at -80°C before being freeze dried and sent for GA quantification at the Plant Hormone Quantification Service in the Institute for Plant Molecular and Cell Biology (IBMCP), Valencia, Spain. GA are quantified using 30 mg of samples dry weight by Ultra Performance Liquid Chromatography-Mass Spectrometry (UPLC-MS).

Fourteen GA forms produced in the two GAs biosynthesis pathways regulated by the activities of GA20-oxidases (GA20ox), GA3-oxidases (GA3ox) and GA2-oxidases (GA2ox) were investigated (Supplementary material figure S1). They include bio-active forms (GAs 4 and 1), degradation forms (GAs 51, 34, 29 and 8) and intermediate forms (GAs 12, 15, 24, 53, 44 and 19).

4.6. Statistical analyses

All statistical analyses were performed with R software (R Development Core team, 2013). We investigated the effects of the combination of (i) the tree treatment (control, leaf removal, and fruit removal), (ii) the scale (tree, shoot, branch, and one side of the Y-shape tree) at which treatments were performed and (iii) the condition within the tree (foliated, defoliated, fruiting and non-fruiting). The effect of all these combinations was tested on photosynthesis, NSC concentrations, GA concentrations and FI proportion, with a one-way ANOVA followed by a Tukey HSD test for pairwise comparison. Linear models were used for continuous variables and a general linear model of the binomial family was used for FI proportion. For GA and due to the low number of replicates (one per tree and condition), the effect of fruit presence/absence was also tested using Kruskal-Wallis test gathering samples from control ON and fruiting parts of trees (originated from branch and Y-Shape treatments) and from control OFF and non-fruiting parts of trees.

The dataset of additional trees with a large range of crop loads, obtained in 2015, 2016 and 2017 was used to fit an exponential relationship between the tree crop load and the mean fruit weight (exponential adjustment). The residuals between observed values for a given fruit removal treatment and fruit weight over different crop loads were used to test the impact of local fruit removal treatments under comparable crop load conditions. A linear model between residuals and treatments was then built and the t-value (coefficient of the model divided by its standard error) associated to each treatment was used to assess if the treatment effect was different from 0 (general trend between tree crop load and mean fruit weight).

5. Results

5.1. Tree fruiting status between treatments

Fruit number was not significantly lower for fruit removal treatments compared to control trees in 2016 but the higher TCSA values for these treatments (mainly for shoot and branch treatment) led to a decrease in crop load values (significant for branch treatment only) (Table 1). In 2017, a significant decrease in crop load was observed for branch and half tree treatments mainly due to lower fruit number. For fruit removal at the shoot scale crop load was also lower than for control trees but this decrease remained non-significant. For leaf removal treatment TCSA and fruit number values were not significantly different from control trees in both years, although higher fruit number were observed for half-tree treatments (Table 1).

Table 1: Mean values of fruit number, trunk cross sectional area (TCSA) and crop load estimated as the fruit number per trunk cross sectional area (fruit.cm⁻²) for different treatments and scales at which treatments were performed and for the control ON trees of ‘Golden delicious’ apple cultivar in 2016 and 2017.

Tree treatment	Scale	Year					
		2016			2017		
		Fruit number	TCSA	Crop load	Fruit number	TCSA	Crop load
Control ON	Tree	366 ^{ab}	27.7 ^b	12,1 ^a	601 ^{ab}	36.5	20,7 ^{ab}
Leaf removal	Shoot	432 ^{ab}	33.0 ^{ab}		464 ^b	34.1	
	Branch	528 ^{ab}	33.7 ^{ab}		591 ^{ab}	36.3	
	Half-tree	655 ^a	34.7 ^{ab}		960 ^a	25.7	
Fruit removal	Shoot	411 ^{ab}	49.9 ^{ab}	8,5 ^{ab}	581 ^{ab}	37.6	15,9 ^{ab}
	Branch	366 ^{ab}	53.9 ^a	6,8 ^b	294 ^b	35.6	8,2 ^b
	Half-tree	279 ^b	28.1 ^b	9,98 ^{ab}	350 ^b	28.7	12,2 ^b
Treatment effect		*	**	*	**	ns	**

For each “Half-tree” tree, two TCSA values were considered and corresponded to both sides of trees. Crop load values for “Half-tree” trees was computed as the mean of crop loads on the two sides. Treatment effect was estimated with a one-way ANOVA on three trees for each combination of treatment and scale at which treatment was performed. ** significant at $0.001 < P < 0.01$, * significant at $0.01 < P < 0.05$ and ns non-significant. A Tukey’s HSD test for pairwise comparisons was made after ANOVA and different letters in a column indicate statistically different values among all treatments.

5.2. Floral induction in SAM occurs after treatment onset.

The complete fruit removal performed sequentially in springs 2016 and 2017 on a subset of ON trees allowed evaluating the date after which the inhibition of FI by fruit presence was no longer reversible. The quantification of FI proportion in the following spring revealed that FI was no longer possible at 70 DAFB (Table 2). At that date, FI proportion reached values similar to those of control ON trees. Conversely, when fruit removal was performed before 50 DAFB, FI proportion was close to 100% as observed for OFF control trees, in both years (Table 2). Assuming that dates of FI were similar for all the buds in trees, this suggests that FI likely occurred during a short period between 50 and 70 DAFB. This shows that our experimental design was relevant since treatments were performed before 50 DAFB at a date when the SAM fate was not yet determined.

Table 2: Proportion of shoot apical meristems (SAM) induced to flower in ‘Golden delicious’ apple trees subjected to complete fruit removal performed sequentially from 30 to 70 days after full bloom (DAFB), in 2016 and 2017 and for control OFF and ON trees. FI proportions were evaluated based on the floral bud proportion, as the ratio of the total number of reproductive buds to the total number of growing buds, on six branches per tree, in the next spring, after the year of treatment.

Treatment	Floral induction 2017		Floral induction 2018	
	Date of fruit removal		Date of fruit removal	
	2016 (DAFB)	FI proportion	2017 (DAFB)	FI proportion
Control OFF	-	97%	-	100%
Fruit removal	30	95%	-	-
	36	79%	37	98%
	42	70%	43	100%
	50	76%	50	90%
	56	40%	58	56%
	70	18%	-	-
Control ON	-	19%	-	29%

5.3. FI proportion is affected by leaf and fruit presence and by their distance to the SAM

Leaf removal did not impact FI on ON trees, with values close to zero on both foliated and defoliated parts, whatever the scale at which leaf removal was performed (Figure 2, right side). In the foliated parts of the defoliated OFF trees FI proportion was similar to the control OFF trees (between 0.9 and 1, Figure 2, left side). In contrast, a strong and significant decrease in FI proportion was observed in the defoliated compared to the foliated parts of trees after leaf removal on half of the branches (-29% and -19% for 2017 and 2018 respectively) or half of the tree (-74% and -63% for 2017 and 2018 respectively). Stronger decrease in the defoliated side of Y-shape trees scale than on defoliated branches was observed, suggesting an impact of the distances to the remaining leaves on FI. This distance effect was also found by the absence of any significant decrease in FI on the defoliated shoots (-6% and -10% for 2017 and 2018 respectively) of trees subjected to leaf removal at the shoot scale (Figure 2). Local fruit removal had also a strong effect on FI proportion within the tree (Figure 2 A and B, right side). FI proportions were lower in the fruiting than in the non-fruiting parts. Consistently with the distance effect observed after leaf removal treatments, FI proportion increased in non-fruiting parts compared to the fruiting ones when the distances to the remaining fruit increased. In 2018, the increase in FI proportion between fruiting and non-fruiting parts was equal to 50.1% for Y-shape trees while it only reached 29% when fruit removal was performed at the shoot scale.

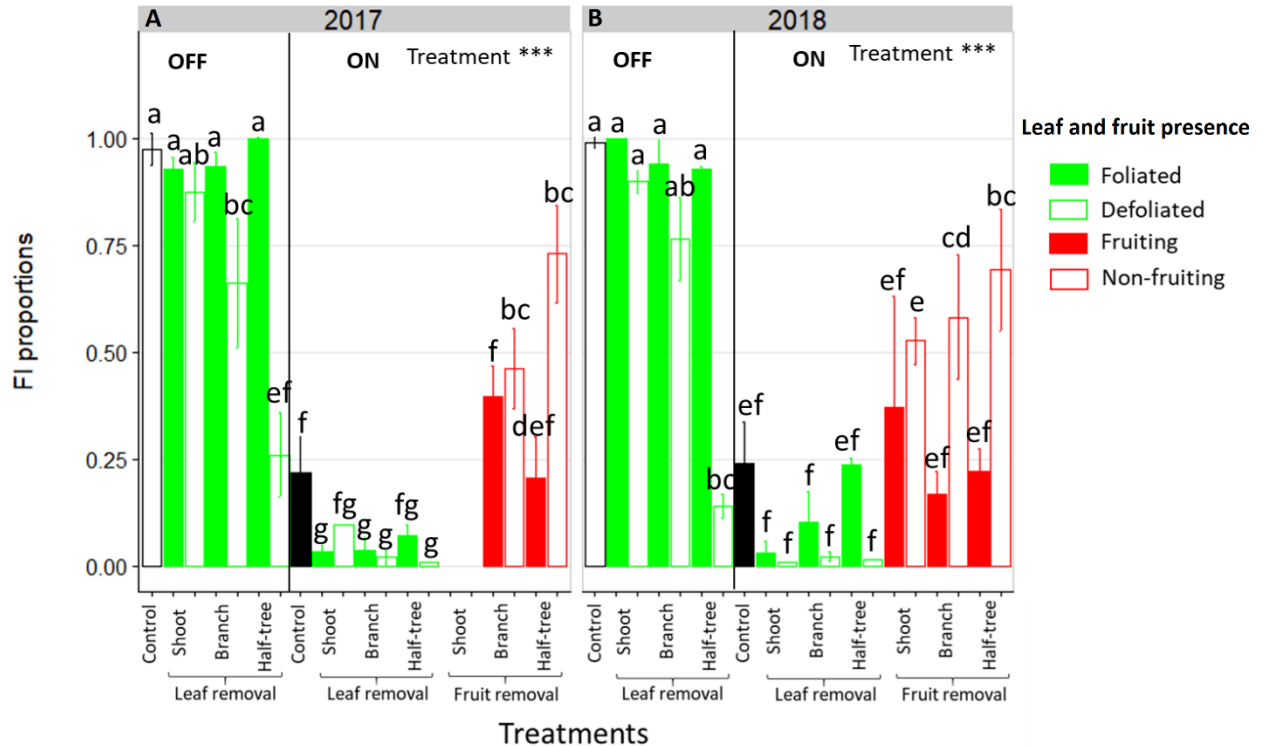


Figure 2. Bar plot representation of FI proportion in ON and OFF 'Golden Delicious' apple trees for the different treatments in 2017 (A) and 2018 (B). Each bar represents the value for one combination of tree treatments and tree scale at which treatments were performed and conditions within the trees (leaf or fruit presence) and lines represent the standard deviation among measurements (3 measurements for each treatment combination). The dataset was fitted with a glm model (binomial family) and leaf and fruit presence effect was assessed with one-way-ANOVA. *** significant at $P < 0.001$. A Tukey's HSD test for pairwise comparisons was made after the analysis and different letters indicate statistically different values among all conditions.

5.4. Mean fruit weight is affected by distances between leaves and fruit

As for FI, mean fruit weight depended on the distances to remaining leaves in trees subjected to leaf removal (Figure 3). Indeed, mean fruit weight decreased of 53% and 59% in 2016 in the defoliated parts of trees subjected to leaf removal at the branch scale or on half of Y-Shape trees, respectively compared to the foliated parts. Conversely, this decrease was no longer significant (equal to 2%) when defoliation was performed at the shoot scale. In both foliated and defoliated parts of these trees (defoliation at the shoot scale), mean fruit weight was not significantly different to what observed for control ON trees. Fruit removal increased mean fruit weight compared to control ON trees. Nevertheless, this increase was higher when fruit removal was performed at the branch scale or on one side of Y-Shape trees than after fruit removal at the shoot scale.

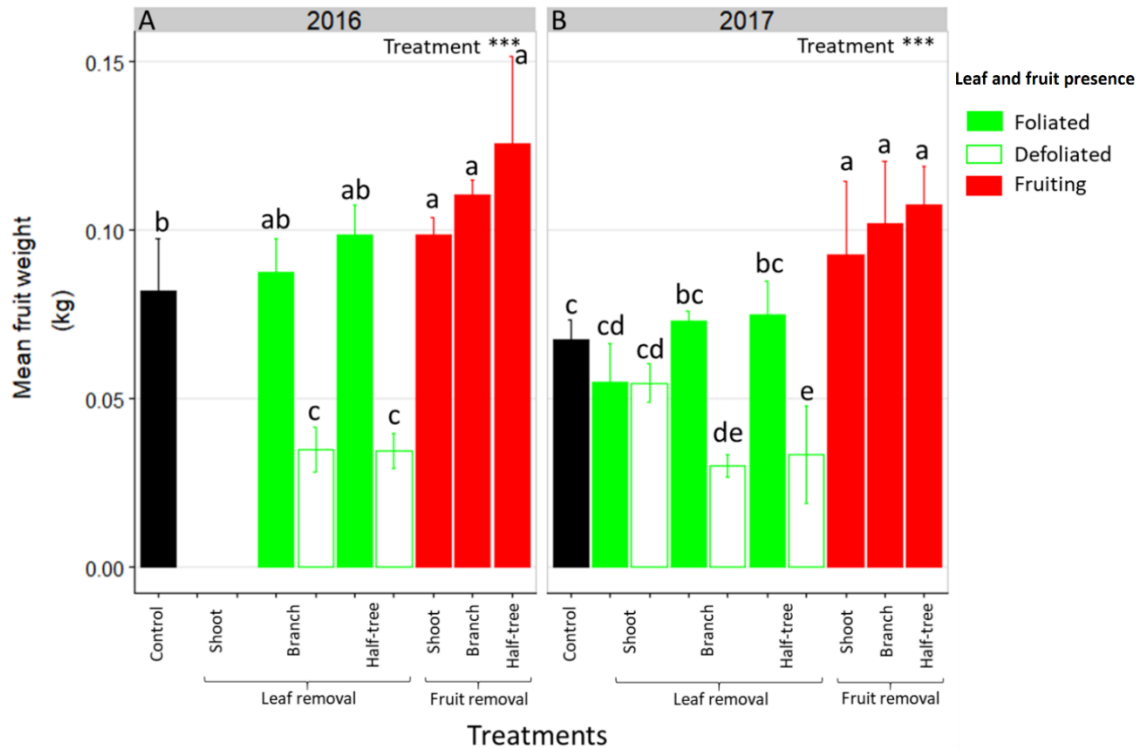


Figure 3. Bar plot representation of mean fruit weight in ON ‘Golden Delicious’ apple trees for the different treatment combinations in 2016 (A) and 2017 (B). Each bar represents the value for one combination of tree treatments and tree scale at which treatments were performed and condition within the trees (leaf or fruit presence) and lines represent the standard deviation among measurements (3 measurements for each treatment combination). Data is not represented for leaf removal at shoot scale in 2016 due to problems in identification of fruit from foliated or defoliated shoots. Leaf and fruit presence effect was estimated with a one-way-ANOVA. *** significant at $P < 0.001$. A Tukey’s HSD test for pairwise comparisons was made after the analysis and different letters indicate statistically different values among all combinations.

The general trend of mean fruit weight over crop loads, for the additional control trees over three years, displayed a negative relationship ($R^2 = 0.71$ between fitted and observed values, Figure 4 and supplementary material Figure S2) with highest mean fruit weights equal to around 0.25kg and lowest ones to 0.08kg. For the fruit removal treatment, the analysis of residuals to the relationship between crop load and mean fruit weight (Table 3) showed that the mean fruit weight in the fruiting shoots (2016) and branches (2016 and 2017) after fruit removal treatments was similar to that of control trees with similar crop load and with a homogeneous distribution of fruit within the tree. A slight increase in residual values (around +0.02 kg) was observed when fruit removal was performed on one side of the Y shape trees in both years or on half of the shoots in 2017. These results suggest that fruit weight was mainly determined by the tree crop load whatever the distance to remaining fruits after fruit removal.

Table 3: Mean values of residuals extracted from exponential adjustments between the mean fruit weight (kg) and tree crop loads (Supplementary Material Figure S2) on ‘Golden delicious’ apple trees. Data are presented for different treatments and scales at which treatments were performed and depending on fruit removal conditions.

Tree treatments	Mean fruit weight residuals			
	Scale	Fruit presence	2016	2017
Fruit removal	Shoot	Fruiting	-0.002 (ns)	+0.013 (*)
	Branch	Fruiting	0.001 (ns)	0.001 (ns)
	Half-tree	Fruiting	+0.029 (***)	+0.021 ^a (***)

A linear model between residuals and treatments was built and the *t*-value (coefficient of the model divided by its standard error) associated to each treatment was then used to assess if the treatment effect was different from 0 (general trend between tree crop load and mean fruit weight, Supplementary Material Figure S2). ns non significant, * and *** significant at $0.01 < P < 0.05$ and at $P < 0.001$, respectively. The exponential adjustment was fitted on the additional set of trees without any treatment and displaying contrasted crop load in 2015, 2016 and 2017.

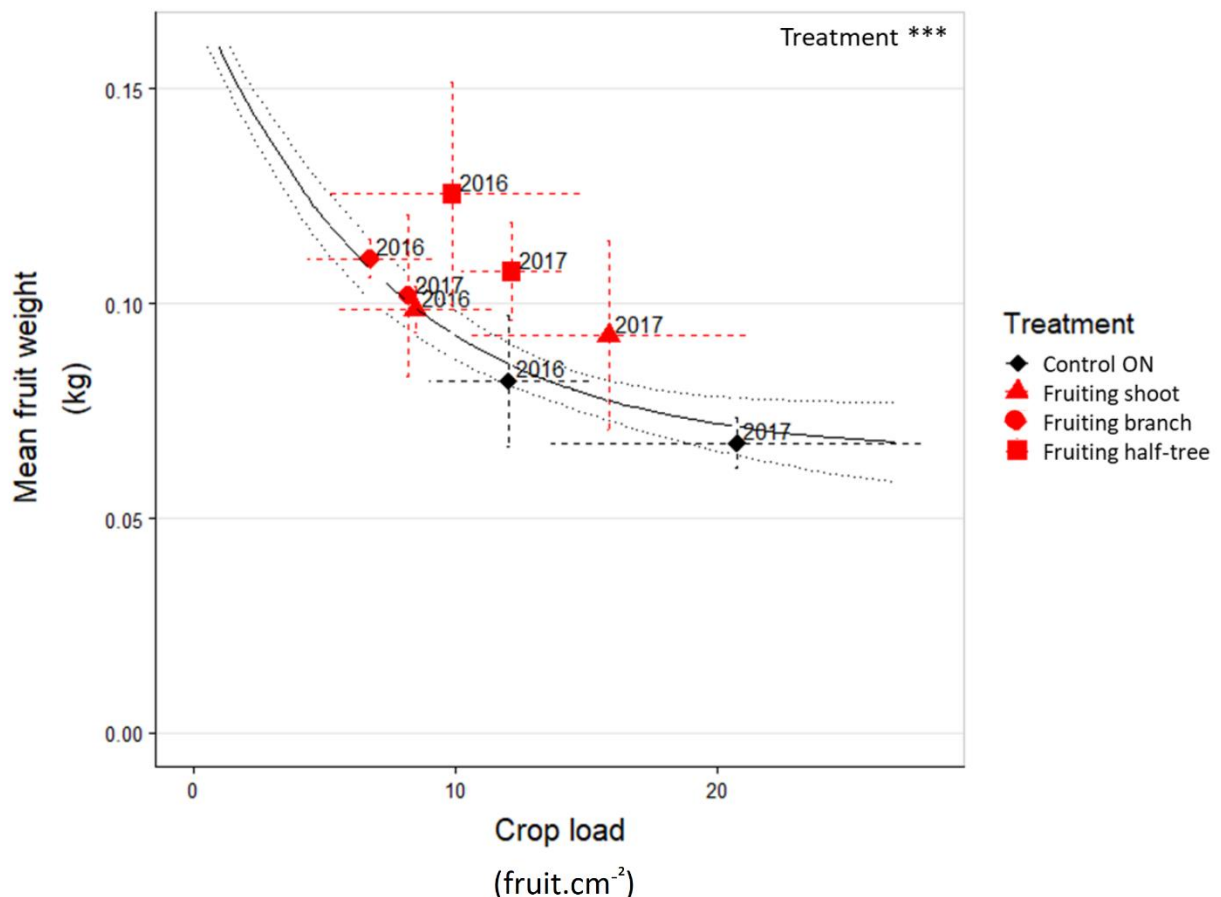


Figure 4. Relationship between mean fruit weight and crop load in ON ‘Golden Delicious’ apple trees for control trees and the different fruit removal treatment combinations in 2016 and 2017. Each point represents the value for one combination of tree treatments, tree scale at which treatments were performed and condition within the trees (fruit presence) and lines represent the standard deviation among measurements (3 measurements for each treatment combination). The continuous black line represents the exponential function fitted on the additional trees dataset (supplementary material Figure S2). The dotted grey lines represent the deviation interval of the fitted values.

5.5. Relationships between FI and mean fruit weight variability and carbon availability

Photosynthesis rate was higher for ON trees compared to OFF ones (mean values 7.6 and 14.3 $\mu\text{mol}\cdot\text{m}^{-2}\cdot\text{s}^{-1}$ for OFF and ON control trees, respectively; Figure 5). Moreover, no significant difference in photosynthetic rates (mean value 15.76 $\mu\text{mol}\cdot\text{m}^{-2}\cdot\text{s}^{-1}$ for all fruit removal treatment) was observed between the different fruiting and non-fruiting parts of trees subjected to fruit removal. This suggests that fruit presence stimulated photosynthesis whatever the distances to the fruit.

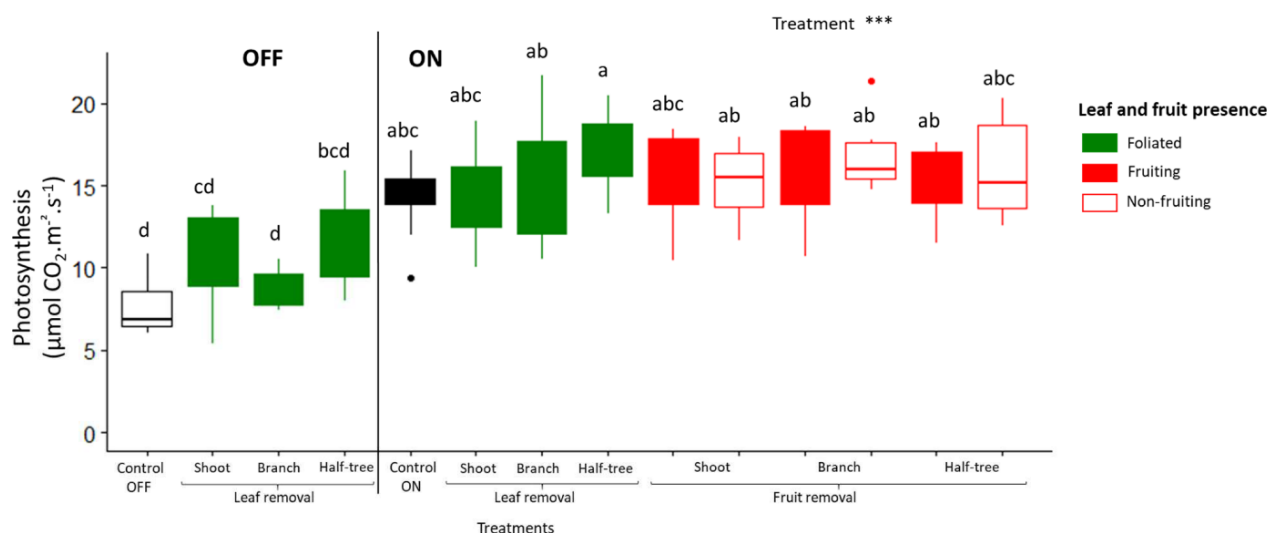


Figure 5. Boxplot representation of leaf photosynthetic activity in August 2017 for 'Golden Delicious' apple trees for the different treatments (control, leaf removal, and fruit removal), tree scales (tree, shoot, branch, and one side of Y-shape trees) at which treatments were performed and conditions within the tree (foliated, defoliated, fruiting and non-fruiting) for ON and OFF trees. Nine replicates were used for each treatment combinations (3 samples \times 3 trees). Treatment effect was estimated with a one-way-ANOVA considering all the combinations together. *** significant at $P < 0.001$. A Tukey's HSD test for pairwise comparisons was made after the analysis and different letters indicate statistically different values.

Starch concentration varied among organs, with low values in SAM and leaves (Figure 6 A, B) and higher values in stems and wood (Figure 6 C, D). Lower values of starch concentration in leaves, stem and wood was observed in ON trees compared to OFF ones whereas no difference between both treatments was observed in SAM. (Figure 6 B). In OFF trees, no impact of defoliation treatments was observed on starch concentrations in SAM, stems and wood (Figure 6, left sides), although a decrease in FI proportion was observed in defoliated parts of OFF trees. In contrast, in ON trees, significantly higher starch concentration were found in the SAM, stems and wood when comparing the leafy parts to defoliated ones (Figure 6 B, C, D). For these trees, this effect of leaf removal was similar regardless of the distances to the remaining leaves since no difference was observed between defoliation at the shoot, branch or half tree scale. The effect of fruit removal on starch concentration was observed in wood only, through a greater concentration in the non-fruiting than in the fruiting parts of defoliated shoot, branch and one side of the Y-shape tree treatments (Figure 6D). No clear impact of the distances to the remaining fruit was observed on starch concentrations in wood, as the decrease in starch content were similar whatever the scale at which fruit removal was performed.

Regarding, the soluble sugars content (sorbitol, sucrose, fructose and glucose) in SAM (supplementary material Figure 3), sorbitol displayed higher concentrations than the three other sugars. Moreover, treatment effects (fruit and leaf removal) on soluble sugars content in SAM were observed on sorbitol concentration, only after leaf removal treatments on both OFF and ON trees.

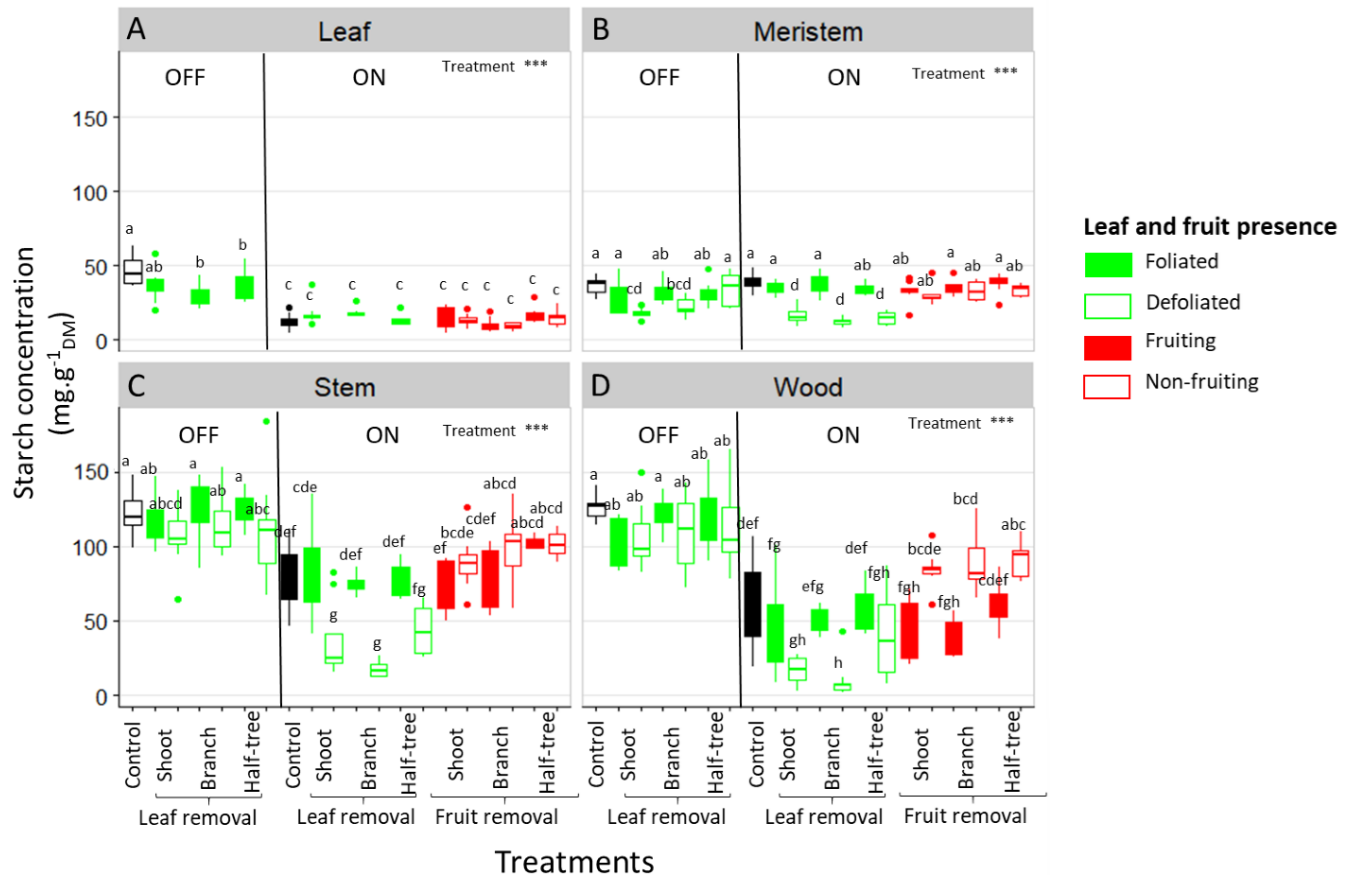


Figure 6. Boxplot representation of starch concentration in the leaves (A), shoot apical meristems (B), stems (C) and one-year-old wood (D) of ON and OFF 'Golden Delicious' apple trees for the different treatments, tree scales at which treatments were performed and conditions within the trees (leaf or fruit presence). Nine replicates were used for each treatment combinations (3 samples × 3 trees). Treatment effect was estimated with a one-way-ANOVA considering all the combinations together. *** significant at $P < 0.001$. A Tukey's HSD test for pairwise comparisons was made after the analysis and different letters indicate statistically different values among all treatments.

5.6. GA9 (precursor of active form) and GA1 (active form) decrease in fruit presence

In the early-13-hydroxylating pathway (supplementary material Figures S5 and S6), three forms were found in abundance (Table 4): GA44 (inactive form), GA1 (active form), and GA8 (degradation form). In the non-hydroxylating GA pathway, maximal GA concentrations were found for GA9 (Table 4) which is the last inactive form before GA4 synthesis. Variations in SAM GA contents were observed among all the sampled trees (supplementary material Figure S6). Nevertheless, differences were significant between SAM from fruiting and non-fruiting parts of trees. GA9 concentration was significantly higher in the SAM collected on the non-fruiting trees or parts of trees (gathering control OFF trees and in non-fruiting branches and sides of Y-shape trees) than in those collected on fruiting trees or parts of trees (gathering control ON trees, fruiting branches and sides of Y-shape trees) (Table 4). Even though not significant, higher concentration was observed in the non-fruiting side of the Y-shape tree than in the non-fruiting branches, suggesting a possible effect of distances to the remaining fruit. In addition, a slightly higher but non-significant GA1 concentration was observed in the SAM of non-fruiting parts of the trees than in the fruiting ones. Conversely, GA8 concentration was higher in control ON than in control OFF trees and in fruiting than in non-fruiting branches when fruit removal was performed on half of the branches. Nevertheless, no difference between fruiting and non-fruiting branches was observed for the Y-Shape trees. Finally, leaf removal did not influence any GA concentration.

Table 4: Concentrations (ng.g⁻¹) of GA9, 44, 1 and 8 in shoot apical meristems sampled at 58 days after full bloom on ‘Golden Delicious’ apple trees under different treatments (leaf or fruit removal), performed at different scales (branch, half-tree).

Tree treatment	Scale	Fruit presence	Pathways			
			Non-hydroxylating	Early-13-hydroxylating		
			GA9	GA44	GA1	GA8
Control ON	Tree	Fruiting	0.43	1.53	2	18.67 ^a
Control OFF	Tree	Non-Fruiting	2.05	0.86	2.48	2.21 ^b
Fruit removal	Branch	Fruiting	0.4	1.22	2.4	15.6 ^{ab}
		Non-Fruiting	1.2	1.43	1.9	3.34 ^b
	Half-tree	Fruiting	0.21	2.04	1.92	3.83 ^b
		Non-Fruiting	2.57	1.41	5.87	4.77 ^{ab}
Leaf removal	Branch	Fruiting (foliated)	0.6	2.64	2.36	3.65 ^b
		Fruiting (defoliated)	0.34	1.76	1.88	4.84 ^{ab}
Treatment effect			ns	ns	ns	**
Mean value of fruiting parts		Fruiting	0.39	1.92	2.14	6.98
Mean value of non-fruiting parts		Non-Fruiting	1.89	1.42	3.89	4.06
Fruit presence effect			**	ns	ns	ns

*Treatment effect on GA concentration was estimated with a one-way ANOVA considering the tree treatment (control, leaf removal, and fruit removal), and the scale (tree, shoot, branch, and one side of the Y-shape tree) at which treatments were performed. ** significant at 0.001<P<0.01 and ns non-significant. When significant differences were observed, a Tukey’s HSD test for pairwise comparisons was made and different letters indicate statistically different values among treatments. The different conditions were then gathered depending on fruit presence, and the fruit presence effect was estimated with Kruskal Wallis test.. ** significant at 0.001<P<0.01 and ns non-significant.*

6. Discussion

6.1. Relative roles of carbohydrates and GA in flower induction

Our study investigated the impact of the tree carbon balance on floral induction by exploring the relation between NSC contents in all the organs and SAM status (floral induced or not) after organ manipulations (leaf or fruit removal). After defoliation treatments, the decrease in FI proportion in the defoliated branches and half-side of OFF trees was not associated with any decrease in starch content in all organs including SAM (Figures 5). In addition, NSC concentration, whatever the forms (soluble or starch), did not vary between fruiting and non-fruiting parts in all the organs including SAM (Figures 5 and S4), while a decrease in FI was observed in fruiting parts compared to non-fruiting parts. Together these results on trees subjected to leaf or fruit removal suggest that FI is not related to the tree carbon balance and carbohydrate availability in SAM.

Other possible effects of leaf removal independently of the carbon production and primary metabolism (here analyzed through NSC and starch content) could be implicated. Indeed, leaves are likely to be sources of FT protein, considered as the florigen which is transported to SAM where it activates flowering (Corbesier *et al.*, 2007b,a; Mathieu *et al.*, 2007; Tamaki *et al.*, 2007). Nevertheless, other carbohydrates than starch and NSC may have role in FI, especially signaling molecules such as trehalose-6-phosphate (T6P, Ponnu *et al.*, 2011; Lastdrager *et al.*, 2014). In *Arabidopsis* T6P has been shown to affect flowering, by inducing FT production and the expression of flowering-time (SPL) genes in SAM that in turn regulate flowering as a function of plant age (Wahl *et al.*, 2013).

GA4 has been shown to target key flowering genes in SAM, in *Arabidopsis* (Eriksson *et al.*, 2006). In apple tree, GA4 and GA1 may inhibit FI (Ramírez *et al.*, 2001; Ramírez *et al.*, 2004). In the present study, the inactive GA9 preceding GA4 in the non-hydroxylating pathway accumulated in OFF trees, and in non-fruiting branches and side of Y-shape trees (Table 4, supplementary material Figure S5). Nevertheless, no difference in GA4 concentrations was found in SAM between fruiting and non-fruiting conditions. In addition, in the hydroxylating pathway, GA1 was slightly higher in non-fruiting tree parts and in OFF trees (Table 4, supplementary material Figure S5) whereas GA8 slightly accumulated in fruit presence. Altogether these results are consistent with the downregulation of *MdGA2ox* transcripts in OFF trees (or its up-regulation in ON trees), observed in Guitton *et al.*, (2016). They suggest that the last steps of GA catabolism could be less active in absence of fruit (conversely more active in presence of fruit). Therefore, the putative role of GA on controlling FI is supported by our results and previous findings even though their inhibitory or activating effect remains to be clarified. Moreover, further research would be needed to investigate the ability of GAs, likely produced by seeds (Dennis and Nitsch, 1966a), to directly act on SAM FI in the apple tree.

6.2. Response of floral induction and fruit growth to changing source-sink distances

In this study, leaf and fruit removal at different scales of plant organization allowed us to clarify the impact of distances between organs on FI and fruit growth. Similar FI proportion was observed between foliated and defoliated shoots and between fruiting and non-fruiting ones (Figure 2) when leaf or fruit removal was performed at the shoot scale, thus implying transport at short distances of signals originated from leaves (activators) and fruits (inhibitors). This suggests that shoots can be considered as non-autonomous and prone to exchanges of inhibiting/activating signals.

In contrast, leaf presence in the foliated parts of trees subjected to defoliation at the branch scale or on one side of Y-Shape trees did not promoted FI in the defoliated parts of these trees (Figure 2). In that case, distances were too long, possibly for florigen transport, consistently with previous studies having underlined the lack of evidence of FT long distance transport in woody plants (Putterill and Varkonyi-Gasic, 2016). Similarly, FI was only slightly affected by fruit presence at long distance since FI in the non-fruiting branches or sides of Y-Shape trees was slightly lower or even similar to that observed on OFF trees. This suggests that the inhibiting signal produced by fruits may not be transported at long distances in the tree structure or in low quantity, only. GA transport at relatively

long distances has been demonstrated but in small annual plants, with GA20 being the mobile form in *Pisum sativum* (Binenbaum *et al.*, 2018) and GA12 the form transported through the xylem in *Arabidopsis thaliana* (Regnault *et al.*, 2015). Interestingly, the different GA forms issuing from the hydroxylated and non-hydroxylated pathways may involve different transporters (Binenbaum *et al.*, 2018). However, studies on the transport of these forms and the distances at which they could be transported in more complex plants such as in fruit trees are still needed.

Fruit weight was also strongly affected by the distances to the remaining leaves after leaf removal (Figure 3). As for FI, similar fruit weights were observed between neighboring leafy and non-leafy shoots, when defoliations were performed at shoot scale. This is consistent with previous studies on peach where non-fruiting shoots contributed to fruit growth in nearby fruiting shoots (Walcraft *et al.*, 2004). Conversely, a strong decrease in fruit weight and starch concentrations in all organs were observed on defoliated branches or defoliated parts of Y-Shape trees. This is in accordance with previous studies of carbon labeling on young walnut and peach trees, that have shown limitation of carbon transport at long distance leading to almost complete autonomy of branches even when exposed to source limitation through shading, leaf removal or girdling (Lacointe *et al.*, 2004; Volpe *et al.*, 2008). These results are also consistent with leaf removal effect on fruit growth and reserve accumulation in young fuyu trees and mature *Carpinus*, *Fagus* and *Tilia* forest trees (Choi *et al.*, 2003; Hoch, 2005).

Conversely, long distance transport of carbohydrates was suggested by the results after fruit removal. Indeed, mean fruit weight in the fruiting parts of trees subjected to fruit removal was similar or even higher to that observed in control trees with a homogeneous crop load (Figure 4, Table 3). Moreover, starch concentration in stems and leaves of non-fruiting parts of ON trees (Figure 6D) was lower than that observed in OFF trees suggesting carbohydrate export to the fruiting parts of the trees even at long distances to sustain fruit growth. Nevertheless, it is noticeable that a part of the carbon excess produced in the non-fruiting parts was allocated to the reserve organs. This confirms the major role of reserves as an active sink in perennial trees (Silpi *et al.*, 2007). The low NSC content observed in leaves of the non-fruiting parts can be interpreted as resulting from carbon export and prevented photosynthesis inhibition by starch accumulation (Wünsche *et al.*, 2000), thus leading to a similar photosynthesis rate in fruiting and non-fruiting parts of the trees (Figure 5). These results are in contradiction with other experimental results showing an impact of the local source-sink conditions on photosynthesis activity (Poirier-Pocovi *et al.*, 2018). Such differences could result from the tree crop load we observed whatever the fruit removal scale (shoot, branch or half tree), ranging from 6.8 to 20,7 fruits/cm² (Table 1) and corresponding to high crop load conditions, in comparison to previous studies or usual orchard management (Wünsche *et al.* 2000).

A discrepancy on the distance effects on fruit growth between trees subjected to leaf and fruit removal may appear from our results (Figure 3). However, this apparent discrepancy results from the nature of each treatment. First, leaf removal likely affected the transpiration flux (e.g. Pataki *et al.*, 1998) and may have disturbed the long distance transport of carbohydrates (e.g. Hölttä *et al.*, 2009, Nikinmaa *et al.*, 2013). Second, large within tree source-sink imbalances existed in the trees subjected to fruit removal with the non-fruiting parts displaying low sink demand and large carbohydrate supply and the fruiting parts displaying high sink demand. This imbalance could be the driver of carbon fluxes even at long distance while in the trees subjected to leaf removal fruit sink demand remained high in all the tree parts thus limiting carbon fluxes from the remaining leaves to the distant fruit (Walcraft *et al.*, 2004).

7. Conclusion

Our results show that SAM floral induction is not directly associated to the tree carbon balance nor organ starch content and NSC availability in SAM but more probably to the combination of activating and inhibiting signals originated from leaves and fruit. Having performed leaf and fruit removal at different scales of tree organization provides new clues for understanding the distances at which these signals can act within the tree. At short distances (neighboring shoots), these signals are able to move from sources (leaves and fruit) to sinks (SAM) to act on FI while they cannot reach SAM at longer distances (branches and sides of Y-shape trees). Moreover, this study suggests that carbohydrates can move at longer distances from branch to branch in condition of high source-sink imbalances within the tree and in absence of any perturbation of the vascular fluxes. Finally, this study brings new considerations on carbohydrate and hormone transports within the fruit trees that can be then integrated in functional structural plant model (e.g Vos *et al.*, 2009) to simulate floral induction and fruit growth over years.

Funding

This work was funded by the ANR-DFG Alternapp project and by the PhD grant accorded to F. Belhassine by INRA BAP department and ITK.

Aknowledgments

The authors thank the AFEF team, SudExpé for technical support during experiments, UMR PIAF for having provided LICOR 6400 device, CIRAD biochemistry platform for NSC analyses and IBMCP for GA quantification. The authors also thanks Dr. B. Guitton for his implication in the gibberellins results analysis. This manuscript has been released as a Pre-Print at <https://www.biorxiv.org/content/10.1101/612317v1>.

Competing interests

Damien Fumey was employed by ITK company. The authors declare that this study received funding from ITK company. ITK was involved in designing the study, data collection and decision to publish. All other authors declare no competing interests or conflict of interest.

Author Contributions

BP, FB, EC, JJK and DF conceived and designed the study; BP, FB, SB, DF and SM collected the data; SB did biochemistry analyses; FB and BP analyzed data and FB, BP and EC wrote the manuscript; all authors approved the final version.

8. Supplementary Material

Table S1. Overview of the different treatments, the number of tree replicates used and the main objectives of each manipulation

Treatments	Crop status	Year	Tree replicates	Objective
Additional trees	OFF to ON	2015	69	Build a relationship between crop load and mean fruit weight
		2016	103	
		2017	65	
Fruit removal at different dates	ON	2016	6	Estimate FI timing
		2017	4	
Control	ON	2016	3	Compare the trees subjected to leaf and fruit removal to non-modified conditions
		2017	3	
	OFF	2016	3	
		2017	3	
Leaf removal at different scales	ON	2016	3	Evaluate the effect of leaf removal and distances on floral induction and fruit weight
		2017	3	
	OFF	2016	3	
		2017	3	
Fruit removal at different scales	ON	2016	3	Evaluate the effect of leaf removal and distances on floral induction and fruit weight
		2017	3	

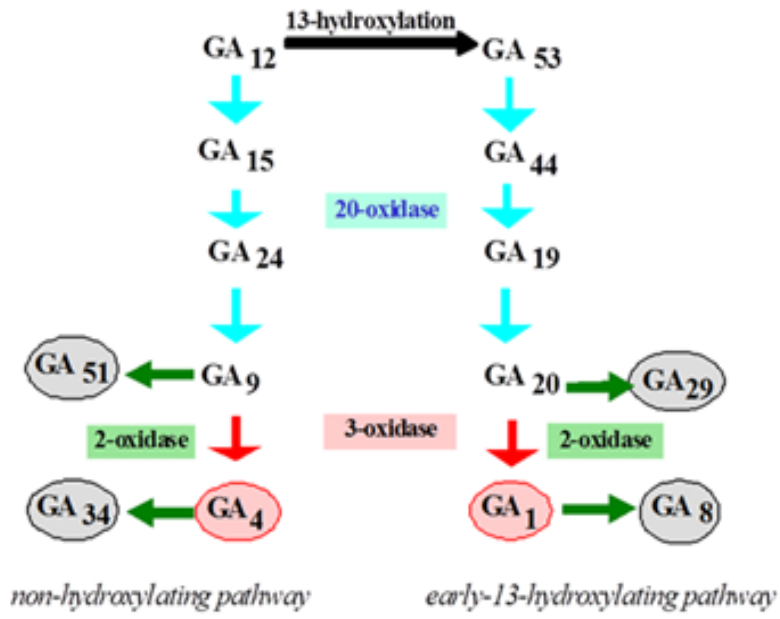


Figure S1. Schematic representation of the gibberellin biosynthesis pathways

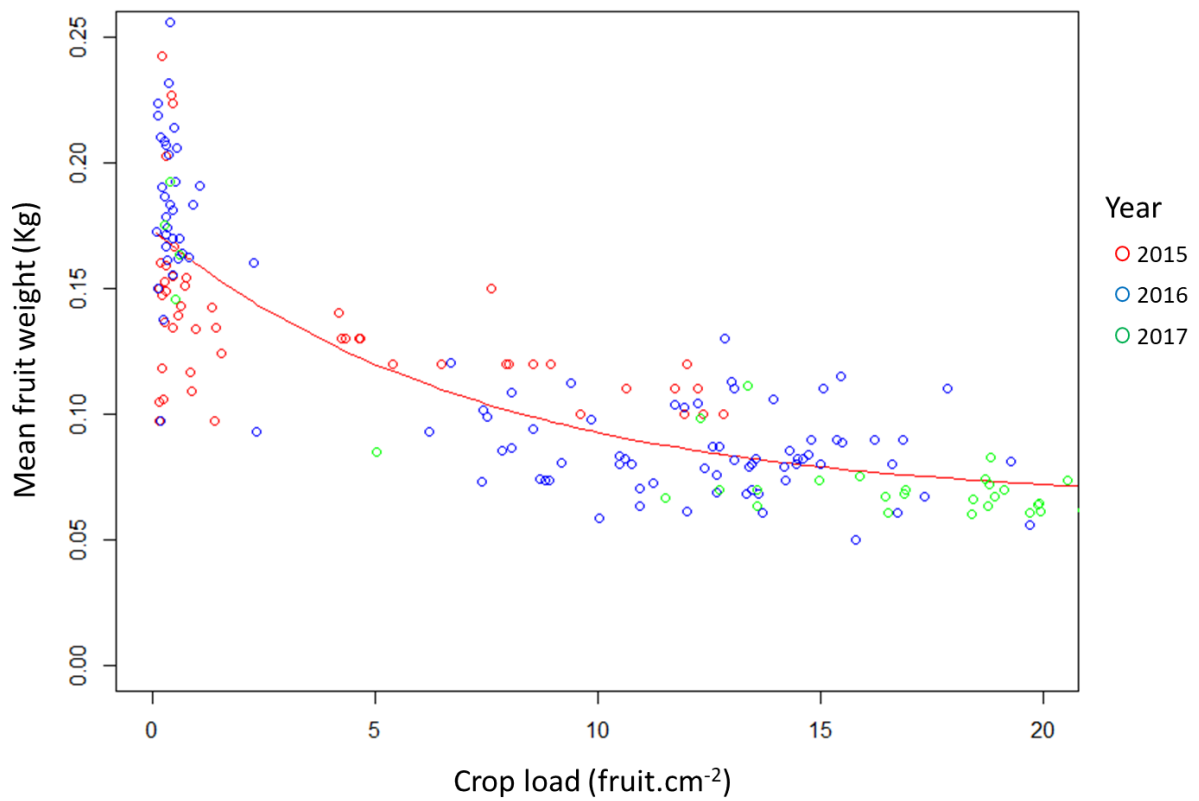


Figure S2. Relationship between crop load and mean fruit weight estimated on the additional ‘Golden Delicious’ apple control trees in 2015, 2016 and 2017. The continuous line represents the result of the exponential adjustment over the whole dataset ($Y = 0.5 \times \exp(-0.2 \times x) + 0.06$). $R^2 = 0.71$ between fitted and observed values.

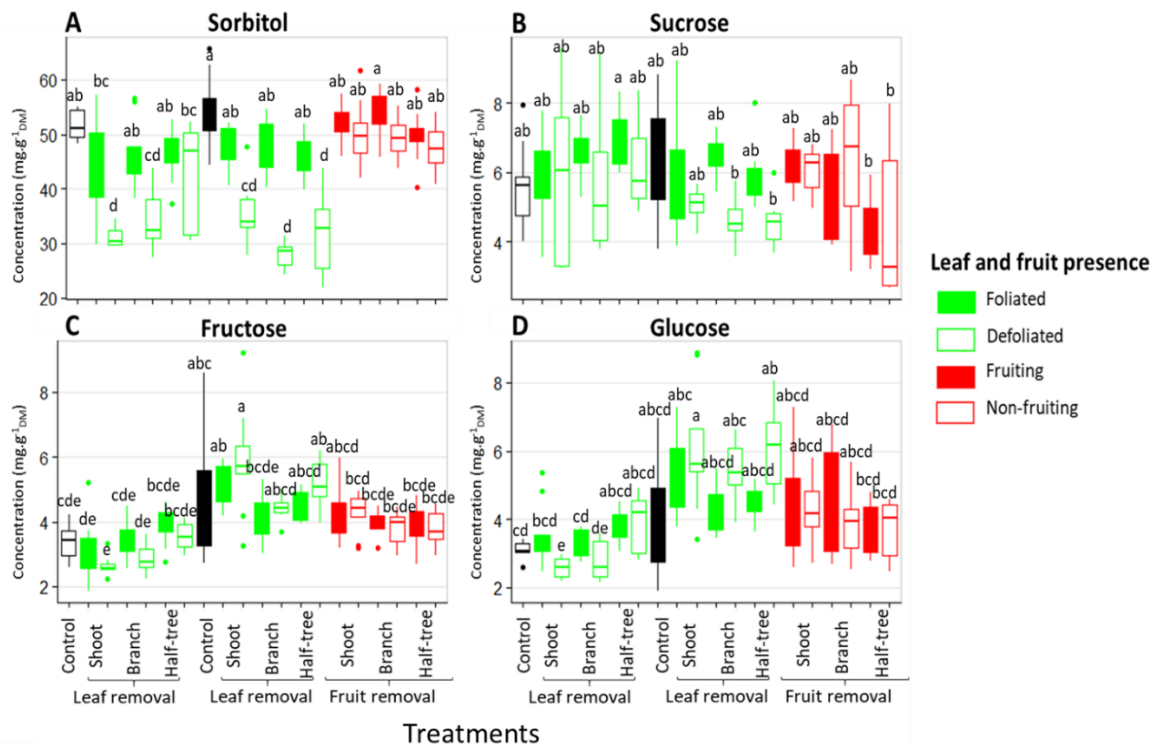


Figure S3. Boxplot representation of sorbitol (A), sucrose (B), fructose (C) and glucose (D) concentration in shoot apical meristems of ‘Golden Delicious’ apple trees for the different combinations of tree treatment, tree scale at which treatments were performed and conditions (leaf or fruit presence) within the trees. Nine replicates were used for each treatment combinations (3 samples \times 3 trees). Treatment effect was estimated with a one-way-ANOVA considering all the combinations together. *** significant at $P < 0.001$. A Tukey’s HSD test for pairwise comparisons was made after the analysis and different letters indicate statistically different values among all treatments.

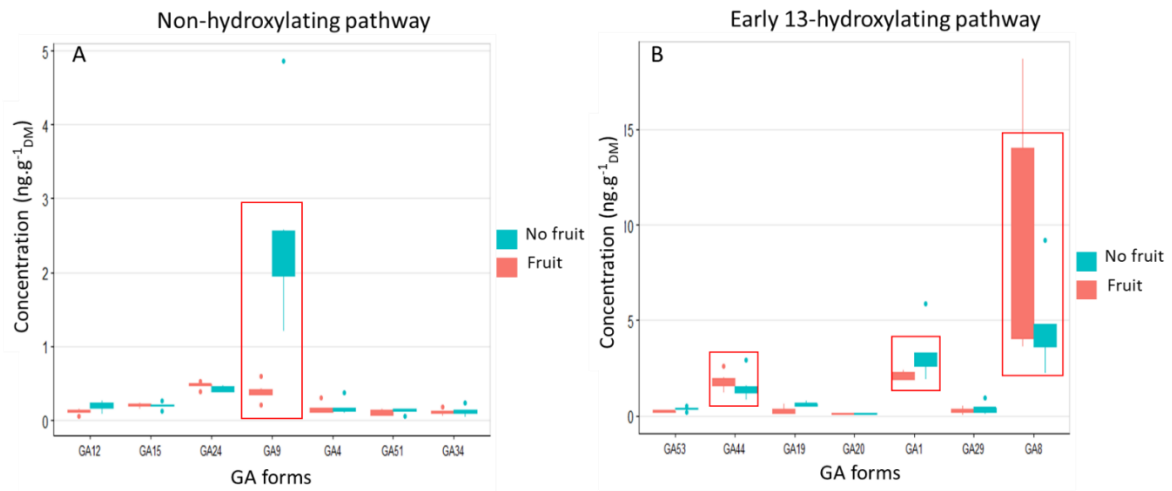


Figure S4. Boxplot representation of concentrations of all gibberellin forms ($\text{ng}\cdot\text{g}^{-1}$) from the non-hydroxylating (A) and the early-13-hydroxylating (B) pathways in shoot apical meristems of 'Golden Delicious' apple with or without fruits at 58 days after full boom. Samples were gathered according to fruit presence at the base of the shoot bearing the shoot apical meristem whatever the treatment to which trees have been subjected.

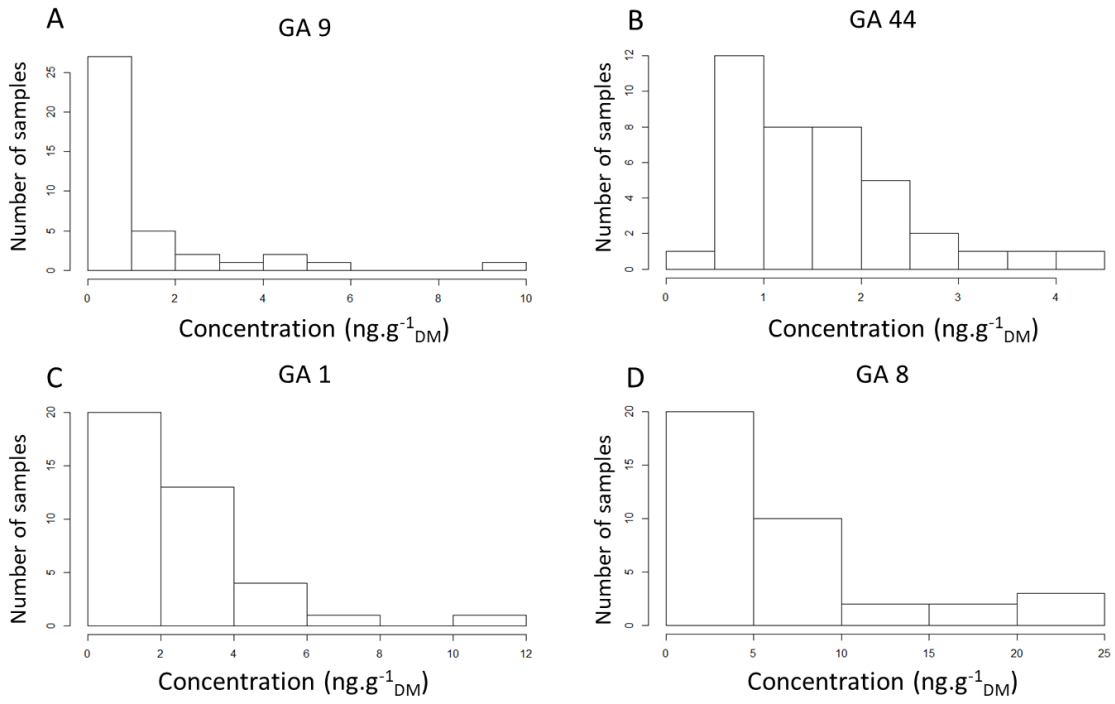


Figure S5. Distribution of concentrations of GA9 (A), GA44 (B), GA1 (C) and GA8 (D), in shoot apical meristems of 'Golden Delicious' apple trees for all the studied treatments at 58 days after full boom.

IV. Modelling transport of inhibiting and activating signals and their combined effects on floral induction: application to apple tree

This chapter corresponds to a scientific paper already published in Scientific Reports.

<https://doi.org/10.1038/s41598-020-69861-8>

1. Résumé

L'induction florale (IF) dans les méristèmes apicaux (SAM) est supposée être déclenchée par des signaux endogènes et antagonistes. Dans les arbres fruitiers, l'IF se produit uniquement dans une partie des SAM et est déterminée par des signaux activateurs ou inhibiteurs provenant respectivement des feuilles et des fruits. Nous avons développé un modèle pour quantifier sur des structures 3D l'effet combiné de ces signaux et des distances auxquelles ils agissent sur les SAM. Le transport du signal a été simulé en considérant un paramètre d'atténuation du signal, tandis que le devenir des SAM a été déterminé par des fonctions de probabilité qui dépendent des quantités de signal qui atteignent le SAM. Le comportement du modèle a été évalué sur des structures simples avant d'être calibré et validé sur un jeu unique de données expérimentales de pommiers numérisés en 3D avec des charges en fruits contrastées et soumis à la suppression des feuilles et des fruits à différentes échelles d'organisation des arbres. Les estimations des paramètres du modèle et les comparaisons de deux fonctions de combinaison de signaux nous ont amenés à formuler de nouvelles hypothèses sur les mécanismes impliqués dans l'IF: (i) le signal activateur pourrait être transporté à des distances plus courtes que le signal inhibiteur (environ 50 cm vs 1 m) (ii) les deux signaux agissent conjointement pour déterminer l'IF. Par ailleurs les SAM sont apparus comme étant plus sensible au signal inhibiteur qu'activateur. Enfin, la généralité du modèle paraît prometteuse pour étudier plus en détail le déterminisme physiologique et architectural de l'IF dans des plantes présentant des systèmes ramifiés.

2. Abstract

Floral induction (FI) in shoot apical meristems (SAM) is assumed to be triggered by antagonistic endogenous signals. In fruit trees, FI occurs in some SAM only and is determined by activating and inhibiting signals originating from leaves and fruit, respectively. We developed a model to quantify on 3D structures the combined impact of such signals and distances at which they act on SAM. Signal transport was simulated considering a signal 'attenuation' parameter, whereas SAM fate was determined by probability functions depending on signal . Model behavior was assessed on simple structures before being calibrated and validated on a unique experimental dataset of 3D digitized apple trees with contrasted crop loads and subjected to leaf and fruit removal at different scales of tree organization. Model parameter estimations and comparisons of two signal combination functions led us to formulate new assumptions on the mechanisms involved: (i) the activating signal could be transported at shorter distances than the inhibiting one (roughly 50 cm vs 1m) (ii) both signals jointly act to determine FI with SAM being more sensitive to inhibiting signal than activating one. Finally, the genericity of the model is promising to further understand the physiological and architectural determinism of FI in plants.

3. Introduction

Timing and intensity of floral induction (FI) are key processes in plants that strongly determine their reproductive ability. Most of the fruit trees have the particularity to induce floral transition in meristems the year before flowering (Monselise and Goldschmidt, 1982) and in part of the population, only (Wilkie *et al.*, 2008). FI usually takes place in spring when fruit growth also occurs, which can in turn affect vegetative growth and the proportion of meristems that are floral induced. The most known illustrations of this potential conflict between growth and FI are biennial bearing and masting that are associated with one year of high flowering intensity following one or many years of low fruit load (Samach and Smith, 2013). Moreover, within a tree canopy, meristems are subjected to contrasted conditions due to variations in microclimate, shoot polymorphism or fruit location (Costes *et al.*, 2008). Such variations in local conditions can affect flowering as shown by the positive correlation between shoot length and FI (Nielsen and Dennis, 2000; Lauri and Trottier, 2004), or by the decreasing proportion of FI in fruiting tree parts (Palmer *et al.*, 1991). Several hypotheses have been proposed to explain the existing within-tree and between years variability in FI (Wilkie *et al.*, 2008; Hanke *et al.*, 2007). Among them, the competition for carbon under high crop load conditions could explain FI inhibition. This assumption is consistent with the differential expressions of genes involved in carbon metabolism between meristems of apple trees subjected to defruited or fruited conditions (Guitton *et al.*, 2016). Nevertheless, experimental findings suggest that the tree carbon economy is not directly involved in FI control in apple (Belhassine *et al.*, 2019). Another assumption, based on seedless varieties, considers that FI is probably affected by inhibiting signals produced by seeds of fruit, mainly gibberellins (GA) (Dennis and Nielsen, 1999). Other molecules could also be implicated to activate FI such as FLOWERING LOCUS T (FT) protein produced by leaves and considered as the florigen (Hanke *et al.*, 2007; Corbesier and Coupland, 2006).

In a previous study (Belhassine *et al.*, 2019) the impact of leaf and fruit presence on within-tree FI variability was investigated in 'Golden Delicious' cv. Results confirmed the existence of promoting and inhibiting signals, originating from leaves and fruit, respectively. This study also showed (i) that FI was determined not only by the local conditions at the shoot scale but also by the fruit number and leaf area in the neighborhood and (ii) that the intensity of these signals strongly decreases with the distance between meristems and emitting sources. Finally, and consistent with other studies (Corbesier and Coupland, 2006), the existence of signal transport in both acropetal and basipetal directions within the tree was suggested. This previous study (Belhassine *et al.*, 2019) provided a strong experimental background from which it could be possible to infer and quantify the respective effect of inhibiting and activating signals in the within tree variability in FI, as well as their combined effects and the distance at which the emitting organs can act.

Mathematical models applied to plant growth and development are promising tools to analyze the impact of hidden processes not directly accessible from experiments through model parameter fitting procedures and subsequent interpretation of parameter values (Cournède *et al.*, 2011). In the current case of analysis of the within-tree variability in FI, functional structural plant models appear highly relevant (Vos *et al.*, 2009). They can combine an explicit description of plant architecture (topology and organ geometry) together with the simulation of transport of different types of molecules (water, carbon, hormones, etc.). These models rely on mathematical formalisms developed to describe and simulate plant architectural development such as multi-scale representation (Godin and Caraglio, 1998), strings of customized plant modules in L-Systems (Lindenmayer, 1968) or graphs (Hemmerling *et al.*, 2008). Within-plant fluxes or molecule transports have been modeled in FSPM with a special consideration on carbon allocation (Lacointe, 2000). It is usually assumed that assimilates are allocated depending on sink demand and distances between sources and sinks with an impact of distances modulated by an empirical resistance (Balandier *et al.*, 2000; Lescourret *et al.*, 2011; Pallas *et al.*, 2016). More mechanistic models are based on an electric analogy for describing carbohydrate movements within the phloem (Allen *et al.*, 2005) or include a mechanistic modeling of coupled phloem/xylem transport (Seleznayova *et al.*, 2018). Signal fluxes

within plants have also been modelled, especially for the simulation of basipetal auxin transport and its consequence on bud outgrowth (Prusinkiewicz *et al.*, 2009; Renton *et al.*, 2012) on small single stem plants, without complex branching systems (*Arabidopsis Thaliana*, pea). In apple tree, initial models have been proposed to simulate inhibiting and activating signal transports and their consequences on FI (Pellerin *et al.*, 2012; Pallas *et al.*, 2016). By changing manually signal quantity thresholds inducing flowering, these models were promising to represent biennial bearing. However, they were not calibrated on observed data.

In this study, we built a model that simulates the transports of both inhibiting and activating signals in 3D branching structures with the aim to further analyze the determinants of FI in fruit trees. This model was adapted from two previous ones, for carbon allocation (Reyes *et al.*, 2019) and for bidirectional transport (Pallas *et al.*, 2016). The model assumes a decrease in signal quantity with the distances from the emitting sources. FI in shoot apical meristems (SAM) was simulated based on inhibition and activation probability laws depending on both the quantity of inhibiting and activating signals. By fitting the model to a unique dataset on 3D digitized apple trees manipulated for their number of leaves and fruit (Belhassine *et al.*, 2019), we quantified the combined impact of such signals and distances at which they act on SAM within trees and explored the underlying mechanisms that could explain within tree variability in FI.

4. Material and methods

4.1. Model overview

The model was developed in Python and uses libraries from the OpenAlea platform (Pradal *et al.*, 2008). The model runs on 3D tree architectures coded in Multiscale Tree Graphs (MTG) (Godin and Caraglio, 1998) with three scales (tree, stem segments and metamers) and augmented with organ 3D coordinates (Godin *et al.*, 1999). Segments are the parts of the stem between two branching points or one branching point and the axis extremity. Metamers are represented for the stem segments corresponding to the most recent shoots only and are composed of one leaf, one internode and an inflorescence if present (Supplementary Information Fig. S1). Fruit and leaves produce signals moving within the structure depending on the distance with an ‘attenuation’ parameter that can be tuned in order to simulate different signal distributions i.e. homogeneity within the structure or local supply. These signals reach SAM and determine their fate with probabilities depending on signal quantities. FI is simulated on the SAM located in terminal position of annual shoots. In its current version the model runs on static tree structures, consistent with our modeling aim since FI usually occurs after the end of shoot vegetative growth in adult apple trees (Foster *et al.*, 2003).

4.2. Inhibiting and activating signal amounts and transport

Equations for signal transport (inhibiting and activating) between annual shoots and SAM were adapted from previous studies dedicated to carbon allocation between sources and sinks (Balandier *et al.*, 2000; Reyes *et al.*, 2019). These formalisms consider carbon allocation as dependent on distances between sources and sinks and on sink strength values depending on organ type and age. In our case, SAM are considered as target organs for inhibiting and activating signal with similar abilities to accumulate inhibiting or activating signal whatever the SAM. Annual shoots are considered as sources of inhibiting and activating signals originating from fruit and leaves, respectively. The quantity of signal originated from each annual shoot is computed as the sum of signals coming from each individual fruit and leaf in a given shoot. Since the equation previously proposed (Reyes *et al.*, 2019) considered relative values of sink strength, the signal distribution from each annual shoot was rewritten to account for similar SAM abilities to accumulate signals as follows:

$$q_{ij} = \frac{Q_i \times \frac{1}{1 + d_{ij}}^r}{\sum_{k=1}^n (Q_i \times \frac{1}{1 + d_{ik}}^r)} \quad (1)$$

where n is the number of SAM in a tree, q_{ij} is the quantity of signal exported by annual shoots (inhibiting or activating signal) i to SAM j , Q_i the quantity of signal produced by annual shoot i , d_{ij} the distance following the topological pathway between i and j and r an ‘attenuation’ parameter modulating the distance effect. For r values close to 0, the signal is equally distributed within the structure whereas it is transported at shorter distance when r values increase (Fig. 1a). Assuming that r can be different depending on the type of signal considered (inhibiting or activating signal), we defined two parameters, r_- , r_+ for the inhibiting and activating signal, respectively. We considered a normalized value equal to 1 for the inhibiting signal produced by each fruit. In order to account for a possible effect of the variations in leaf area between shoots on FI, we set the quantity of activating signal as equal to individual leaf area. For consistency with the parameters associated with inhibiting signals, variables and parameters associated with activating signal were normalized (ranging between 0 and 1) by dividing their value by the mean shoot leaf area observed in trees.

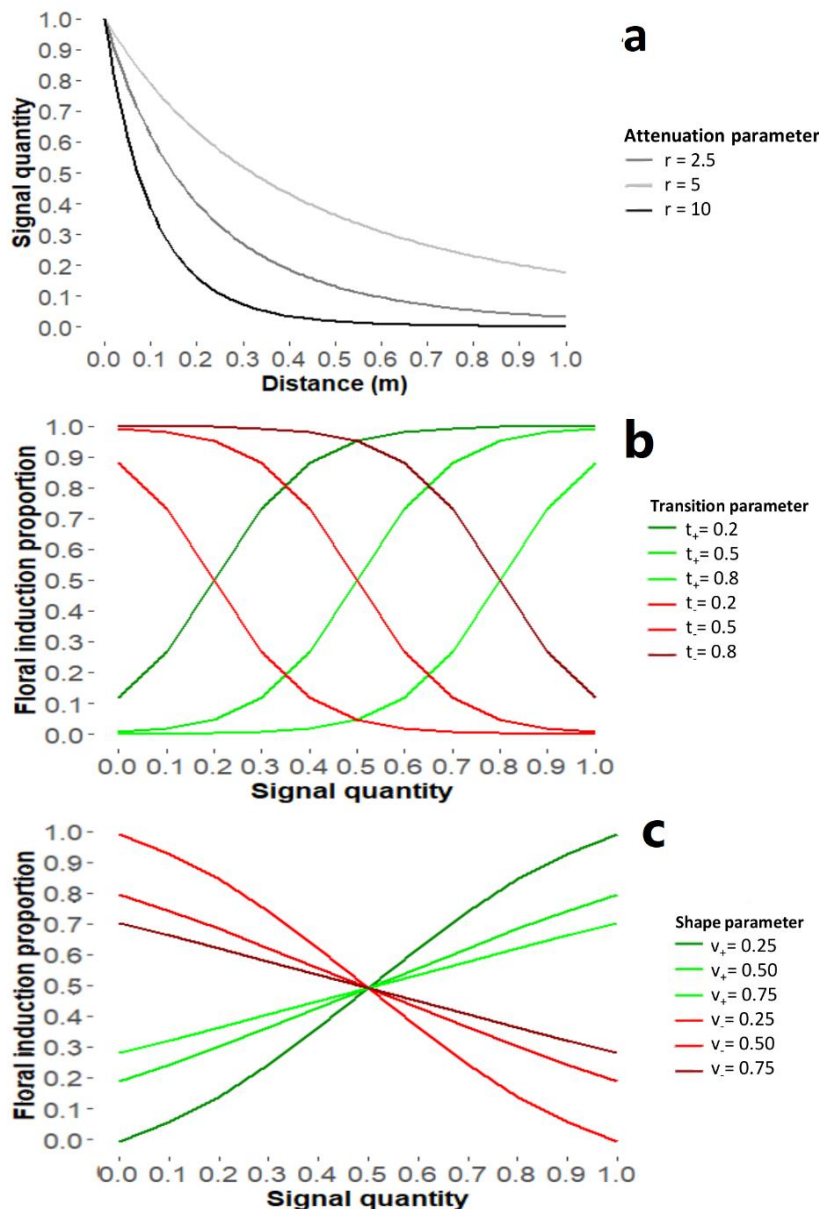


Figure 1. Representation of equations for signal transport and effects on floral induction. (a) Relationship between distance to meristems and signal quantity (activating and inhibiting) for different signal ‘attenuation’ values (r_- , r_+), (b) Relationship between signal quantity (activating and inhibiting) and floral induction proportions for different ‘transition’ values (t_- , t_+), (c) Relationship between signal quantity (activating and inhibiting) and floral induction proportions for different ‘shape’ values (v_- , v_+).

After computations of fluxes, the quantity of signal (Supplementary Information Fig. S3) reaching each SAM j (Q_{Fj}) is then computed as the total quantity of signal originated from all the sources including the shoot bearing the considered SAM:

$$Q_j = \sum_{i=1}^N (q_{ij}) \quad (2)$$

Where N is the number of annual shoots. In the following Q_F^+ and Q_F^- are used for the quantity of activating and inhibiting signal, respectively.

Distances between SAMs and shoots are computed based on the organ topological position and 3D coordinates in the MTG. The distance d_{ij} between shoots and SAM (i, j) in the tree structure is computed as the sum of the Euclidean distances between (i) the base and the barycenter of each annual shoot, (ii) plus the distances between the successive bases of the plant components and the SAMs in the topological path (iii) plus the distance between the base of the annual shoot bearing the SAM and its extremity²⁹.

4.3. Computation of floral induction probability

A sigmoidal function is used to compute the probability of FI (P_j) associated with the activating produced by leaves (P_j^+) or inhibiting signal quantity produced by fruit (P_j^- by the fruit) for each SAM j , as follows:

$$P_j^+ = \frac{1}{1 + \exp\left(\frac{-(Q_j - t_+)}{v_+}\right)} \quad \text{and} \quad P_j^- = 1 - \frac{1}{1 + \exp\left(\frac{-(Q_j - t_-)}{v_-}\right)} \quad (3)$$

with, t_+ and t_- being parameters called 'transition' values (Fig. 1b) indicating the signal quantity (Q_F^+ or Q_F^-) for which SAM have 50% chance to be activated or inhibited and v_+ and v_- parameters called 'shape factor' accounting for variations in the slope of the function. When v_+ or v_- are close to 0, the probability changes rapidly from 0 to 1 when the values of Q_F^+ or Q_F^- exceed or fall behind t_+ or t_- whereas the transitions are more progressive when v_+ or v_- values increase (Fig. 1c).

These parameters are used to represent some uncertainty in SAM fate (floral induced or not) for a given value of inhibiting and activating signals.

Two formalisms were considered for combining the effect of fruit and leaves on FI. In the first one, FI probability (P_j) in SAM j is determined by the most limiting factor only:

$$P_j = \min[P_j^-, P_j^+] \quad (4)$$

In the second formalism a cumulative effect of both signals determines SAM FI probability, assuming a multiplicative function:

$$P_j = P_j^- \times P_j^+ \quad (5)$$

4.4. Model behavior assessment on simple structures

The model was applied to simple tree structures in order to analyze model consistency and sensitivity to parameter values. The first structure consisted of a branch composed of six shoots equidistant from each other, bearing or not leaves or fruit. Here, we aimed at testing the effect of the signal 'attenuation' parameter (r, r_+) on the quantity of signal reaching SAMs located at different distances from signal sources.

The second application was performed on two complete branches with different spatial distributions of fruit and leaves. In a first case, fruit and leaf distributions were similar in the two branches, with half of the shoots bearing either fruit or leaves. In the second case, all the fruit or leaves were located on one branch only and the other one was completely either defruited or defoliated. Here we aimed at testing a wide range of signal 'attenuation' (r, r_+) and 'transition' parameter (t, t_+)

values in order to evaluate the intertwined effects created by the model, between tree architecture, signal transport and SAM sensitivity to the quantity of signals.

Lastly, we analyzed model formalisms (“limiting factor”, “multiplicative formalism”; equations 4&5) used to integrate the combined effects of inhibiting and activating signals on SAM FI. We used a structure composed of four contrasted branches, i.e. a leafy and fruiting branch, a foliated branch without fruit, a fruiting branch without leaf and a defoliated and non-fruiting branch. The two formalisms were used with a wide range of ‘transition’ values (t_-, t_+) to modify the SAM sensitivity to both signals.

4.5. Description of the experimental dataset

Data used for building the tree 3D representations and for calibration and validation purpose were taken from experiments carried out in 2017 on 10-year-old apple trees (cv. ‘Golden Delicious’) orchard, located at the SudExpé experimental station in Marsillargues, in the south of France (43°66’N 4°18’E). In this experiment described in Belhassine *et al.* (2019), leaves and/or fruit were removed in different parts of the tree (Supplementary Information Fig. S2). On trees set in ON (high fruit load) or OFF (crop load close to 0) conditions, fruit or leaves were removed on half of the shoots and half of the branches of trees trained as “solaxe” (one main vertical trunk) and on one side of trees with a Y-Shape (two main trunks). An additional set of trees not subjected to fruit or leaf removal but displaying a natural variability in crop load were observed during three years (2015-2016-2017).

SAM FI proportion in trees was estimated at full bloom in the spring following treatment onset, as the ratio of the total number of reproductive buds to the total number of growing buds in the different parts of the trees (leafy, non-leafy or fruiting, non-fruiting). Tree crop load was estimated as the fruit number at harvest divided by the trunk cross sectional area (TCSA, cm²) estimated in autumn after fruit harvest (Wünsche *et al.*, 2000).

4.6. Input architectures

Architecture description was performed on one “solaxe” tree and one Y-shape tree displaying TCSA values (20.4 and 24.7 cm², for solaxe and Y-Shape trees, respectively) close to the mean values observed in the orchard. 3D coordinates were acquired using an electromagnetic 3D digitizer (3Space Fastrak; Polhemus Inc., Colchester, VT, USA) at the trunk base, branching points and top and bases coordinates of each annual shoot (Supplementary Information Fig. S1). The 3D structures, including tree entities organized in three topological scales and their coordinates, were saved in MTG format and used to reconstruct leaf location and area along annual shoots and to reproduce *in silico* experimental treatments of leaf and fruit removal. Leaf area distribution along annual shoots was reconstructed based on allometric relationships as previously proposed (Sonohat *et al.*, 2006) (Supplementary Information Methods S1). To build allometric relationships, data were collected on both 60 short (<5cm) and long shoots (>5cm) and individual leaf areas were estimated with a leaf area meter (LI 3100 Area Meter, LI-COR, Lincoln, NE, USA) every three leaves along the shoots. Mature leaves were sampled after fruit harvest to build these allometric relationships. On ON trees, one fruit was added in the MTG at the base of each annual shoot (consistent with thinning practices in the field).

4.7. Estimation of parameter values and model assessment

The model output extends the MTG with new attributes for each SAM j corresponding to the quantities of activating and inhibiting signals reaching it after transport ($Q_{F,j}^+$ and $Q_{F,j}^-$), its probability of FI associated with received activating (P_j^+) or inhibiting signals (P_j^-) and its final FI probability combining both signals (P_j). Parameters associated with either activating or inhibiting signal effects on FI were estimated separately on leaf and fruit removal treatments, respectively. Activating signal parameters (r_+, t_+, v_+) were estimated on non-fruiting structures subjected to leaf removal at

different scales (shoot, branch, and half-tree) or not (control OFF trees). Inhibiting signal parameters (r , t , v) were estimated on leafy and fruiting tree structures subjected to fruit removal at different scales (shoot, branch and half-tree) or not (control ON trees) and on leafy non-fruiting tree structure (control OFF trees). Simulated FI proportion (i.e. proportion of meristems that were floral induced) were compared to the observed FI ones in the different parts of the trees (leafy or non-leafy, fruiting or non-fruiting). Simulated proportions were computed as the average FI probability of each bud in the different parts of the trees. The parameter values of the simulation displaying the lowest error between simulated and observed FI for all conditions (tree and local treatments) were selected as the best solution in the calibration procedure. Two steps in the calibration procedure were done. A first step consisted in exploring a wide range of values by varying r_+ and r_- from 0 to 15 (step = 0.1), t_+ , t_- from 0 to 1 (step = 0.1) and v_+ and v_- between 0.01, 0.1, 0.3 and 0.6 for activating and inhibiting signals respectively (6644 simulations in total). In a second step, the range of values close to the best solutions was narrowed down to refine estimations (1155 simulations).

Model validations were performed in two steps. First, the two sets of parameter values for activating and inhibiting signals obtained from calibration were used to simulate FI probability in fruiting trees subjected to leaf removal. The two functions which represent the combined effect of both signals on SAM FI, i.e. with a “limiting factor” or a multiplicative formalism, were compared through simulated SAM FI proportions. Second, validations were performed on the digitized “solaxe” tree on which contrasted crop loads were obtained by *in-silico* fruit removal. FI proportions simulated for these different *in silico* crop loads were compared to the relationship between FI and crop load obtained from the additional trees displaying contrasting crop load in the experiment.

Model calibration and validation quality was evaluated using RMSE (root mean square error), bias (absolute sum of differences divided by replicate number) and R^2 between observed and simulated values.

5. Results

5.1. Model behavior and sensitivity to model parameters

The ‘attenuation’ parameter of the inhibiting signal (r) was varied on a simple structure composed of six shoots located at an equal distance from each other (15 cm) and with three sources (fruit) (Fig. 2a). When no signal ‘attenuation’ ($r=0$) was considered, inhibiting signal was equally transported to the six SAMs (Fig. 2b): each one had an inhibiting signal value equal to 0.5 which represented the number of fruits divided by the shoot number. When r values are increased, the quantity of inhibiting signal reaching each meristem (Q_F^-) increased and decreased in SAM of fruiting and non-fruiting shoots, respectively. For the highest values of r (roughly over 15) Q_F^- was equal to 0 in the SAM of non-fruiting shoot and 1 in the ones of fruiting shoots. When considering medium values of r , differences between fruiting and non-fruiting shoot resulted from the distance of each shoot to the other ones. Among non-fruiting shoots, the ranking of Q_F^- in SAM depended on its distance to all fruit, with SAM of shoot 3 (sum of distances to the fruit=45 cm) displaying the highest quantity, SAM 6 (90 cm) the lowest and SAM 5 (75 cm) a medium value.

Similarly, SAM 1 and 2 of fruiting shoots displayed higher Q_F^- than SAM 4 because they were located close to each other and could exchange inhibiting signal. In another simulation set, the sources of activating (leaves) signals were varied on the same simple structure considering leafy and non-leafy shoots to analyze the effect of attenuation parameter associated with activating signal (r_+) on activating signal quantity in SAM (Q_F^+ , Supplementary Information Fig. S3). Similar results for the signal quantities variations in SAM were obtained since model assumptions were symmetric for both inhibiting and activating signals.

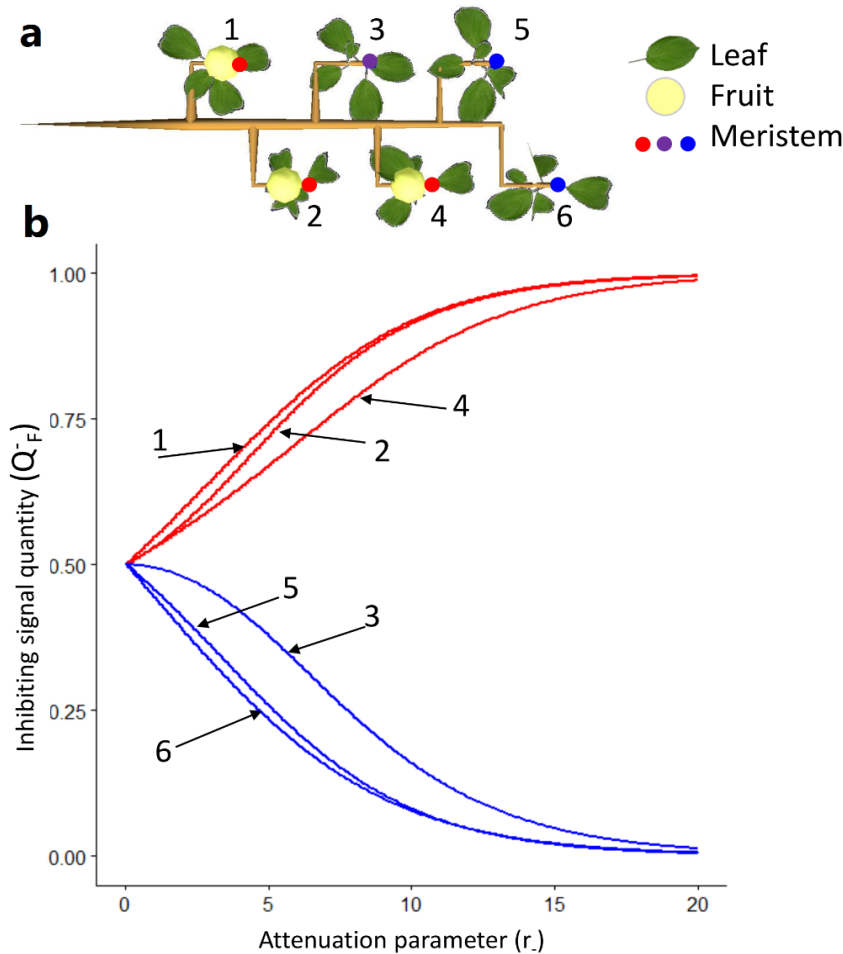


Figure 2. Inhibiting signal concentration (Q_F^-) in six meristems for different values of the signal ‘attenuation’ parameter ($r.$) (b). Simulations were performed on a simple structure composed of six shoots and three fruit, each shoot being located at 15 cm from each other (a). 1, 2 and 4 are fructing shoots and 3, 5 and 6 are non-fructing shoots.

The impact of the signal ‘attenuation’ ($r.$) and ‘transition’ parameters ($t.$) on SAM floral induction probability depending on inhibiting signal (P^-) was assessed on simple structures composed of two branches with contrasted location of fruit (random fruit removal on both branches, Fig. 3d; one fructing and one non-fructing branch, Fig. 3a). On the two structures and except for $r.= 0$ (homogeneous distribution of signal between each SAM), P^- was higher in SAM located on non-fructing branches or shoots than in SAM located in fructing branches or shoots (Fig. 3b,c). The contrast in P^- between fructing branches/shoots and non-fructing ones increases when $r.$ values increase due to transport of the inhibiting signal at shorter distances (Fig. 3b,c). Moreover, the contrast in P^- between fructing and non-fructing parts was lower when fruit were removed randomly on both branches (Fig. 3e,f) than when removal was performed at the branch scale (Fig. 3b,c). This results from the lower distances between fructing and non-fructing shoots when fruit removal was performed on half of the shoots than between fructing and non-fructing branches when fruit removal was performed at the branch scale. The effect of $t.$ parameter (indicating the signal quantity threshold for which P^- was equal to 50%), was consistent with its expected impact as P^- increases when $t.$ increases. As expected from model equations, P^- was equal to 1 in all conditions when $t.$ was equal to 1. Model behavior was similar when considering the impact of leaf removal at different scales (shoot or branch, Supplementary Information Fig. S4) on floral induction probability associated with the activating signal (P^+) on the same two-branches structures since model hypotheses for inhibiting and activating signal were symmetric.

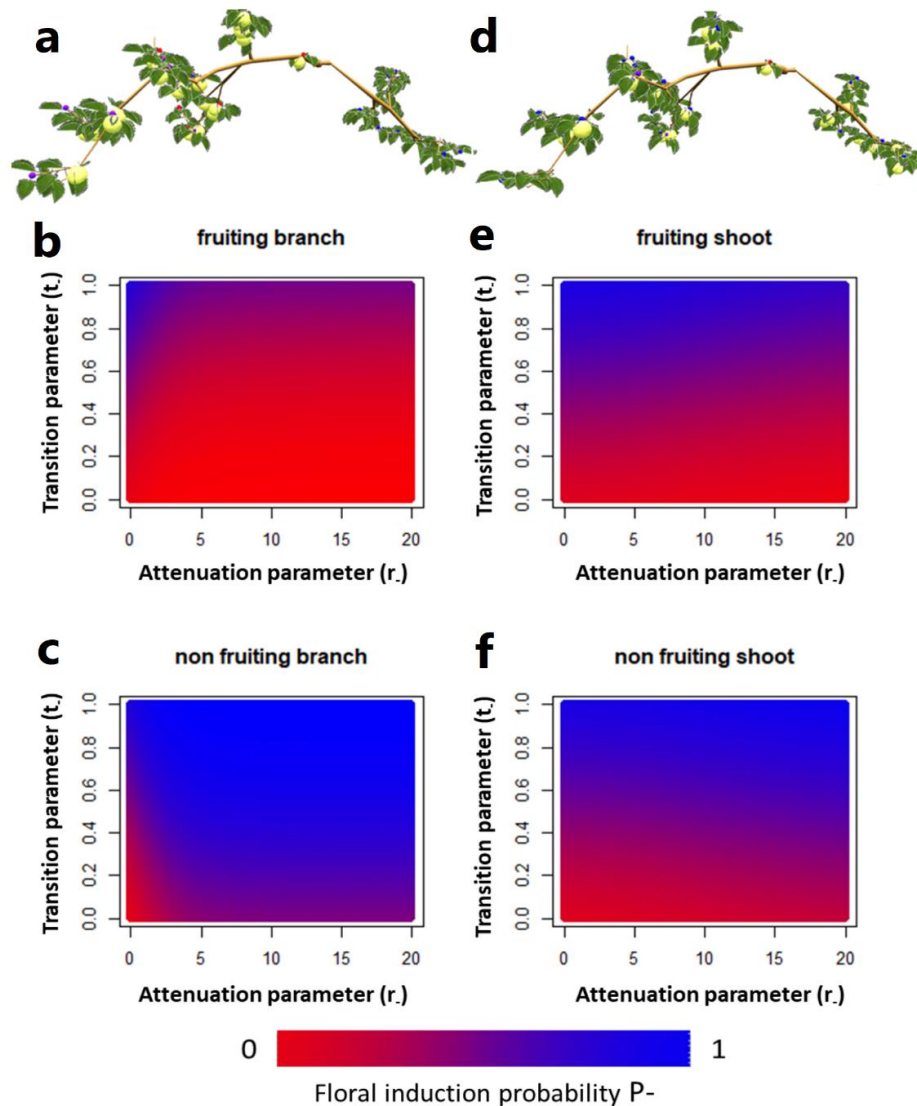


Figure 3. Mean floral induction probability (P) in shoot apical meristems depending on the quantity of inhibiting signal produced by fruit for different values of the signal ‘attenuation’ (r) (200 values) and ‘transition’ parameters (t) (100 values). Simulations were performed on two hypothetical structures composed of two branches with one fruiting and one non-fruiting branch (a) and two branches with homogeneous fruit removal on half of the shoots (d). (b) and (c) represent the mean floral induction proportion in fruiting and non-fruiting branches, respectively for the structure represented in (a). (e) and (f) represent the mean floral induction proportion in fruiting and non-fruiting shoots, respectively for the structure represented in (d). Simulations were performed assuming a shape parameter value (v) equal to 0.25.

Simulations were then performed to analyze model behavior when effects both of leaves and fruit are taken into account. In these simulations, resulting FI probability (P) were calculated by either the function assuming a limiting-factor (Supplementary Information Fig. S5) or the multiplicative (Fig. 4) formalism on simple structures composed of four branches bearing leaves and fruit or not. In these simulations, signal (inhibiting and activating) transport could occur between branches to simulate some inhibiting and activating signal quantities in non-fruiting and non-leafy branches, respectively. When medium values for ‘transition’ parameters ($t=t_r=0.5$) were considered, P was, as expected, the highest in non-fruiting and leafy branches, i.e. in presence of activating signal and in absence of inhibiting one, whatever the chosen function (multiplicative, Fig. 4 or limiting factor formalism, Supplementary Information Fig. S5). For the three other branch configurations and whatever the

formalism, P were close to 0 due to either high inhibiting signal quantity in fruiting branches (Fig. 4b 1,3; Supplementary Information Fig. S5b 1,3) or low activating signal quantity in non-leafy branches (Fig. 4b 3,4; Supplementary Information Fig. S5b 1,3). When varying the transition parameter values, lower P were simulated by the multiplicative formalism than by the limiting factor one. This was mainly observed for fruiting and foliated branches (Fig. 4b 1 and Fig S5b 1) and non-fruiting and defoliated branches (Fig. 4b 4 and Supplementary Information Fig S5b 4) when $t_- < 0.7$ and $t_+ > 0.3$, respectively. In those cases, an additional effect on P of the less-limiting factor (activating signal in foliated branches, or inhibiting signal in fruiting branches) was simulated by the multiplicative formalism. This effect was due to fruit presence in neighboring branches in the non-fruiting defoliated branch or leaf absence in the neighborhood for the fruiting leafy branch.

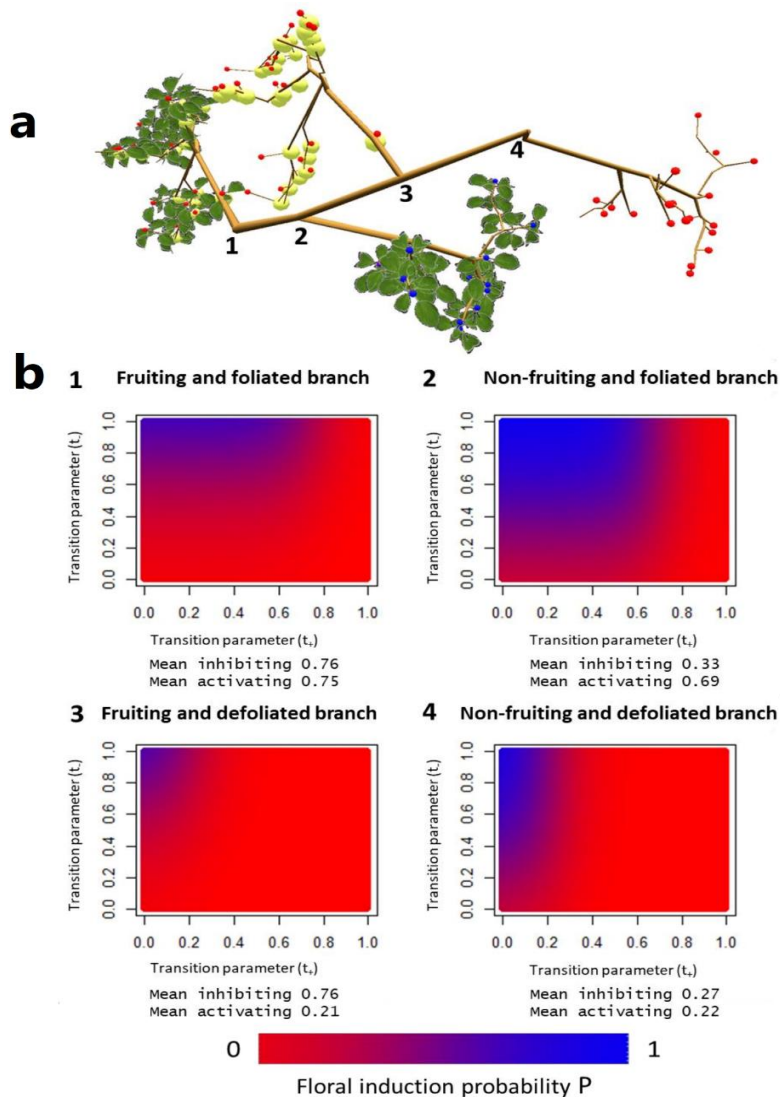


Figure 4. Mean floral induction probability (P) in shoot apical meristem for different ‘transition’ parameter values for the activating (t_+) and inhibiting (t_-) signals (100×100 values). Floral induction proportions were computed on a hypothetical structure composed of one fruiting and leafy branch (1), one non-fruiting and leafy branch (2), one fruiting and non-leafy branch (3) and one non-fruiting and non-leafy branch (4) (a). (b) represents the mean floral induction proportion in the different branches. Mean inhibiting and mean activating below the heatmaps represent the mean of the inhibiting and activating signals quantities for all meristems in each branch. Simulations were performed assuming a multiplicative effect of the inhibiting and activating signal on floral induction. In these simulations ‘shape’ parameters (v_-, v_+) equal to 0.25 and ‘attenuation’ parameters (r_+, r_-) equal to 2.5 were used.

5.2. Model calibration and associated parameters values

Model calibration performed separately on trees with leaf or fruit removal were highly relevant when confronting observed and simulated FI proportions in the different parts of the trees subjected to local fruit and leaf removal (Fig. 5). R^2 and RMSE were equal to 0.90 and 0.072 and 0.93 and 0.001, for the calibration performed on trees with leaf or fruit removal, respectively

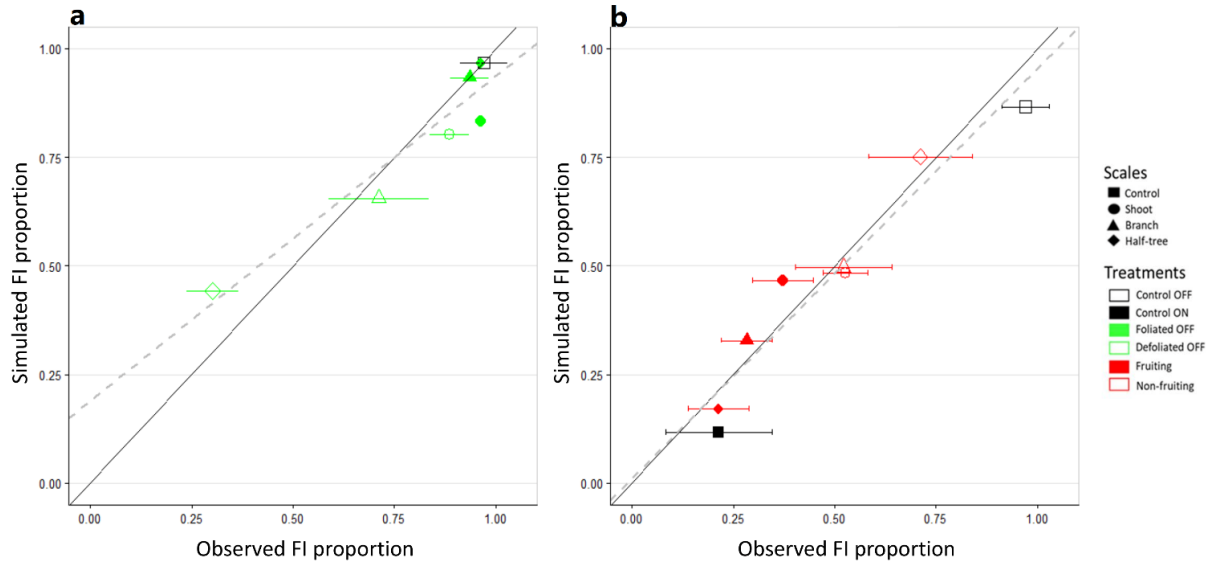


Figure 5. Observed and simulated floral induction proportions for the treatments used for calibration. Parameters associated with either activating or inhibiting signal effects on floral induction were estimated separately on leaf (a) and fruit removal (b) treatments, respectively. Treatments were performed by removing fruit or leaves on half of the shoot (shoot scale), or half of the branches (branch scale) or on one side of trees with a Y-Shape (half-tree scale). Bars represent the observed standard deviation in floral induction proportion (3 tree replicates). Continuous line represents the 1:1 line and the dashed ones are the linear fit between observed and simulated proportions ($R^2 = 0.90$ and 0.93 for a and b, respectively).

This calibration procedure resulted in a set of estimated parameters related to either activating or inhibiting signal. The estimated 'transition' parameter value (Table 1) was lower for the activating signal (0.09) than for the inhibiting signal (0.49), revealing that low quantities of activating signal were enough to trigger FI. The estimated signal 'attenuation' value was higher for the activating signal (5.0) than for the inhibiting one (2.9). These values correspond to roughly less than 10% of the emitted signal reaching a SAM when located at more than 1.2m or 0.5m from sources of activating and inhibiting signals (leaves and fruit), respectively (Supplementary Information Fig. S6). Estimated 'shape' parameter values were similar for both activating and inhibiting signals (0.25) and account for a noticeable uncertainty in SAM fate for a given quantity of signal. Indeed, although the 'transition' value for the inhibiting signal (0.49) represents the quantity of signal needed to reach a FI probability of 0.5, this probability was equal to 0.27 when the quantity of inhibiting signal was high (0.75) and still remained non null (0.11) for an quantity of signal equal to 1 (Supplementary Information Fig. S6).

Table 1 Values of ‘attenuation’ (r_+ , r_-), ‘transition’ (t_+ , t_-) and ‘shape’ (s_+ , s_-) parameters estimated for activating and inhibiting signals respectively and RMSE, R^2 and bias between observed and simulated FI proportion.

Calibration dataset											
Activating signal						Inhibiting signal					
r_+	t_+	s_+	RMSE	R^2	Bias	r_-	t_-	s_-	RMSE	R^2	Bias
5.0	0.09	0.25	0.116	0.90	0.072	2.7	0.47	0.25	0.059	0.93	0.001

Distributions of simulated FI probability depending on the quantities of inhibiting and activating signals in the different SAMs of trees subjected to either leaf or fruit removal provided additional information about the underlying signal and distance effects FI probability in the different tree parts (Fig. 6). Inhibiting and activating signal quantity were slightly lower in leafy compared to non-leafy parts and in non-fruiting parts compared to fruiting ones when removals were performed at the shoot scale (Fig. 6a,b). These small differences were consistent with the observed low differences in FI proportion between leaf/non-leafy or fruiting/non-fruiting shoots and resulted from the short distances between neighboring shoots within tree structures. Among shoots of a given type (leafy, non-leafy, fruiting, non-fruiting), variations in the quantity of inhibiting and activating signals were quite low when treatments were performed at the shoot scale. This likely resulted from (i) the low variation in the observed individual shoot leaf areas (e.g more than 75% of the shoots had leaf area between 80 and 120cm² in the “solaxe” tree, Supplementary Information Fig. S7) and (ii) because of the low variation of the number of fruits per shoot (all shoots were considered as bearing one fruit in ON trees).

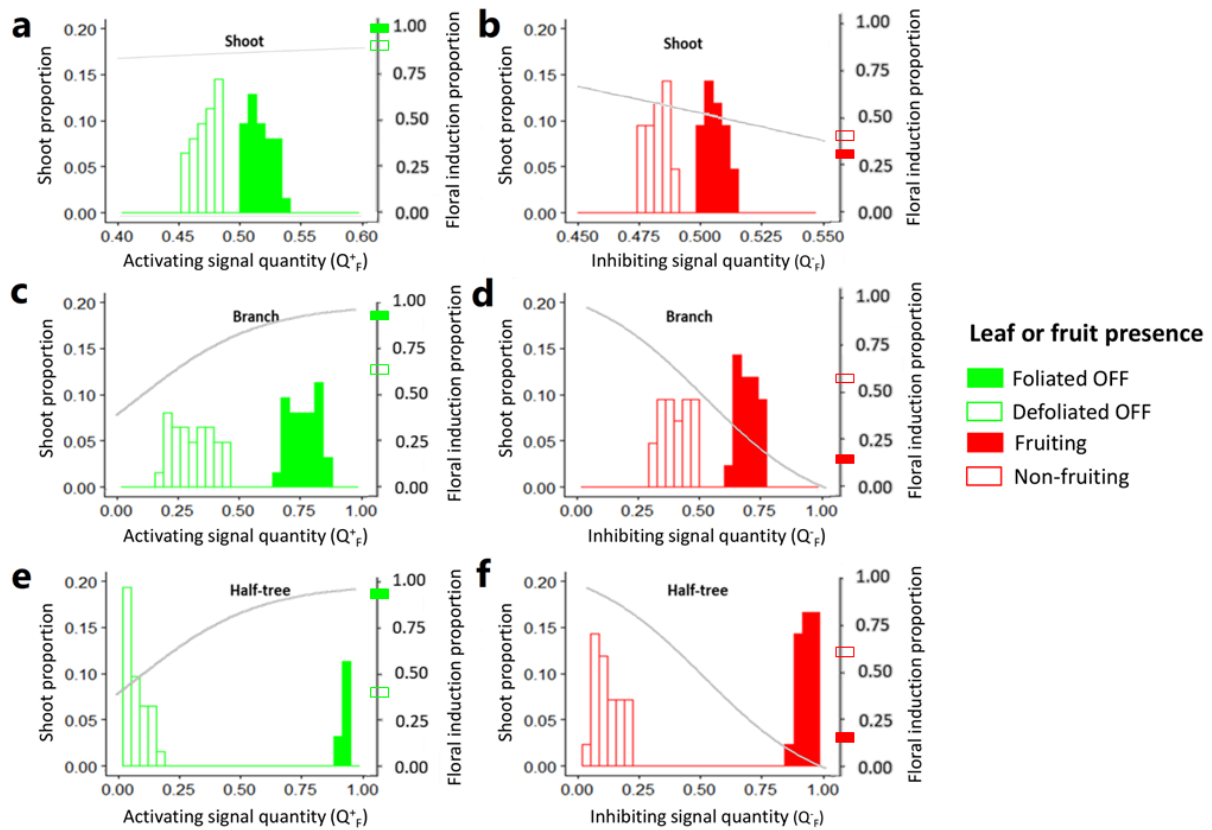


Figure 6. Distribution of simulated signal quantity in shoot apical meristem and resulting floral induction proportions depending on activating (a,c,e) and inhibiting (b,d,f) quantities in the different experimental conditions (see Belhassine et al., 2019 for details). Treatments were performed by removing fruit or leaves on half of the shoot (a,b), half of the branches (c,d) or on one side of trees with a Y-Shape (e,f). Shoot proportions depending on signal quantity are represented by bars and the resulting FI probability with a continuous grey curve. Crosses on Y axes and grey curves represent the observed and simulated FI proportions, respectively. Blank and colored crosses are used for the foliated/fruited tree parts and defoliated/defruited parts, respectively.

Differences in signal quantity (Q_F) between the different tree parts were stronger when organ removals were considered at coarser scales (branch or half-tree) with a greater impact of leaf/fruit removals on half-trees, consistent with the increasing distances to the remaining fruit or leaves (Fig. 6c,d,e,f). These differences were of greater extent for leaf removal than for fruit removal due to the higher estimated signal ‘attenuation’ parameter value for the activating signal (r^+) than for inhibiting one (r^-) (Table 1). Nevertheless, and consistent with observed data, the simulated impact of leaf removal on FI probability was lower than that of fruit due to lower estimated ‘transition’ parameter (t) values for the activating signal. Finally, quite large variability in signal quantities was obtained in the different SAMs of non-leafy (Q_F^+) and non-fruited parts (Q_F^-) when treatments were performed at the branch or half tree scale. This variability probably resulted from the spatial distribution of SAM within the tree, with SAM at branch bases closer to the sources of signals coming from other branches than ones located at branch extremities.

5.3. Signal combined effect and model validation

Model validation was performed on ON trees subjected to leaf removal at different scales (shoot, branch and half-tree) by using the set of parameters previously estimated and with the two formalisms proposed to account for their combined effects (limiting factor or multiplicative formalism, Table 2). Bias values showed that both formalisms underestimated the effect of signal combination on proportion of meristems that were floral induced. However, this bias was lower and

the differences among treatments were better simulated ($R^2=0.47$) with the multiplicative formalism. Nevertheless, the range of variation in the observed FI proportions was low, with FI proportion close to 0 in all the treatments considered. We thus performed another set of in-silico experiments to complement the validation step. Trees with contrasted crop loads (ratio of harvested fruit number to trunk cross sectional area) were represented by removing varying proportion of fruit on ON trees. FI proportion were in overall adequate agreement with the estimated relationship with tree crop load, built from field observations ($R^2=0.95$, RMSE= 0.112) (Fig. 7). Model outputs were in agreement with observations for crop load values higher than 5 fruit cm^{-2} and tended to underestimate FI proportions for lower crop load values. Nevertheless, differences between observed and simulated FI proportions remained lower than 10%.

Table 2 RMSE, R^2 and bias between observed and simulated FI proportion for the validation dataset and for the limiting factor or multiplicative formalism.

Validation dataset							
Range of variation (FI proportion observed value)	Limiting factor			Multiplicative formalism			
	RMSE	R^2	Bias	RMSE	R^2	Bias	
0.03-0.15	0.089	0.004	0.036	0.055	0.47	0.063	

Validations were performed using the calibrated sets of parameter values for activating and inhibiting signals. Simulations were performed on fruiting trees subjected to leaf removal at different scale (shoot, branch and half-tree).

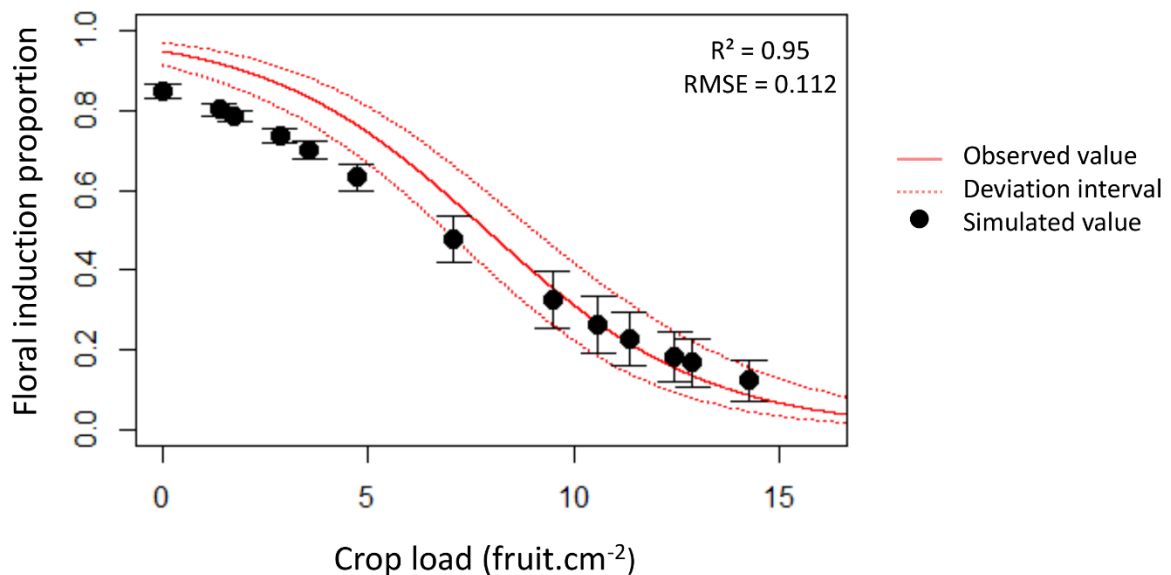


Figure 7. Simulation of floral induction proportions depending on crop load. Black points represent the simulated floral induction proportion for different values of crop loads using the set of parameters estimated after the calibration procedure. The continuous line represents the result of the exponential adjustment performed on experimental data ($y = \exp(-0.3721 \times x + 2.9273) / (1 + \exp(-0.3721 \times x + 2.9273))$). The relationship was built on “additional” control trees in 2015, 2016 and 2017. The dotted red lines represent the deviation interval of the fitted values. Bars represent the within tree standard deviation of FI in the simulations.

6. Discussion

6.1. A model-based approach for quantifying the respective roles of leaves and fruit on FI

This study proposes a new model that simulates for the first time FI variability in a fruit tree as the result of the combined effects of its architecture, inhibiting and activating signals and SAM sensitivity to these signals. The model proved its ability to represent experimental observations in which the within-tree distribution of inhibiting and activating sources were artificially modified (Belhassine *et al.*, 2019). It was also able to rebuild the relationship between tree crop load and the proportion of flowering SAMs in the next year as previously observed (Wünsche and Ferguson, 2005). The model assumes that signal attenuation is related to distances from emitting sources and that FI could be determined using probability functions depending on the combination of both signal quantities. It uses a generic formalism adapted for representing all types of plant architectures (MTG) (Godin and Caraglio, 1998). The proposed model could thus be applied to other fruit tree species in which FI varies within the tree and between years (e.g. peach, olive, plum and walnut trees). This study focused on FI proportion in SAM located in terminal position on annual shoots and did not account for meristem fate in axillary position along medium and long stems. This simplification is relevant for adult apple trees displaying short shoots mainly (Costes *et al.*, 2008). In the case of younger trees or other fruit trees bearing buds in axillary positions (e.g. *Prunus* sp.), our model would also be relevant for computing axillary flowering probability but it should be complemented with other sub-models to account for the position of axillary meristems in the flowering zones along the parent shoot (Costes *et al.*, 2014). Generating a potential floral zone in the tree structure could be achieved using statistical models, as done previously (Renton *et al.*, 2006), or more mechanistically by simulating shoot growth dynamics within the growing season (Miguault *et al.*, 2017). Indeed, FI occurrence was observed to be associated with a decrease in plastochron and shoot growth cessation (Crabbé, 1984; Lauri *et al.*, 1998).

Previous models for simulating signal transport in plants were developed to represent basipetal auxin polar transport at short distances within a monopodial stem (Prusinkiewicz *et al.*, 2009; Renton *et al.*, 2012). Our approach relied on a more general formalism previously proposed for source-sink models to represent fruit growth variability (Lescourret *et al.*, 2011; Pallas *et al.*, 2016; Reyes *et al.*, 2019). In our model, no preferential direction in signal fluxes was assumed as previous studies showed that fruit and leaf influence occurs in both acropetal and basipetal directions (Haberman *et al.*, 2016). In this tree structure, the quantity of inhibiting signal produced by each fruit was assumed to be similar, since it is associated with a constant seed number per fruit (source of GA) for a given genotype. The quantity of activating signal was assumed to be associated with shoot leaf area values based on previous results showing the close relationship between shoot vigor or length and FI (Lauri and Trottier, 2004).

6.2. Parameter estimation leads to new assumptions on the physiological process involved in the within-tree variability in floral induction

A heuristic approach was carried out by adjusting parameter values ('attenuation', 'transition' and 'shape' parameters) to a set of experimental data. The estimated parameter values allowed us to propose new hypotheses explaining the within tree variability in FI in apple trees.

The signal 'attenuation' parameters represent the distance effect and the decrease in the influence of fruit and leaves. It could be associated with the rate of hormone or protein accumulation or degradation during their transport from the emitting sources to SAM (Wolters and Jürgens, 2009). The estimated values of 'attenuation' parameters were relatively higher for the activating signal than for the inhibiting one. This result is consistent with the relatively short distance of the action of the florigen, i.e FT protein, in fruit trees (Freiman *et al.*, 2015; Putterill *et al.*, 2016). Molecules other than FT could have an activating effect on FI. Among them sugar signaling molecules such as trehalose-6-phosphate were observed to affect flowering time in *Arabidopsis thaliana* by inducing FT production

(Wahl *et al.*, 2013). The present study also provides quantitative support to the assumption of the relatively long-distance transport of an inhibiting signal originating from fruit that could correspond to a GA mobile form, especially GA12 that was observed to be transported in small plants (Regnault *et al.*, 2015; Binenbaum *et al.*, 2018). However, molecules other than GA could also be involved such as auxin that can act as a second messenger and can be transported over long distances (Hanke, 2007).

The 'transition' parameter represents the sensitivity of SAMs to the quantity of signals they receive. The estimated values suggest that a low quantity of activating signal corresponding to 33 cm² of shoot leaf area only ($t_x=0.12$ when normalized values were used) is enough to activate FI. Such an area is very low compared to the range of shoot leaf areas observed in apple tree (Willlaume *et al.*, 2004). This means that in most agronomic cases and for trees not subjected to any drastic defoliation, the quantity of signal produced by leaves does not limit FI. This result suggests to reinterpret the observed positive correlation between shoot leaf area and FI (Neilsen and Dennis, 2000; Lauri and Trottier, 2004). Increasing leaf area does not likely activate by itself FI. This relationship between shoot leaf area and FI could result from a longer distance between fruit and SAM that may in turn reduce inhibiting signal quantity reaching SAM. In apple trees, large genotypic variability in shoot length exists (Lauri and Lespinasse, 1993) that has been associated with a higher tendency to return bloom each year in cultivars bearing fruit on long shoots than those bearing on spurs (short shoots). Such relationships seem to disappear when exploring the variability within a segregating population (Segura *et al.*, 2008). In that context, it is likely that each genotype may have different physiological regulations, for instance different quantity of inhibiting signal produced in relation with the observed genotypic variability in seed number per fruit (Celton *et al.*, 2014). The modeling approach proposed, integrating both architectural and functional traits (quantity of signal, signal transport, meristem sensitivity), could be a promising way to explore the determinant of the genotypic variability in FI.

Model outputs support a combined effect of activating and inhibiting signals on FI since the multiplicative formalism, even though not stringent enough, was better at simulating FI in fruiting and non-leafy parts of the trees than the formalism based on a "limiting factor". This can be interpreted as the likely implication of both signals in a common pathway responsible for FI. This assumption is consistent with previous studies showing an impact of GA on the floral pathway integrator SOC whose activity is also regulated by FT (Mouradov *et al.*, 2002; Lee and Lee, 2010).

Finally, model limitations to represent FI within apple tree structure mainly result from the large value of the shape parameter representing the level of uncertainty in the SAM FI for a given quantity of signals. It is likely that the model hypotheses, assuming a role of leaves and fruit only, are not sufficient to represent all the complex processes involved in within tree variability in FI. Indeed several pathways are known to be involved, including climatic conditions, in particular temperature (Bernier *et al.*, 1993), which can be modified by the microclimate conditions within the canopy. Moreover, in our model we did not consider any preferential direction in signal fluxes (acropetal or basipetal) which could locally affect FI proportion. Although it is known that GA (Regnault *et al.*, 2015) and FT (Aki *et al.*, 2008) can move in the vascular xylem-phloem system, no results exist on a possible preferential transport for the signaling molecules (with the transpiration and water flux or with the phloem mass flow).

7. Conclusion

In this study, we developed a new generic model for simulating the transport of inhibiting and activating signals within tree structures that was calibrated using a unique set of experimental data in apple trees. Although the nature of the signal remains to be elucidated, the estimation of model parameter values and the comparisons of two signal combining functions allowed us to propose new assumptions regarding the respective influences of inhibiting and activating signals and the distance effects in the determination of FI. Model outputs support the hypothesis that inhibiting and activating signals interact to determine FI, with the SAM being more sensitive to inhibiting signal than activating one, and that fruit signals act at longer distances than leaves. Moreover, leaf area in actual agronomic conditions is likely non-limiting for FI. This model thus opens new perspectives to understand further the physiological and architectural determinants of FI in trees.

Acknowledgments

The authors thank the other AFEF team members and SudExpé for technical support during experiments and UMR PIAF for having provided the digitizing device. F. Belhassine PhD was funded by INRA (BAP department) and ITK company. This work was also partly funded by the ANR-DFG Alternapp project.

Author contributions

BP, FB, EC, and DF conceived and designed the study; BP, FB, DF, CP and JC implemented the model; FB and BP run and analyzed simulations; FB, SM and BP collected the experimental data; BP, FB and EC wrote the manuscript; CP revised the manuscript.

Competing interest

The authors declare no competing interests.

Data availability

The dataset and model implementation are available from the corresponding author upon request.

8. Supplementary Material

The following supplementary information is available for this article:

Methods S1. Description of the allometric relationships used for individual leaf area reconstruction

Measurements were performed on 60 short shoots ($\leq 5\text{cm}$) and 60 long shoots ($>5\text{cm}$) to estimate leaf area number, values and distribution along each shoot. The following allometric relationships were thus established:

For the number of leaves (N_L) for each shoot type:

$$N_L = 42.8 \times l + 4.24$$

With l the length (m) of each shoot computed from 3D coordinates of the base and top of the shoots. ($R^2=0.52$)

Individual leaf areas (L_{ai}) along each shoot were computed as the product between the maximal individual leaf area (L_M) depending on shoot type and a relative leaf area ranging between 0 and 1 (R_i) and used to represent the leaf area profile along shoots, as follows:

$$L_{ai} = R_i \times L_M$$

Based on measurements L_M was set to 38.6 and 27.6 cm^2 for short and long shoots, respectively.

R_i was computed from a quadratic equation depending on the relative rank of the leaf (r_i) along shoots with r_i defined as the ratio of leaf insertion rank to shoot leaf number (N_L)

For short shoots, $R_i = -1.03 \times R_i^2 + 1.8 \times R_i + 0.15$ ($R^2=0.95$)

For long shoots, $R_i = -0.93 \times R_i^2 + 0.87 \times R_i + 0.80$ ($R^2=0.96$)

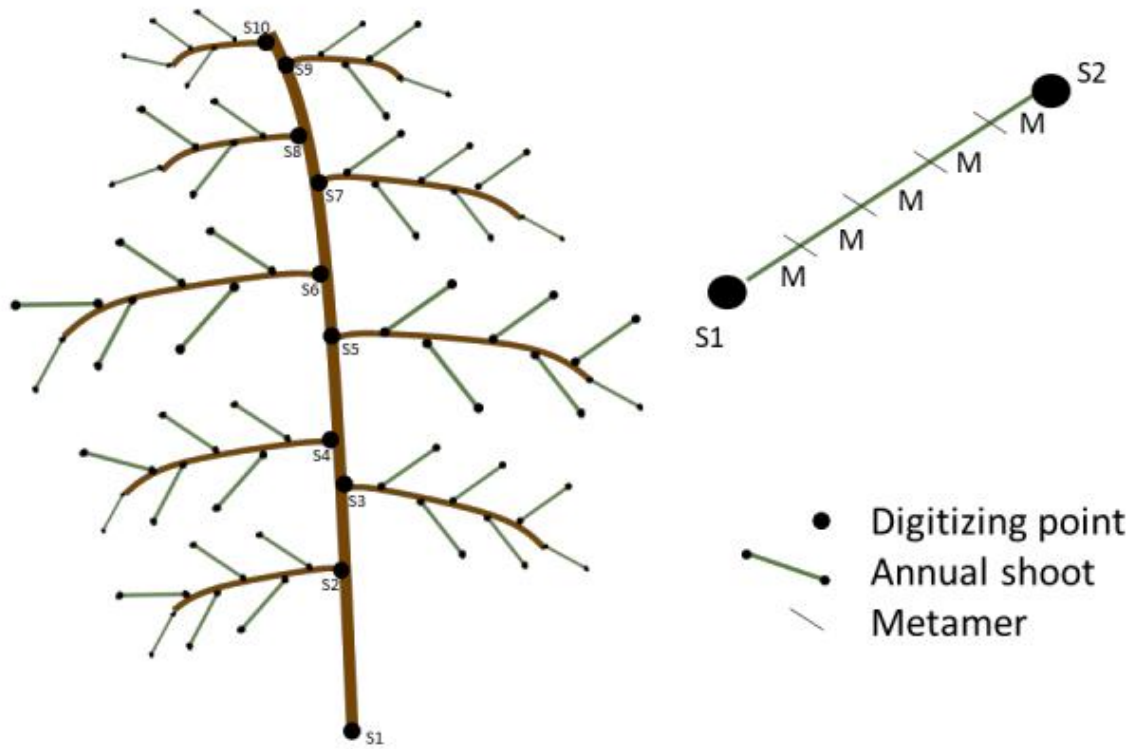


Fig. S1 MTG structure used in the model with three scales (tree, stem segment and metamer). The green segments represents annual shoots. M represent metamers considered in this MTG for the most recent shoots, only. Black points refer to the different digitizing points on the trees which are used to separate each stem segment.

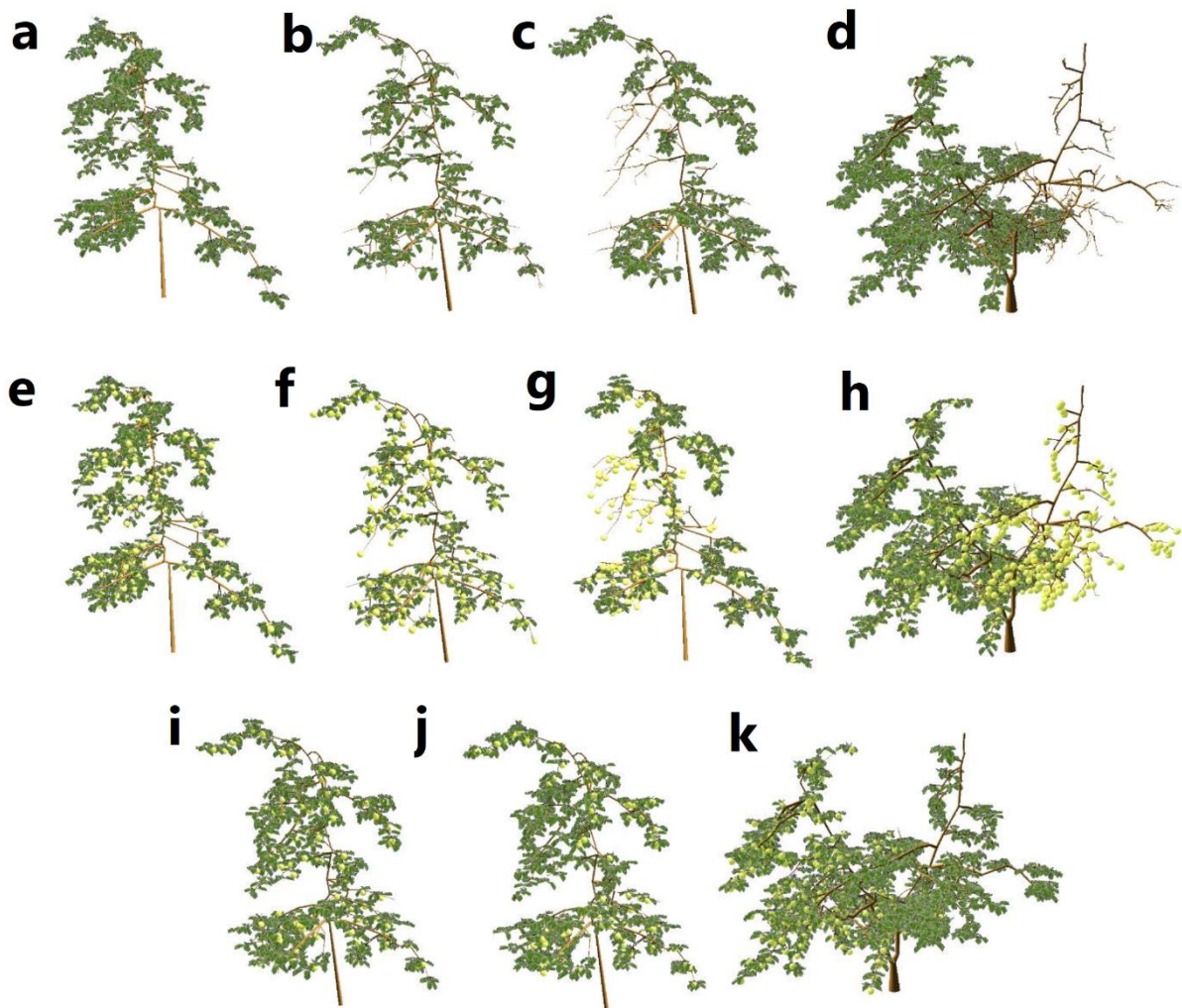


Fig. S2 3D visualization of tree structures used for calibration (a,b,c,d,e,i,j,k) and validation (f,g,h) of the model's parameters. (a) is the representation of control trees in OFF conditions. (b), (c) and (d) defoliated OFF trees at the shoot, branch and half-tree (Y-Shape tree) scales, respectively. (e) control trees in ON conditions. (f), (g) and (h) defoliated ON trees at the shoot, branch and half-tree scale, respectively. (i), (j) and (k) defruited ON trees at the shoot, branch and half-tree scale, respectively.

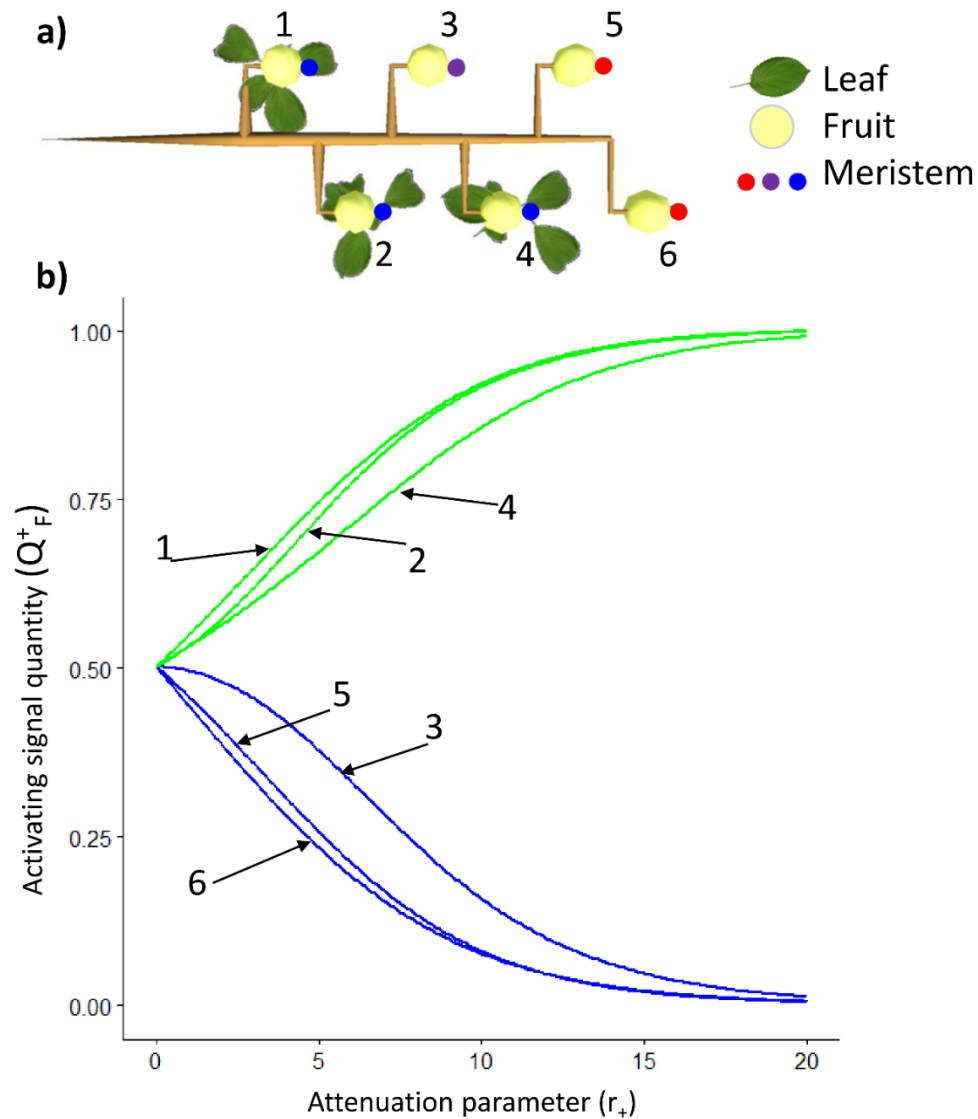


Fig. S3 Activating signal concentration (Q_F^+) in six meristems for different values of the signal 'attenuation' parameter (r_+) (b). Simulations were performed on a hypothetical structure composed of six shoots, half of them leafy, each shoot being located at 15 cm from each other (a). 1, 2 and 4 are leafy shoots and 3, 5 and 6 are non-leafy shoots.

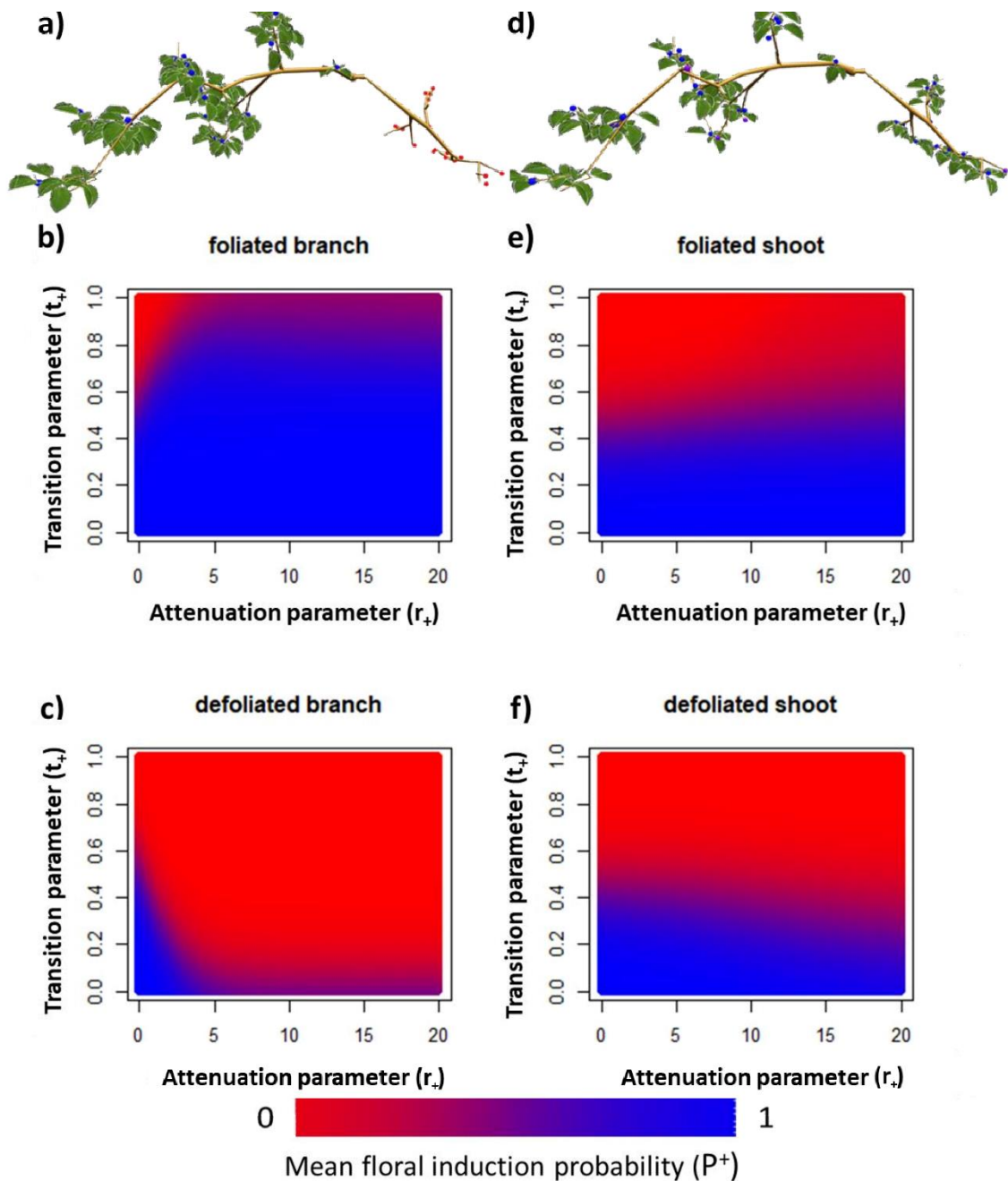


Fig. S4 Mean floral induction probability (P^+) depending on the quantity of activating signal produced by leaves for different values of the signal 'attenuation' (r_+) (200 values) and 'transition' parameters (t_+) (100 values). Simulations were performed on two hypothetical structures composed of two branches with one leafy and one non-leafy branch (a) and two branches with homogeneous leaf removal on half of the shoots (d). (b) and (c) represent the mean floral induction proportion in leafy and non-leafy branches, respectively for the structure represented in (a). (e) and (f) represent the mean floral induction proportion in leafy and non-leafy shoots, respectively for the structure represented in (d). Simulations were performed assuming a shape parameter value (v_+) equal to 0.25.

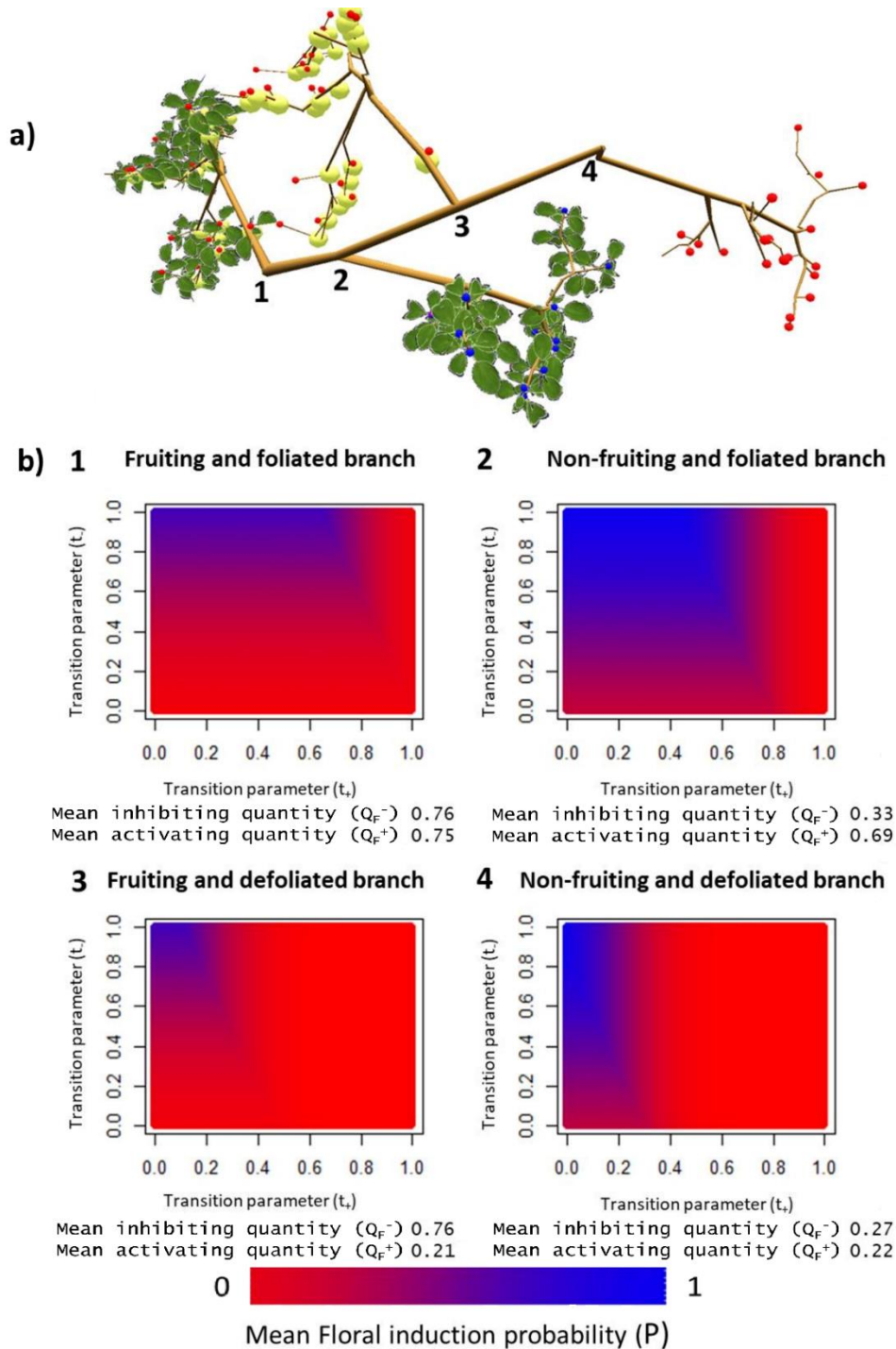


Fig. S5 Mean floral induction probability (P) in shoot apical meristem for different ‘transition’ parameter values for the activating (t_+) and inhibiting (t_-) signals. Floral induction proportions were computed on a hypothetical structure composed of one fruiting and leafy branch (1), one non-fruiting and leafy branch (2), one fruiting and non-leafy branch (3) and one non-fruiting and non-leafy branch (4) (a). (b) represent the mean floral induction proportion in the different branches. Mean inhibiting and mean activating above the heatmaps represent the mean of the inhibiting and activating signals quantities for all meristems in each branch. Simulations were performed with the limiting-factor formalism to account for the effect of the inhibiting and activating signal on floral induction. In these simulations ‘shape’ parameters (v_+ , v_-) equal to 0.25 and ‘attenuation’ parameters (r_+ , r_-) equal to 2.5 were used.

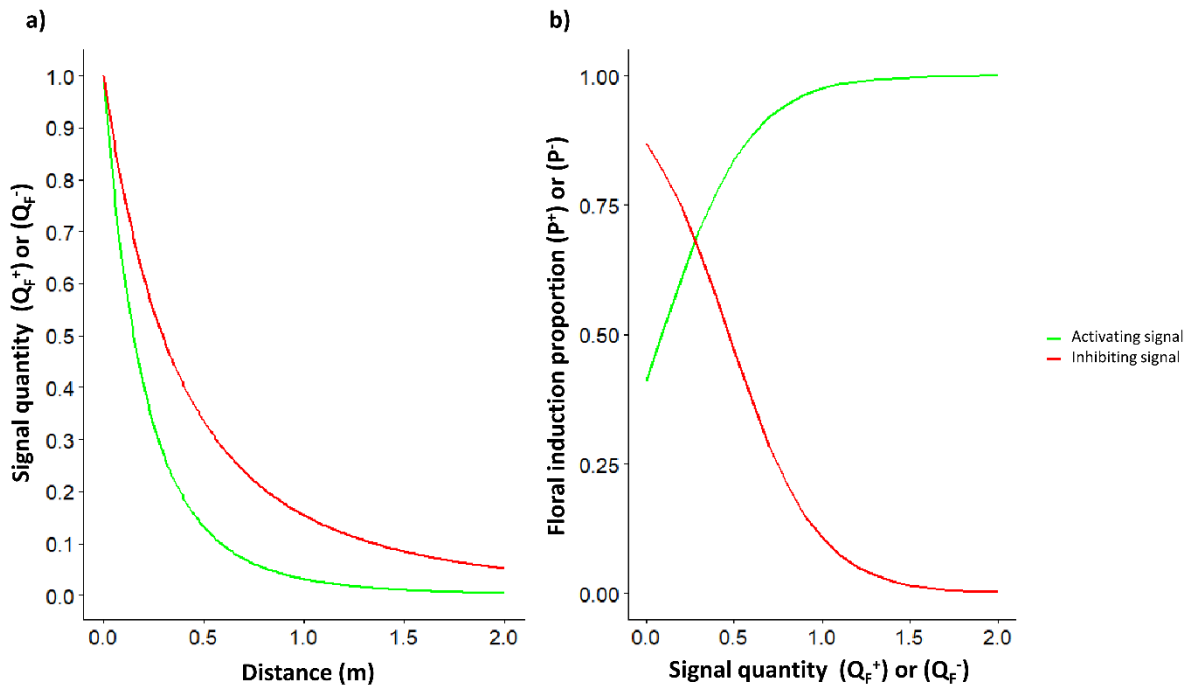


Fig. S6 (a) Representation of equations for activating (green) and inhibiting (red) signal quantity (Q_F^+ and Q_F^-) depending on distances from the emitting sources, with the values of 'attenuation' parameters ($r_+ = 5$ and $r_- = 2.7$) estimated after model calibration. (b) Representation of floral induction proportion for different activating (green) and inhibiting (red) signal quantity (Q_F^+ and Q_F^-), with 'transition' and 'shape' parameter values ($t_+ = 0.09$, $v_+ = 0.25$ and $t_- = 0.47$, $v_- = 0.25$) estimated after model calibration.

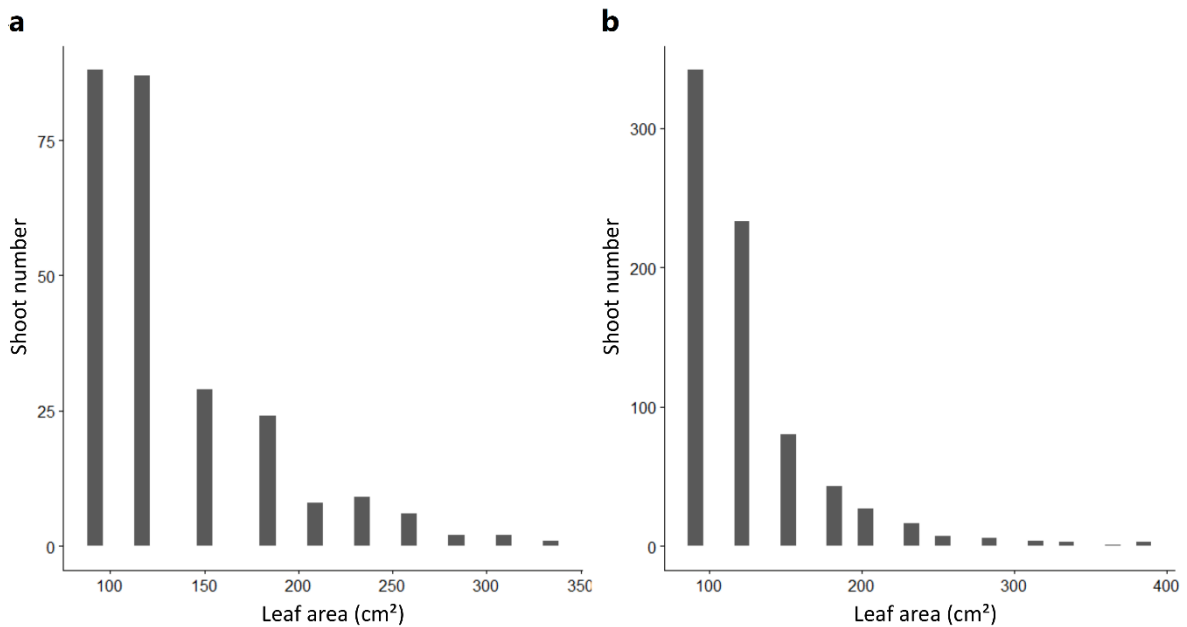


Fig. S7 Distribution of shoot leaf areas for the tree structures used for simulations with one main axis (Solaxe, a) and two main axes (Y-shape, b).

- V. Analyses of the impact of carbon balance, hormonal concentrations and architecture on floral induction in genotypes issued from an apple tree core collection reveals complex genotypic-based regulations.**

1. Résumé

Il existe une grande variabilité génotypique de l'architecture et du fonctionnement des arbres fruitiers. Cependant, il n'est pas encore établi dans quelle mesure la variabilité de l'induction florale (IF) entre les géotypes peut être expliquée par la variabilité de l'architecture et du fonctionnement des arbres. Des études précédentes ont suggéré que l'IF est déterminée par la compétition pour le carbone tandis que d'autres ont suggéré que la signalisation hormonale, principalement les gibbérellines (GA) produites par les pépins des fruits, peut également affecter l'IF. De plus, une grande variabilité a été observée dans les comportements de floraison associés à des caractéristiques architecturales telles que la position des bourgeons dans la branche ou la longueur des pousses annuelles.

Cette étude a été réalisée pendant cinq ans (2014-2019) sur six géotypes différents de pommier avec des architectures contrastées et issus d'une collection variétale de pommiers. L'établissement de l'architecture, la floraison et la production qui en résultent ont été suivis de la plantation jusqu'à cinq ans après, grâce à des relevés manuels de la topologie et à l'aide de mesures réalisées par du Lidar terrestre. Durant deux années (2018-2019), ces mesures ont été complétées par des quantifications de l'activité photosynthétique et de la teneur en carbohydrates non structuraux dans les feuilles, les pousses annuelles et les méristèmes apicaux. Le contenu en hormones (AIA, ABA, GA et cytokinines) des méristèmes a aussi été quantifié. Des morphotypes architecturaux ont été définis sur la base des traits architecturaux, en utilisant une approche de classification hiérarchique.

Les résultats de cette étude ont montré que les relations entre la photosynthèse, l'accumulation d'amidon dans les feuilles et les pousses annuelles pouvaient changer en fonction des géotypes et des caractéristiques architecturales. De plus, ces résultats montrent que la variabilité du bilan carboné entre les géotypes explique mal la variabilité génotypique observée pour l'IF. Les résultats ont également suggéré que les gibbérellines et les cytokinines étaient impliquées dans la variabilité de l'IF. Enfin, cette étude a souligné que la mise en place d'une architecture végétale dans les premières années après la plantation, sous la dépendance de signaux hormonaux (AIA et ABA), joue un rôle clé dans le déclenchement de l'alternance de production.

Cette étude donne de nouveaux indices pour mieux comprendre les déterminismes de la variabilité génotypique dans l'IF et ouvre la voie à l'intégration des caractéristiques génotypiques dans des approches de modélisation.

2. Abstract

Large genotypic variability in fruit tree architecture and functioning exists. Nevertheless, it is unknown at which extent floral induction (FI) variability between genotypes can be explained by the variability in tree architecture and functioning. Previous studies suggested that FI is determined by the competition for carbon while others suggested that hormone signaling, mainly gibberellins (GA) produced by seeds in fruits, can also affect FI. Moreover, a large variability in flowering behaviors associated with architectural traits such as bud position within the branch or length of annual shoots has been observed.

This study was carried out over five years on six different apple genotypes with contrasted architectures issued from an apple core collection. Architecture development as well as the resulting flowering and production were followed from planting to five years after planting with topological and T-Lidar measurements. In the third and fourth years, these measurements were complemented with quantifications of leaf photosynthesis activity and non-structural carbon content in leaf, stem and apical meristems and hormonal contents (AIA, ABA, GA and cytokinines) in meristems. On these genotypes, architectural morphotypes were defined based on architectural traits using a clustering approach.

This study showed that the relationship between photosynthesis and starch accumulation in leaves and stems could change depending on genotypes and architectural characteristics. Moreover, the variability in carbon balance between genotypes poorly explained the observed genotypic variability in FI. The results also suggested that gibberellins and cytokinins were implicated in FI variability. Finally, this study emphasized that the establishment of plant architecture in the first years after planting, under the control of hormonal signaling (AIA and ABA), plays a key role in the onset of biennial bearing.

Finally, new clues were provided to further understand the determinisms of genotypic variability in FI and the way was opened for the integration of genotypic characteristics into modelling approaches.

3. Introduction

Alternate bearing has been described as a common phenomenon for different perennial species (Monselise and Goldschmidt, 1982), but its causes are still unclear. This alternation in fruit production has been suggested to be linked to fluctuations in bud floral induction (FI) and controlled through physiological and molecular mechanisms (Wilkie *et al.*, 2008). FI involves morphological and physiological changes that lead to the transition of meristems from vegetative to reproductive state. The tree crop load has been widely reported to be inversely proportioned to flowering in the next spring, and fruit thus suspected to act as an inhibitor of floral induction (Nielsen and Dennis, 2000). This phenomenon in turn leads to between-years fluctuations in floral induction and subsequently fruit production. Two main hypotheses have been suggested to explain such fluctuations in FI. The first hypothesis concerns competition for carbohydrate and states that the number of floral induced meristems is directly affected by the tree carbohydrate status (Monselise and Goldschmidt, 1982). The second hypothesis concerns phytohormones and suggests that gibberellins, cytokinins or ABA, could act in regulating flower induction or differentiation (Bangerth, 2009; Smith and Samach, 2013; Xing *et al.*, 2015). In particular, gibberellins which would originate from fruit, have been considered as inhibitors of FI in fruit trees (Dennis and Nielsen, 1999; Ramírez *et al.*, 2004; Wilkie *et al.*, 2008; Guitton *et al.*, 2016). Moreover, the roles of FLOWERING LOCUS T (FT) gene and protein, considered as the florigen (Corbesier *et al.*, 2007), has been proposed to be conserved in numerous fruit species (Putterill and Varkonyi-Gasic, 2016). To quantify tree alternate bearing behavior, which is by definition a pluri-annual trait, different indexes have been proposed. Biennial bearing index (BBI), initially proposed by Hoblyn *et al.* (1936) and Wilcox (1944), has become an accepted standard and has been used to analyze yield (mass of fruit) variations at different scales: whole areas, individual trees, and branches in several fruit species (see Durand *et al.* 2013 for a review). The biennial bearing index (BBI) estimates the intensity of deviation in yield during successive years. The larger the oscillation around the general yield trend, the higher the index. Durand *et al.* (2013) proposed to enrich the indices considered by normalizing the BBI and by two other indices, autocorrelation and entropy. Autocorrelation index allows to know whether genotypes have a regular, irregular or biennial bearing pattern and represents the synchronization of flowering buds or fruiting shoots of a tree in each year. The three indices (BBI, auto-correlation and entropy) have been used to characterize and classify genotypes of apple bi-parental segregation populations in Durand *et al.* (2013) and (2017). In the apple tree, alternate bearing has been shown to be under genetic control and the QTL detected on a genetic map on which candidate genes were located, suggested that gibberellin-related genes are more likely to play a role than flowering genes (Guitton *et al.*, 2011).

In addition to the two previous assumptions, several studies have underlined relationships between tree architecture and shoot morphology on the one hand and FI of the shoot apical meristem (SAM) on the other hand. In apple trees, architecture has been categorized into four classes based on branch orientation and position along the trunk, flowering position within branches and flowering regularity over years (Lespinasse, 1992; Lauri 1995). Type I presents a columnar shape with many short laterals emerging from the main trunk and producing flowers. Type IV has a vigorous growth, with flowering occurring at the tips of long branches located on the upper part of the tree. Type II and III are intermediate architectures, bearing fruit from spurs for the first case and on medium and long branches close to the trunk for the other case. Apple cultivars from type I and II categories have been considered as prone to alternative bearing while cultivars from type III and IV are considered as regular. In addition to this “qualitative” classification, a number of studies have been performed to highlight and quantify the architectural patterns in fruit trees (Costes *et al.*, 2006). The evolution of tree architecture during ontogeny has been also been investigated, showing that the shoot length within the tree progressively decreases with a similar trend in all branches of different orders (Costes *et al.*, 2003). During this decrease, flowering occurs at particular locations and times with patterns of recurrence in flowering that depends on the genotype (Costes and Guédon, 2012).

As for alternate bearing, previous studies have shown that several architectural and morphological variables, such as internode length, branching, tree height and geometry, act in the tree regularity despite changes throughout tree life and for different GU types (Segura *et al.*, 2008). Several QTL have been associated with those traits. Despite not yet being demonstrated, it is likely that genetic variations in plant architecture involve changes in hormonal ratios (Ward and Leyser, 2004; Smith and Samach, 2013). In particular, auxin is well known for its involvement in the regulation of apical dominance (Cline, 1991).

To investigate the physiological mechanisms that could explain the genotype variability in biennial bearing, 16 genotypes issued from a bi-parental population (X3263 x Belrène) and belonging to three classes (biennial, regular with a high production of floral buds every year and regular with desynchronized bud fates in each year) have been studied (Pallas *et al.*, 2018). The authors have shown that FI variability among genotypes was not directly associated with the observed variation in photosynthesis activity nor in leaf and stem starch concentration considered as a proxy of the intensity of trophic competition. In this study, it was observed that the genotypic variation in photosynthesis or NSC content was mainly determined by crop load values that strongly varied between genotypes since trees in ON and OFF years were considered. While informative, different limitations in this study can be mentioned since (i) this study did not consider NSC concentrations in meristems while it is the organ in which FI occurs, (ii) it did not include any quantification of hormone concentrations, and (iii) it did not describe the architectural differences between genotypes that could explain part of the variability in FI, as suggested by Lauri (1995).

Thus, the general objective of the present study was to further investigate the relationships between architectural, physiological and FI genetic variations by comparing different genotypes. For this purpose, we selected six genotypes from an apple core collection (Lassois *et al.*, 2016). This collection has been phenotyped for the genetic variation of morphological traits and transpiration on a high throughput phenotyping platform (Lopez *et al.*, 2015). The establishment of the tree architecture was followed from planting until three to four years of growth in order to identify their respective characteristics and define morphotypes. Together with this architectural description, physiological measurements were performed: photosynthesis activity, carbohydrate concentrations (starch, sorbitol, sucrose, glucose and fructose) and hormone concentrations (gibberellins, cytokinins, abscisic acid and auxin). Relationships between tree architecture, physiology, fruit production and floral induction variability were then explored to further investigate the possible determinants of FI genotypic variability.

4. Material and methods

4.1. Plant material and growing conditions

The experiment was carried out from 2014 to 2019 on a subset of six genotypes (Table 1) from the INRA apple core collection composed of 242 genotypes (Lassois *et al.*, 2016). The orchard was located at DIASCOPE, the INRA experimental station in Mauguio, in the south of France (43°36' N, 03°58' E). The collection was planted in winter 2014. The orchard was composed of ten rows of 100 trees, using four replicates per genotype planted facing each other. Two replicates of each genotype of the collection were grown under summer water deficit conditions but two trees per genotype used in this study were grown under optimal growth conditions, with required irrigation, fertilization, weed removal, and pest management (Figure S1). The current study applies to six of these 242 genotypes with two replicates per genotype (Figure S2). The selected genotypes comprised three genotypes identified as vigorous and three as non-vigorous in Lopez *et al.* 2015 (Table 1).

Table 1. Genotypes used for architecture and physiological analyses (from Lopez et al. 2015)

Genotype code	Genotype name	Vigor
X0337	Cassou	vigorous
X6917	Président roulin	vigorous
X8323	Beau soleil	vigorous
X0342	Rouge d'oriule	non-vigorous
X8717	France deliquet	non-vigorous
X9234	St-Jacques St- Chamond	non-vigorous

In springs during the five years of the experiment, all the trees were thinned by leaving only one fruit per inflorescence. In 2018, when physiological measurements were performed, trees were thinned before performing the physiological measurements in order to get comparable crop load values close to 4 fruits.cm⁻² in order to avoid crop load effects.

Table 2. Dates of acquisition of architecture, production and functioning variables

Date	Data collected
March 2015	Topological description of six genotypes: GU produced in 2014
March 2016	Topological description of six genotypes: GU produced in 2015
March 2017	Topological description of six genotypes: GU produced in 2016
September 2017	Fruit harvesting
October 2017	Scanning of the six genotypes with leaves using a T-Lidar
February 2018	Scanning of the six genotypes without leaves using a T-Lidar
March 2018	Topological description of three genotypes : GU produced in 2017 + floral GU of 2018
June 2018	Photosynthesis measurements on the six genotypes
June 2018	Organ sampling for carbohydrates and hormones measurements on the 6 genotypes
September 2018	Fruit harvesting
April 2019	Flowering proportion estimations on four branches per tree

4.2. Architectural description

Tree components and their topological organization (succession and branching) were described during winter, i.e. before budburst (February-March), from 2015 until 2017 for the six genotypes. Because this data collection was time consuming (up to four complete days of measurement for one tree), three genotypes only (X0337, X0342 and X6917) were described in 2018 (Table 2). Each year, the topological description concerned the annual shoots produced in the previous year, except for 2018 where the number of floral growth unit (GU) produced in 2018 was also recorded. The tree topology was noted using Multiscale Tree Graph encoding method (MTG, Godin and Caraglio, 1998). Four organization levels (tree, axes, growth units and internodes), three axes categories depending on their lengths (short, medium and long, Costes *et al.*, 2003) and four GU types (long, medium, short and floral) were distinguished. Topological variables were extracted from MTGs using the MTG library of the OpenAlea platform (Pradal *et al.*, 2008). For each year, the number of floral, short, medium and long vegetative growth units (respectively lower than 5cm, between 5 and 15 cm and longer than 15cm following Costes *et al.* 2003) was extracted from these MTGs. Topological description was performed on the two individuals per genotype except for X8717 that had one individual (X8717_1) only.

Other architectural variables were reconstructed from terrestrial LiDAR-generated data, based on two measurement campaigns. The first campaign was performed in October 2017 on leafy trees and the other one in February 2018 on non-leafy trees to allow observation of the perennial structures when trees were four-year-old. Data acquisition was performed following the high throughput

protocol presented in Coupel-Ledru *et al.*, 2019. Scans of the first campaign were used to estimate the height of each individual tree, their volume and their total leaf area using the PlantGL software (Pradal *et al.*, 2009). The estimation of tree volume was based on an estimation of their convex volume, and total leaf area was estimated from an allometric relationship based on the tree alpha volume and leaf area (see Coupel-Ledru *et al.*, 2019 for a complete description). Scans of the second campaign allowed estimating the total number of axes in each individual tree. This variable was computed after tree skeletization performed using the PlantScan3D software (Boudon *et al.*, 2014) and consisted of counting the number of branching points within the structure. The total cumulative length of these axes was then computed.

4.3. Yield component and tree crop load management by fruit removal

At harvest, fruit were collected on each tree. Fruit were counted per tree and weighed together. The mean fruit weight was estimated as the ratio of the total fruit weight to the number of fruits per tree. Crop load was estimated as the harvested fruit number per tree was divided by its trunk cross sectional area (Francesconi *et al.*, 1996). After having measured the trunk circumference at 10 cm above the grafting zone each spring on each tree, the trunk cross sectional area of each tree was computed assuming a cylinder shape of the trunk. Crop load was estimated in three other ways: the harvested fruit number per tree was divided by its leaf area; the harvested fruit mass per tree was divided by its trunk cross sectional area; and finally by dividing the harvested fruit mass by its leaf area.

4.4. Leaf photosynthesis and organ concentration in non-structural carbohydrates (NSC)

Leaf photosynthesis and NSC concentrations were measured on all the trees (6 genotypes x 2 replicates) in the second half of June 2018 on fully expanded leaves belonging to short or medium shoots and that were fully exposed to sunlight. Measurements were performed on leaves belonging to four fruiting (bourse shoot) and four non-fruiting (vegetative shoots or bourse shoot without fruit) shoots for each tree from 12 June to 03 July 2018. Photosynthesis was recorded between 8 and 12 am, using a LI-COR gas exchange system (LI-6400, LICOR, Lincoln, Nebraska, USA) set under controlled conditions within the measurement chamber, known to be non-limiting for photosynthesis (photosynthetic photon flux density = $1800 \mu\text{mol}^{-2} \text{s}^{-1}$, relative humidity = RH = 70%, $\text{CO}_2 = 400\text{ppm}$, $T = 25^\circ\text{C}$) (Massonnet *et al.*, 2007).

After each photosynthesis measurement, the leaf, the annual shoot bearing the leaf (referred to as “stem” in the following) on which photosynthesis measurements were performed and its SAM were sampled to measure their NSC concentration (starch, sorbitol, sucrose, glucose, and fructose). As for photosynthesis, eight replicates of all these organs were sampled on each tree (four fruiting and four non-fruiting shoots). Samples were placed in liquid nitrogen immediately after harvest. Afterwards, they were stored at -20°C for about one week before being freeze-dried and ground to fine powder using a ball grinder. The duration and the speed of grindings were adapted to each type of organ. NSC concentrations were then determined following the protocol described in Pallas *et al.* (2018).

4.5. Hormone concentrations in SAM

SAMs sampled for NSC measurements were also used for the measurement of their hormones concentrations. Since individual SAM weight was not enough for performing hormone quantifications, three meristems having similar fruit presence condition (fruiting and non-fruiting shoots) were gathered for each tree. This resulted in only two samples per tree. All samples were conserved at -80°C before being sent for hormone quantification to the Plant Hormone Quantification Service at the Institute for Plant Molecular and Cell Biology (IBMCP), Valencia, Spain. Six GA forms involved in the metabolism of active GAs (GA4 and GA1) and suspected to be implicated in FI regulation were quantified (Figure S3 A). Three cytokinin forms (IP, Tz, DHZ), abscisic acid (ABA) and indoleacetic acid (IAA) were also quantified to investigate their possible role in FI (Figure S3 B). All these NSC and hormone measurements were also performed in June 2019, but data are not presented in this chapter because laboratory analyses are still underway.

4.6. Determination of FI proportions and BBI

FI proportion were estimated from 2014 to 2018 for X0337, X0342 and X6917 genotypes, from their topological description by considering the proportion of floral growth units to all growth units produced in a given year. For the three other genotypes, X8232, X8717 and X9234, the flowering proportion was computed based on topological records available from 2014 until 2017 (no topological records in 2018). In spring 2019, a different protocol was used to estimate FI because topological measurements were too time consuming. In this year, FI proportion in SAM was estimated at full bloom on all the trees of the experiment as the ratio of the total number of reproductive buds to the total number of growing buds counted on six randomly chosen branches.

The determination of genotype bearing patterns was done using normalized biennial bearing index (BBI) (Durand *et al.*, 2013). BBI was computed as residuals of the general trend between the FI proportion values over years. High values of BBI refer to genotypes with irregular or biennial bearing patterns.

4.7. Statistical analyses

All statistical analyses were performed with R software (R Development Core team, 2013). We investigated the effect of crop load and genotypes on continuous quantitative variables (photosynthesis, NSC concentrations and hormones concentrations...) with two a one-way ANOVA, separately. Fruit presence effects on the same variables were estimated by a two-way-ANOVA with genotype and fruit presence effect. Moreover, due to the low number of replicates for some architectural and production variables (one per tree) and hormones concentrations (two per tree), the effect of genotype was also tested using Kruskal-Wallis test. These analyses (ANOVA or Kruskal-Wallis) were followed by a Tukey HSD test for pairwise comparisons. The different distributions of GU types (short, medium, long, floral) in 2015, 2016 and 2017 were compared among genotypes using chi-square test.

Principal component analysis (PCA) was used to determine groups of variables and genotypes according to variables related to architecture. A clustering of genotypes (Ward method) was also performed on a set of selected architectural traits to determine morphotypes among the genotypes. Physiological variables (photosynthesis, NSC and hormone concentration) were then computed depending on the morphotype group. Significant differences between groups were tested with Kruskal-Wallis test.

Correlation analyses between crop load values (the four different calculations were tested), and physiological (carbon metabolism-related variables, hormone concentrations), or architectural variables and floral induction were performed. The Pearson coefficient was estimated for each correlation and its significance was tested.

5. Results

5.1. Dynamics of tree architectures and flowering

Large significant differences in the number of growth units (GU) among genotypes were observed in the first years of tree development (Figure 1). In 2016, when trees were 3-year-old, the number of GU ranged from 28 (X0337) to 477 (X6917) and in 2017, this number ranged from 95 to 673 for these two genotypes. The proportion of GU types (floral and short, medium and long vegetative) for each year showed a significant impact of the genotype (based on a Chi-square test), except in 2014. Although these differences were significant, some similarities between genotypes were observed. Over the four successive growth years, the proportions of medium and long GU decreased in favor of short and floral GU for the all the genotypes (Figure 1). Short and floral GU became the major type from the second year of growth for all the genotypes, except X0342. Indeed, X0342 which had the lowest number of GU produced per year stayed producing around 50% of long GU each year from 2014 to 2017. Moreover, in all genotypes, some compensation appears to exist between short and floral GU from a year to the next one. This behavior was particularly clear for the two largest

genotypes (X0337 and X6917) that displayed an alternation in the number of floral GU from 2015 to 2017. Such a behavior corresponds to alternating flowering that started after the year of abundant flowering, i.e. in the second year for X0337 and in the third year for X6917.

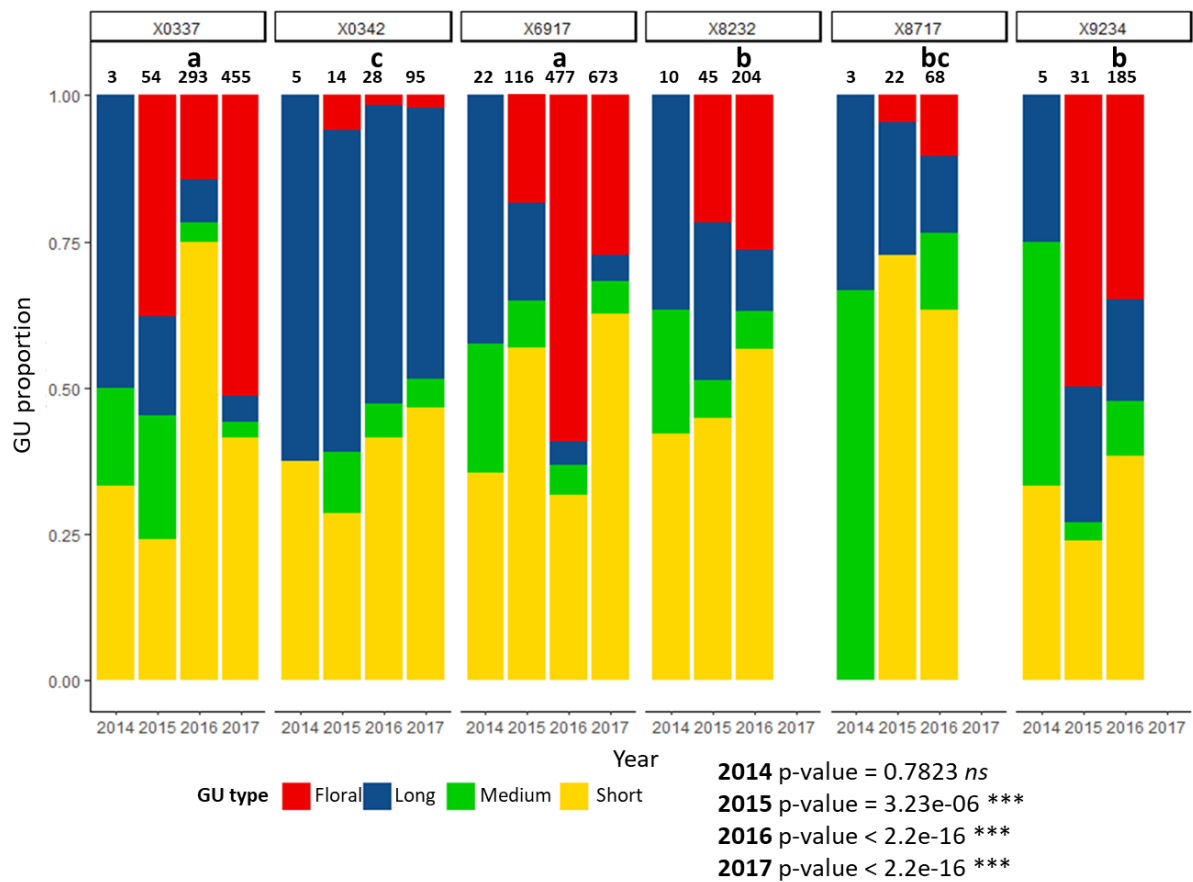


Figure 1. Mean annual growth units (GU) proportions depending on their type (floral, short, medium and long vegetative) in six genotypes of the apple tree core collection, from the first year after planting (2014) to the fourth (2017). Total number of GU per year is mentioned above bars. Differences in GU proportions among genotypes in 2016 were tested with a Kruskal-Wallis test and different letters above GU numbers indicate significant differences among genotypes. Differences in GU proportions among genotypes were tested with a chi-square test considering each year separately. P-values of chi-square tests for each year are reported under the bar plots. Mean values were calculated on two individuals per genotype except for X8717 that had one individual, only. No architectural description was done in 2017 on genotypes X8232, X8717 and X9234.

The flowering behavior of the different genotypes appeared even more clearly when the dynamics of within-tree flowering proportion was plotted over the six years of the experiment (2014-2019; Figure 2). As suggested by the number of short and floral GU, X0337 appeared as a biennial flowering genotype, with the two replicates being synchronized (2016 and 2018 being two years of low flowering and 2017 and 2019 of high flowering). X6917 presented an irregular flowering behavior with a peak of flowering in 2016, followed by low flowering in 2017 for both tree replicates, but with a decrease more pronounced in one of the replicates. Then the two replicates entered into an alternating flowering with opposite phases in the next two years. X0342 displayed low flowering proportion until 2017 and started flowering massively in 2018 but alternated in 2019 with a similar behavior for both replicates. X8232 displayed low to medium flowering in the first three years (2014-2016), especially for one tree replicate, but with an increase in 2019. X8717 kept a very low flowering proportion over the four years of observation. X9234 displayed an alternating flowering behavior

between 2014, 2015 and 2016 and contrasted individual trees behavior in 2019. Unfortunately, for X8232, 8717 and 9234 no data were recorded in 2017 and 2018 limiting our ability to clearly describe their bearing behavior.

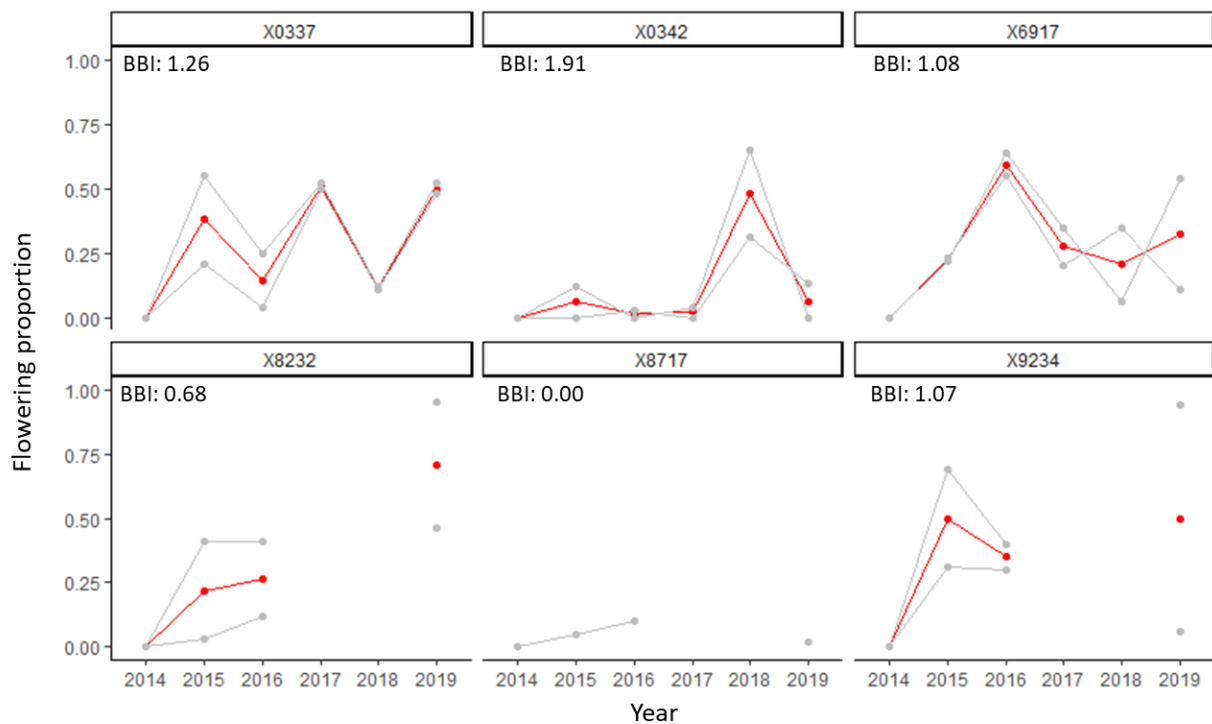


Figure 2. Flowering proportion (number of floral buds / numbers of growing buds) from 2014 to 2019 and biennial bearing index (BBI) for the six genotypes from the apple core collection. Analyses were performed on two individuals per genotype, except X8717. Red lines represent the mean flowering proportion of the two replicates of each genotype and grey lines represent flowering proportion of each individual tree. FI proportion were extracted from topological descriptions from 2014 to 2018 and estimated on six branches per tree in 2019. No architectural description was done in 2017 and 2018 on genotypes X8232, X8717 and X9234.

The total GU number per tree was strongly and positively correlated between consecutive years in the first three years (Figure 3). A significant correlation between the number of GU and TCSA was observed in 2016 (0.61*). The total leaf area estimated in 2017 was also slightly correlated to TCSA measured in 2018 and to the number of GU but the correlation was significant in 2017 (i.e. in the same year), only.

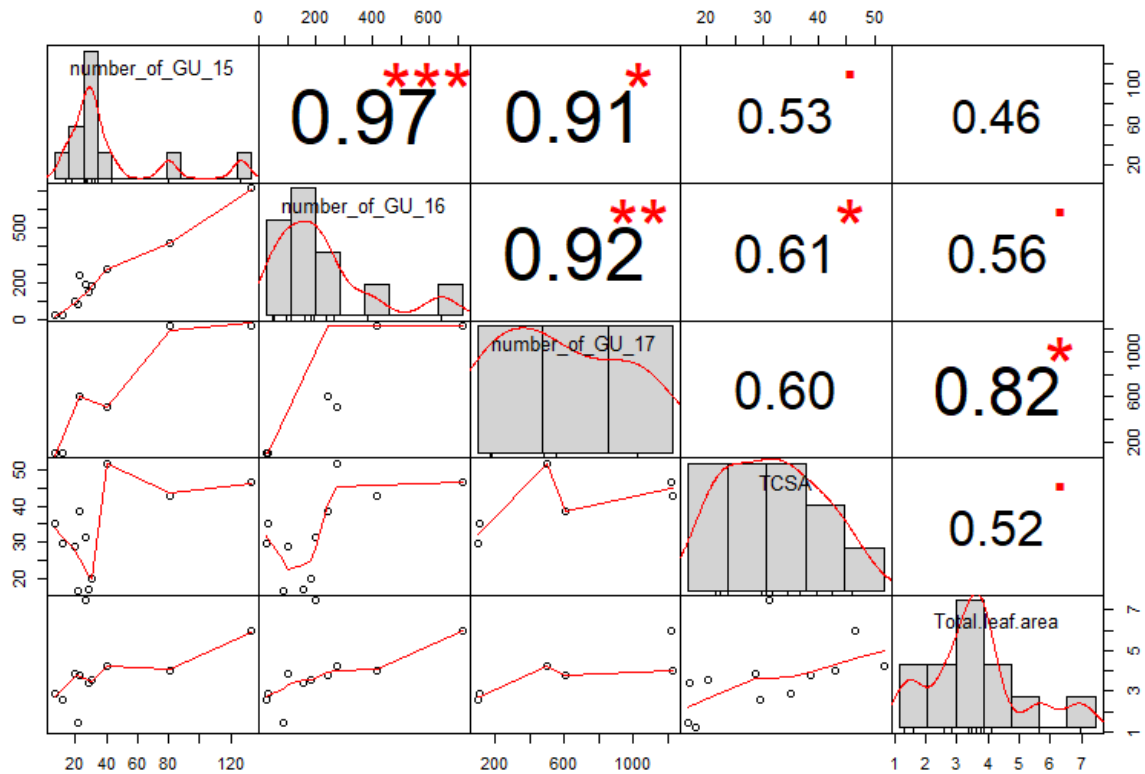


Figure 3. Correlations between total GU number per tree from 2015 to 2017, TCSA in 2017 and total leaf area in 2017 for the twelve trees of six genotypes selected from the apple core collection. For each correlation, the Pearson coefficient is represented in the right upper panel together with the significance of the P-values. *** significant at $P < 0.001$, ** significant at $0.001 < P < 0.00$, * significant at $0.01 < P < 0.05$ and . significant at $0.05 < P < 0.1$.

Depending on their type, correlations between the numbers of GU per tree in each year were then estimated. First, the number of vegetative GU depending on their type in 2015, 2016 and 2017 were compared to the number of floral GU formed in the following year (Figure 4). Significant correlation was obtained between the number of short GU in 2015 and 2016 and the number of floral GU in 2016 and 2017 (0.90*** and 0.89* respectively). In 2018, the number of floral GU were less correlated to short GU number (0.71) but was strongly correlated to the number of medium GU in 2017 (0.86*). This correlation between the number of floral and medium GU was also observed in the two previous years (0.94** and 0.86* for 2015, 2016 respectively).

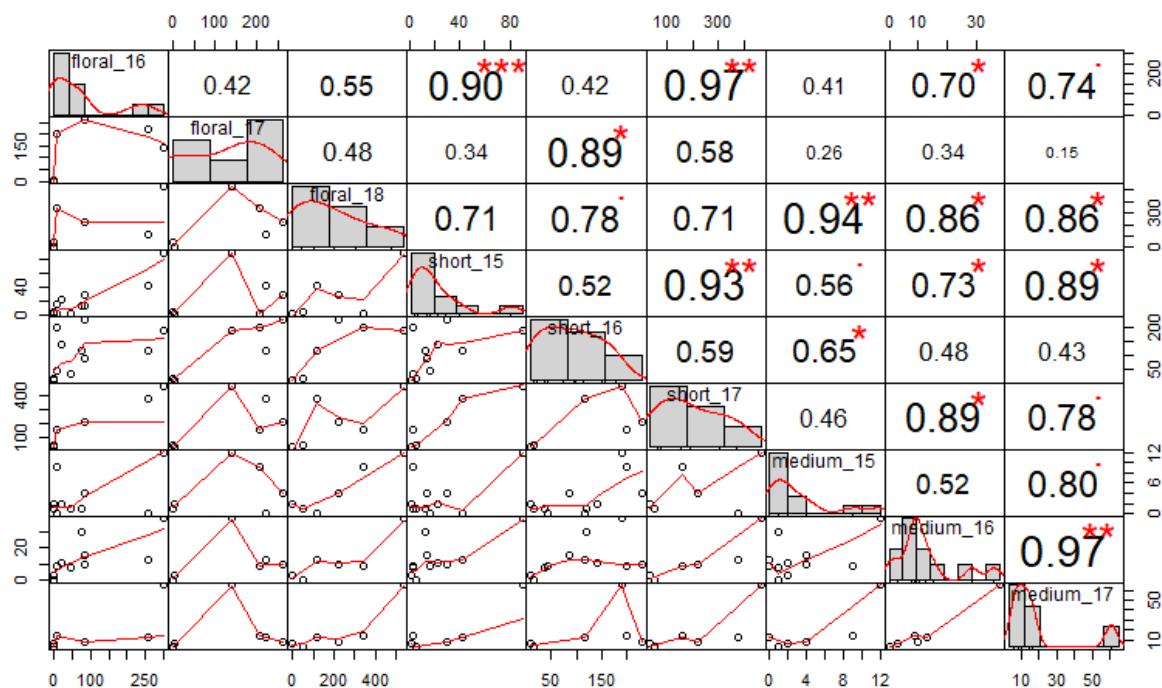


Figure 4. Correlations between the different types of GU (short, medium, long and floral) from 2015 to 2018 for the twelve trees of six genotypes selected from the apple core collection. For each correlation, the Pearson coefficient is represented in the right upper panel together with the significance of the P-values. *** significant at $P < 0.001$, ** significant at $0.001 < P < 0.01$, * significant at $0.01 < P < 0.05$ and . significant at $0.05 < P < 0.1$.

5.2. Classification of genotypes based on architectural and production traits

Analyses of the differences in architectural characteristics and production traits among genotypes were performed on a set of architectural variables computed from T-Lidar scans in 2018 (total leaf area (TLA), number of axes, total axis length, height and volume) complemented by the trunk cross sectional area, which was manually measured, and mean fruit weight and number recorded in 2018 (Table 3). Five variables had significant differences (if tested with ANOVA) among genotypes ($P < 0.001$): tree volume, total axis length, TCSA (expressed as fruit number per TLA), height and number of axes. X6917 and X8717 were the two extreme genotypes, X6917 having the highest values for all the architectural variables, except height and X8717 the lowest ones. Differences between these two genotypes were very large: for instance, the volume of X6917 was almost six times the volume of X8717. Although differences were observed between genotypes for total leaf area, mean fruit weight and number of harvested fruit, they were not significant when tested with ANOVA or Kruskal Wallis likely due to large variability between replicates within genotype.

A clustering analysis was performed to identify morphotypes based on the five architectural variables previously described. The clustering allowed the identification of four groups. Groups 2 and 4 represented the genotypes with the largest and lowest tree volumes, total leaf area, number of axes and total length. Group 2 included genotype X6917 and group 4 genotype X8717, consistent with results presented in Table 3 showing that X6917 can be considered as the “biggest” and X8717 as the smallest genotype. Groups 1 and 3 displayed intermediate values for the variables (Table 4). Group 1 included the two trees of X0337 genotype that corresponded to the tallest trees with the highest TCSA and intermediate values of total leaf area, number of axes and total axis length. Group 3 included the two trees of the three other genotypes (X0342, X8232 and X9234). Those genotypes exhibited almost similar total leaf area, number and total axis length values to group 1, but significantly lower TCSA, height and volume than the other group.

Table 3. Mean values of architectural and production variables estimated in 2018 with T-Lidar acquisition and at harvest for six genotypes selected from the apple core collection.

Genotype	Number of axes	Total length (m)	TCSA (cm ²)	Total leaf area (m ²)	Height (m)	Volume (m ³)	Fruit number	Mean fruit weight (Kg)	Croup load (Fruit.m ⁻²)
X0337	187.5 ^b	29.64 ^{bc}	37.03 ^a	4.01 ^a	3.18 ^a	3.49 ^b	88.5	0.20 ^{ab}	22.0
X0342	131.0 ^b	18.95 ^{bc}	22.72 ^{ab}	2.74 ^{ab}	2.38 ^b	2.41 ^b	78.0	0.15 ^{ab}	28.6
X6917	616.5 ^a	71.37 ^a	38.58 ^a	5.02 ^a	2.35 ^b	6.96 ^a	108.5	0.23 ^a	20.3
X8232	186.5 ^b	29.62 ^{bc}	14.31 ^b	3.51 ^{ab}	2.43 ^b	2.80 ^b	121.0	0.08 ^b	34.5
X8717	68.0 ^b	11.28 ^c	14.01 ^b	1.33 ^b	1.79 ^b	1.07 ^b	37.5	0.13 ^{ab}	27.0
X9234	295.5 ^b	46.25 ^{ab}	22.20 ^{ab}	5.67 ^a	2.15 ^b	3.49 ^b	114.0	0.19 ^{ab}	16.3
Genotype effect ANOVA	0.002 **	0.001 **	0.003 **	0.081 .	0.002 **	0.001 **	0.81 <i>ns</i>	0.05 .	0.63 <i>ns</i>
Genotype effect	0.11	0.06	0.08	0.08	0.13	0.07	0.64	0.09	0.52

Genotype effect was estimated with a one-way ANOVA and with a Kruskal-Wallis test.

*** significant at 0.001 < P < 0.01, . significant at 0.05 < P < 0.1 and ns non-significant. A Tukey's HSD test for pairwise comparisons was made after these analyses and different letters in a column indicate statistically different values among genotypes.*

Table 4. Mean values of architectural variables of the four groups identified after the clustering.

Group	TCSA (cm ²)	Total leaf area (m ²)	Number of axes	Total length (m ²)	Height (m)	Volume (m ³)	Trees assigned in the group	Group description
1	45.16	4	187.5	296	3.18	3.48	X0337_1, X0337_3	High trees with intermediate number of axes
2	44.74	5.01	616.5	71.4	2.34	6.96	X6917_1, X6917_3	Large trees with many axes
3	26.97	3.97	204.3	31.6	2.32	2.9	X0342_1, X0342_3, X8232_1, X8232_3, X9234_1, X9234_3	Medium size trees with intermediate number of axes
4	17.33	1.32	68	11.3	1.79	1.06	X8717_1, X8717_3	Small trees with few axes

Data were evaluated from T-Lidar measurements except for TCSA which was evaluated manually.

This clustering was complemented by a PCA analysis performed on the six genotypes. The same six architectural variables used for the clustering were used in the PCA. The first two axes of the PCA explained more than 88% of the variance (67.87% and 20.25% for GU 1 and 2 respectively, Figure 5A). The first axis was strongly associated with the variability in most of the variables associated with tree vigor (TCSA, total leaf area, number of axes, volume and total length) while the second axis was associated to tree height, only which is, as a consequence, poorly associated to the five other architectural variables (Figure 5 and Table 5). The representation of the four groups identified with the clustering on the PCA graphs is consistent with the clustering: Group 1 that is located in the central top corresponds to tall trees, group 2 at the bottom right refers to large trees, group 3 in the middle represents the intermediate trees and group 4 at the bottom correspond to small trees (Figure 5 B).

Fruit number and mean weight were contrasted between the different groups and for genotypes within the same group (Figure 6). Group 2 displayed the highest fruit number and mean weight and group 4 displayed the lowest fruit number and mean weight. Group 1 presented intermediate fruit number and high mean fruit weight. Within group 3, X0342 displayed fruit number and mean weight slightly below the average observed on mean values of all genotypes together. X8232 displayed high fruit number and the lowest fruit weight of all genotypes and X9234 displayed medium value of fruit weight and average fruit number even if the two replicates were contrasted in 2018.

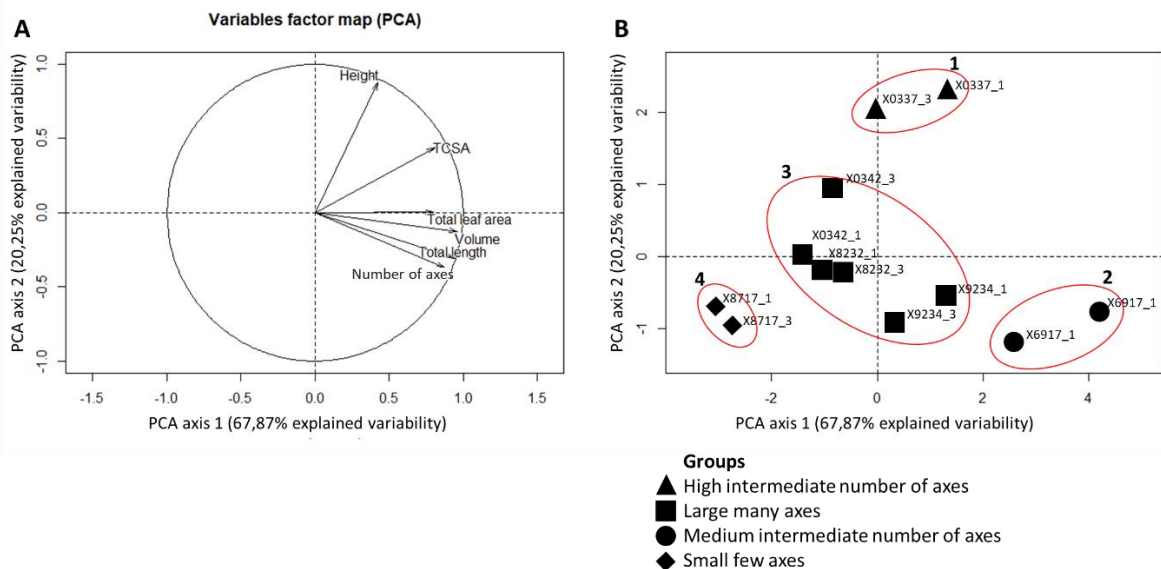


Figure 5. Projection of the architectural variables (A) and individuals (B) on the two first axes of the principal component analysis (PCA). Red circles define the morphotype groups identified after the clustering.

Table 5. Contribution of the selected architectural variables and correlation between variables and dimension (between parentheses) on the PCA dimensions and percentage of explained variances for each dimension.

Contribution	Dim.1		Dim.2		Dim.3		Dim.4		Dim.5	
TCSA	16.14	(-0.81)	15.96	(-0.44)	13.68	(-0.26)	52.4	(-0.28)	1.47	(-0.03)
Total leaf area	15.82	(-0.8)	0	(0)	69.33	(-0.59)	5.77	(-0.09)	0.62	(-0.02)
Number of axes	18.88	(-0.88)	11.19	(-0.37)	14.6	(-0.27)	1.37	(-0.05)	34.55	(-0.14)
total length	22.02	(-0.95)	7.71	(-0.31)	0.65	(-0.06)	1.21	(-0.04)	1.87	(-0.03)
Height	4.47	(-0.43)	63.82	(-0.88)	0.1	(-0.02)	25.38	(-0.2)	6.09	(-0.06)
Volume	22.68	(-0.96)	1.33	(-0.13)	1.64	(-0.09)	13.87	(-0.15)	55.39	(-0.18)
Percentage of explained variance	67.87		20.25		8.32		2.54		0.93	

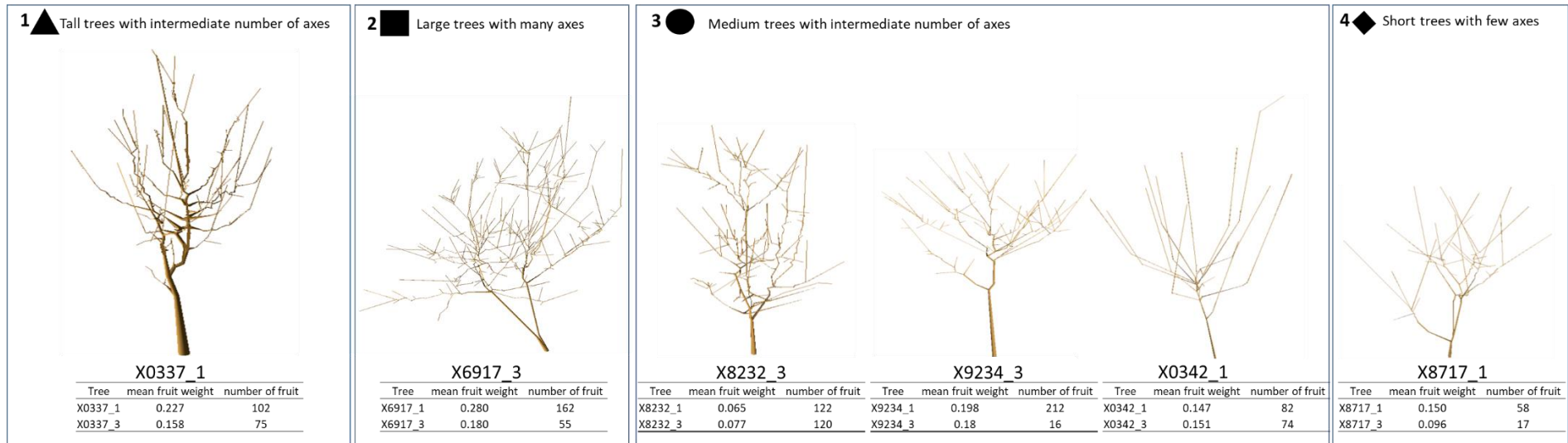


Figure 6. 3D representation of one of the two individuals digitized for the six genotypes in 2017. Each genotype is represented in the group of morphotype identified in the clustering. Mean number of harvested fruit and mean fruit weight in 2018 are indicated for both individuals of each genotype below the 3D representation. Symbols (triangle, square, circle, diamond) for each group are those used in the following figures.

In 2018, we chose to set the crop load as similar for all the genotypes (target value = 4 fruits cm⁻²TCSA) to be able to observe genotypic variability in functional variables independently from crop load variation (Table 6). Unfortunately, this practice was not very successful. For the majority of trees, the crop load was lower than the target value, probably due to some natural fruit drop after thinning. Among the different trees three of them displayed higher values than the others (above 6 fruits cm⁻² TCSA) and two of them displayed low values close to 0 because they did not produce enough flower in this year to reach the target values.

Crop loads were calculated using four different ways to account either for the number of fruit or for their mass with respect to TCSA or total leaf area: fruit number by TCSA (Fruit cm⁻²) or by total leaf area (Fruit m⁻²) and fruit mass by TCSA (Kg cm⁻²) or TLA (Kg m⁻²). In the following, this crop load based on fruit number per total leaf area (Fruit m⁻²) was considered in most of the analyses for analyzing crop load effect on functional variables.

Table 6. Tree crop load in 2018

Genotype	Tree	Crop load (fruit cm ⁻² TCSA)	Crop load (fruit m ⁻² total leaf area)	Crop load (Kg cm ⁻² TCSA)	Crop load (Kg m ⁻² total leaf area)
X0337	X0337_1	1.97	23.96	1.20	14.61
	X0337_3	1.95	20.00	0.41	4.26
X0342	X0342_1	2.76	31.46	0.73	8.29
	X0342_3	2.11	25.83	0.49	6.06
X6917	X6917_1	3.47	27.00	3.67	28.56
	X6917_3	1.28	13.65	2.61	27.75
X8232	X8232_1	6.06	34.15	0.72	4.08
	X8232_3	7.07	34.92	0.68	3.34
X8717	X8717_1	3.46	39.55	0.82	9.31
	X8717_3	0.95	14.44	0.24	3.67
X9234	X9234_1	6.79	28.45	1.41	5.93
	X9234_3	0.56	4.12	2.30	17.06

Four different ways to calculate croploads to account either for the number of fruit or for their mass with respect to TCSA or total leaf area: fruit number by TCSA (Fruit cm⁻²) or by total leaf area (Fruit m⁻²) and fruit mass by TCSA (Kg cm⁻²) or TLA (Kg m⁻²).

5.3. Leaf photosynthesis and leaf, stem and SAM starch concentration

Leaf photosynthesis displayed values between 10.91 and 16.71 μmol.m⁻².s⁻¹ depending on the genotype and tree (Figure 7 A). Significant differences among genotypes were observed for this variable (p-values < 0.001 **). Two groups of genotypes were highlighted after a pairwise comparison: the genotypes X8232, X8717 and X9234 exhibited lower leaf photosynthesis (mean value = 11 μmol.m⁻².s⁻¹) than genotypes X0337, X0342 and X6917 (mean value = 15.14 μmol.m⁻².s⁻¹). Differences can be observed between the two tree replicates of a same genotype. These differences between the tree of a given genotype were mainly observed for genotypes X0337 and X9234. For genotype X9234, these differences could result from the contrasted crop load observed between the two replicates: X9234_1 with the highest photosynthesis rates also displayed higher crop load (28.44 fruit.m⁻² total leaf area) than X9234_3 (4.12 fruit.m⁻² total leaf area). Whatever the genotype, photosynthesis was similar in the leaves of shoots bearing or not fruit (data not shown, two-way ANOVA, P=0.4). Moreover, it could be observed that high photosynthesis rates were found in genotypes bearing the biggest fruit (X0337, X6917 and X0342) whereas the lowest rates were found in genotypes bearing the smallest fruits (X8232 and X8717) (Figure 6 and 8 A). Nevertheless, such a relationship is not relevant for X9234 that bore big fruit but had low photosynthesis rates.

Starch concentration in leaves was strongly impacted by genotype and responded negatively to crop load (Figure 7 B). Three groups of genotypes were distinguished after a pairwise comparison: the

genotypes X0337, X6917, X8717 and X9234 exhibited low starch concentration in leaf (mean value = 26.7 mg.g⁻¹) compared to the genotypes X8232 (mean value = 84.3 mg.g⁻¹) and X0342 (mean value = 78.8 mg.g⁻¹). Differences could be observed between the two replicates of a same genotype. Such between-individual variability was mainly observed for genotypes X8232 and X9234.

Starch concentration in stem was significantly impacted by genotype and increased with crop load (Figure 7 C). X0337, X0342, X8717 and X9234 had low starch concentration in stem (mean value = 39.6 mg.g⁻¹) compared to the genotypes X8232 (mean value = 61.2 mg.g⁻¹) and X6917 (mean value = 55.2 mg.g⁻¹). Differences could be observed between the two tree replicates for all genotypes. Such differences could result from the variability observed in crop load between replicates (see Table 6).

A significant genotypic effect was observed in starch concentration in SAMs (Figure 7 D). The lowest starch concentration in SAM was observed for X0337 and X8717 (mean value = 6.5 mg.g⁻¹) while X0342 exhibited the highest concentration (mean value = 17.6 mg.g⁻¹). Differences can be observed between the two tree replicates for genotypes X0342 and X9234 that also probably results from contrasted crop load values between both replicates. As for photosynthesis, fruit presence (fruiting, non-fruiting shoots) effect was not significant on NSC concentration in SAM, stems and leaves (one-way ANOVA, data not shown).

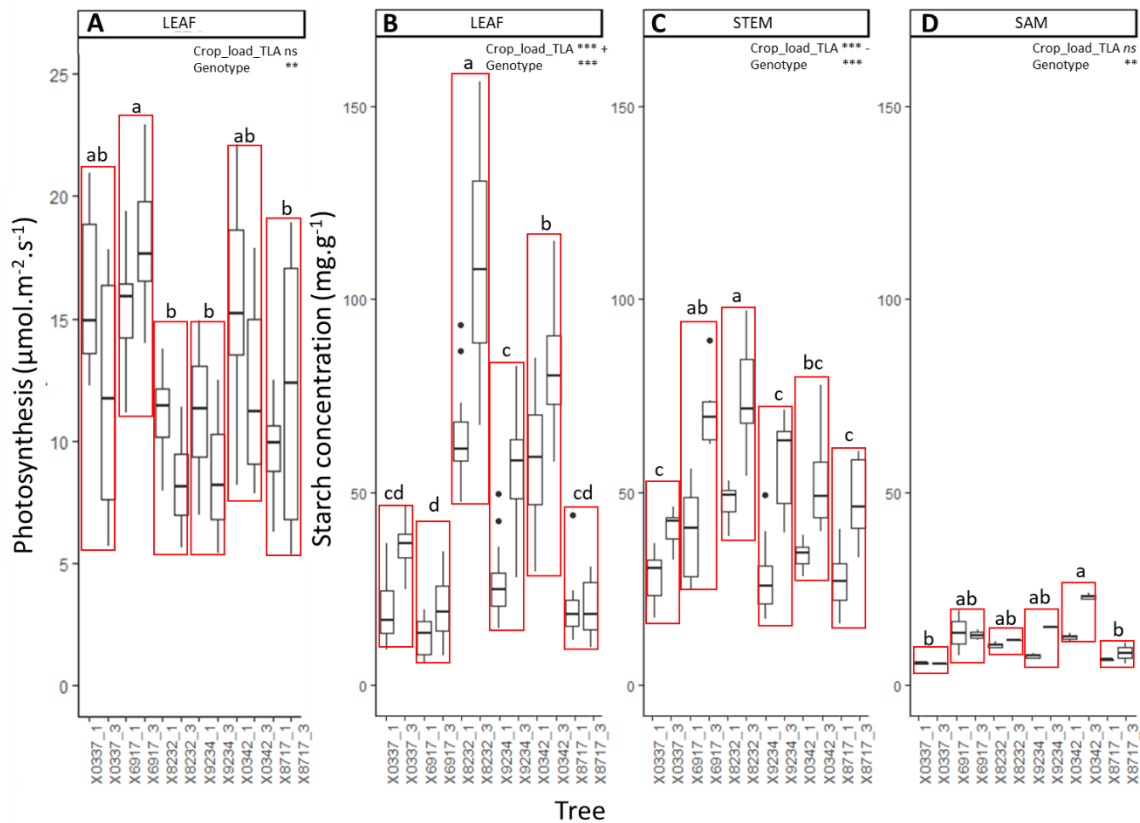


Figure 7. Boxplot representation of (A) leaf photosynthetic activity ($\mu\text{mol m}^{-2} \text{s}^{-1}$) starch concentration in (B) leaf, (C) stem and (D) shoot apical meristem (SAM) for the twelve trees of six genotypes of the apple core collection. Crop load effect was estimated by a one-way-ANOVA. Genotype and fruit presence effects were estimated by a two-way-ANOVA. *** significant at $P < 0.001$, ** significant at $0.001 < P < 0.01$ and ns non-significant. A Tukey's HSD test for pairwise comparisons between genotypes was made gathering together all the measurements made on each genotype and different letters indicate statistically different values. In the boxplot, for each individual data of non-fruiting and fruiting shoots are considered together representing a total number of 8 replicates.

5.4. Leaf, stem and SAM sorbitol concentration

Sorbitol concentration in leaves was strongly impacted by genotype and increased with crop load (Figure 8 A). Three groups of genotypes were distinguished after a pairwise comparison: the genotypes X0337, X6917, X8232 and X8717 exhibited low sorbitol concentration in leaf (mean value = 96.9 mg g⁻¹) compared to the genotypes X9234 (mean value = 117.3 mg g⁻¹) and X0342 (mean value = 107.9 mg g⁻¹). Differences can be observed between the two replicates of a same genotype. Such between tree variability was mainly observed for genotypes X8717 and X9234.

Sorbitol concentration in stem was significantly impacted by the genotype and not impacted by the crop load (Figure 8 B). X6917 and X8232 had the lowest sorbitol concentration in stem (mean value = 54.6 mg g⁻¹). X0342 and X8717 had the highest sorbitol concentration in stem (mean value = 67.7 mg g⁻¹) while X0337 and X9234 had intermediate concentrations (mean value = 62.1 mg g⁻¹).

Sorbitol concentration in SAM was significantly impacted by genotypes (Figure 8 C). The lowest sorbitol concentration in SAM was observed for X0337 (mean value = 37.1 mg g⁻¹) and the highest sorbitol concentration was observed for X8717 (mean value = 67.2 mg g⁻¹). The other genotypes displayed intermediate concentrations (mean value = 53.1 mg g⁻¹).

Fruit presence (fruiting vs non-fruiting shoots) significantly impacted sorbitol concentration in stem only (One way ANOVA, data not shown).

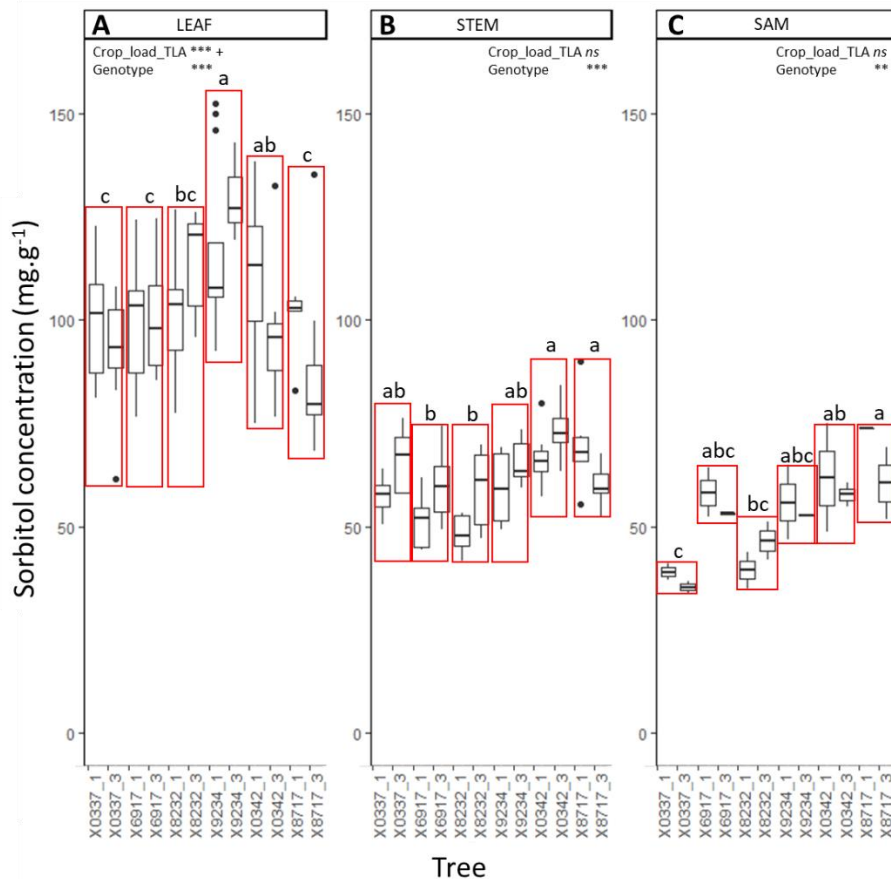


Figure 8. Boxplot representation of sorbitol concentration in (A) leaf, (B) stem and (C) shoot apical meristem (SAM) for the trees of the six genotypes of apple core collection. Crop load effect was estimated by a one-way-ANOVA. Genotype and fruit presence effects were estimated by a two-way-ANOVA. *** significant at $P < 0.001$, ** significant at $0.001 < P < 0.01$, * significant at $0.01 < P < 0.05$ and ns non-significant. A Tukey's HSD test for pairwise comparisons among genotypes was made gathering all measurements on each genotype and different letters indicate statistically different values. In the boxplot, for each individual data of non-fruiting and fruiting shoots are considered together representing a total number of 8 replicates.

5.5. Correlations between NSC organ concentrations and photosynthesis

When all samples were considered together, a general trend was found over the six genotypes with a decrease in photosynthesis when the starch concentration increased in leaves (Figure 9 A). Genotypes with high photosynthesis (X0337 and X6917) displayed low starch concentration and genotypes with low photosynthesis (X8232) had high starch concentration in leaf. Nevertheless, this behavior was not observed for all the genotypes. X9234 and X8717 with low photosynthesis had also low starch concentration in leaf and X0342 with high photosynthesis displayed high starch concentration in leaves. As a consequence, the correlation coefficient was quite low.

Moreover, the negative relationship between photosynthesis and leaf starch concentration did not exist for some genotypes if the correlations were examined for each genotype separately. Indeed, the negative relationship was significant for X8232 and X9234, only. For X0337 and X6917, a positive correlation between starch concentration and photosynthesis was obtained and no correlation was observed for X0342 and X8717.

Photosynthesis was also negatively correlated to sorbitol concentration in leaves if the six genotypes were considered together. Nevertheless, similar to photosynthesis the correlation was quite low and this relationship was changing if genotypes were considered separately. A negative correlation was observed for X8232 and X9234 (figure 9 B) while the correlation was positive for X6917. Positive correlations were obtained between starch concentrations in leaves and stems if the six genotypes were considered together (figure 9 C) or if X0337, X0342, X8232 and X9234 were considered separately. The relationship was no longer significant for X8717 and X6917. No correlation appeared between starch and sorbitol concentrations in leaf if all the genotypes were considered together. If the genotypes were considered separately, a negative correlation was observed for X8717, only (figure 9 D).

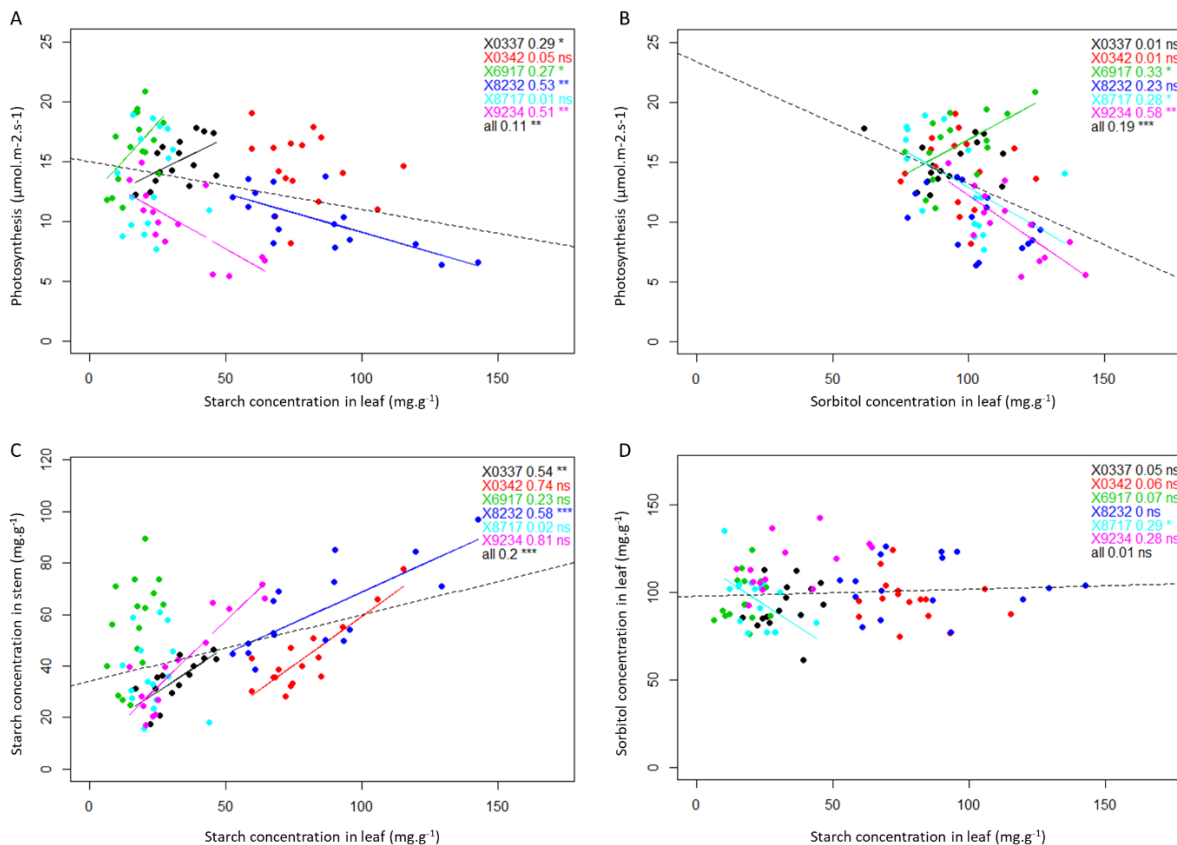


Figure 9. Correlation between (A) starch concentration in leaf ($\text{mg}\cdot\text{g}^{-1}$) and photosynthesis, (B) sorbitol concentration in leaf ($\text{mg}\cdot\text{g}^{-1}$) and photosynthesis, (C) starch concentration in leaf ($\text{mg}\cdot\text{g}^{-1}$) and starch concentration in stem ($\text{mg}\cdot\text{g}^{-1}$) and (D) starch concentration in leaf ($\text{mg}\cdot\text{g}^{-1}$) and sorbitol concentration in leaf ($\text{mg}\cdot\text{g}^{-1}$) for the twelve trees of six genotypes of the apple core collection. Different genotypes have different colors. Dotted black line represents the linear regression computed on the whole dataset and continuous colored lines represent the linear regression between variables for the different genotypes when considered separately. The values of the determination coefficient (R) of the Pearson correlation and their significance are represented in the top right corner of each graph for each genotype and for the whole dataset. *** significant at $P < 0.001$ and ** significant at $0.001 < P < 0.01$. Continuous black line represents the linear regression between the two variables. For each individual data of non-fruiting and fruiting shoots are considered together representing a total number of 8 replicates.

5.6. Correlations between photosynthesis, TCSA and crop load

A significant positive correlation was observed between photosynthesis and TCSA when all genotypes are considered (Figure 10 A, $r = 0.57$ ***). However, X8717 and X9234 did not conform to this correlation since the two replicates of these genotypes had contrasted photosynthesis rates for comparable TCSA. When photosynthesis was correlated to crop load, a negative relationship was found (Figure 10 B). However, tree X9234_3 displaying the lowest photosynthesis and crop load was not considered in the calculation of correlation coefficient.

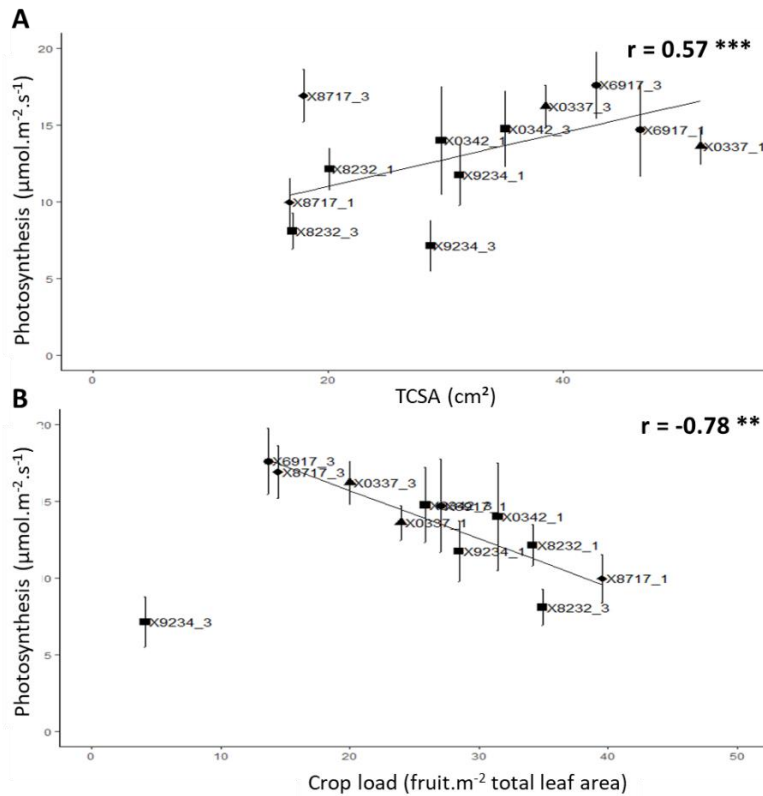


Figure 10. Correlation between (A) photosynthesis ($\mu\text{mol m}^{-2} \text{s}^{-1}$) and trunk cross sectional area (TCSA in cm^2) and (B) photosynthesis ($\mu\text{mol m}^{-2} \text{s}^{-1}$) and crop load (fruit.m^{-2} total leaf area) for the twelve trees of the six genotypes selected in core collection. Continuous lines represent the linear regression over the whole dataset. The value of the correlation coefficient (r) of the Pearson correlation and its significance is represented in the top right corner of each graph. $***$ significant at $P < 0.001$ and $**$ significant at $0.001 < P < 0.01$. In B) data of X9234_3 tree was excluded from the correlation analysis. For each individual data point, non-fruiting and fruiting shoots are considered together representing a total number of 8 replicates. Bars represent the standard deviation.

5.7. Carbon metabolism in the different classes of tree architectures

Photosynthesis and NSC concentration in leaf, stem and SAM were compared among the four architectural classes previously established (Table 7). A significant group effect was observed for all the variables. Group 1 which was characterized by tall trees with high fruit number and mean weight exhibited high photosynthesis associated with the lowest concentrations of starch in stem and sorbitol in leaf and SAM. Similarly, group 2 that contains large trees and displayed the highest fruit number and mean weight, had the highest photosynthesis and starch concentration in stem and the lowest concentrations of starch in leaves and sorbitol in stem. Group 3 characterized by trees of medium size with high fruit number and low mean fruit weight displayed the lowest photosynthesis and the highest starch and sorbitol concentrations in leaves. Group 4, with small trees having the lowest fruit number and mean weight, had intermediate photosynthesis and the highest sorbitol concentrations in stem and SAM.

Table 7. Photosynthesis rate and NSC concentrations in leaf, stem and SAM for the four architectural classes identified with the clustering methods (see table 2)

Group	Photosynthesis ($\mu\text{mol m}^{-2} \text{s}^{-1}$)	Starch leaf (mg g^{-1})	Starch stem (mg g^{-1})	Starch SAM (mg g^{-1})	Sorbitol leaf (mg g^{-1})	Sorbitol stem (mg g^{-1})	Sorbitol SAM (mg g^{-1})
1	14.9 ^{ab}	32.0 ^b	34.5 ^b	5.6 ^b	92.1 ^b	61.8 ^{ab}	37.1 ^b
2	16.2 ^a	16.8 ^c	55.3 ^a	13.2 ^a	96.1 ^{ab}	55.6 ^b	55.7 ^a
3	11.3 ^c	66.2 ^a	49.2 ^a	13.3 ^a	105.9 ^{ab}	62.1 ^{ab}	52.3 ^a
4	13.4 ^b	22.5 ^c	37.7 ^b	7.4 ^b	95.5 ^b	64.8 ^a	67.2 ^a
Group effect	4.39e-05 ***	2.61e-11 ***	1.77e-03 ***	3.45e-03 ***	3.31e-02 **	4.61e-02 **	1.95e-02 **

Group effect was estimated with a Kruskal-Wallis test. A Tukey's HSD test for pairwise comparisons was made after these analyses and different letters in a column indicate statistically different values among genotypes.

5.8. Genotypic variability in SAM hormone concentrations

Among the different forms of hormones analyzed (6 GA forms, IAA, ABA and 3 cytokinines), few differences in the concentrations were statistically significant among genotypes. This is mainly due to high variability between the two replicates for each genotype (Figure 11). Genotype significantly impacted five hormones only: two gibberellin forms (GA9 and GA1), abscisic acid (ABA), auxin (IAA) and one cytokinin form (DHZ, dihydrozeatin) (Figure 11). Among these five forms, crop load effect was significant for ABA and DHZ, only.

For GA9 which is the precursor of the active form GA4 in the non-hydroxylating pathway, a single genotype, X3307, had a different and higher concentration than the others (mean value = 7.1 and 2.2 ng.g^{-1} for X3307 and for the five other genotypes, respectively). Among the five other genotypes, despite being non-significantly different, X6917 exhibited the lowest concentration (0.69 ng.g^{-1}). Regarding GA1, which is the active form of the other GA pathway (early-13-hydroxylating pathway), X0342 and X8232 had higher concentration than the other genotypes (mean value = 45.6 and 50.1 ng.g^{-1} for X0342 and X8232, respectively compared to 6.25 ng.g^{-1} for the other genotypes).

Larger contrast was found among genotypes for ABA concentration. X8717 and X9234 had significantly higher ABA concentration (mean value = 6830 and 6365 ng.g^{-1} respectively), X6917 exhibited the lowest values (mean value = 1880 ng.g^{-1}), and X0337, X0342 and X8232 intermediate values (mean value = 4731 ng.g^{-1}). Regarding IAA concentration, a significant genotypic effect was found, mainly associated with the high concentration observed for X0342 (mean value = 39.8 ng.g^{-1}) compared with the other five genotypes (mean value = 10.25 ng.g^{-1}). Finally, DHZ concentration was significantly different between X8717 (highest mean value = 3.28 ng.g^{-1}) and X0337 (lowest value = 0.31 ng.g^{-1}), while it was similar for the other genotypes. Nevertheless, strong variability between tree replicates was observed, with tree X8717_1 displaying a DHZ concentration three times higher than tree X8717_3.

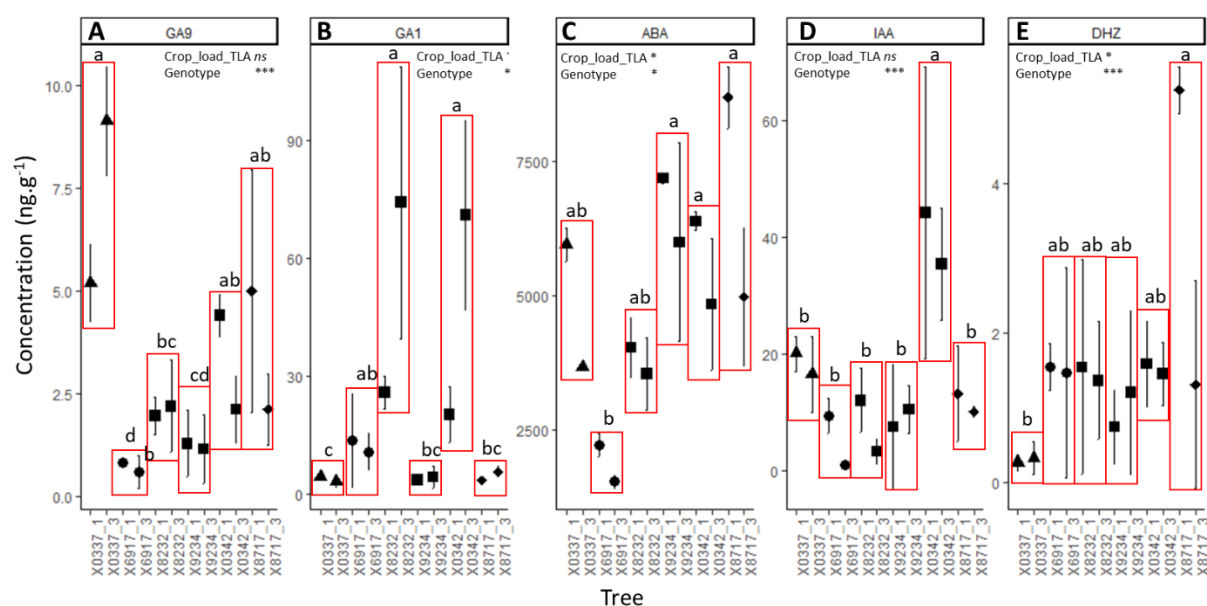


Figure 11. Boxplot representation of hormone concentrations in shoot apical meristem (SAM) for the trees of the six genotypes of the apple core collection. On these graphs, only the hormones displaying significant differences between genotypes are represented. Two replicates were used for each tree. Crop load effect was estimated by a one-way-ANOVA. Genotype and fruit presence effects were estimated by a two-way-ANOVA. *** significant at $P < 0.001$, * significant at $0.01 < P < 0.05$, . significant at $0.05 < P < 0.1$ and ns non-significant. Genotype effect was also estimated with a Kruskal-Wallis test. A Tukey's HSD test for pairwise comparisons was made after the analysis and different letters indicate statistically different values among all genotypes. Bars represent the standard deviation.

5.9. SAM hormones concentration in the different classes of tree architectures

SAM hormone concentrations were compared between the four architectural groups (Table 8). A significant group effect was observed for GA9 only, based on a Kruskal-Wallis test. Nevertheless, Tukey pairwise test showed significant differences among groups. Group 1 had the highest GA9 and GA8 concentrations and the lowest GA1 concentration among the four groups. Group 1 was also characterized by intermediate ABA concentration in SAM and the lowest DHZ. Conversely, group 2 displayed the lowest GA9 concentration. It had also intermediate GA1 and GA8 concentration and the lowest ABA concentration. Group 3 presented the highest GA1 concentration of all groups, and intermediate GA9 and GA8 concentrations. Group 3 displayed high ABA concentration. Finally, group 4 had the lowest GA8 concentration and intermediate GA9 and GA1 concentrations. Group 4 had the highest ABA concentration and its DHZ concentration was contrasted between the two replicates of the single genotype (X8717) present in this group. Nevertheless, these differences among group should be interpreted with caution due to the low level of significance of the differences probably due to large within tree and within genotype variability.

Table 8. Hormone concentrations in SAM for the four architectural groups identified in the clustering analysis (see table 2).

Group	GA9 (ng g ⁻¹)	GA4 (ng g ⁻¹)	GA34 (ng g ⁻¹)	GA20 (ng g ⁻¹)	GA1 (ng g ⁻¹)	GA8 (ng g ⁻¹)	ABA (ng g ⁻¹)	IAA (ng g ⁻¹)	DHZ (ng g ⁻¹)	IP (ng g ⁻¹)	Tz (ng g ⁻¹)
1	7.17 ^a	0.79	0.32	0.87	3.8 ^b	10.8 ^a	4800 ^{ab}	18.2	0.31 ^b	0.43	1.5
2	0.72 ^c	0.98	0.3	1.02	12.2 ^{ab}	8.7 ^{ab}	1880 ^b	5.2	1.52 ^a	0.28	1.22
3	2.23 ^b	0.98	0.47	1.01	33.3 ^a	7.8 ^{ab}	5252 ^a	18.7	1.28 ^{ab}	0.25	1.93
4	3.57 ^{ab}	0.86	0.31	0.55	4.7 ^{ab}	5.7 ^b	6829 ^a	11.6	3.28 ^{ab}	0.2	3.25
Group effect	0.039*	0.46	0.12	0.24	0.16	0.15	0.14	0.27	0.15	0.61	0.22

Group effect was estimated with a Kruskal-Wallis test. A Tukey's HSD test for pairwise comparisons was made after these analyses and different letters in a column indicate statistically different values among genotypes.

5.10. Correlations between NSC organ concentrations and hormone concentration in SAM

All correlations were examined but only those significant ones are commented below. The most significant correlation was observed between starch concentration in leaves and GA1 in SAM (Figure 12 A, R² = 0.86***, positive correlation). This correlation was mainly determined by X0342 and X8232, which presented the highest GA1 concentration and the highest starch concentrations, although large differences between their replicates existed. A negative correlation but less significant was observed between GA4 in SAM and leaf photosynthesis (Figure 12 B, R = -0.59*). This negative correlation was mainly caused by the strong contrast between X9234 replicates displaying contrasted crop load values, and to a lesser extent by the contrast between X8232 replicates. Both ABA and TZ concentration in SAM decreased with the increase in starch concentration in stem (Figure 12 C and D respectively, R = -0.67* and -0.63* respectively). No clear impact of genotype was observed for these correlations but it was noticeable that the same trees had the highest (X6917_3, X9232_3) and lowest concentrations (X8717_1, X9234_1, X0337_1) for both ABA and Tz. Consequently, a positive correlation was also found between Tz and ABA (Figure 12 E). Moreover, a significant negative correlation was found between Tz and GA8 (Figure 12 F, R = -0.72**). This correlation involved the variability among replicates and genotypes.

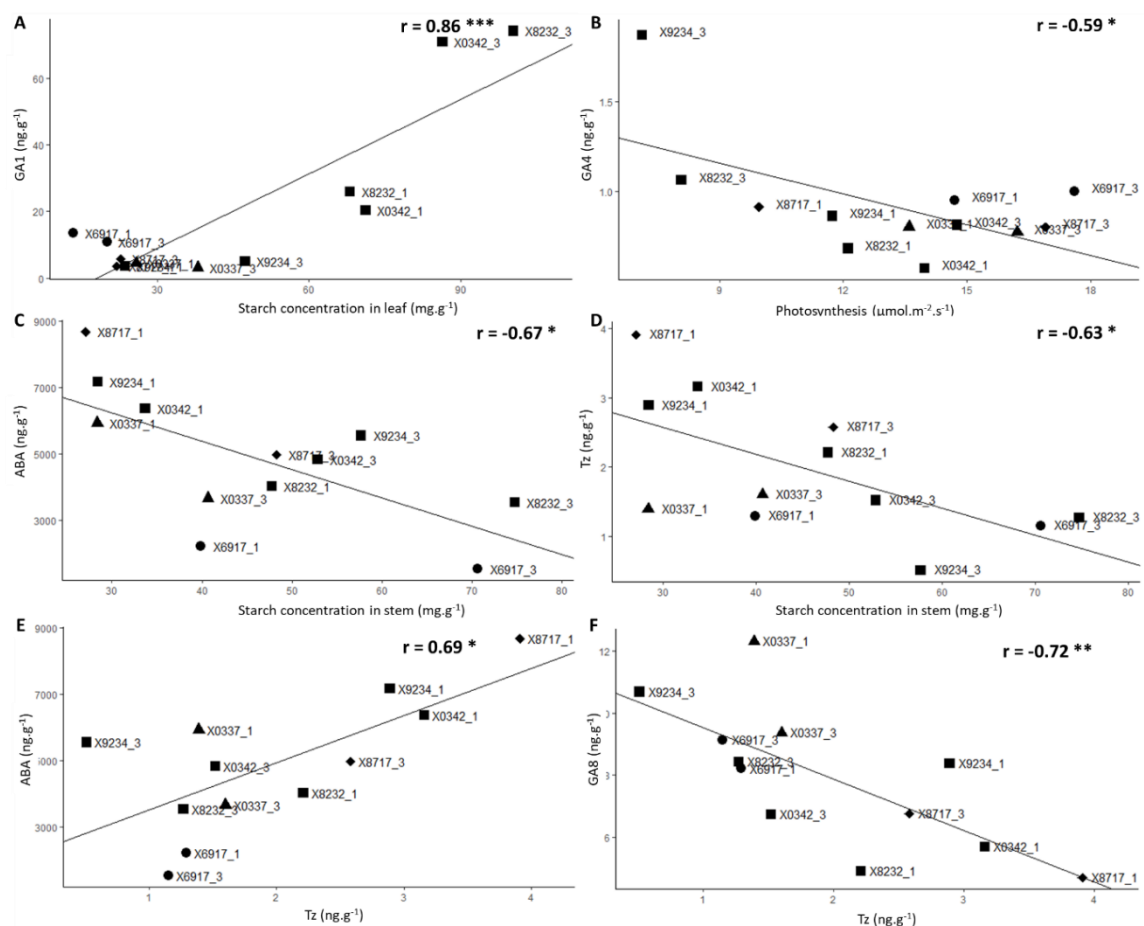


Figure 12. Correlation between (A) starch concentration in leaf (mg g^{-1}) and GA1 (ng g^{-1}), (B) photosynthesis ($\mu\text{mol m}^{-2} \text{s}^{-1}$) and GA4 (ng g^{-1}), (C) starch concentration in stem (mg g^{-1}) and ABA (ng g^{-1}), (D) starch concentration in stem (mg g^{-1}) and Tz (ng g^{-1}), (E) Tz (ng g^{-1}) and ABA (ng g^{-1}) and (F) Tz (ng g^{-1}) and GA8 (ng g^{-1}) for the twelve trees from six genotypes of apple core collection. Continuous black line represents the linear regression between the two variables. Correlations coefficients and its significance are represented in the top right corner of each graph. Each point represents the mean value computed on 2 replicates. Photosynthesis, starch and hormones concentrations were measured in 2018.

5.11. Correlations between physiology-related variables and architectural traits

As the topology was recorded in 2018 (measurement of the 2017 growth season) on three genotypes only, the correlations between architectural and physiology-related variables were calculated with six trees only. In those calculations, the architectural variables related to the 2017 growth season were correlated with physiology-related variables in 2018, i.e. the year after.

Among the architectural variables, the number of short GU was correlated to several organ hormone and NSC concentrations. It was negatively correlated with starch in leaf and sorbitol in SAM (Figure 13 A, B) with r equal to -0.89^* and -0.87^* respectively. These correlations resulted from the contrast between X6917 (both replicates displaying low starch in leaf and sorbitol in stem with high number of short GU) and X0342 (both replicates displaying high starch in leaf and sorbitol in stem with low number of short GU). X0337 had intermediate behavior that fitted the global relationship. Moreover, the number of short GU was negatively correlated to ABA and IAA concentrations (Figure 13 C, D). These correlations resulted from the contrast between X6917 (both replicates displaying low ABA and IAA in SAM with high number of short GU) and X0342 (both replicates displaying high ABA and IAA in SAM with low number of short GU). The number of short GU was positively correlated to GA4 concentration (Figure 13 E, $r = 0.84^*$). Again, this correlation relied on the contrast between X0342

(both replicate displaying low GA4 in SAM with low number of short GU) and X6917 (both replicate displaying high GA4 in SAM with high number of short GU).

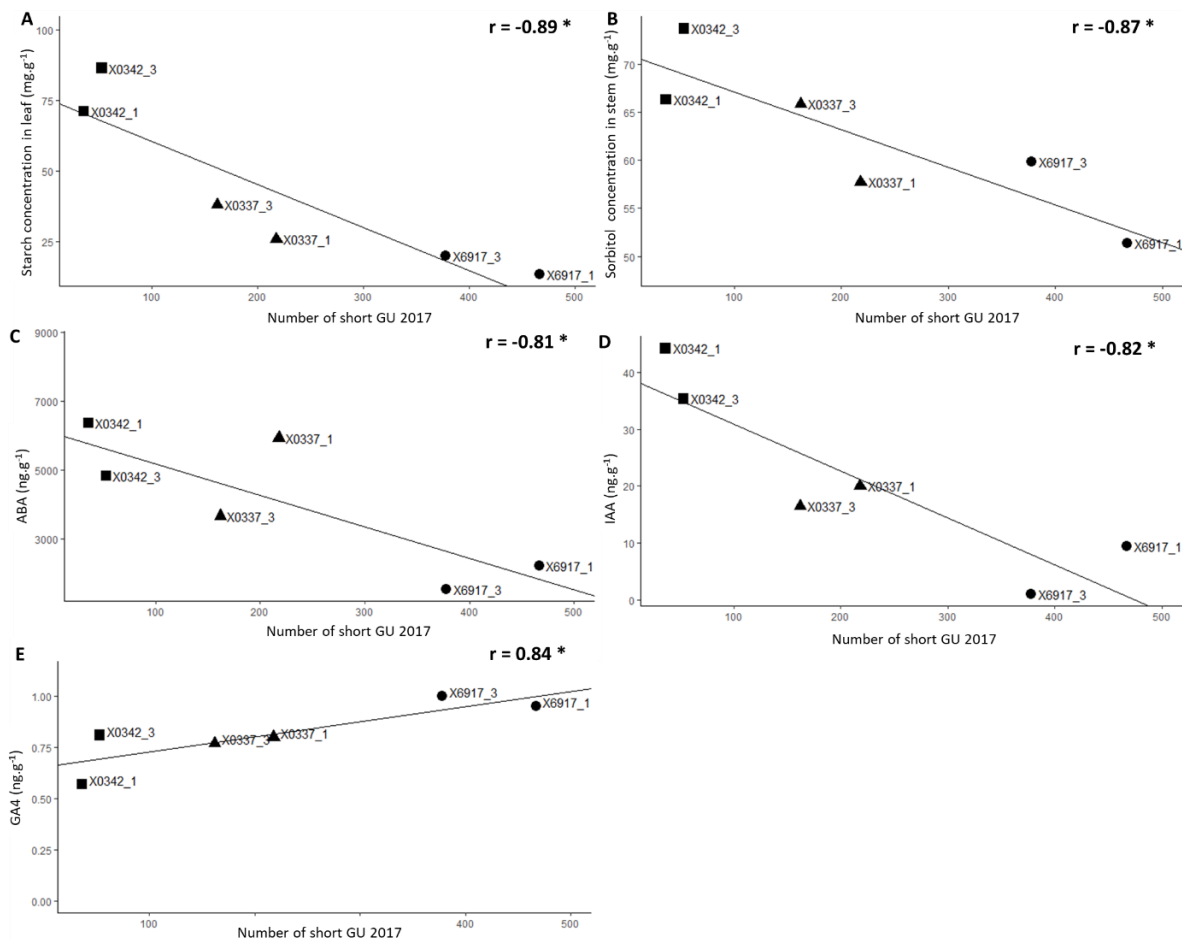


Figure 13. Correlation between the number of short GU in 2017 and (A) starch concentration in leaf (mg g^{-1}), (B) sorbitol concentration in stem, (C) ABA (ng g^{-1}), (D) IAA (ng g^{-1}) and (E) GA4 (ng g^{-1}) for the six trees from three genotypes of apple core collection. Continuous black line represents the linear regression between the two variables. Correlations coefficients and their significance are represented in the top right corner of each graph. Each point represents the mean value computed on two replicates. Topological data are extracted from trees digitalization in 2017 and starch, sorbitol and hormones concentrations were measured in 2018.

A negative significant correlation was found between the number of long and floral GU produced in 2017 (Figure 14 A, $r = -0.93^{**}$). This was mainly due to the contrast between X0342 (both replicates displaying low number of floral GU with high number of long GU) and X0337 (both replicates displaying high number of floral GU with low number of long GU). X6917 had an intermediate behavior. However, the contrast between the replicates of X0337 and X6917 also contributed to the significance of this relationship. For the two replicates of X0342 a comparable low number of floral GU for roughly similar numbers of long GU (42 and 47 for the two replicates) were observed.

A strong correlation was found between the number of long GU in 2017 and GA8 concentrations in 2018 (Figure 14 B, $r = -0.98^{***}$). This correlation was also due to the contrast between X0342 (both replicates displaying low GA8 with high number of long GU) and X0337 (both replicates displaying high GA8 with low number of long GU). X6917 had an intermediate behavior. The contrast observed between the replicates of the three genotypes also contributed to the significance of this relationship.

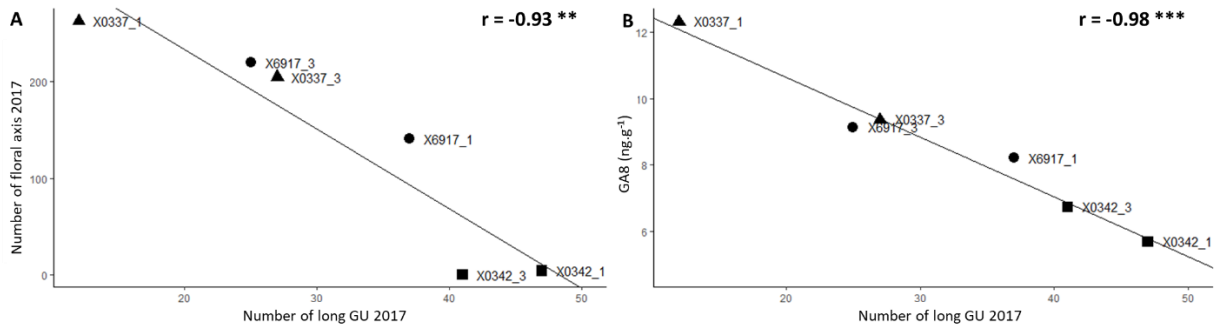


Figure 14. Correlation between (A) the number of long GU in 2017 and the number of floral GU in 2017 and (B) the number of long GU in 2017 and GA8 (ng g⁻¹) in 2018 for the six trees from three genotypes of apple core collection. Continuous black line represents the linear regression between the two variables. *Correlations* coefficients and its significance are represented in the top right corner of each graph. Each point represents the mean value computed on 2 replicates. Topological data are extracted from tree digitalization in 2017 and GA concentrations were measured in 2018.

5.12. Correlations between physiology-related variables, number of floral GU and floral induction

Crop loads calculated in 2018 were plotted against FI proportion in the next spring (Figure 15). When calculated with the number of fruits per leaf area unit or TCSA, the tree crop load was inversely correlated to the proportion of FI in the next spring (Figure 15 A and B) whereas such a correlation was not observed with the crop load calculated with the fruit weight (per leaf area unit or TCSA, Figure 15 C and D). This suggests that fruit number affects FI more than individual fruit sink strength, here represented by mean fruit weight. All trees and genotypes contributed to the observed negative relationship except X8282 (in light grey in Figure 15) whose trees exhibited high FI despite high values of crop loads. The correlation coefficient value between crop load and FI was estimated for each estimated crop load excluding the genotype X8282. The highest *r* value was obtained with the crop load estimated in fruit number by total leaf area (0.71).

Examining in more detail each tree within the relationship between FI proportion and crop load highlighted that the two replicates of X0337, X0342, X6917 and X9234 reacted as expected as their FI proportion decreased with the increase in crop load (Fig 15 A). However, replicates of X9234 were highly contrasted, consistently with their contrasted production in 2018 and 2019. In contrast to the two tree replicates of X8232 that displayed high FI proportion even though crop loads were high, the two replicates of X8717 maintained low FI proportion for two different crop load values. This suggests that these two genotypes had specific flowering behavior, more independent of the crop load than expected.

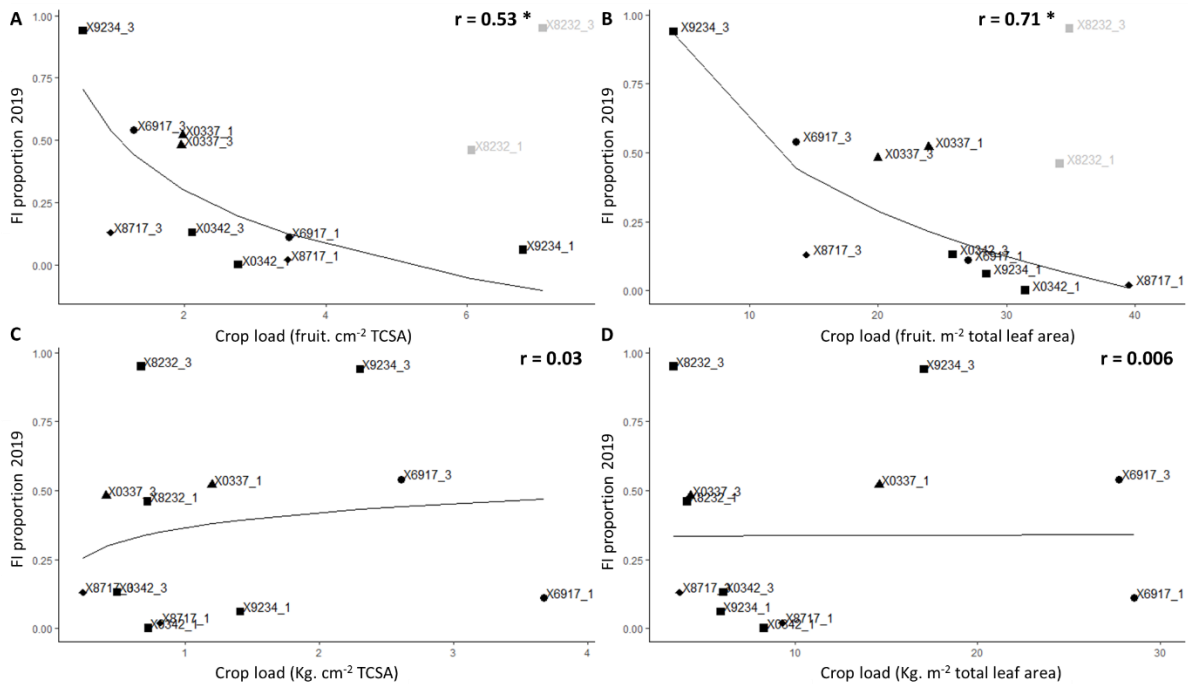


Figure 15. Correlations between floral induction proportion in 2019 and crop load in 2018 expressed by four different ways of estimation for the twelve trees from six genotypes of the apple core collection. Crop load was expressed as (A) fruit number by TCSA (Fruit cm^{-2}), (B) fruit number by total leaf area (Fruit m^{-2}), (C) fruit mass by TCSA (Kg. cm^{-2}) and (D) fruit mass by total leaf area (Kg. m^{-2}). Continuous black line represents the linear regression between the two variables. Correlations coefficients and its significance are represented in the top right corner of each graph. Each point represents the mean value computed on 4 replicates. The grey points in (A) and (B) correspond to X8232 replicates that were excluded from the regression.

A strong correlation was found between the number of floral GU in 2017 and GA8 concentrations in 2018 (Figure 16 A, $R=0.92^{**}$). This correlation was opposite to the one observed between long GU and GA8 (figure 14 B), as the number of long and floral GU were negatively correlated. The obtained correlation was mainly due to the contrast between X0342 (both replicate displaying low GA8 with low number of long GU) and X0337 (both replicate displaying high GA8 with high number of long GU). X6917 had an intermediate behavior. The contrast observed between the replicates of the three genotypes also contributed to the significance of this relationship.

The number of floral GU produced in 2018 was negatively correlated to starch concentration in leaves measured in the same year (Figure 16 B, $R = -0.85^{*}$). The correlation observed is mainly due to the contrast between X0342 (both replicate displaying high starch concentration in leaf with low number of long GU) and X0337 (both replicate displaying low starch concentration in leaf with high number of long GU). The contrast observed for X6917 was probably related to the contrast in crop load observed for the replicates of this genotype (Figure 15).

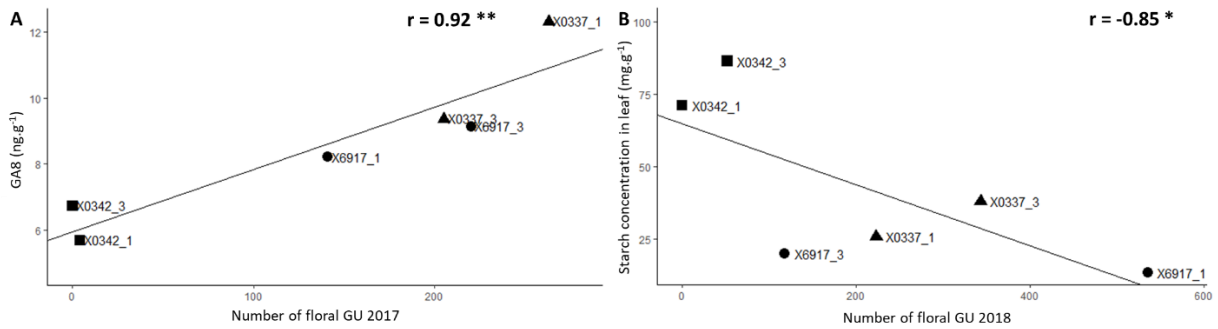


Figure 16. Correlation between (A) the number of floral GU in 2017 and GA8 (ng g^{-1}) in 2018 and (B) the number of floral GU in 2018 and starch concentration in leaf (mg.g^{-1}) in 2018 for the six trees from three genotypes of apple core collection. Continuous black line represents the linear regression between the two variables. Correlations coefficients and their significance are represented in the top right corner of each graph. Each point represents the mean value computed on 2 replicates. Architecture data is extracted from tree digitalization in 2017 and starch and GA concentrations were measured in 2018.

Correlations between physiology-related variables observed in 2018 and the proportion of floral GU in the next spring (2019), representing the proportion of FI, were of moderate intensity. FI proportion in 2019 was positively correlated to sorbitol in leaf and starch in stem (Figure 17 A and C respectively). The correlation between sorbitol in leaf and FI was mainly due to high starch concentrations in leaf and stem for X8232_3 and X9234_3 that displayed high FI. The other individuals were spread around the general trend. For starch in stem, X8232_3, X9234_3 and X6917_3 contributed to the relationship with high values of starch and FI. Nevertheless, such relationships disappeared when looking at particular genotypes. For instance, X0337 displayed average FI proportion of 0.5 for low and comparable starch in stem and sorbitol in leaf concentrations. X0342 and X8717 both displayed low FI proportion whatever starch and sorbitol concentrations in stem and leaves.

FI proportion in 2019 was positively correlated to GA4 in SAM (Figure 17 D). FI proportion in X8232 and X9234_3 were higher for high GA4 concentration and FI proportion in X0342_3 were the lowest for low GA4 concentration. The other individuals were spread around the general trend. FI proportion decreased proportionally with SAM concentration in sorbitol and Tz (Figure 17 B and E respectively). All individuals were spread around the general trend, always with X8232_3 and X9234_3 had higher FI values than the other genotypes.

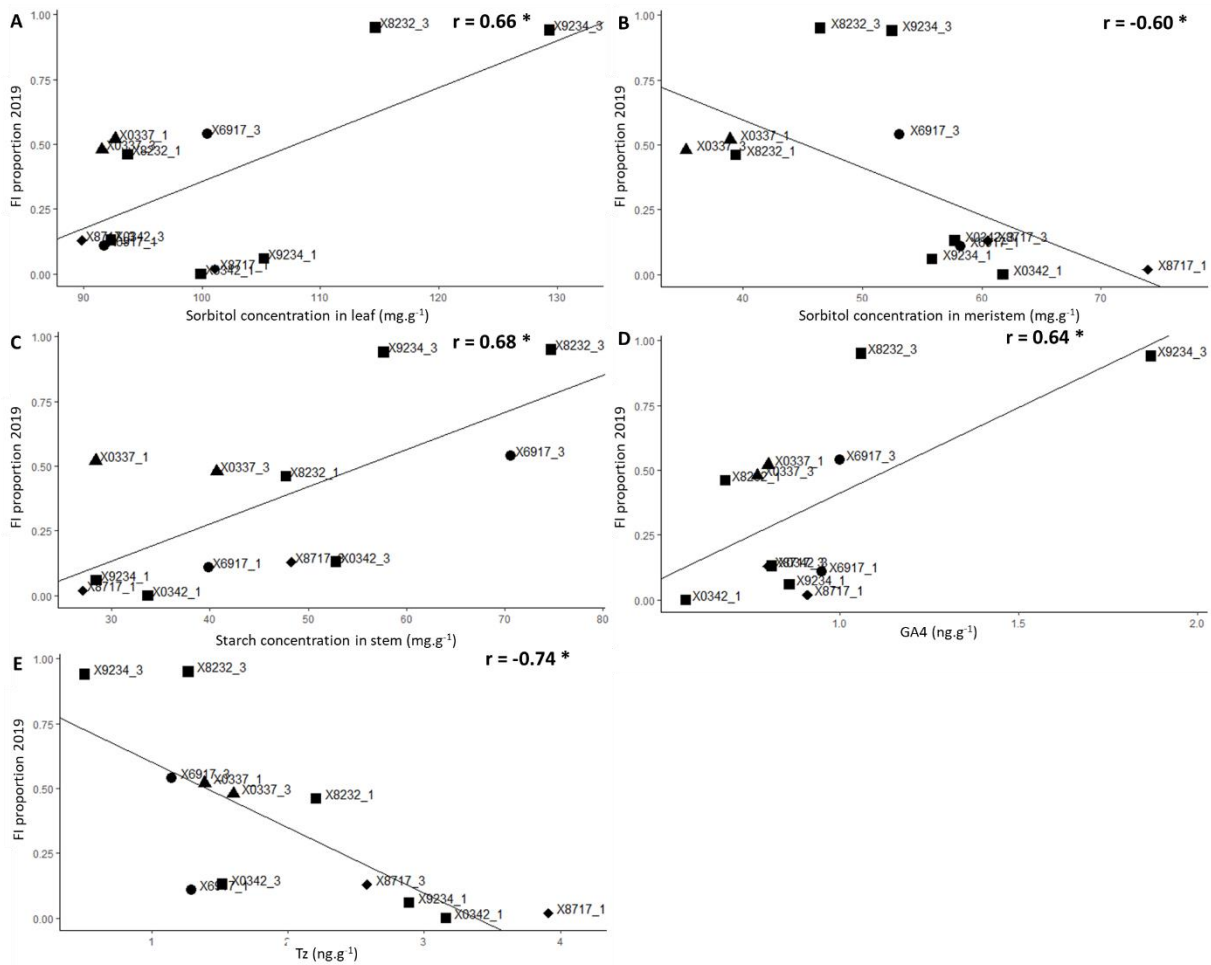


Figure 17. Correlation between (A) sorbitol concentration in leaf ($\text{mg}\cdot\text{g}^{-1}$) and FI proportion in 2019, (B) sorbitol concentration in SAM ($\text{mg}\cdot\text{g}^{-1}$) and FI proportion in 2019, (C) starch concentration in stem ($\text{mg}\cdot\text{g}^{-1}$) and FI proportion in 2019, (D) GA4 ($\text{ng}\cdot\text{g}^{-1}$) FI proportion in 2019 and (E) Tz and FI proportion in 2019 for the twelve trees from six genotypes of apple core collection. Continuous black line represents the linear regression between the two variables. Correlations coefficients and their significance are represented in the top right corner of each graph. Each point represents the mean value computed on two replicates. Starch, sorbitol and hormones concentrations were measured in 2018. FI proportion in 2019 was computed as the mean of the number floral buds divided by the number of all buds in four branches per tree.

6. Discussion

6.1. Genotypic variability in tree architecture

This study was carried out on six apple tree genotypes observed in a previous experiment as representative of the architectural diversity observed in a core collection of this species (Lopez *et al.*, 2015). As this classification has been performed when the trees were one year old and before the present experiment (Lopez *et al.*, 2015), we had to examine the consistency of this initial choice. In the study of Lopez *et al.* (2015), the core collection genotypes were classified in six groups according to their total leaf area and other morphological traits (e.g. internode length, basal diameter and number of leaves). Clustering on traits of architecture and functioning performed by Coupel-Ledru *et al.* (2019) on the trees of the core collection in 2017 (four year old trees) separated the core collection in groups mainly depending on tree volume, leaf area, light interception efficiency (STAR) and functional traits to a lower extent (e.g. photo-assimilation, vegetation and water deficit indices).

For the three genotypes initially considered as vigorous (X0337, X6917, X8232), two of them were clearly correctly classified. Indeed X0337 and X6917 were the highest (group1) and X6917 the most

voluminous (group 2). From the pictures (sup Fig. S2), X0337 could correspond to type II (Lespinasse, 1977): tall and erect, rapid entrance into production but strongly alternating bearer. X6917 corresponds to a more open shape with GU bending after fruiting and could be considered as a type IV. Nevertheless it was a strongly alternating bearer since the third year. X8232's growth dynamics was slower, as well as its entrance into production. Despite high number of GU, quite high and third in volume it was classified in group 3 due to a low TCSA. Therefore, for this genotype, the pluri-annual diagnostic led to a slightly different classification than the initial one. From the photos (Figure S2), X8232 appears close to X0337 and could be a type II as well. In the three "low vigorous" genotypes, classification of X8717 is consistent with its initial diagnostic. Quite open in shape, it corresponds to a small genotype, probably type III or IV but the fruiting did not occur massively enough to see the final branch shape. Similarly, X0342 appears as a medium size, quite weak tree. Despite in group 3, its current classification appears consistent with the initial one. In contrast, X9234 appears taller and more voluminous than initially expected with a high number of axes. Quite weak and with low number of GU in the first three years, it was much more branched when the classification was done, in 2018. This miss-classification could thus result from an intense branching that may have occurred lately. Finally, among the six genotypes four maintained their initial class whereas two changed their behavior (X8232, X9234), mainly because of diametral growth and branching respectively, two processes characterizing tree development from young to adult stages.

In the classification performed by Coupel-Ledru *et al.* (2019) on the trees when they were four-year-old, X6917 (vigorous based on Lopez *et al.* 2015) was classified as a large tree with large volume and with high STAR values. X0342 and X9234 classified as non-vigorous were separated in two groups based on STAR values (very high for X9234 and quite low for X0342). X0337 and X8232 (vigorous) were classified in the same group of medium-size tree with high STAR values. More surprisingly, X8717 which is the "smallest" tree in our study was classified in the same group.

In this study and consistently with previous studies on tree ontogeny (Costes *et al.*, 2003; Renton *et al.*, 2006), the types of annual GU changed over years with an increase in the proportion of short and floral GU at the expense of long ones. This decrease in the proportion of long GU was associated with the end of the "juvenile" or "adolescent" (Costes and Guédon 2012) stage and the beginning of production. This decrease was observed in all the genotypes from two until four years after planting, except for X0342 that maintained a relatively high number of long GU in the first four years of growth. The length of the juvenile phase has been associated to the tree vigor in terms of trunk diameter (Visser, 1964), consistently with low flowering proportion over the years observed for genotypes with small TCSA.

6.2. Genotypic variability in crop loads, carbohydrate metabolism and relationship with architecture

In 2018, when physiological measurements were performed medium-high crop load values were observed for most of the genotypes (between 1 and 4 fruits.cm⁻²), even though higher values (between 6 and 7 fruits.cm⁻²) were observed for X8232. Moreover, due to opposite alternation phases, tree replicates of X9234 had contrasted crop loads (close to 0 fruits.cm⁻² for the tree in OFF year and close to 7 fruits.cm⁻² for the tree in ON year).

Genotypic differences in photosynthetic activity were observed for the six genotypes. These difference remains in a range of values comparable to what has been observed for instance for 'Braeburn' cultivar with comparable crop loads (Wünsche *et al.*, 2000). Genotypic variability in photosynthesis activity has been already previously detected when studying apple hybrids issuing from a bi-parental cross (Pallas *et al.*, 2018). In this study, the variability was mainly associated to the contrasted crop loads observed and a positive relationship between crop load and photosynthesis common for all genotypes was detected consistently with other studies performed on one cultivar, only (Palmer *et al.*, 1997; Wünsche *et al.*, 2000). A threshold for photosynthesis saturation has also been detected for crop load values higher than 2.5 fruits cm⁻² TCSA. In the present study, such an increase in photosynthesis activity was not detected when the tree with the lowest crop load

(X9234_3) was excluded from the analysis (Figure 10). This probably results from the high crop loads that were high enough to lead to photosynthesis saturation. In this condition, this saturating photosynthesis rate was observed to be genotype dependent. This genotype-based photosynthesis saturation rate could be associated with TCSA suggesting the importance of other sink demands than fruit, i.e. primary and secondary growth on the determination of photosynthesis activity (Lauri *et al.*, 2010). Altogether these results suggest that in trees that are relatively young, vegetative growth and sinks other than fruit could drive leaf photosynthetic rates.

Previous studies indicate that the photosynthesis rate is highly related to the down-regulation of leaf photosynthesis by low export of sugars out of leaves which can be usually estimated by starch and/or sorbitol concentration in leaves (Zhou and Quebedeaux, 2003; Franck *et al.*, 2006). Such relationships were observed for two genotypes mainly, even though a general trend was observed when considering the whole genotypic variability. This probably reveals that the existence of this feedback regulation of photosynthesis by sugar accumulation depends on the genotypes (Figure 9). For two genotypes (X8232 and X9234), high photosynthesis rates were observed along with low starch and sorbitol accumulation in leaves, consistently with the previous studies that have shown that starch accumulation in leaves inhibits photosynthesis (Wünsche *et al.*, 2000; Zhou and Quebedeaux, 2003). In X8717, the negative feedback could exist but was probably driven by sorbitol concentration in leaves rather than starch. However, in X0337 and X6917, photosynthesis was positively correlated to starch concentrations in leaves but starch concentration in leaves remained low for these genotypes. This low amount of starch was likely associated to high sink demand since they also displayed the highest fruit size and vegetative development. It could be hypothesized that in this case, low starch concentration did not inhibit photosynthesis activity, and that the positive relationship between starch and photosynthesis, observed in a small range of starch values, results from a high production of carbohydrate when photosynthesis increases.

Genotypic differences in carbon allocation between leaf and stem appeared from the differences in the ratio between starch concentration in leaf and stem (Figure 9 C). This ratio was the lowest for X6917 (0.3) and at the highest for X0342 (1.8) and the contrast in carbon allocation between these two genotypes is consistent with the higher internode length for X0342 compared to X6917 (estimated as the ratio between total axis length and number, Table 3).

Among the other correlations found significant between hormone concentrations in SAM and physiological variables, ABA was negatively correlated to starch in stem. The negative correlation between ABA and starch concentration in stem (Figure 12 C) supports previous results about the up-regulation of ABA for low sugar availability conditions (Jossier *et al.*, 2009). The lowest ABA concentration was found in SAM of X6719 that had the highest photosynthesis rate of all genotypes. This is consistent with previous findings about ABA control of stomatal behavior and gas exchange under stress conditions (Jones and Mansfield, 1970).

6.3. Genotypic variability in hormones and relationship to tree architecture

Large genotypic variability was observed in SAM hormone concentrations, between genotypes but also between both replicates of each genotype. Each genotype exhibited a specific combination of hormonal concentrations. Among them, X8717 had high ABA and DHZ concentration, X0342 high GA1 and IAA concentration and X0337 high GA9 concentration. Among the six genotypes studied, SAMs of the six genotypes tended to have higher GA concentration than what was observed in 'Golden Delicious' (Belhassine *et al.*, 2019). For the active GA forms, GA4 concentrations were between 0.05 and 0.54 ng.g⁻¹ of dry matter for Golden and between 0.34 and 3.42 ng.g⁻¹ of dry matter for the genotypes and GA1 concentrations were between 0.68 and 10.87 ng.g⁻¹ of dry matter for Golden and between 2.15 and 98.69 ng.g⁻¹ of dry matter for the genotypes. Among the GA forms, GA9 emerged with differences among the genotypes and had different concentrations between fruiting and non-fruiting shoots in 'Golden Delicious'. GA9, precursor of active GA4, was significantly higher in SAMs of X0337 (Figure 11 A). In addition, the active GA1 was found significantly higher in SAMs of X0342 and X8232 (Figure 11 B) even though no difference had been found between fruiting

and non-fruiting shoots of Golden Delicious. A possible implication of GA in shoot elongation remains consistent with our results (Eriksson *et al.*, 2006), since the degradation form of the active GA1 (GA8) increased when the number of long axes increased (Figure 14B). On the other hand the increase in short GU number with GA4 concentration could be associated with an effect of GA on the branching intensity as observed in previous studies (Van Hooijdonk *et al.*, 2010)

X8717 displayed low concentration in hormones except for ABA and DHZ for which it had the highest concentrations. ABA is known to be involved in plant reactions to stress and the inhibitory action of ABA on shoot growth has already been reported by previous studies (Wilkinson and Davies, 2002). As X8717 is a small morphotype with a low fruiting potential (Table 5, Figure 6), we can assume that this genotype is not adapted to the environment in which the trees grew. This stressful condition is likely to result from the Mediterranean, warm and dry in summer not favorable to an old and non-vigorous variety (Lassois *et al.*, 2016). Although being the smallest genotype, topology description indicates that X8717 developed more GU than X0342 in 2016 (Figure 1). This is consistent with the high IAA concentration found in X0342 SAMs. Indeed IAA is well known to be an inhibitor of axillary bud outgrowth, through apical dominance involving auxin transport in basipetal direction (Booker *et al.*, 2003). In addition, the high number of GU in X8717, likely associated to high number of axes, is consistent with its high DHZ concentration (Figure 11 E) as cytokinins are known to act as antagonist to IAA by stimulating the growth of lateral buds (Bangerth *et al.*, 2000; Rameau *et al.*, 2015). Moreover, the positive correlation between ABA and another cytokinin form (Tz) (Figure 12 E) observed when considering all the genotypes together is compatible with the antagonism between cytokinins and ABA to IAA in the control of axillary buds.

6.4. Relationship between floral induction, physiology traits and architecture

The negative correlation observed between the number of long and floral GU (Figure 14 A) is consistent with floral induction occurring when the tree growth decreases (Costes *et al.*, 2003) and at the end of their juvenile period (Costes and Guédon, 2012). The current results together suggest that this relationship is conserved among genotypes with diverse architectures. In the present study, this relationship could result from the relatively young age of the trees, suggesting different dates of entry into production depending on the genotype. X0342 maintained a high number of long GU while exhibiting few floral GU whereas X0337 and X6917 displayed low proportion of long GU starting from the second year of growth and an alternation in short and floral GU proportions over successive years.

FI proportion correlated to starch concentration in stem (Figure 17 C), but with a low correlation coefficient. Contrasted FI proportions for comparable starch concentrations in stem were observed in this correlation, indicating the lack of strong relationship between carbon balance estimated from stem starch and FI. This observation is similar to previous results showing that FI inhibition is not related to carbon status (Belhassine *et al.*, 2019). A decrease in FI proportion was observed for most of the genotypes when crop load values (expressed in number of fruit per leaf area) increased. This is consistent with the well documented crop load effect on flowering (Jonkers, 1979; Monselise and Goldschmidt, 1982). Nevertheless, such a relationship disappears when crop load was expressed by mass of fruit (Figure 15) revealing that FI is more affected by fruit number rather than fruit sink strength, and thus supporting the hypothesis that carbon balance does not affect directly FI. However, two genotypes displayed flowering behavior independent of crop load: X8232 maintaining high FI proportion in high crop loads and X8717 maintaining low FI proportion for contrasted crop loads. This suggests that the sensitivity of SAM FI to the presence of fruit could differ among genotypes. The strong impact of the number of fruits could be related to the impact of the number of seeds, as previously suggested by Neilsen and Dennis (2000). Nevertheless, no clear experimental result is available to be able to confirm the existence of genotypic variability in seed number.

Exogenous applications of GA1 and GA4 have been shown to inhibit floral initiation in 'Golden Delicious' (Ramírez *et al.*, 2004). Moreover, heavily cropping 'Fuji' trees had higher concentrations of GA1 and GA4 in SAMs than concentrations found on thinned trees (Kittikorn *et al.*, 2010). Active GA4 was positively correlated to FI proportion in 2019 (Figure 17 D), with high FI proportion found in trees with high GA4 concentration. Although this effect was contradictory to what observed by Ramírez *et al.* (2004), this result reinforces an implication of GA4 in controlling FI. Ramírez *et al.*, (2004) also proposed that floral induction in SAM is promoted when cytokinins exceed GA concentration in 'Golden Delicious' seeds. Our hormones quantification did not conform to this observation, as all genotypes had lower concentrations of cytokinins than of gibberellins in SAM. Moreover, increasing Tz concentration in SAM was negatively associated to FI proportion (Figure 17 E), meaning that Tz is more likely inhibiting FI.

7. Conclusion

This study was carried out on genotypes contrasted for architectural traits as observed with previous classifications (Coupel-Ledru *et al.*, 2019). Concentration patterns of hormones (mainly GA, IAA and ABA) and tree carbohydrate to a lesser extent appeared to act on plant growth and development. Changes in the proportion of annual GU changed over years with an increase in the proportion of short and floral at the expense of long GU, consistently with previous studies on tree ontogeny. Although their tendency to decrease, the high proportions of long GU for some genotypes at the end of the experiment indicate that they did not overcome the juvenile phase yet and are still in transition to the mature phase. As a consequence, genotype bearing patterns and FI are likely to change with tree ontogeny. Nevertheless, our results reinforce the assumption of hormones (GA and cytokinines) implication in FI in apple trees.

8. Supplementary Material

	Irrigation North										Irrigation South									
	1	2	3	4	5	6	7	8	9	10	1	2	3	4	5	6	7	8	9	10
1	X0036	X0036	X6468	X6468	X8743	X8743	X1556	X1556	X8939	X8939										
2	X0048	X0048	X6471	X6471	X8746	X8746	X8398	X8398	X8386	X8386										
3	X0156	X0156	X6518	X6518	X8749	X8749	X1180	X1180	X9391	X9391										
4	X0337	X0337	X6905	X6905	X8750	X8750	X8415	X8415	X1225	X1225										
5	X0342	X0342	X6917	X6917	X8751	X8751	X1344	X1344	X8220	X8220										
6	X0344	X0344	X6918	X6918	X8933	X8933	X2361	X2361	X8751	X8751										
7	X0352	X0352	X6920	X6920	X8934	X8934	X0972	X0972	X6917	X6917										
8	X0380	X0380	X7195	X7195	X8937	X8937	X1314	X1314	X8215	X8215										
9	X0395	X0395	X7197	X7197	X8939	X8939	X8404	X8404	X8740	X8740										
10	X0404	X0404	X7199	X7199	X8972	X8972	X4442	X4442	X8411	X8411										
11	X0421	X0421	X7200	X7200	X9080	X9080	X8256	X8256	X1239	X1239										
12	X0468	X0468	X7203	X7203	X9090	X9090	X0700	X0700	X1071	X1071										
13	X0522	X0522	X7204	X7204	X9115	X9115	X9153	X9153	X4681	X4681										
14	X0585	X0585	X7358	X7358	X9118	X9118	X4915	X4915	X0036	X0036										
15	X0591	X0591	X7759	X7759	X9122	X9122	X8933	X8933	X1307	X1307										
16	X0599	X0599	X8199	X8199	X9124	X9124	X2104	X2104	X8200	X8200										
17	X0600	X0600	X8200	X8200	X9128	X9128	X4004	X4004	X1077	X1077										
18	X0640	X0640	X8201	X8201	X9130	X9130	X8972	X8972	X8743	X8743										
19	X0666	X0666	X8202	X8202	X9148	X9148	X1076	X1076	X8937	X8937										
20	X0667	X0667	X8203	X8203	X9151	X9151	X2318	X2318	X2949	X2949										
21	X0695	X0695	X8209	X8209	X9152	X9152	X1705	X1705	X8396	X8396										
22	X0700	X0700	X8211	X8211	X9153	X9153	X8227	X8227	X0968	X0968										
23	X0710	X0710	X8212	X8212	X9166	X9166	X1212	X1212	X8692	X8692										
24	X0778	X0778	X8214	X8214	X9171	X9171	X8713	X8713	X0421	X0421										
25	X0849	X0849	X8215	X8215	X9176	X9176	X2316	X2316	X8706	X8706										
26	X0942	X0942	X8218	X8218	X9177	X9177	X2320	X2320	X2428	X2428										
27	X0960	X0960	X8220	X8220	X9179	X9179	X2302	X2302	X8247	X8247										
28	X0968	X0968	X8222	X8222	X9185	X9185	X8252	X8252	X8732	X8732										
29	X0972	X0972	X8223	X8223	X9186	X9186	X0352	X0352	X1682	X1682										
30	X1064	X1064	X8224	X8224	X9190	X9190	X8223	X8223	X8405	X8405										
31	X1071	X1071	X8226	X8226	X9191	X9191	X4898	X4898	X8228	X8228										
32	X1076	X1076	X8227	X8227	X9202	X9202	X1095	X1095	X7203	X7203										
33	X1077	X1077	X8228	X8228	X9234	X9234	X1363	X1363	X1552	X1552										
34	X1095	X1095	X8229	X8229	X9246	X9246	X8214	X8214	X9234	X9234										
35	X1176	X1176	X8232	X8232	X9250	X9250	X8392	X8392	X0710	X0710										
36	X1180	X1180	X8233	X8233	X9251	X9251	X8224	X8224	X8407	X8407										
37	X1186	X1186	X8236	X8236	X9252	X9252	X1227	X1227	X1982	X1982										
38	X1206	X1206	X8237	X8237	X9256	X9256	X9090	X9090	X8201	X8201										
39	X1212	X1212	X8238	X8238	X9259	X9259	X9080	X9080	X8199	X8199										
40	X1225	X1225	X8239	X8239	X9267	X9267	X8697	X8697	X8694	X8694										
41	X1227	X1227	X8242	X8242	X9389	X9389	X0404	X0404	X8229	X8229										
42	X1235	X1235	X8244	X8244	X9391	X9391	X9115	X9115	X8390	X8390										
43	X1239	X1239	X8245	X8245	X9421	X9421	X8238	X8238	X8436	X8436										
44	X1269	X1269	X8246	X8246	X9429	X9429	X8719	X8719	X9429	X9429										
45	X1301	X1301	X8247	X8247	X9433	X9433	X9176	X9176	X0344	X0344										
46	X1307	X1307	X8249	X8249	X9436	X9436	X8249	X8249	X6905	X6905										
47	X1314	X1314	X8250	X8250	X9437	X9437	X1846	X1846	X1206	X1206										
48	X1344	X1344	X8252	X8252	X0898	X0898	X0695	X0695	X9185	X9185										
49	X1363	X1363	X8256	X8256	X8934	X8934	X8750	X8750	X9122	X9122										
50	X1552	X1552	X8380	X8380	X0942	X0942	X1269	X1269	X9166	X9166										

Figure S1. Disposition of the 12 trees (highlighted in yellow) in the orchard. WW rows corresponded to well-watered trees and WS rows correspond to water-stressed trees.

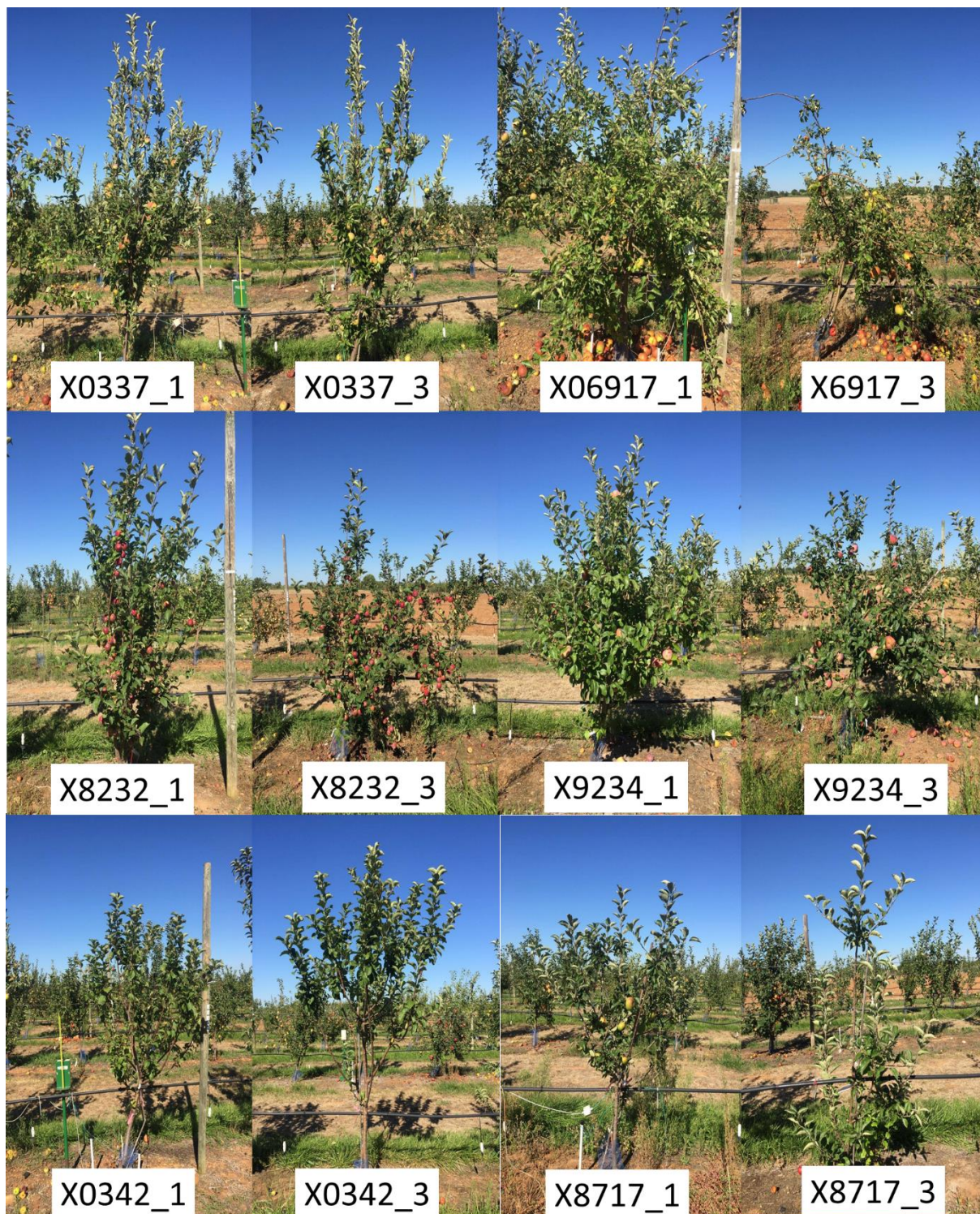


Figure S2. Photograph of the 12 trees of the six genotypes in summer 2017

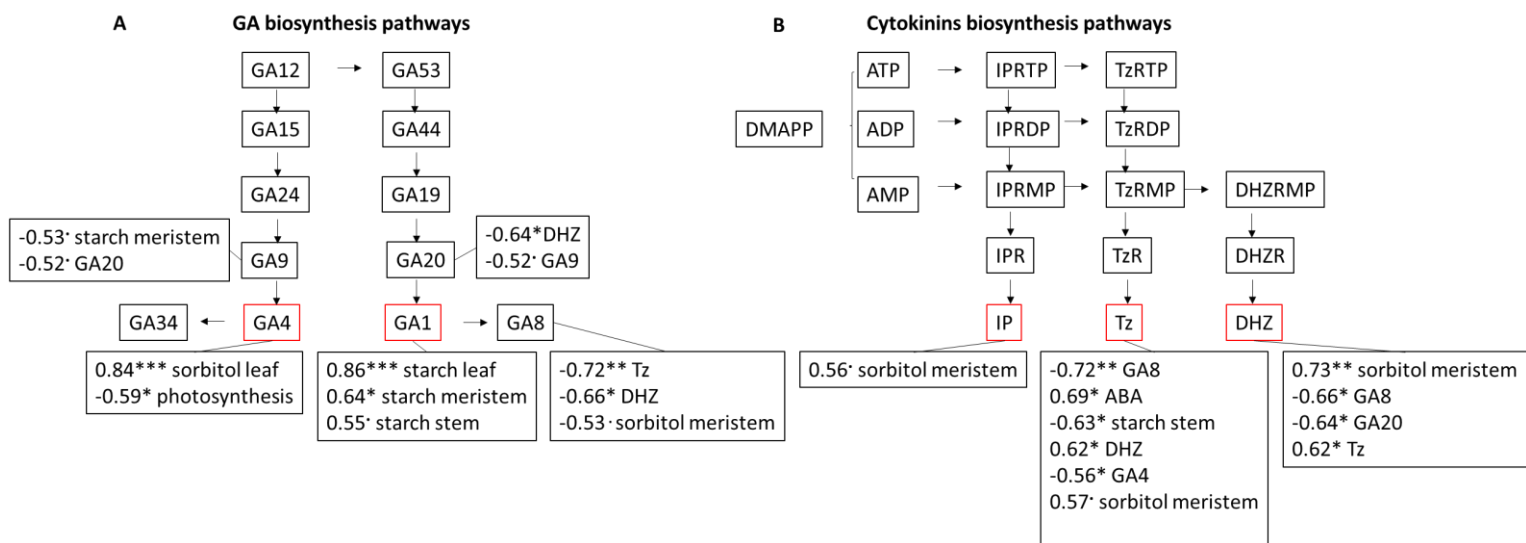


Figure S3. Schematic representation of biosynthesis pathways of (A) active gibberellin and (B) cytokinin forms and their most significant correlations with other measured physiological variables.

VI. General discussion

1. Analysis of inhibiting and activating signals effect on floral induction through an experimental approach

1.1. Main physiological mechanisms analyzed in this study.

The results of the first experiment showed a strong effect of leaf and fruit removal practices on FI proportion at the tree level. As expected, a decrease in the number of leaves resulted in a decrease in FI proportion whereas a decrease in the number of fruits resulted in an increase of FI proportion. Palmer *et al* have already studied effects of part-tree thinning on flowering of apple tree. However, this study did not take into account the effect of leaves nor considered the implication of non-structural carbohydrate contents in organs including shoot apical meristem (SAM) in the growth season on the next year flowering. The innovation of our study was thus to show that these effects of leaves and fruit are variable depending on the scale of the tree at which leaf and fruit removal practices were carried out, suggesting a major effect of the distances between the leaves, fruit and meristems on FI control. Changing the scales of leaf and fruit removals suggests that signals can move from the signal sources (leaves and fruit) to the target organs (meristems) but can act on FI at a short distance only (between neighboring shoots), while they cannot reach longer distances (other branches and half of Y-shaped trees). In addition, the spatial variability of FI was not associated with a spatial variability in photosynthetic activity, neither with starch content in organs, nor with the availability of non-structural carbohydrates in the meristems. These results supported what had already been proposed on the low involvement of carbon in the control of FI (Pallas *et al.*, 2018; Belhassine *et al.*, 2019).

Nevertheless, carbon transport at long distances is suggested by the results we obtained with respect of within-tree variability of fruit weight and photosynthesis. Indeed, under high crop load conditions, no difference in photosynthesis was observed between fruiting and non-fruiting tree parts. This observation confirms that under high sink demand, leaves export assimilates at long distances to sustain this demand, thus stimulating photosynthesis in non-fruiting tree parts (Wunsche *et al.*, 2000). An impact of the local source-sink conditions on photosynthesis activity was observed in another study (Poirier-Pocovi *et al.*, 2018) probably due to lower crop loads that did not trigger a whole-tree saturation in photosynthesis.

Gibberellin involvement in FI was suggested by the quantifications of different GA forms, particularly for GA9. Moreover, the correlations found on the set of genotypes between GA4 and GA8 and flowering proportion and number of inflorescences per tree reinforced the probable implication of these hormones in the control of FI. Results of both experiments showed that gibberellin concentrations exhibited a large variability in the buds of the same tree even under the same conditions of leaves and fruits presence. This variation could be related to the desynchronization of the meristems within the tree and the variability of phenological stages in the sampled meristems. Histological observations of apple tree meristems of short shoots (spurs) have revealed that the changes from vegetative to reproductive stages occur between 39 and 53 days after full bloom (Foster *et al.* 2003, Hanke *et al.* 2007). We sampled similar meristems in this period, but it remains unknown at which stages active GA could affect the meristem transition toward FI. Moreover, a strong polymorphism of the shoots is observed in the apple tree (Fulford, 1966; Costes *et al.*, 2003) ranging from short (spurs) to long shoots that can reach one meter in length or more. This variability is mainly determined by the date of shoot growth arrest (Chen *et al.* 2019). As long shoot types can be floral induced, FI may occur at different periods of time in the growth season since FI and meristem growth arrest have to be synchronized (Fulford, 1966). Moreover, a polycyclic growth can occur in the development of apple branches mainly on young trees (Costes and Guédon, 2012), with the possibility of producing more than one unit of growth (Chen *et al.*, 2019). This implies that at sampling time, some meristems had not yet performed their transition to flowering.

Our study focused on FI proportion in SAM located in terminal position of annual shoots and did not account for meristem fate in axillary position along medium and long shoots. This simplification is relevant for adult apple trees displaying short shoots mainly (e.g. Costes *et al.* 2003). Nevertheless, in

medium and long shoots, FI appears in axillary buds in some specific zones along parent shoots (Costes *et al.* 2014). This positioning has been observed to be strongly associated with changes in the rate of leaf emergence from the SAM and in the intensity of apical dominance (Barnola and Crabbé, 1991; Lauri and Térouanne 1998). Therefore, further experiments coupling an evaluation of the rate of shoot development and timing of FI in axillary buds would be relevant to disentangle the combined effects of shoot ontogenetic properties and inhibiting and activating signals on the determination of FI.

The study of flowering genes expression revealed that FI occurs before the first signs of histological transformation from vegetative to reproductive stages could be observed in the meristems (Hättasch *et al.*, 2008). From this perspective, it would be interesting to look at the expression genes involved in the regulation of the enzymes of GA biosynthesis pathways. This could be highly relevant since the study by Guitton *et al.*, (2016) detected that genes linked to the expression of GA2ox and GA20ox, which contribute to catabolism and metabolism of active GA forms, respectively, appeared to be regulated differently in SAM of trees under ON and OFF conditions. These results suggest that it would be interesting to jointly examine the gene expression of GA pathways and the amounts of different forms in SAM to further analyze GA implication on FI. Gene expression quantification and profiling by microarray or qRT-PCR are therefore other alternatives to estimate the levels of activities of the different genes involved in hormonal and sugar pathways signaling (Celton *et al.*, 2011; Gibson, 2005; Guitton *et al.*, 2016; Olszewski *et al.*, 2002). Moreover, it would be possible to predict the effects of enzyme activities on GA production, including feedback effects, along the biosynthesis by combining enzyme activity measurements together with a mathematical modeling approach (Middleton *et al.* 2012).

Although gibberellins are suspected to be the source of the inhibitory signal, little information is available about their transport in plants. Long-distance transport of GA has been observed on non-bioactive precursors (GA12) rather than on bioactive forms (Regnault *et al.*, 2015). A recent review on GA transport reported the nitrate transporter 1/peptide (NPF) and SWEET transporters family as gibberellin transporters but their biological importance remained weak because of poor genetic support (Binenbaum *et al.*, 2018). Moreover, we can suspect the action of other hormones on FI, such as abscisic acid, auxin and cytokinins that can act as a second messenger (Hanke and al., 2007) and can be transported over long distances (Kanno *et al.*, 2012; Prusinkiewicz *et al.*, 2009; Wang *et al.*, 2006).

Another difficulty in hormone quantifications was that meristems were not isolated from the bud. Sample thus contained preformed leaves and bud scales together with the meristematic tissues. The hormone concentrations attributed to the meristems could therefore be biased by the content of the other bud structures.

As carbon was found as not directly involved in FI, the nature of the activating signal remains to be elucidated. Assumptions about the nature of the activating signal involved in FI can be made based on the knowledge available in other species. For instance, signaling molecules, such as trehalose-6-phosphate (T6P) produced in leaves may have a role in FI (Ponnu *et al.*, 2011; Lastdrager *et al.*, 2014). This molecule, which is found only in trace amounts in most plants, is assumed to play a key role as signaling the plant carbon status. In *Arabidopsis*, T6P has been shown to affect development and flowering and to be required for the production of the FT protein, considered as the florigen (Corbesier *et al.*, 2007a; Corbesier *et al.*, 2007b; Wahl *et al.*, 2013). The leaves are also likely to be sources of FT protein, which is assumed to be transported by phloem to SAM where it activates flowering (Mathieu *et al.*, 2007; Tamaki *et al.*, 2007). It could act possibly downstream of *CONSTANS* (*CO*) gene (Cho *et al.*, 2018). Moreover FD, expressed in SAM is required for FT to promote flowering through the activation of a floral meristem identity gene, *APETALA 1* (Abe *et al.*, 2005). Quantifying T6P and expression of genes encoding for FD and FT protein in SAM would confirm their presence in

SAM of apple and would help understanding of their role in FI (Guitton *et al.*, 2016; Wahl *et al.*, 2013).

1.2. Analysis of the main determinants of genotypic variability in floral induction

The genetic diversity considered in this present study was based on an apple core collection of French varieties and does not include the worldwide observed diversity (Lassois *et al.*, 2016). The use of this core collection aimed at having a large allelic diversity in the genotypes studied, and at maximizing the variability in architectural traits and bearing habits. This diversity was indeed larger than the one considered in previous studies performed on biparental segregated population, as for instance the one derived from the cross between 'Belrène' cultivar and the INRA hybrid X3263 in which a large variability in flowering and production patterns has been observed (Durand *et al.*, 2017; Pallas *et al.*, 2018). Other approaches further extending the diversity studied could have been done. For instance, the use of wild relatives distributed worldwide (Cornille *et al.*, 2014) represent potentially sources of diversity for apple architecture, physiology and flowering.

During the first four years of growth, the coding methodology proposed by Godin and Caraglio (1998) was used to describe the topology of trees in the form of MTG. The main limitation of topology acquisition in MTG is that this method, although very precise and informative, was time-consuming. Indeed, each year it was harder and more time consuming to describe the trees due to the increasing number of growth units over the years (the biggest tree produced 673 growth units in 2017). Four days of annotation were necessary to obtain a complete tree description in 2017. 3D reconstruction of the architecture of the six genotypes was obtained from digitizers that record directly the 3D points of interest (Sinoquet *et al.*, 1997). Such a dataset is highly relevant for further modeling work, but the method for data collection was also time-consuming and hardly applicable on large trees. Terrestrial LIDAR scans (T-LIDAR) represent a new way to acquire 3D representation, related to plant topology and geometry (Côté *et al.*, 2009) that were used to analyze the genotypic differences in tree shape and light interception descriptors of the apple core collection (Coupel-Ledru *et al.*, 2019). This method is also adapted for the reconstruction of tree topology using tree skeletization procedure (Boudon *et al.*, 2014). Nevertheless, some limits with this method also exist such as self-occlusion problems that limit the full description of shoot branching and successions. Other methods can also be used for characterizing genotypes physiological properties, based on high-throughput measurements with airborne images (Gomez-Candon *et al.*, 2016). Vegetation indices and proxies of tree transpiration can be extracted from thermal and multi-spectral images. Moreover, regarding photosynthesis, *in planta* measurement based on chlorophyll fluorescence, even though not high throughput could be used in future studies. In particular, the semi-empirical I_{PL} index derived from fluorescence measurements (Losciale *et al.*, 2015) has been used to quantify the genotypic variability in photosynthesis of the core collection (Coupel-Ledru *et al.*, 2019). Genotypic variability in carbohydrates and hormones could also be assessed by modern spectroscopic techniques such as near infrared spectroscopy (NIRS) measurements. Indeed, a previous study performed on nine apple cultivars could discriminate differences between cultivars, based on fruit samples (Eisenstecken *et al.*, 2019). However, preliminary work to calibrate the relationships between the trait of interest and absorbance curves on a large set of genotypes would be necessary.

In this study, a combined effect of GA and cytokinines on FI was suggested by the results on the genotypic variability. Hormones were only measured for SAMs, but it would be interesting to analyze hormone content in other organs. Quantification of gibberellins in fruit or seed could represent a good option to evaluate the relationship between GA concentrations in the supposed sources organ and in SAM (Ramírez *et al.*, 2001). Moreover, different amounts of inhibiting signals produced could be in relation with the observed genotypic variability in seed number per fruit (Celton *et al.*, 2014). Correlation between GA concentrations in seeds and SAM would support the hypothesis of GA transport between these two organs. Furthermore, quantification of ABA, IAA and cytokinins in roots and stems could help understanding their implication in FI in relation with apical dominance and branching patterns, as previously in the 'Wijcik McIntosh' mutant (Petersen and Krost, 2013).

From the whole tree topology description six genotypes over the years, a clear difference in the dynamics of setting up the tree architecture was revealed. Despite stable architectural traits for several genotypes which maintained either vigorous growth and branching or weak ones among years, other genotypes changed their behavior during their development. The importance of the dynamics in tree architecture in the first years of tree development and its consequence on FI has been underlined since the studies of Hallé *et al.* (1970).

From the whole tree topology description six genotypes over the years, a clear difference in the dynamics of setting up the tree architecture was revealed. Despite stable architectural traits of four genotypes that maintained either vigorous or weak growth and branching over the years, two genotypes changed their behavior during their development. The importance of the dynamics in tree architecture in the first years of tree development and its consequence on FI has been underlined since the studies of Hallé and co-workers (1970). Moreover, the genotypes appeared in transition between juvenile and mature phases, even though they exhibited contrasted dynamics, evaluated through changes in proportions of long and floral GUs, depending on each genotype. The dynamics of architectural establishment strongly affected genotypic production patterns. The two genotypes that exhibited alternate bearing were characterized by a high and synchronized flowering in their second or third year of growth. This confirms the importance of meristem synchronization in the setting up of biennial bearing (Durand *et al.*, 2013; Koenig and Knops, 2005). The other three genotypes did not exhibit strong irregularity during their first 5 years of growth. Also, the two most vigorous genotypes, which had larger TCSA and number of axes, appeared to be able to achieve greater and earlier production than small genotypes, consistently with previous observations (Visser, 1965). Consequently, since small genotypes did not fully enter in the adult phase at the end of our experiment, no conclusions could be formulated concerning their regularity. Alternate bearing after tree maturity, which occurs three to five years after planting, is related to synchronicity in SAM FI. Such synchronicity can result from tree ontogeny, i.e. the decrease of long GU (Costes and Guédon, 2012) or from climatic accidents such as frost (Nagy *et al.*, 2009). Therefore, to draw conclusions about genotypes regularity in the core collection, more observation will be needed in the coming years. In addition, the trees in this study have been thinned, which undoubtedly limited the appearance of natural alternation in some genotypes. This is particularly true for 2018, when genotypes were thinned to have comparable crop loads.

In this study, FI was used to estimate alternate bearing, but this factor is probably not enough to assess the genotypes bearing patterns. Indeed, large variability in fruit set also exists in apple trees. This variability could result from genotypic characteristics with some genotypes more prone to fruit drop during the growing season (Celton *et al.* 2014) than others. Moreover, a strong inverse relationship between floral induction and fruit set, likely related to the carbon balance (Lakso *et al.*, 2007), can limit the consequences of high flowering in one year on next year production (Lordan *et al.*, 2019; Pallas *et al.*, 2018).

2. Modeling of FI variability and its determinisms

2.1. Added value of the modeling approach and limitation

The hypotheses that emerged from the first experiment were used to develop a model for simulating the transport of signals that could affect FI within a tree branching structure. This model complements and renews previous models that have been proposed to simulate inhibiting and activating signal transports and their consequences on FI (Pellerin *et al.*, 2012; Pallas *et al.*, 2016). Indeed, these models were not calibrated on observed data and did not simulate the within-tree variability of FI. As the activating signal appeared to be related to leaf presence but independent on the carbon balance, the total leaf area was used as an approximation of the amount of activating signal. This choice was also based on previous results showing the close relationship between shoot vigor or length and FI (Neilsen and Dennis, 2000; Lauri and Trottier, 2004). In addition, the estimated values of the parameters made it possible to quantify the distances at which the activating and inhibiting signals could be transported from the leaves and fruit to the meristems (approximately 50

cm vs 1 m, respectively). Thus, the model results suggest that the activating signal could be transported at shorter distances than the inhibiting signal. Moreover, when combining the respective effects of both signals in the meristem, the model suggests that meristems were less sensitive to the activator signal than to the inhibitor signal.

The current limitation of this model results from the limited insight into the nature of the signals moving to trigger or repress floral induction. In addition, the model does not consider any preferential direction in signal fluxes (acropetal or basipetal) which could locally affect FI proportion, while such a mechanism could be hypothesized.

The model is not dynamic at neither on intra-annual nor inter-annual time scales. As explained before, it is likely that FI occurs at different periods within the growth season, depending on the shoot length (Costes *et al.*, 2014b). Indeed, studies that described floral transition in meristems focused on short shoots (Foster *et al.*, 2003; Hanke *et al.*, 2007). However, long annual shoots, often developing until summer, are also able to flower in apical position (Costes and Guédon, 2012). Therefore, FI even though happening in short shoots around 50 days after full bloom, could occur later and consequently in different trophic and temperature conditions. It can be thus postulated that the tree carbon status could drive the growth potential of the shoots by determining their growth duration whereas FI could occur in SAM only when growth decreases or even ceases. The assumption of such a relationship between intra-bud growth before growth cessation and FI has been previously proposed by Barnola and Crabbé (1991). Coupling the model developed in this study to the dynamic model MappleT (Costes *et al.*, 2008) would allow considering shoot growth development and cessation during the season. Moreover, a photosynthesis model (for example Sinoquet *et al.*, 2001) and a carbon allocation model (for example Reyes *et al.*, 2019) with retroactions on growth would make the model able to simulate within tree variation in growth and development depending on trophic condition (crop load for instance) or/and abiotic stresses. Furthermore, the model proposed in the current study simulates FI for a considered year, only with no feed-back on the tree's architecture in the next year. In that context, the Markov models implemented in MappleT could be used to simulate transitions in meristem fates in the following year while the model developed in this thesis could quantify the intensity of FI in the developing shoots. Coupling MappleT model with photosynthesis and carbon allocation modules would be facilitated by the generic MTG structure and the availability of those models on the OpenAlea platform, designed to facilitate the integration of models (Pradal *et al.*, 2008; Albasha *et al.*, 2019; Barillot *et al.*, 2019).

Another limit of the modelling approach arises from the absence of any simulation of meristem fate in axillary position along medium and long GU, considering that adult trees produce short GU only (Costes *et al.*, 2008). However, for younger trees or other fruit trees bearing floral buds in axillary position (e.g. *Prunus* sp.) it would be necessary to consider both flowering probability and the bud position along parent shoots (Costes *et al.*, 2014). Studies showed that floral induction is associated with the decrease in plastochron and shoot growth cessation (Crabbé, 1984; Lauri and Terouanne, 1998; Costes and Guédon, 2002). Once again, generating potential floral zone in the tree structure could be achieved using markovian models (Renton *et al.*, 2006) or more mechanistically by simulating shoot growth dynamics within the growing season depending on growing degree days (Migault *et al.*, 2017). Integrating the effects of fruit set in modeling approaches as in other studies (Lordan *et al.*, 2019) would be a step further in the development of a decision-making tool to predict fruit production over the years and conduct agronomic practices such as thinning of flowers. In that context and since fruit set is known to be affected by current year trophic condition (Lakso *et al.*, 2006), the use of a carbon-based model allowing to estimate fruit set would be relevant.

2.2. Perspectives to account for genotypic variability in the model for simulating floral induction variability

First simulations on hypothetical structures showed that our model is able to reproduce many different FI behaviors. High values of resistance parameters can lead to some shoot autonomy and promote alternation at the shoot scale whereas low values for this parameter lead to similar distribution of signal amount in all the buds, which can induce alternation at the tree scale. High values for the transition parameters for inhibiting signal can be associated with a bourse-over-bourse behavior (Lauri *et al.*, 1997) and high shape values can lead to random determination of FI and regularity at the tree scale with half of buds floral-induced in each year (Durand *et al.* 2013). Our modeling approach integrating both architectural and functional traits could be thus an interesting way to explore further these intertwined relationships between tree physiology (amount of signal, signal fluxes, meristem sensitivity), architecture and FI on in a context of genotypic variability.

The experiment performed on genotypes suggested that there were variations in the quantity of signals that correlated with architectural variations, and that both processes affected FI. It might be possible to conduct dedicated experiments on genotypes to further characterize the nature of the signals and their transport as well as tree architecture, but *in silico* modeling approach aiming at deciphering the architectural and physiological effects on IF on a large tree population seems very helpful. 3D structures obtained from digitized genotypes are now available to initiate the adaptation of the model to six genotypes. However, other high throughput methods such as T-LIDAR scans can be used for architecture characterization of a large set of genotypes, as previously discussed.

For physiological variables, we can hypothesize that the amount of signal produced by each genotype could vary especially in relation with the observed genotypic variability in seed number (Celton *et al.* 2014) which are known to be a source of GA. Since the activating signal was found as not limiting under usual agronomic condition, a model-based approach could be carried out on the inhibiting signal only. Using the set of parameters validated for 'Golden delicious', it would be possible to run simulations for the other six genotypes, in order to assess the part of architectural variability explaining the variability in FI. The next step would be to carry out a sensitivity analysis of the model on contrasted architectures to assess the most influential parameters on the simulations and their redundancy. The same methods as those used by Da Silva *et al.* (2014) and Perez *et al.* (2017) (metamodeling approach) for analyzing sensitivity of architectural traits on light interception and carbon assimilation could thus be performed for analyzing the effect of model parameters on FI. This approach would help defining the most influencing parameter on FI before trying to estimate model parameters on a larger set of genotypes than those used in this study.

It could be argued that the simplicity of the model would facilitate the fitting procedure of the model to a large set of genotypes using simple model inversion procedure. Such kind of model inversion procedures have been performed in previous studies by the GreenLab model (Cournède *et al.*, 2011; Letort *et al.*, 2008; Mathieu *et al.*, 2008).

VII. Résumé général

1. Contexte général

La floraison et la reproduction peuvent se produire à différents âges ou stades de développement chez les plantes polycarpiques. Pour la plupart des arbres tempérés, la floraison a lieu chaque année, mais avec de grandes irrégularités d'intensité selon les années. L'un des phénomènes les plus connus associés à cette irrégularité de production est l'alternance de production qui se caractérise par une année de reproduction intense (année ON) suivie d'une année de reproduction faible ou nulle (année OFF) (Monselise and Goldschmidt, 1982). Ce phénomène est particulièrement observé chez les espèces fruitières et présente des enjeux économiques cruciaux. En effet, l'alternance de production génère des problèmes économiques associés à une trop faible production en années OFF et une production de fruits de faible calibre avec des qualités organoleptiques altérées en années ON. Les processus liés à l'alternance de production ont été étudiés depuis de plusieurs années dans le but d'atténuer ses effets. Ces études ont engendré des pratiques agronomiques pour diminuer la floribondité en année de forte charge, notamment par la pulvérisation d'éclaircissants chimiques et plus récemment par l'éclaircissage mécanique. Cependant ces pratiques présentent un coût économique non négligeable pour les agriculteurs ainsi que des risques environnementaux dans le cas des éclaircissants chimiques. Dans ce contexte, il est donc nécessaire d'étudier en détail les mécanismes physiologiques déterminant de l'alternance de production afin d'optimiser les pratiques agronomiques. Un autre moyen pour résoudre le problème d'alternance pourrait être de sélectionner des variétés naturellement peu alternantes pour limiter les besoins en éclaircissants et/ou les coûts associés à d'autres méthodes d'éclaircissages.

Des observations ont montré que l'alternance de production est liée principalement à des fluctuations de l'induction florale (IF) dans les bourgeons. L'IF correspond à des changements morphologiques et physiologiques qui conduisent à la transition des méristèmes de l'état végétatif à l'état reproducteur (Bangerth, 2009). Chez le pommier, comme chez de nombreux fruitiers de climat tempéré, l'IF survient l'année précédant la floraison (Abbott, 1969), ce qui signifie que le nombre potentiel de fruits d'un arbre est déterminé l'année précédant la récolte. Cette IF se produit entre de 50 à 60 jours après la pleine floraison (Haberman *et al.*, 2016a), dans des conditions de forte compétition puisqu'il s'agit de la période de fort développement végétatif et du début du développement des fruits. Chez les arbres fruitiers, deux hypothèses principales ont été proposées pour expliquer les variations interannuelles de l'induction florale. La première hypothèse concerne la compétition entre les organes en croissance (fruits, pousses et racines) et les méristèmes pour les carbohydrates produits par la photosynthèse (Nielsen and Dennis, 2000). En année de forte charge en fruits, cette compétition est forte et donc susceptible de priver les méristèmes des assimilats, qu'on suppose nécessaires pour l'IF, conduisant ainsi à de faibles floraisons et fructification l'année suivante. La deuxième hypothèse suggère que les fruits produisent des substances, probablement des gibbérellines produites par les pépins dans le cas du pommier, qui inhibent l'IF dans les méristèmes à proximité (Chan and Cain, 1967). Certaines études se sont concentrées sur la productivité des arbres fruitiers en caractérisant les relations entre rendement, bilan carboné, et intensité des stress biotiques et abiotiques (Palmer *et al.*, 1991; Wunsche *et al.*, 2000). D'autres études ont aussi montré que la présence de feuilles favorisait la floraison (Davis, 2002; Haberman *et al.*, 2016a). Cependant, il n'est pas encore clair si ces facteurs affectent directement l'IF ou d'autres composantes du rendement (nouaison, masse de fruits) (Lauri *et al.*, 1996). L'architecture des arbres s'est également révélée importante pour la régularité de la production, notamment du fait de la distribution spatiale des bourgeons floraux au sein de l'arbre. En effet, dans une structure d'arbre, tous les méristèmes ne fleurissent pas nécessairement au cours d'une année donnée. Pour le pommier, il a été montré qu'en fonction de la variété, les méristèmes sont plus ou moins synchronisés et que les différences de régularité entre variétés sont en partie liées aux différences d'organisation topologique et de ramification (Costes *et al.*, 2003; Durand *et al.*, 2013). Ainsi, un lien a été suggéré entre la variabilité architecturale observée entre variétés et les rythmes interannuels de floraison. Il est généralement admis que les géotypes présentant une démographie de pousses

annuelles avec une majorité d'axes de longueur moyenne ont une tendance à être plus réguliers que les génotypes ayant une majorité d'axes courts (Costes and Guédon, 2012).

Récemment, des études ont été réalisées pour analyser le lien potentiel entre la variabilité génotypique du mode de production (régulier, irrégulier, biennal, synchronisé ou pas) et le métabolisme carboné (Pallas *et al.* 2018). Les auteurs ont conclu que la variabilité de l'IF entre les génotypes n'était pas directement associée à des contrastes d'activité photosynthétique ou de disponibilité en carbone, remettant ainsi en question l'implication des relations source-puits de carbone dans la détermination de l'IF. De nouvelles hypothèses sur l'implication d'hormones telles que les gibbérellines et sur l'impact de la variabilité architecturale entre les organes dans la détermination de l'IF ont émergé de ces études et de détection de zones du génome associés à des caractères quantitatifs associés à l'alternance de production (QTLs ; Guitton *et al.*, 2012). Néanmoins, l'approfondissement de ces hypothèses et leur confrontation à des expérimentations reste nécessaire.

Cette thèse, qui porte sur le pommier comme cas d'étude, repose sur l'hypothèse que l'IF dans l'arbre fruitier dépend à la fois de l'architecture définie par l'organisation spatiale des différents organes aériens (fruits, feuilles, rameaux et méristèmes) et de signaux inhibiteurs ou activateurs. Ces signaux pourraient être liés à l'intensité de la compétition pour le carbone et/ou à des signalétiques hormonales. De plus, ce travail s'inscrit dans un contexte d'analyse de la variabilité génotypique avec pour objectif d'élucider davantage quelle part de la variabilité génotypique de la régularité de l'IF au cours des années pourrait résulter de la variabilité de l'architecture de l'arbre et/ou de la variabilité des processus physiologiques (hormonaux et carbonés principalement).

La stratégie générale de cette thèse reposait sur la complémentarité entre les approches expérimentales et de modélisation pour expliquer la variabilité de l'IF au sein de l'arbre et entre les différentes années d'une part et sa variabilité génotypique d'autre part. Des expériences sur la variabilité spatiale, temporelle et génotypique de l'induction florale ont été menées pour permettre l'étude des interactions entre les variables structurelles et fonctionnelles supposées être liées à l'IF. Les résultats obtenus à partir de ces expériences ont été utilisés pour développer une approche de modélisation dans laquelle l'IF dans les méristèmes était supposée être sous le contrôle des signaux inhibiteurs et activateurs se déplaçant à l'intérieur de la structure et agissant sur les méristèmes pour déterminer l'IF.

2. Objectifs

Cette thèse comportait trois objectifs. Le premier objectif était de déterminer sur une expérimentation menée sur le génotype 'Golden delicious' l'importance relative des différents signaux supposés responsables de l'IF chez le pommier et de quantifier l'impact de leurs distances aux méristèmes apicaux sur l'IF. Le deuxième objectif était de développer un modèle générique permettant d'estimer des quantités de signaux activateurs et inhibiteurs à différentes distances au sein de structures complexes d'arbres et de tester la capacité du modèle à simuler la variabilité intra-arbre de l'IF observée expérimentalement. En calibrant le modèle sur le jeu de données récolté dans la première expérimentation, ce travail de modélisation a eu pour objectif d'étudier de façon quantitative les effets conjoints des signaux inhibiteurs et activateurs sur l'induction florale ainsi que les distances auxquelles ils sont susceptibles d'agir dans la structure. Le troisième objectif était d'étudier les bases architecturales et physiologiques susceptibles d'expliquer la variabilité génotypique de l'IF par l'exploration de variables architecturales et fonctionnelles (hormonales et carbonés) parmi six variétés de pommier, contrastées en termes d'architecture.

3. Démarche expérimentale

Une première expérimentation visait à quantifier la contribution relative de la variation intra-arbre du contenu en carbohydrates et en gibbérellines sur l'IF. De plus, cette expérimentation a permis d'analyser plus en détail à quelle distance les effets des fruits et des feuilles avaient un impact sur le

devenir des méristèmes. Cette expérimentation a été réalisée entre 2016 et 2019 sur la variété Golden dans la station expérimentale SudExpé située à Marsillargues dans l'Hérault.

Pour répondre à ces questions, nous avons manipulé localement les relations sources-puits au sein de l'arbre afin de modifier l'intensité de la compétition trophique et les distances entre les méristèmes, les feuilles et les fruits. Sur des arbres placés en charges en fruits élevées (arbres ON) ou faibles (arbres OFF), nous avons réduit de moitié le nombre de feuilles (sources de carbone) ou de fruits (sources de gibbérellines et puits de carbone). Ces manipulations ont été effectuées à différentes échelles dans les arbres (pousses, branches et un côté des arbres en forme de Y). Nous avons alors examiné les variations intra-arbre de l'acquisition (activité photosynthétique des feuilles) et de l'accumulation (concentration de carbohydrates non structuraux dans les organes végétatifs) de carbone résultant de ces manipulations. Parallèlement, nous avons évalué la teneur en gibbérellines dans les méristèmes apicaux. Nous avons ensuite exploré leur possible implication sur les variations locales de l'IF mesurée pendant trois années au printemps. L'approche statistique d'analyses de données a consisté à analyser par analyse de variance (i) les effets combinés des traitements à l'échelle de l'arbre (contrôle, suppression de feuilles ou de fruits), (ii) de l'échelle à laquelle le traitement a été effectué (arbre, rameaux, branche ou moitié de l'arbre) et (iii) des conditions locales à l'intérieur de l'arbre (folié vs défolié, fructifié vs défructifié).

Une deuxième expérimentation a été menée entre 2014 et 2018 à l'UE Diascope à Mauguio dans l'Hérault. Cette expérimentation a eu pour objectif d'étudier six génotypes (deux répétitions par génotype) issus d'une collection de variétés de pommier et présentant des contrastes d'architecture. Les génotypes utilisés dans cette étude ont été identifiés par Lopez *et al.*, (2015), lorsque les arbres étaient âgés d'un an, comme ayant une vigueur élevée ou faible (trois génotypes pour chaque catégorie) en fonction de variables telles que la surface foliaire totale ou la hauteur. La mise en place de l'architecture des génotypes a été étudiée depuis la plantation jusqu'à trois à quatre ans de croissance afin d'identifier leurs caractéristiques respectives et de définir des morphotypes. Parallèlement à cette description architecturale, des mesures physiologiques ont été effectuées telles que l'évaluation du taux de photosynthèse, des dosages de carbohydrates (amidon, sorbitol, saccharose, glucose et fructose) dans les organes et d'hormones (gibbérellines, cytokinines, acide abscisique et auxine) dans les méristèmes. L'approche statistique retenue a combiné des analyses de corrélation entre les variables en explorant à la fois la variabilité inter et intra-génotype avec des analyses multivariées ayant pour but de déterminer des groupes de morphotypes. Nous avons ensuite associé ces groupes avec les valeurs des variables physiologiques qui leur sont spécifiques pour déterminer les liens possibles entre architecture et fonctionnement sur ce sous-échantillon de variétés. Les relations entre l'architecture des arbres, la physiologie, la production et la variabilité de l'induction florale ont ensuite été explorées pour approfondir les connaissances sur les déterminants possibles de la variabilité génotypique FI. Dans ce chapitre seules les données des mesures physiologiques acquises en 2018 sont présentées car les analyses 2019 notamment pour les dosages biochimiques et hormonaux n'ont pas encore été finalisées.

4. Démarche de modélisation

Nous avons développé un modèle générique pour quantifier l'impact combiné des signaux activateurs (en provenance des feuilles) et inhibiteurs (entre provenance des fruits) et des distances auxquelles ils agissent sur l'IF dans les arbres. Ce modèle a été développé en reprenant des formalismes précédemment utilisés dans deux modèles, pour l'allocation du carbone entre organes (Reyes *et al.*, 2019) et pour le transport bidirectionnel de messagers inhibiteurs (Pallas *et al.*, 2016). Dans le modèle développé dans cette thèse les feuilles et les fruits sont respectivement considérés comme des sources de signaux activateurs et inhibiteurs de l'induction florale. La quantité de signaux produits par chaque feuille est considérée comme proportionnelle à sa surface et celle originaire des fruits est proportionnelle au nombre de fruits dans la structure. Le transport du signal dans ces structures a été simulé dans des représentations 3D d'arbres grâce au format MTG, en considérant une atténuation du signal en fonction des distances entre organes. L'intensité de cette atténuation a

été modulée par un paramètre d'atténuation assimilables à une résistance au transport. Le devenir de chaque méristème est déterminé en fonction de la quantité de signaux l'atteignant et de lois de probabilité. Ces lois de probabilité comprennent deux paramètres : un paramètre représentant la quantité de signal permettant un taux moyen d'induction de 50% et un autre paramètre permettant de simuler un aléa dans la détermination du devenir du méristème. La combinaison des effets des deux signaux a été prise en compte en utilisant deux formalismes, un formalisme multiplicatif (probabilité d'induction = effet activateur x (1 – effet inhibiteur) et un autre basé sur l'effet unique du facteur le plus limitant (manque de signal activateur ou abondance de signal inhibiteur). Le comportement du modèle a été évalué sur des structures simples avant d'être calibré sur des architectures de pommier de la variété 'Golden delicious' soumises à des suppressions de feuilles ou de fruits et digitalisées au cours de la première expérimentation. Des validations des taux d'induction florale simulés ont été effectuées sur les arbres qui avaient été soumis à la fois à des suppressions de feuilles et de fruits. Les valeurs des paramètres du modèle ont été interprétées de façon à estimer l'impact des distances aux sources émettrices sur les quantités de signaux reçus et la sensibilité des méristèmes apicaux à la combinaison de signaux inhibiteurs et activateurs.

5. Principaux résultats

Les résultats de la première expérimentation ont montré un fort effet des pratiques de défoliation et de défructification sur le taux d'IF. Globalement et comme attendu, une diminution du nombre de feuilles a entraîné une diminution du taux d'IF alors qu'une diminution du nombre de fruits a permis d'augmenter celle-ci. Le caractère novateur de cette étude a été de montrer que ces effets sont variables selon l'échelle de l'arbre à laquelle sont faites les pratiques de défoliation et de défructification suggérant un effet majeur des distances entre les feuilles, les fruits et les méristèmes sur l'IF. De plus il a été montré que la variabilité spatiale de l'IF résultant de ces manipulations n'est pas associée à une variabilité spatiale de l'activité photosynthétique ni à la teneur en amidon des organes ou à la disponibilité carbohydrates non structuraux dans les méristèmes apicaux. Ceci suggère un impact de signaux activateurs provenant des feuilles et inhibiteurs provenant des fruits indépendants du bilan carboné. L'étude des effets sur l'IF selon les échelles de défoliation/défructification (rameau, branche, moitié des arbres) suggère qu'à courte distance (pousses avoisinantes), ces signaux peuvent se déplacer des sources (feuilles et fruits) aux puits (méristèmes apicaux) pour agir sur l'IF alors qu'ils ne peuvent pas atteindre de plus longues distances (branches et moitié d'arbres en forme de Y). Par contre une implication des gibbérellines, notamment de la GA9 a été suggérée. Bien que non directement reliée au déterminisme de l'IF, cette étude a par contre montré que les carbohydrates peuvent se déplacer d'une branche à l'autre en cas de déséquilibres source-puits élevés dans l'arbre afin de permettre la croissance des fruits même si ceux-ci sont situés à longue distance des sources de photo-assimilats.

La première expérimentation a été réalisée sur un seul génotype et n'était pas informative sur les variables physiologiques ou architecturales sous-jacentes qui pourraient expliquer la variabilité de l'IF entre les génotypes et les différents patterns de production qui pourraient en résulter. Les résultats de la deuxième expérimentation ont permis de pousser plus loin les connaissances sur les relations entre la variabilité génotypique de l'architecture, de la physiologie et de l'induction florale. D'après la classification effectuée par Coupel-Ledru *et al.* 2019, les génotypes utilisés dans cette étude apparaissent représentatifs de l'ensemble de la diversité de la population avec le génotype X8717 représentatif d'un groupe de petits arbres, X6917 d'un groupe de grands arbres et les quatre autres génotypes représentatifs d'arbres de taille moyenne. A travers leurs différences de taille et d'intensité de production, ces groupes avaient aussi des correspondances avec les types architecturaux établis par Lespinasse (1977). La baisse des proportions d'unités de croissances longues indiquait que les génotypes évoluaient vers la sortie de la juvénilité et l'entrée en production. L'effet des génotypes sur la photosynthèse n'était pas lié à la présence des fruits, mais plutôt aux différents besoins pour la croissance primaire et secondaire qui dépassaient les demandes des fruits. Les contrastes observés dans le stockage de l'amidon correspondaient aussi à des

contrastes dans le nombre et la longueur des unités de croissance. Concernant les différences hormonales observées entre les génotypes, elles étaient surtout associées à la croissance avec des associations et des oppositions entre gibbérellines, ABA, IAA et cytokinines. Les interactions trouvées pour gibbérellines (GA4 et GA8) permettent de renforcer l'hypothèse d'une implication de ces hormones dans le contrôle de l'induction florale. D'un autre côté, les résultats des carbohydrates confortent ce les résultats précédents sur la faible implication du carbone dans le contrôle de l'induction florale (Belhassine *et al.*, 2019; Pallas *et al.*, 2018).

Les hypothèses sorties de la première expérimentation ont servi à concevoir le fonctionnement du modèle de transport de signaux. Comme il paraissait indépendant du bilan carboné mais lié à la présence de feuilles, le signal activateur dans le modèle a été estimé à travers la surface foliaire. De même, le signal inhibiteur a également été considéré comme indépendamment du bilan carboné et sa quantité a été considéré comme dépendant du nombre de fruits. Les premiers tests du modèle réalisés sur des structures simplifiées (pousses, branche avec différente surface ou un nombre variable de nombre de fruits) ont montré que le modèle était capable de reproduire les effets de présences de feuilles et de fruits et de leurs distances respectives aux méristèmes sur l'induction florale. En confrontant le modèle aux résultats expérimentations issus de la première expérimentation, les calibrations et validations du modèle ont montré une capacité à s'ajuster aux données observées et à les simuler ($R^2 > 0.90$) suggérant que le modèle est adéquat pour rendre compte la variabilité intra-arbre de l'IF. De plus, les valeurs estimées des paramètres ont permis d'évaluer quantitativement les distances auxquelles pourraient être transportés les signaux activateur et inhibiteur en provenance des feuilles et fruits (environ 50 cm vs 1 m, respectivement). Ainsi le signal activateur pourrait être transporté à des distances plus faibles que le signal inhibiteur. De plus, il a été montré, lors de la combinaison des effets respectifs des signaux dans le méristème, qu'il existait une sensibilité plus faible au signal activateur qu'au signal l'inhibiteur. Les résultats des simulations suggèrent malgré tout, une certaine variabilité du devenir des bourgeons pour une quantité de signal donné. Ceci pourrait être dû au fait que le modèle, en prenant en compte uniquement les signaux inhibiteurs et activateurs en provenance des feuilles et fruits, ne considère pas d'autres mécanismes potentiellement impliqués dans le déterminisme de l'IF. Malgré tout et bien que la nature des signaux ne soit pas spécifiée, cette étude fournit de nouvelles hypothèses sur les rôles respectifs des feuilles et des fruits et sur les distances auxquelles ces organes agissent sur l'IF.

6. Conclusions et perspectives

Ce travail de thèse s'inscrit dans le cadre de l'étude de l'étude des mécanismes impliqué dans l'IF et dans sa variabilité génotypique chez le pommier. Pour répondre aux objectifs de la thèse, des approches expérimentales en écophysiologie du pommier qui englobent la variabilité architecturale et génotypique ainsi que l'élaboration d'un modèle qui permet de simuler le transport de signaux activateurs et inhibiteur de floraison dans une structure d'arbre ont été mis en œuvre.

Au moyen des manipulations effectuées sur le nombre des feuilles et des fruits, une base de données caractérisant les relations sources-puits à différents niveaux et les effets de distances sur le transport des signaux a été construite. Les résultats expérimentaux et de modélisation ont montrés que le bilan carboné n'est pas directement associé à la floraison. Cependant bien que cette thèse donne certains indices sur la nature des signal activateur et inhibiteurs ceux-ci restent encore à élucider.

En ce qui concerne la nature du signal inhibiteur, des différences d'accumulation de certaines formes de gibbérellines (principalement GA9) en fonction de la présence ou de l'absence des fruits soutiennent l'hypothèse que les gibbérellines aient un rôle sur le contrôle de l'IF. Des recherches supplémentaires seraient nécessaires pour étudier la capacité des gibbérellines, probablement produites par les pépins (Dennis and Nitsch, 1966), à agir directement sur SAM FI dans le pommier. Des approches complémentaires d'analyse de transcriptomique pour étudier l'expression des gènes impliqués dans la biosynthèse des GA pourraient alors être également envisagées. Dans notre étude,

les dosages de gibbérellines ont montré une large variabilité de concentrations dans les bourgeons d'un même arbre et soumis aux mêmes conditions de présences de feuilles et de fruits. Cette variation pourrait résulter de la désynchronisation des méristèmes au sein de l'arbre et de la variabilité de stades phénologiques dans les méristèmes prélevés. Par ailleurs, le dosage a été effectué sur des bourgeons contenant des méristèmes, mais aussi les feuilles préformées et les écailles. Les concentrations attribuées aux méristèmes apicaux pourraient donc être biaisée par le contenu des autres structures des bourgeons. Enfin, bien que nous ayons mis en avant des variations des quantités de GA selon les génotypes étudiés, la source de cette variabilité reste encore à élucider. Des dosages complémentaires de GA sur les pépins (lieu supposé de production de GA) de différents génotypes pourraient alors être envisagés.

L'étude de la variabilité de l'architecture entre les génotypes étudiés a montré une implication des concentrations en hormones des méristèmes (principalement GA, IAA et ABA) sur la croissance et le développement des arbres. Bien qu'elles présentaient une tendance à la baisse, les proportions élevées d'unités de croissance longues indiquaient que les génotypes n'avaient pas encore dépassé la phase juvénile et étaient toujours en transition vers la phase mature. Les rythmes de production des génotypes sont ainsi susceptibles de changer avec l'ontogenèse des arbres. Par conséquent, aucune conclusion n'avait pu être tirée concernant la régularité des génotypes à partir les premières années de croissance. Néanmoins, les résultats renforcent l'hypothèse d'une implication de GA dans FI dans le pommier alors que l'économie de carbone serait plus cruciale pour le développement végétatif.

D'après les résultats de la modélisation, il apparaît clairement que les effets des fruits et des feuilles n'ont lieu qu'à courte distance même si l'effet des fruits semble être observée à des distances légèrement plus longues que les feuilles. Pour confirmer les informations biologiques obtenues à partir de ce travail de modélisation, d'autres expériences sont nécessaires afin d'examiner d'abord les molécules impliquées dans le signal inhibiteur et activateur. En effet, bien que les gibbérellines soient soupçonnés d'être la source du signal inhibiteur, d'autres molécules peuvent être impliquées comme l'auxine et les cytokinines qui peuvent agir comme un second messager et peuvent être transportée sur de longues distances (Hanke *et al.*, 2007). Les études s'intéressant la transition florale dans les méristèmes ont été réalisés sur des pousses courtes (Foster *et al.*, 2003; Hanke *et al.*, 2007). Cependant, les pousses longues, se développant souvent jusqu'à l'été, peuvent également fleurir en position apicale (Costes et Guédon, 2012). Par conséquent, même si l'IF se produit environ 50 jours après la pleine floraison dans les pousses courtes, elle pourrait se produire plus tard dans les pousses longues et par conséquent dans différentes conditions trophiques et de température (Chen *et al.*, 2019). Le couplage du modèle développé dans cette étude avec le modèle dynamique MappleT (Costes *et al.*, 2008) permettrait d'avoir une structure qui se développe au cours de la saison et ainsi de simuler l'induction florale temporellement aux dates d'arrêt de fonctionnement des méristèmes comme suggéré par de précédentes études (Barnola et Crabbé 1991). De plus, le couplage à un modèle de photosynthèse (par exemple Sinoquet *et al.*, 2001) et d'allocation de carbone (par exemple Reyes *et al.*, 2019) intégrant des rétroactions sur la croissance, permettront au modèle de simuler la variation de la croissance et du développement au sein des arbres en fonction de l'état trophique ou/et des stress abiotiques. En outre, le modèle proposé dans la cette étude simule l'IF pour une année considérée, mais sans rétroaction sur l'architecture de l'arbre au cours de l'année suivante. Dans ce contexte, les modèles de Markov mis en œuvre dans MappleT pourraient être utilisés pour simuler la croissance potentielle l'année suivante tandis que le modèle développé dans cette thèse pourrait moduler cette structure potentielle en quantifiant l'intensité de l'induction florale dans les pousses en développement. L'exploration de la sensibilité de l'induction florale aux variations des paramètres de résistance au transport et sensibilité à la quantité de signal a également montré que le modèle pouvait être adapté pour représenter un comportement génotypique contrasté. Utiliser ce modèle pour mieux comprendre le déterminisme physiologique ou architectural de cette variabilité génotypique pourrait donc être une approche prometteuse.

VIII. References

- Abbott D.L. 1969.** Role of bud scales in the morphogenesis and dormancy of the apple fruit bud. In Long Ashton Symp, 2d, Univ of Bristol.
- Abbott DL. 1984.** The apple tree: physiology and management. Grower Books, London.
- Abe M, Kobayashi Y, Yamamoto S, Daimon Y, Yamaguchi A, Ikeda Y, Ichinoki H, Notaguchi M, Goto K, Araki T. 2005.** FD, a bZIP protein mediating signals from the floral pathway integrator FT at the shoot apex. *Science* **309**: 1052–1056.
- Adam B, Dones N, Sinoquet H. 2004.** VegeSTAR v.3.1. A software to compute light interception and photosynthesis by 3D plant mock-ups. In: Fourth International Workshop on Functional-Structural Plant Models, Montpellier, France. 414.
- Aki T, Shigyo M, Nakano R, Yoneyama T and Yanagisawa S. 2008.** Nano scale proteomics revealed the presence of regulatory proteins including three FT-like proteins in phloem and xylem saps from rice. *Plant and Cell Physiol.* **49**: 767–790.
- Albasha R, Fournier C, Pradal C, Chelle M, Prieto JA, Louarn G, Simonneau T, Lebon E. 2019.** HydroShoot: a functional-structural plant model for simulating hydraulic structure, gas and energy exchange dynamics of complex plant canopies under water deficit—application to grapevine (*Vitis vinifera*). *In Silico Plants* **1**: 1–26.
- Allen M, Prusinkiewicz P, Dejong T. 2005.** Using L-Systems for Modeling the Architecture and Physiology of Growing Trees: The L-PEACH Model. *New Phytologist* **166**: 869–880.
- Balandier P, Lacoite A, Le Roux X, Sinoquet H, Cruziat P, Le Dizès S. 2000.** SIMWAL: A structural-functional model simulating single walnut tree growth in response to climate and pruning. *Annals of Forest Science* **57**: 571–585.
- Ball JT, Woodrow IE, Berry JA. 1987.** A model predicting stomatal conductance and its contribution to the control of photosynthesis under different environmental conditions. In: *Progress in photosynthesis research*, Springer: 221–224.
- Bangerth F, Li CJ, Gruber J. 2000.** Mutual interaction of auxin and cytokinins in regulating correlative dominance. *Plant Growth Regulation* **32**: 205–217.
- Bangerth KF. 2009.** Floral induction in mature, perennial angiosperm fruit trees: Similarities and discrepancies with annual/biennial plants and the involvement of plant hormones. *Scientia Horticulturae* **122**: 153–163.
- Barillot R, Chambon C, Fournier C, Combes D, Pradal C, Andrieu B. 2019.** Investigation of complex canopies with a functional–structural plant model as exemplified by leaf inclination effect on the functioning of pure and mixed stands of wheat during grain filling. *Annals of botany* **123**: 727–742.
- Barnola P, Crabbé J. 1991.** La basitonie chez les végétaux ligneux. Déterminismes et variabilité d’expression. In : *L’Arbre, Biologie et développement*, 2ème Colloque International sur l’Arbre. Montpellier, France. 381–396.
- Barritt BH, Konishi BS, Dilley MA. 1997.** Tree size, yield and biennial bearing relationships with 40 apple rootstocks and three scion cultivars. In: VI International Symposium on Integrated Canopy, Rootstock, Environmental Physiology in Orchard Systems **451**. 105–112.
- Barthélémy D, Caraglio Y. 2007.** Plant architecture: A dynamic, multilevel and comprehensive approach to plant form, structure and ontogeny. *Annals of Botany* **99**: 375–407.
- Battaglia M, Sands PJ. 1998.** Process-based forest productivity models and their application in forest management. *Forest Ecology and Management* **102**: 13–32.
- Bäurle I, Dean C. 2006.** The Timing of Developmental Transitions in Plants. *Cell* **125**: 655–664.
- Belhassine F, Martinez S, Bluy S, Fumey D, Kelner J, Costes E, Pallas B. 2019.** Impact of Within-Tree Organ Distances on Floral Induction and Fruit Growth in Apple Tree: Implication of Carbohydrate and Gibberellin Organ Contents. *Frontiers in Plant Science* **10**: 1233.
- Bell G. 1980.** The Costs of Reproduction and Their Consequences. *The American Naturalist* **116**: 45–76.
- Berman ME, Dejong TM. 2003.** Seasonal patterns of vegetative growth and competition with reproductive sinks in peach (*Prunus persica*). *Journal of Horticultural Science and Biotechnology* **78**: 303–309.

Bernier, G., Havelange, A., Houssa, C., Petitjean, A. and Lejeune P. 1993. Physiological signals that induce flowering. *Plant Cell* **5**: 1147–1155.

Binenbaum J, Weinstain R, Shani E. 2018. Gibberellin Localization and Transport in Plants. *Trends in Plant Science* **23**: 410–421.

Blazquez MA, Weigel D. 2000. Integration of floral inductive signals in Arabidopsis. *Nature* **404**: 889–892.

Bonhomme M, Peuch M, Ameglio T, Rageau R, Guillot A, Decourteix M, Alves G, Sakr S, Lacoïnte A. 2010. Carbohydrate uptake from xylem vessels and its distribution among stem tissues and buds in walnut (*Juglans regia* L.). *Tree Physiology* **30**: 89–102.

Booker J, Chatfield S, Leyser O. 2003. Auxin acts in xylem-associated or medullary cells to mediate apical dominance. *Plant Cell* **15**: 495–507.

Borner R, Kampmann G, Chandler J, Gleißner R, Wisman E, Apel K, Melzer S. 2000. A MADS domain gene involved in the transition to flowering in Arabidopsis. *Plant Journal* **24**: 591–599.

Boss PK. 2004. Multiple Pathways in the Decision to Flower: Enabling, Promoting, and Resetting. *The Plant Cell Online* **16**: S18–S31.

Boudon F, Preuksakarn C, Ferraro P, Diener J, Nacry P, Nikinmaa E, Godin C. 2014. Quantitative assessment of automatic reconstructions of branching systems obtained from laser scanning. *Annals of Botany* **114**: 853–862.

Brisson N, Gary C, Justes E, Roche R, Mary B, Ripoche D, Zimmer D, Sierra J, Bertuzzi P, Burger P. 2003. An overview of the crop model STICS. *European Journal of Agronomy* **18**: 309–332.

Buck-Sorlin G, De Visser PHB, Henke M, Sarlikioti V, Van Der Heijden GWAM, Marcelis LFM, Vos J. 2011. Towards a functional structural plant model of cut-rose: Simulation of light environment, light absorption, photosynthesis and interference with the plant structure. *Annals of Botany* **108**: 1121–1134.

Buck-Sorlin GH, Kniemeyer O, Kurth W. 2005. Barley morphology, genetics and hormonal regulation of internode elongation modelled by a relational growth grammar. *New Phytologist* **166**: 859–867.

Casadebaig P, Guillioni L, Lecoeur J, Christophe A, Champolivier L, Debaeke P. 2011. SUNFLO, a model to simulate genotype-specific performance of the sunflower crop in contrasting environments. *Agricultural and Forest Meteorology* **151**: 163–178.

Castillo-Llanque F, Rapoport HF. 2011. Relationship between reproductive behavior and new shoot development in 5-year-old branches of olive trees (*Olea europaea* L.). *Trees - Structure and Function* **25**: 823–832.

Celton JM, Kelner JJ, Martinez S, Bechti A, Touhami AK, James MJ, Durel CE, Laurens F, Costes E. 2014. Fruit self-thinning: A trait to consider for genetic improvement of apple tree. *PLoS ONE* **9**: e91016.

Celton JM, Martinez S, Jammes MJ, Bechti A, Salvi S, Legave JM, Costes E. 2011. Deciphering the genetic determinism of bud phenology in apple progenies: A new insight into chilling and heat requirement effects on flowering dates and positional candidate genes. *New Phytologist* **192**: 378–392.

Celton JM, Kelner JJ, Martinez S, Bechti A, Khelifi Touhami A, James MJ, Durel CE, Laurens F, Costes E. 2014. Fruit Self-Amicissement: A Trait to Consider for Genetic Improvement of Apple Tree. *PLoS ONE* **9**(3): e91016.

Chan BG, Cain JC. 1967. The effect of seed formation on subsequent flowering in apple. *Proceedings of the American Society for Horticultural Science* **91**: 63–68.

Chandler J, Wilson A, Dean C. 1996. Arabidopsis mutants showing an altered response to vernalization. *The Plant Journal* **10**: 637–644.

Chelle M, Andrieu B. 1999. Radiative models for architectural modeling. *Agronomie* **19**: 225–240.

Chelle M, Hanan J, Autret H. 2004. FSPM 04 Lighting virtual crops: the CARIBU solution for open L-systems. In *Proceedings of the 4th international workshop on functional–structural plant models* 194.

- Chen D, Pallas B, Martinez S, Wang Y, Costes E. 2019.** Neoformation and summer arrest are common sources of tree plasticity in response to water stress of apple cultivars. *Annals of Botany* **123**: 877–890.
- Chevreau E, Lespinasse Y, Gallet M. 1985.** Inheritance of pollen enzymes and polyploid origin of apple (*Malus x domestica* Borkh.). *Theoretical and Applied Genetics* **71**: 268–277.
- Cho LH, Pasriga R, Yoon J, Jeon JS, An G. 2018.** Roles of Sugars in Controlling Flowering Time. *Journal of Plant Biology* **61**: 121–130.
- Choi ST, Park DS, Song WD, Kang SM, Shon GM. 2003.** Effect of different degrees of defoliation on fruit growth and reserve accumulation in young ‘Fuyu’ trees. *Acta Horticulturae* **601**: 99–104.
- Cieslak M, Seleznyova AN, Hanan J. 2011.** A functional-structural kiwifruit vine model integrating architecture, carbon dynamics and effects of the environment. *Annals of Botany* **107**: 747–764.
- Cline MG. 1991.** Apical dominance. *The Botanical Review* **57**: 318–358.
- Corbesier L, Coupland G. 2006.** The quest for florigen: a review of recent progress. *Journal of Experimental Botany* **57**: 3395–3403.
- Corbesier L, Vincent C, Jang S, Fornara F, Fan Q, Searle I, Giakountis A, Farrona S, Gissot L, Turnbull C, et al. 2007a.** Long-Distance Signaling in Floral Induction of *Arabidopsis*. *Science* **316**: 1030–1034.
- Corbesier L, Vincent C, Jang S, Fornara F, Fan Q, Searle I, Giakountis A, Farrona S, Gissot L, Turnbull C, et al. 2007b.** FT protein movement contributes to long-distance signaling in floral induction of *Arabidopsis*. *Science* **316**: 1030–1033.
- Cornille A, Giraud T, Smulders MJM, Roldán-Ruiz I, Gladieux P. 2014.** The domestication and evolutionary ecology of apples. *Trends in Genetics* **30**: 57–65.
- Costes E, Crespel L, Denoyes B, Morel P, Demene M-N, Lauri P-E, Wenden B. 2014.** Bud structure, position and fate generate various branching patterns along shoots of closely related Rosaceae species: a review. *Frontiers in Plant Science* **5**: 1–11.
- Costes E, Guédon Y. 2002.** Modelling branching patterns on 1-year-old trunks of six apple cultivars. *Annals of Botany* **89**: 513–524.
- Costes E, Guédon Y. 2012.** Deciphering the ontogeny of a sympodial tree. *Trees - Structure and Function* **26**: 865–879.
- Costes E, Lauri P, Regnard JL. 2006.** Analyzing Fruit Tree Architecture: Implications for Tree Management and Fruit Production. *Horticultural Reviews* **32**: 1–61.
- Costes E, Sinoquet H, Godin C, Kelner JJ. 1998.** 3D digitizing based on tree topology: application to study the variability of apple quality within the canopy. In: *V International Symposium on Computer Modelling in Fruit Research and Orchard Management* **499**: 271–280.
- Costes E, Sinoquet H, Kelner JJ, Godin C. 2003.** Exploring within-tree architectural development of two apple tree cultivars over 6 years. *Annals of Botany* **91**: 91–104.
- Costes E, Smith C, Renton M, Guédon Y, Prusinkiewicz P, Godin C. 2008.** MAppleT: Simulation of apple tree development using mixed stochastic and biomechanical models. *Functional Plant Biology* **35**: 936–950.
- Côté J, Widlowski J, Fournier RA, Verstraete MM. 2009.** Remote Sensing of Environment The structural and radiative consistency of three-dimensional tree reconstructions from terrestrial lidar. *Remote Sensing of Environment* **113**: 1067–1081.
- Coupel-Ledru A, Pallas B, Delalande M, Boudon F, Carrié E, Martinez S, Regnard JL, Costes E. 2019.** Multi-scale high-throughput phenotyping of apple architectural and functional traits in orchard reveals genotypic variability under contrasted watering regimes. *Horticulture Research* **6**: 52.
- Cournède PH, Letort V, Mathieu A, Kang MZ, Lemaire S, Trevezas S, Houllier F, De Reffye P. 2011.** Some parameter estimation issues in functional-structural plant modelling. *Mathematical Modelling of Natural Phenomena* **6**: 133–159.
- Crabbé JJ. 1984.** Vegetative vigor control over location and fate of flower buds, in fruit trees. *Flowering and Fruit Set in Fruit Trees* **149**: 55–64.
- Da Silva D, Favreau R, Auzmendi I, Dejong TM. 2011.** Linking water stress effects on carbon partitioning by introducing a xylem circuit into L-PEACH. *Annals of Botany* **108**: 1135–1145.

- Da Silva D, Han L, Costes E. 2014.** Light interception efficiency of apple trees: A multiscale computational study based on MAppleT. *Ecological Modelling* **290**: 45–53.
- Da Silva D, Han L, Faivre R, Costes E. 2014.** Influence of the variation of geometrical and topological traits on light interception efficiency of apple trees: Sensitivity analysis and metamodelling for ideotype definition. *Annals of Botany* **114**: 739–752.
- Dauzat J, Clouvel P, Luquet D, Martin P. 2008.** Using virtual plants to analyse the light-foraging efficiency of a low-density cotton crop. *Annals of Botany* **101**: 1153–1166.
- DeJong TM, Grossman YL. 1994.** A Supply and Demand Approach to Modeling Annual Reproductive and Vegetative Growth of Deciduous Fruit Trees. *HortScience* **29**: 1435–1442.
- DeJong TM, Grossman YL. 1995.** Quantifying sink and source limitations on dry matter partitioning to fruit growth in peach trees. *Physiologia Plantarum* **95**: 437–443.
- Deleuze C, Houllier F. 1997.** A transport model for tree ring width. *The Finnish Society of Forest Science and The Finnish Forest Research Institute* **31**: 239–250.
- Dennis F, Nitsch P. 1966.** Identification of gibberellins A4 and A7 in immature apple seeds. *Nature* **211**: 781–782.
- Dennis FG, Neilsen JC. 1999.** Physiological factors affecting biennial bearing in tree fruit: The role of seeds in apple. *HortTechnology* **9**: 317–322.
- Dennis FG. 2000.** The history of fruit thinning. *Plant Growth Regulation* **31**: 1–16.
- DeReffye P, Heuvelink E, Guo Y, Hu B, Zhang B-G. 2009.** Coupling Process-Based Models and Plant Architectural Models: A Key Issue for Simulating Crop Production. In: Cao W., White J.W., Wang E. (eds) *Crop Modeling and Decision Support*. Springer, Berlin, Heidelberg: 130-147
- Dong Q, Louarn G, Wang Y, Barczy JF, De Reffye P. 2008.** Does the structure-function model GREENLAB deal with crop phenotypic plasticity induced by plant spacing? A case study on tomato. *Annals of Botany* **101**: 1195–1206.
- Durand JB, Allard A, Guitton B, van de Weg E, Bink MCAM, Costes E. 2017.** Predicting flowering behavior and exploring its genetic determinism in an apple multi-family population based on statistical indices and simplified phenotyping. *Frontiers in Plant Science* **8**: 1–15.
- Durand JB, Guitton B, Peyhardi J, Holtz Y, Guédon Y, Trottier C, Costes E. 2013.** New insights for estimating the genetic value of segregating apple progenies for irregular bearing during the first years of tree production. *Journal of Experimental Botany* **64**: 5099–5113.
- Duursma RA, Falster DS, Valladares F, Sterck FJ, Percy RW, Lusk CH, Sendall KM, Nordenstahl M, Houter NC, Atwell BJ, et al. 2012.** Light interception efficiency explained by two simple variables: A test using a diversity of small- to medium-sized woody plants. *New Phytologist* **193**: 397–408.
- Eisenstecken D, Stürz B, Robatscher P, Lozano L, Zanella A, Oberhuber M. 2019.** The potential of near infrared spectroscopy (NIRS) to trace apple origin: Study on different cultivars and orchard elevations. *Postharvest Biology and Technology* **147**: 123–131.
- Eriksson S, Bohlenius H, Moritz T, Nilsson O. 2006.** GA4 is the active gibberellin in the regulation of LEAFY transcription and Arabidopsis floral initiation. *The Plant Cell* **18**: 2172–2181.
- Escobar-Gutiérrez A, Gaudillère J. 1996.** Distribution, métabolisme et rôle du sorbitol chez les plantes supérieures. *Agronomie* **16**: 281–298.
- Falavigna V, Guitton B, Costes E, Andrés F. 2019.** I Want to (Bud) Break Free: The Potential Role of DAM and SVP -Like Genes in Regulating Dormancy Cycle in Temperate Fruit Trees. *Frontiers in Plant Science* **9**: 1–17.
- Foster T, Johnston R, Seleznyova A. 2003.** A morphological and quantitative characterization of early floral development in apple (*Malus x domestica* Borkh.). *Annals of Botany* **92**: 199–206.
- Francesconi AHD, Lakso AN, Nyrop JP, Barnard J, Denning SS. 1996.** Carbon balance as a physiological basis for the interactions of European red mite and crop load on ‘Starkrimson Delicious’ apple trees. *Journal of the American Society for Horticultural Science* **121**: 959–966.
- Franck N, Vaast P, Génard M, Dauzat J. 2006.** Soluble sugars mediate sink feedback down-regulation of leaf photosynthesis in field-grown *Coffea arabica*. *Tree Physiology* **26**: 517–525.
- Freiman, A, Golobovitch, S, Yablovitz, Z, Belausov, E, Dahan, Y, Peer, R, Sobolev, V. 2015.** Expression of flowering locus T2 transgene from *Pyrus communis* L. delays dormancy and leaf

senescence in *Malus domestica* Borkh, and causes early flowering in tobacco. *Plant Science*. **241**: 164-176.

Fulford RM. 1966. The Morphogenesis of Apple Buds. *Annals of Botany* **30**: 597–606.

Garin G, Fournier C, Andrieu B, Houllès V, Robert C, Pradal C. 2014. A modelling framework to simulate foliar fungal epidemics using functional-structural plant models. *Annals of Botany* **114**: 795–812.

Génard M, Dauzat J, Franck N, Lescourret F, Moitrier N, Vaast P, Vercambre G. 2008. Carbon allocation in fruit trees: From theory to modelling. *Trees-Structure and Function* **22**: 269–282.

Gibson SI. 2005. Control of plant development and gene expression by sugar signaling. *Current Opinion in Plant Biology* **8**: 93–102.

Godin C, Caraglio Y. 1998. A Multiscale Model of Plant Topological Structures. *Journal of Theoretical Biology* **191**: 1–46.

Godin C, Costes E, Sinoquet H. 1999. A method for describing plant architecture which integrates topology and geometry. *Annals of Botany* **84**: 343–357.

Godin C. 2003. Introduction aux structures multi-échelles. Applications à la représentation des plantes. Modélisation et simulation. Rapport HDR, Université de Montpellier 2.

Gómez-Candón D, Virlet N, Labbé S, Jolivot A, Regnard JL. 2016. Field phenotyping of water stress at tree scale by UAV-sensed imagery : new insights for thermal acquisition and calibration. *Precision Agriculture* **17**: 786–800

Goto N, Kumagai T, Koornneef M. 1991. Flowering responses to light-breaks in photomorphogenic mutants of *Arabidopsis thaliana*, a long-day plant. *Physiologia Plantarum* **83**: 209–215.

Griffon S, de Coligny F. 2014. AMAPstudio: An editing and simulation software suite for plants architecture modelling. *Ecological Modelling* **290**: 3–10.

Grossman YL, Dejong T. 1998. Training and pruning system effects on vegetative growth potential, light interception, and cropping efficiency in peach trees. *Journal-American Society For Horticultural Science*. **123**: 1058–1064.

Grossman YL, DeJong TM. 1995. Maximum fruit growth potential following resource limitation during peach growth. *Annals of Botany* **75**: 561–567.

Guitton B, Kelner JJ, Celton JM, Sabau X, Renou JP, Chagné D, Costes E. 2016. Analysis of transcripts differentially expressed between fruited and deflowered ‘Gala’ adult trees: A contribution to biennial bearing understanding in apple. *BMC Plant Biology* **16**: 1–22.

Guitton B, Kelner JJ, Velasco R, Gardiner SE, Chagné D, Costes E. 2011. Genetic control of biennial bearing in apple. *Journal of Experimental Botany* **63**: 131–149.

Guo Y, Ma Y, Zhan Z, Li B, Dingkuhn M, Luquet D, De Reffye P. 2006. Parameter optimization and field validation of the functional-structural model GREENLAB for maize. *Annals of Botany* **97**: 217–230.

Ha TM. 2014. A Review of Plants Flowering Physiology: The Control of Floral Induction by Juvenility, Temperature and Photoperiod in Annual and Ornamental Crops. *Asian Journal of Agriculture and Food Science* **2**: 2321–1571.

Haberman A, Ackerman M, Crane O, Kelner JJ, Costes E, Samach A. 2016. Different flowering response to various fruit loads in apple cultivars correlates with degree of transcript reaccumulation of a TFL1-encoding gene. *The Plant journal* **87**(2): 161–173.

Hammer GL, Van Oosterom E, McLean G, Chapman SC, Broad I, Harland P, Muchow RC. 2010. Adapting APSIM to model the physiology and genetics of complex adaptive traits in field crops. *Journal of Experimental Botany* **61**: 2185–2202.

Han L, Costes E, Boudon F, Cokelaer T, Pradal C, Da Silva D, Faivre R. 2012. Investigating the influence of geometrical traits on light interception efficiency of apple trees: A modelling study with MAppleT. *Proceedings - IEEE 4th International Symposium on Plant Growth Modeling, Simulation, Visualization and Applications*, 152–159.

Hanan J, Prusinkiewicz P. 2008. Foreword: Studying plants with functional – structural models. *Functional Plant Biology* **35**: vi–viii.

Hanke M-V, Flachowsky H, Peil A, Hättasch C. 2007. No Flower no Fruit – Genetic Potentials to Trigger Flowering in Fruit Trees. *Genes, Genomes and Genomics* **1**: 1–20.

Hansen P. 1967. 14C-Studies on Apple Trees III. The Influence of Season on Storage and Mobilization of Labelled Compounds. *Physiologia Plantarum* **20**: 1103–1111.

Hansen P. 1969. 14C-Studies on Apple Trees. IV. Photosynthate Consumption in Fruits in Relation to the Leaf-Fruit Ratio and to the Leaf-Fruit Position. *Physiologia Plantarum* **22**: 186–198.

Hansen P. 1971. 14C-Studies on Apple Trees. VII. The Early Seasonal Growth in Leaves, Flowers and Shoots as Dependent upon Current Photosynthates and Existing Reserves. *Physiologia Plantarum* **25**: 469–473.

Harley CP, Magness JR, Masure MP, Fletcher LA, Degman ES. 1942. Investigations on the Cause and Control of Biennial Bearing of Apple Trees. Technical bulletin (No. 1488-2016-123629). US Government Printing Office.

Hättasch C, Flachowsky H, Kapturska D, Hanke MV. 2008. Isolation of flowering genes and seasonal changes in their transcript levels related to flower induction and initiation in apple (*Malus domestica*). *Tree Physiology* **28**: 1459–1466.

Hayama R, Coupland G. 2004. The molecular basis of diversity in the photoperiodic flowering responses of arabidopsis and rice. *Plant Physiology* **135**: 677–684.

Heide OM, Prestrud AK. 2005. Low temperature, but not photoperiod, controls growth cessation and dormancy induction and release in apple and pear. *Tree Physiology* **25**: 109–114.

Hemmerling R, Kniemeyer O, Lanwert D, Kurth W, Buck-Sorlin GH. 2008. The rule-based language XL and the modelling environment GroIMP illustrated with simulated tree competition. *Functional Plant Biology* **35**: 739–750.

Heuvelink E. 1995. Dry matter partitioning in a tomato plant: one common assimilate pool? *Journal of Experimental Botany* **46**: 1025–1033.

Hoad G V. 1984. Hormonal regulation of fruit-bud formation in fruit trees. *Acta Horticulturae* **149**: 13–23.

Hoblyn TN, Grubb NH, Painter AC, Wates BL. 1936. Studies in Biennial Bearing.—I. *Journal of pomology and horticultural science* **14**: 39–76.

Hoch G. 2005. Fruit-bearing branchlets are carbon autonomous in mature broad-leaved temperate forest trees. *Plant, Cell and Environment* **28**: 651–659.

Hölttä T, Mencuccini M, Nikinmaa E. 2009. Linking phloem function to structure: Analysis with a coupled xylem-phloem transport model. *Journal of Theoretical Biology* **259**: 325–337.

Horvath DP, Anderson J V., Chao WS, Foley ME. 2003. Knowing when to grow: Signals regulating bud dormancy. *Trends in Plant Science* **8**: 534–540.

Izawa T, Oikawa T, Sugiyama N, Tanisaka T, Yano M, Shimamoto K. 2002. Phytochrome mediates the external light signal to repress FT orthologs in photoperiodic flowering of rice. *Genes and Development* **16**: 2006–2020.

Jarvis PG. 1976. The interpretation of the variations in leaf water potential and stomatal conductance found in canopies in the field. *Philosophical Transactions of the Royal Society of London. Biological Sciences* **273**: 593–610.

Ji X, Van Den Ende W, Van Laere A, Cheng S, Bennett J. 2005. Structure, evolution, and expression of the two invertase gene families of rice. *Journal of Molecular Evolution* **60**: 615–634.

Johnson E, Bradley M, Harberd NP, Whitelam CC. 1994. Photoresponses of light-grown phyA mutants of Arabidopsis (phytochrome A is required for the perception of daylength extensions). *Plant Physiology* **105**: 141–149.

Jones RJ, Mansfield TA. 1970. Suppression of stomatal opening in leaves treated with abscisic acid. *Journal of Experimental Botany* **21**: 714–719.

Jonkers H. 1979. Biennial bearing in apple and pear: A literature survey. *Scientia Horticulturae* **11**: 303–317.

Jossier M, Bouly JP, Meimoun P, Arjmand A, Lessard P, Hawley S, Grahame Hardie D, Thomas M. 2009. SnRK1 (SNF1-related kinase 1) has a central role in sugar and ABA signalling in Arabidopsis thaliana. *Plant Journal* **59**: 316–328.

- Jung C, Müller AE. 2009.** Flowering time control and applications in plant breeding. *Trends in Plant Science* **14**: 563–573.
- Jung C, Pillen K, Staiger D, Coupland G, von Korff M. 2017.** Editorial: Recent Advances in Flowering Time Control. *Frontiers in Plant Science* **7**: 2016–2018.
- Kandiah S. 1979a.** Turnover of carbohydrates in relation to growth in apple trees. I. Seasonal variation of growth and carbohydrate reserves. *Annals of Botany* **44**: 175–183.
- Kandiah S. 1979b.** Turnover of Carbohydrates in Relation to Growth in Apple Trees. II. Distribution of ¹⁴C Assimilates Labelled in Autumn, Spring and Summer. *Annals of Botany* **44**: 185–195.
- Kang M, Evers JB, Vos J, De Reffye P. 2008.** The derivation of sink functions of wheat organs using the GREENLAB model. *Annals of Botany* **101**: 1099–1108.
- Kanno Y, Hanada A, Chiba Y, Ichikawa T, Nakazawa M, Matsui M, Koshiba T, Kamiya Y, Seo M. 2012.** Identification of an abscisic acid transporter by functional screening using the receptor complex as a sensor. *Proceedings of the National Academy of Sciences of the United States of America* **109**: 9653–9658.
- Kim D-H, Doyle MR, Sung S, Amasino RM. 2009.** Vernalization: Winter and the Timing of Flowering in Plants. *Annual Review of Cell and Developmental Biology* **25**: 277–299.
- Kittikorn M, Shiraishi N, Okawa K, Ohara H, Yokoyama M, Ifuku O, Yoshida S, Kondo S. 2010.** Effect of fruit load on 9,10-ketol-octadecadienoic acid (KODA), GA and jasmonic acid concentrations in apple buds. *Scientia Horticulturae* **124**: 225–230.
- Kniemeyer OGM. 2008.** Design and Implementation of a Graph Grammar Based Language for Functional-Structural Plant Modelling. PhD Thesis. Brandenburg University of Technology, Cottbus-Senftenberg, Germany.
- Koenig WD, Knops JMH. 2005.** The mystery of masting in trees. *American Scientist* **93**: 340–347.
- Koornneef M, Alonso-Blanco C, Blankestijn-De Vries H, Hanhart CJ, Peeters AJM. 1998.** Genetic interactions among late-flowering mutants of *Arabidopsis*. *Genetics* **148**: 885–892.
- Kotoda N, Hayashi H, Suzuki M, Igarashi M, Hatsuyama Y, Kidou SI, Igasaki T, Nishiguchi M, Yano K, Shimizu T, et al. 2010.** Molecular characterization of flowering LOCUS t-like genes of apple (*malus × domestica borkh.*). *Plant and Cell Physiology* **51**: 561–575.
- Kotoda N, Wada M, Komori S, Kidou S ichiro, Abe K, Masuda T, Soejima J. 2000.** Expression pattern of homologues of floral meristem identity genes LFY and AP1 during flower development in apple. *Journal of the American Society for Horticultural Science* **125**: 398–403.
- Lacointe A, Deleens E, Ameglio T, Saint-Joanis B, Lelarge C, Vandame M, Song GC, Daudet FA. 2004.** Testing the branch autonomy theory: A ¹³C/¹⁴C double-labelling experiment on differentially shaded branches. *Plant, Cell and Environment* **27**: 1159–1168.
- Lacointe A. 2000.** Carbon allocation among tree organs: A review of basic processes and representation in functional-structural tree models. *Annals of Forest Science* **57**: 521–533.
- Lakso AN, Robinson TL, Greene DW. 2006.** Integration of environment, physiology and fruit abscission via carbon balance modeling-Implications for understanding growth regulator responses. In: X International Symposium on Plant Bioregulators in Fruit Production **727**: 321–326.
- Lakso AN, Robinson TL, Greene DW. 2007.** Using an apple tree carbohydrate model to understand thinning responses to weather and chemical thinners. *New York Fruit Quarterly* **15**(3): 16–19.
- Lakso AN, White MD, Tustin DS. 1991.** Simulation modeling of the effects of short and long-term climatic variations on carbon balance of apple trees. VII International Symposium on Orchard and Plantation Systems. **557**: 473-480.
- Lassois L, Denancé C, Ravon E, Guyader A, Guisnel R, Hibrand-Saint-Oyant L, Poncet C, Lasserre-Zuber P, Feugey L, Durel CE. 2016.** Genetic Diversity, Population Structure, Parentage Analysis, and Construction of Core Collections in the French Apple Germplasm Based on SSR Markers. *Plant Molecular Biology Reporter* **34**: 827–844.
- Lassois L, Denancé C, Ravon E, Guyader A, Guisnel R, Hibrand-Saint-Oyant L, Poncet C, Lasserre-Zuber P, Feugey L, Durel CE. 2016.** Genetic Diversity, Population Structure, Parentage Analysis, and Construction of Core Collections in the French Apple Germplasm Based on SSR Markers. *Plant Molecular Biology Reporter* **34**: 827–844.

- Lastdrager J, Hanson J, Smeekens S. 2014.** Sugar signals and the control of plant growth and development. *Journal of Experimental Botany* **65**: 799–807.
- Lauri P. 1995.** Genotypic differences in the axillary bud growth and fruiting pattern of apple fruiting branches over several years—an approach to regulation of fruit bearing. *Scientia Horticulturae* **64**: 265–281.
- Lauri PE, and Lespinasse, JM. 1993.** The relationship between cultivar fruiting-type and fruiting branch characteristics in apple trees. *Acta Horticulturae*. **349**: 259–263.
- Lauri PÉ, Kelner JJ, Trottier C, Costes E. 2010.** Insights into secondary growth in perennial plants: Its unequal spatial and temporal dynamics in the apple (*Malus domestica*) is driven by architectural position and fruit load. *Annals of Botany* **105**: 607–616.
- Lauri PE, Térouanne E, Lespinasse JM, Regnard JL, Kelner JJ. 1995.** Genotypic differences in the axillary bud growth and fruiting pattern of apple fruiting branches over several years-an approach to regulation of fruit bearing. *Scientia Horticulturae* **64**: 265–281.
- Lauri PE, Terouanne E, Lespinasse JM. 1997.** Relationship between the early development of apple fruiting branches and the regularity of bearing - An approach to the strategies of various cultivars. *Journal of Horticultural Science and Biotechnology* **72**: 519–530.
- Lauri PE, Terouanne E. 1998.** The influence of shoot growth on the pattern of axillary development on the long shoots of young apple trees (*Malus domestica* Borkh.). *International Journal of Plant Sciences* **159**: 283–296.
- Lauri PÉ, Trottier C. 2004.** Patterns of size and fate relationships of contiguous organs in the apple (*Malus domestica*) crown. *New Phytologist* **163**: 533–546.
- Lavee S. 2007.** Biennial bearing in olive (*Olea europaea*). *Annales, Series Historia Naturalis* **17**: 102–112.
- Le Roux X, Lacoite A, Escobar-Gutiérrez A, Le Dizès S. 2001.** Carbon-based models of individual tree growth : A critical appraisal. *Annals For.Science* **58**: 469–506.
- Lecigne B, Delagrangé S, Messier C. 2018.** Exploring trees in three dimensions: VoxR, a novel voxel-based R package dedicated to analysing the complex arrangement of tree crowns. *Annals of Botany* **121**: 589–601.
- Lee H, Suh SS, Park E, Cho E, Ahn JH, Kim SG, Lee JS, Kwon YM, Lee I. 2000.** The AGAMOUS-LIKE 20 MADS domain protein integrates floral inductive pathways in Arabidopsis. *Genes and Development* **14**: 2366–2376.
- Lee J, Lee I. 2010.** Regulation and function of SOC1, a flowering pathway integrator. *Journal of Experimental Botany* **61**: 2247–2254.
- Legave JM, Blanke M, Christen D, Giovannini D, Mathieu V, Oger R. 2013.** A comprehensive overview of the spatial and temporal variability of apple bud dormancy release and blooming phenology in Western Europe. *International Journal of Biometeorology* **57**: 317–331.
- Lescourret F, Moitrier N, Valsesia P, Génard M. 2011.** QualiTree, a virtual fruit tree to study the management of fruit quality. I. Model development. *Trees - Structure and Function* **25**: 519–530.
- Lespinasse J-M. 1977.** La conduite du pommier: Types de fructification, incidence sur la conduite de l'arbre. No Folleto 6283
- Lespinasse Y. 1992.** Breeding apple tree: aims and methods. In: Rousselle-Bourgeois F, Rousselle P, eds. Proceedings of the joint conference of the E.A.P.R. breeding and varietal assessment section and the EUCARPIA. potato section. Ploudaniel, France: INRA. 12-17 January: 103–110.
- Lespinasse Y. 1992.** Le pommier. Amélioration des espèces végétales cultivées-objectifs et critères de sélection. INRA, Paris: 579–594.
- Letort V, Cournède PH, Mathieu A, De Reffye P, Constant T. 2008.** Parametric identification of a functional-structural tree growth model and application to beech trees (*Fagus sylvatica*). *Functional Plant Biology* **35**: 951–963.
- Lifschitz E, Eshed Y. 2006.** Universal florigenic signals triggered by FT homologues regulate growth and flowering cycles in perennial day-neutral tomato. *Journal of Experimental Botany* **57**: 3405–3414.

Lin MK, Belanger H, Lee YJ, Varkonyi-Gasic E, Taoka KI, Miura E, Xoconostle-Cázares B, Gendler K, Jorgensen RA, Phinney B, et al. 2007. FLOWERING LOCUS T protein may act as the long-distance florigenic signal in the cucurbits. *Plant Cell* **19**: 1488–1506.

Lindenmayer A. 1968. Mathematical models for cellular interactions in development II. Simple and branching filaments with two-sided inputs. *Journal of Theoretical Biology* **18**: 300–315.

Lopez G, Pallas B, Martinez S, Lauri PÉ, Regnard JL, Durel CÉ, Costes E. 2015. Genetic variation of morphological traits and transpiration in an apple core collection under well-watered conditions: Towards the identification of morphotypes with high water use efficiency. *PLoS ONE* **10**: 1–19.

Lordan J, Reginato GH, Lakso AN, Francescatto P, Robinson TL. 2019. Natural fruitlet abscission as related to apple tree carbon balance estimated with the MaluSim model. *Scientia Horticulturae* **247**: 296–309.

Losciale P, Manfrini L, Morandi B, Pierpaoli E, Zibordi M, Stellacci AM, Salvati L, Corelli Grappadelli L. 2015. A multivariate approach for assessing leaf photo-assimilation performance using the IPL index. *Physiologia Plantarum* **154**: 609–620.

Lovatt CJ. 2010. Alternate Bearing Of ‘Hass’ Avocado: A summary of basic information to assist growers in managing their orchards. *California Avocado Society Yearbook* **93**: 125-140.

Luquet D, Dingkuhn M, Kim H, Tambour L, Clement-Vidal A. 2006. EcoMeristem, a model of morphogenesis and competition among sinks in rice. 1. Concept, validation and sensitivity analysis. *Functional Plant Biology* **33**: 309–323.

Marcelis LFM, Heuvelink E, Goudriaan J. 1998. Modelling biomass production and yield of horticultural crops: a review. *Scientia Horticulturae* **74**: 83–111.

Martinez-Zapater JM, Somerville CR. 1990. Effect of light quality and vernalization on late-flowering mutants of *Arabidopsis thaliana*. *Plant Physiology* **92**: 770–776.

Massonnet C, Costes E, Rambal S, Dreyer E, Regnard JL. 2007. Stomatal regulation of photosynthesis in apple leaves: Evidence for different water-use strategies between two cultivars. *Annals of Botany* **100**: 1347–1356.

Mathieu A, Cournède PH, Barthélémy D, De Reffye P. 2008. Rhythms and alternating patterns in plants as emergent properties of a model of interaction between development and functioning. *Annals of Botany* **101**: 1233–1242.

Mathieu A, Cournède PH, Letort V, Barthélémy D, de Reffye P. 2009. A dynamic model of plant growth with interactions between development and functional mechanisms to study plant structural plasticity related to trophic competition. *Annals of Botany* **103**: 1173–1186.

Mathieu J, Warthmann N, Schmid M, Ku F. 2007. Report Export of FT Protein from Phloem Companion Cells Is Sufficient for Floral Induction in *Arabidopsis*. *Current Biology* **17**: 1055–1060.

Meinke DW, Cherry JM, Dean C, Rounsley SD, Koornneef M. 1998. *Arabidopsis thaliana*: A model plant for genome analysis. *Science* **282**: 662–682.

Michaels SD, Amasino RM. 1999. FLOWERING LOCUS C encodes a novel MADS domain protein that acts as a repressor of flowering. *Plant Cell* **11**: 949–956.

Michaels SD, Amasino RM. 2000. Memories of winter vernalization and the competence to flower. *Plant, Cell & Environment* **23**: 1145–1153.

Middleton AM, Úbeda-Tomás S, Griffiths J, Holman T, Hedden P, Thomas SG, Phillips AL, Holdsworth MJ, Bennett MJ, King JR, et al. 2012. Mathematical modeling elucidates the role of transcriptional feedback in gibberellin signaling. *Proceedings of the National Academy of Sciences of the United States of America* **109**: 7571–7576.

Migault V, Pallas B, Costes E. 2017. Combining genome-wide information with a functional structural plant model to simulate 1-year-old apple tree architecture. *Frontiers in Plant Science* **7**: 1–14.

Mimida N, Kotoda N, Ueda T, Igarashi M, Hatsuyama Y, Iwanami H, Moriya S, Abe K. 2009. Four TFL1/CEN-like genes on distinct linkage groups show different expression patterns to regulate vegetative and reproductive development in apple (*Malus x domestica* Borkh.). *Plant and Cell Physiology* **50**: 394–412.

Minchin PEH, Lacoite A. 2005. New understanding on phloem physiology and possible consequences for modelling long-distance carbon transport. *New Phytologist* **166**: 771–779.

Monselise SP, Goldschmidt EE. 1982. Alternate bearing in fruit trees. *Horticultural Reviews* **4**: 128–173.

Moon J, Suh SS, Lee H, Choi KR, Hong CB, Paek NC, Kim SG, Lee I. 2003. The SOC1 MADS-box gene integrates vernalization and gibberellin signals for flowering in *Arabidopsis*. *Plant Journal* **35**: 613–623.

Mouradov A, Cremer F, Coupland G. 2002. Control of flowering time: Interacting pathways as a basis for diversity. *Plant Cell* **14**: 111–131.

Muñoz-Fambuena N, Mesejo C, González-Mas MC, Primo-Millo E, Agustí M, Iglesias DJ. 2012. Fruit load modulates flowering-related gene expression in buds of alternate-bearing ‘Moncada’ mandarin. *Annals of Botany* **110**: 1109–1118.

Mutasa-Göttgens E, Hedden P. 2009. Gibberellin as a factor in floral regulatory networks. *Journal of Experimental Botany* **60**: 1979–1989.

Nagy PT, Szabo Z, Nyeki J, Dussi MC. 2009. Effects of frost-induced biennial bearing on nutrient availability and fruit disorders in an integrated apple orchard. In: XI International Symposium on Plant Bioregulators in Fruit Production **884**: 753–757.

Nakagawa M, Honsho C, Kanzaki S, Shimizu K, Utsunomiya N. 2012. Isolation and expression analysis of FLOWERING LOCUS T-like and gibberellin metabolism genes in biennial-bearing mango trees. *Scientia Horticulturae* **139**: 108–117.

Naschitz S, Naor A, Genish S, Wolf S, Goldschmidt EE. 2010. Internal management of non-structural carbohydrate resources in apple leaves and branch wood under a broad range of sink and source manipulations. *Tree Physiology* **30**: 715–727.

Neilsen JC, Dennis FG. 2000. Effects of seed number, fruit removal, bourse shoot length and crop density on flowering in ‘spencer seedless’ apple. *Acta Horticulturae* **527**: 137–146.

Nikinmaa E, Hölttä T, Hari P, Kolari P, Mäkelä A, Sevanto S, Vesala T. 2013. Assimilate transport in phloem sets conditions for leaf gas exchange. *Plant, Cell and Environment* **36**: 655–669.

Obeso JR. 2002. The costs of reproduction in plants. *New Phytologist* **155**: 321–348.

Olszewski N, Sun T-P, Gubler F, Hsing Y-I, Zeevaart JAD, Chen L-J, Yu S-M. 2002. Gibberellin Signaling: Biosynthesis, catabolism, and Response pathways. *Plant Cell* **14**: S61–S80.

Onouchi H, Igeño MI, Périlleux C, Graves K, Coupland G. 2000. Mutagenesis of plants overexpressing CONSTANS demonstrates novel interactions among *Arabidopsis* flowering-time genes. *Plant Cell* **12**: 885–900.

Pallas B, Bluy S, Ngao J, Martinez S, Clément-Vidal A, Kelner J-J, Costes E. 2018. Growth and carbon balance are differently regulated by tree and shoot fruiting contexts: an integrative study on apple genotypes with contrasted bearing patterns (J Pereira, Ed.). *Tree Physiology* **38**: 1395–1408.

Pallas B, Costes E, Hanan J. 2016a. Modeling bi-directional signals in complex branching structure: Application to the control of floral induction in apple trees. *Proceedings - IEEE International Conference on Functional-Structural Plant Growth Modeling, Simulation, Visualization and Applications*: 150–157.

Pallas B, Da Silva D, Valsesia P, Yang W, Guillaume O, Lauri PE, Vercambre G, Génard M, Costes E. 2016b. Simulation of carbon allocation and organ growth variability in apple tree by connecting architectural and source-sink models. *Annals of Botany* **118**: 317–330.

Pallas B, Louarn G, Christophe A, Lebon E, Lecoeur J. 2008. Influence of intra-shoot trophic competition on shoot development in two grapevine cultivars (*Vitis vinifera*). *Physiologia Plantarum* **134**: 49–63.

Palmer JW, Cai YL, Edjamo Y. 1991. Effect of part-tree flower thinning on fruiting, vegetative growth and leaf photosynthesis in ‘Cox’s Orange Pippin’ apple. *Journal of Horticultural Science* **66**: 319–325.

Palmer JW, Giuliani R, Adams HM. 1997. Effect of crop load on fruiting and leaf photosynthesis of ‘Braeburn’/M.26 apple trees. *Tree physiology* **17**: 741–6.

Parveaud CE, Chopard J, Dauzat J, Courbaud B, Auclair D. 2008. Modelling foliage characteristics in 3D tree crowns: Influence on light interception and leaf irradiance. *Trees-Structure and Function* **22**: 87–104.

Pataki DE, Oren R, Phillips N. 1998. Responses of sap flux and stomatal conductance of *Pinus taeda* trees to stepwise reductions in leaf area. *Journal of Experimental Botany* **49**: 871–878.

Pellerin BP, Buszard D, Georgallas A, Nowakowski RJ. 2012. A novel framework to consider endogenous hormonal control of apple tree flowering. *HortScience* **47**: 589–592.

Perez RPA, Dauzat J, Pallas B, Lamour J, Verley P, Caliman J-P, Costes E, Faivre R. 2017. Designing oil palm architectural ideotypes for optimal light interception and carbon assimilation through a sensitivity analysis of leaf traits. *Annals of Botany* **121**: 909–926.

Perez RPA, Pallas B, Le Moguedec G, Rey H, Griffon S, Caliman JP, Costes E, Dauzat J. 2016. Integrating mixed-effect models into an architectural plant model to simulate inter- and intra-progeny variability: A case study on oil palm (*Elaeis guineensis* Jacq.). *Journal of Experimental Botany* **67**: 4507–4521.

Perttunen J, Sievänen R, Nikinmaa E. 1998. LIGNUM: A model combining the structure and the functioning of trees. *Ecological Modelling* **108**: 189–198.

Petersen R, Krost C. 2013. Tracing a key player in the regulation of plant architecture: The columnar growth habit of apple trees (*Malus × domestica*). *Planta* **238**: 1–22.

Poirier-Pocovi M, Lothier J, Buck-Sorlin G. 2018. Modelling temporal variation of parameters used in two photosynthesis models: Influence of fruit load and girdling on leaf photosynthesis in fruit-bearing branches of apple. *Annals of Botany* **121**: 821–832.

Ponnu J, Wahl V, Schmid M. 2011. Trehalose-6-Phosphate: Connecting Plant Metabolism and Development. *Frontiers in Plant Science* **2**: 1–6.

Pradal C, Boudon F, Nouguier C, Chopard J, Godin C. 2009. PlantGL: A Python-based geometric library for 3D plant modelling at different scales. *Graphical Models* **71**: 1–21.

Pradal C, Dufour-Kowalski S, Boudon F, Fournier C, Godin C. 2008. OpenAlea: A visual programming and component-based software platform for plant modelling. *Functional Plant Biology* **35**: 751–760.

Pretzsch H, Grote R, Reineking B, Rötzer T, Seifert S. 2008. Models for forest ecosystem management: A European perspective. *Annals of Botany* **101**: 1065–1087.

Prioul JL, Chartier P. 1977. Partitioning of Transfer and Carboxylation Components of Intracellular Resistance to Photosynthetic CO₂ Fixation: A Critical Analysis of the Methods Used. *Annals of Botany* **41**: 789–800.

Prusinkiewicz P, Crawford S, Smith RS, Ljung K, Bennett T, Ongaro V, Leyser O. 2009. Control of bud activation by an auxin transport switch. *Proceedings of the National Academy of Sciences* **106**: 17431–17436.

Prusinkiewicz P, Hammel MS, Mjolsness E. 1993. Animation of plant development. *Proceedings of the 20th Annual Conference on Computer Graphics and Interactive Techniques, SIGGRAPH* **93**: 351–360.

Prusinkiewicz P. 2004. Modeling plant growth and development. *Current Opinion in Plant Biology* **7**: 79–83.

Putterill J, Laurie R, Macknight R. 2004. It's time to flower: The genetic control of flowering time. *BioEssays* **26**: 363–373.

Putterill J, Varkonyi-Gasic E. 2016. FT and florigen long-distance flowering control in plants. *Current Opinion in Plant Biology* **33**: 77–82.

Ramírez H, Benavides A, Robledo V, Alonso R, Gómez J. 2004. Gibberellins and cytokinins related to fruit bud initiation in apple. *Acta Horticulturae* **636**: 409–413.

Ramírez H, Hoard G V, Benavides A, Rangel E, Ramírez H, Hoard G V, Benavides A, Rangel E. 2001. Gibberellins in apple seeds and the transport of [3H]-GA₄. *Revista de la Sociedad Química de México* **45**: 47–50.

Reeves PH, Coupland G. 2001. Analysis of flowering time control in *Arabidopsis* by comparison of double and triple mutants. *Plant Physiology* **126**: 1085–1091.

Regnault T, Davière J-M, Wild M, Sakvarelidze-Achard L, Heintz D, Carrera Bergua E, Lopez Diaz I, Gong F, Hedden P, Achard P. 2015. The gibberellin precursor GA₁₂ acts as a long-distance growth signal in *Arabidopsis*. *Nature Plants* **1**: 1–6.

Renton M, Guédon Y, Godin C, Costes E. 2006. Similarities and gradients in growth unit branching patterns during ontogeny in ‘Fuji’ apple trees: A stochastic approach. *Journal of Experimental Botany* **57**: 3131–3143.

Renton M, Hanan J, Ferguson BJ, Beveridge CA. 2012. Models of long-distance transport: how is carrier-dependent auxin transport regulated in the stem? *New Phytologist* **194**: 704–715.

Reyes F, DeJong T, Franceschi P, Tagliavini M, Gianelle D. 2016. Maximum Growth Potential and Periods of Resource Limitation in Apple Tree. *Frontiers in Plant Science* **7**: 1–12.

Reyes F, Pallas B, Pradal C, Vaggi F, Zanutelli D, Tagliavini M, Gianelle D, Costes E. 2019. MuSCA : a multi-scale source-sink carbon allocation model to explore carbon allocation in plants . An application on static apple-tree structures. *Annals of Botany*: 1–15.

Rolland F, Baena-Gonzalez E, Sheen J. 2006. SUGAR SENSING AND SIGNALING IN PLANTS: Conserved and Novel Mechanisms. *Annual Review of Plant Biology* **57**: 675–709.

Rosenstock TS, Rosa UA, Plant RE, Brown PH. 2010. A reevaluation of alternate bearing in pistachio. *Scientia Horticulturae* **124**: 149–152.

Sachs T. 1999. ‘Node counting’: An internal control of balanced vegetative and reproductive development. *Plant, Cell and Environment* **22**: 757–766.

Sala A, Woodruff DR, Meinzer FC. 2012. Carbon dynamics in trees: Feast or famine? *Tree Physiology* **32**: 764–775.

Samach A, Smith HM. 2013. Constraints to obtaining consistent annual yields in perennials. II: Environment and fruit load affect induction of flowering. *Plant Science* **207**: 168–176.

Searle I, Coupland G. 2004. Induction of flowering by seasonal changes in photoperiod. *EMBO Journal* **23**: 1217–1222.

Segura V, Cilas C, Costes E. 2008. Dissecting apple tree architecture into genetic, ontogenetic and environmental effects: mixed linear modelling of repeated spatial and temporal measures. *New Phytologist* **178**: 302–314.

Seleznyova, AN, & Hanan, J. 2018. Mechanistic modelling of coupled phloem/xylem transport for L-systems: combining analytical and computational methods. *Annals of botany* **121**(5): 991-1003.

Sievänen R, Nikinmaa E, Nygren P, Ozier-Lafontaine H, Perttunen J, Hakula H. 2000. Components of functional-structural tree models. *Annals of Forest Science* **57**: 399–412.

Silpi U, Lacoite A, Kasempap P, Thanysawanyangkura S, Chantuma P, Gohet E, Musigamart N, Clément A, Améglio T, Thaler P. 2007. Carbohydrate reserves as a competing sink: Evidence from tapping rubber trees. *Tree Physiology* **27**: 881–889.

Simpson GG, Dean C. 2002. Arabidopsis, the rosetta stone of flowering time. *Science* **296**: 285–290.

Sinoquet H, Le Roux X, Adam B, Améglio T, Daudet FA. 2001. RATP a model for simulating the spatial distribution of radiation absorption transpirations and photosynthesis within canopies: application to an isolated tree crown. *Plant, Cell and Environment* **24**: 395–406.

Sinoquet H, Moulia B, Bonhomme R. 1991. Estimating the three-dimensional geometry of a maize crop as an input of radiation models: comparison between three-dimensional digitizing and plant profiles. *Agricultural and Forest Meteorology* **55**: 233–249.

Sinoquet H, Rivet P, Godin C. 1997. Assessment of the three-dimensional architecture of walnut trees using digitising.

Smith HM, Samach A. 2013. Constraints to obtaining consistent annual yields in perennial tree crops. I: Heavy fruit load dominates over vegetative growth. *Plant Science* **207**: 158–167.

Sonohat, G, Sinoquet, H, Kulandaivelu, V, Combes, D, Lescourret, F. 2006. Three-dimensional reconstruction of partially 3D-digitized peach tree canopies. *Tree physiology*. **26**(3): 337-351.

Spengler RN. 2019. Origins of the apple: The role of megafaunal mutualism in the domestication of *Malus* and rosaceous trees. *Frontiers in Plant Science* **10**: 1–18.

Sprugel DG, Hinckley TM, Schaap W. 1991. The Theory and Practice of Branch Autonomy. *Annual Review of Ecology and Systematics* **22**: 309–334.

Sprugel DG. 2002. When branch autonomy fails: Milton’s Law of resource availability and allocation. *Tree physiology* **22**: 1119–1124.

- Srikanth A, Schmid M. 2011.** Regulation of flowering time: All roads lead to Rome. *Cellular and Molecular Life Sciences* **68**: 2013–2037.
- Sung S, Amasino RM. 2004.** Vernalization and epigenetics: How plants remember winter. *Current Opinion in Plant Biology* **7**: 4–10.
- Takenaka A, Inui Y, Osawa A. 1998.** Measurement of three-dimensional structure of plants with a simple device and estimation of light capture of individual leaves. *Functional Ecology* **12**: 159–165.
- Tamaki S, Matsuo S, Wong HL, Yokoi S, Shimamoto K. 2007.** Hd3a Protein Is a Mobile Flowering Signal in Rice. *Science* **316**: 1033–1037.
- Tardieu F. 2010.** Why work and discuss the basic principles of plant modelling 50 years after the first plant models? *Journal of Experimental Botany* **61**: 2039–2041.
- Teo G, Suzuki Y, Uratsu SL, Lampinen B, Ormonde N, Hu WK, DeJong TM, Dandekar AM. 2006.** Silencing leaf sorbitol synthesis alters long-distance partitioning and apple fruit quality. *Proceedings of the National Academy of Sciences of the United States of America* **103**: 18842–18847.
- Thorpe MR, Lacomte A, Minchin PEH. 2011.** Modelling phloem transport within a pruned dwarf bean: A 2-source-3-sink system. *Functional Plant Biology* **38**: 127–138.
- Tworokski T, Fazio G. 2015.** Effects of Size-Controlling Apple Rootstocks on Growth, Abscisic Acid, and Hydraulic Conductivity of Scion of Different Vigor. *International Journal of Fruit Science* **15**: 369–381.
- Valverde F, Mouradov A, Soppe W, Ravenscroft D, Samach A, Coupland G. 2004.** Photoreceptor Regulation of CONSTANS Protein in Photoperiodic Flowering. *Science* **303**: 1003–1006.
- Van Hooijdonk BM, Woolley DJ, Warrington IJ, Tustin DS. 2010.** Initial alteration of scion architecture by dwarfing apple rootstocks may involve shoot-root-shoot signalling by auxin, gibberellin, and cytokinin. *Journal of Horticultural Science and Biotechnology* **85**: 59–65.
- Velasco R, Zharkikh A, Affourtit J, Dhingra A, Cestaro A, Kalyanaraman A, Fontana P, Bhatnagar SK, Troggio M, Pruss D, et al. 2010.** The genome of the domesticated apple (*Malus × domestica* Borkh.). *Nature Genetics* **42**: 833–839.
- Visser T. 1964.** Juvenile phase and growth of apple and pear seedlings. *Euphytica* **13**: 119–129.
- Visser T. 1965.** On the inheritance of the juvenile period in apple. *Euphytica* **14**: 125–134.
- Volpe G, Lo Bianco R, Rieger M. 2008.** Carbon autonomy of peach shoots determined by (13)C-photoassimilate transport. *Tree Physiology* **28**: 1805–1812.
- Vos J, Marcelis LFM, Evers JB. 2007.** Functional-structural plant modelling in crop production: adding a dimension. *Frontis* 1–12.
- Vos J, Evers JB, Buck-Sorlin GH, Andrieu B, Chelle M, De Visser PHB. 2009.** Functional-structural plant modelling: A new versatile tool in crop science. *Journal of Experimental Botany* **61**: 2101–2115.
- Wahl V, Ponnu J, Schlereth A, Arrivault S, Langenecker T, Franke A, Feil R, Lunn JE, Stitt M, Schmid M. 2013.** Regulation of Flowering by Trehalose-6-Phosphate Signaling in *Arabidopsis thaliana*. *Science* **339**: 704–707.
- Walcraft a S, Lescouret F, Génard M, Sinoquet H, Le Roux X, Donès N. 2004.** Does variability in shoot carbon assimilation within the tree crown explain variability in peach fruit growth? *Tree Physiology* **24**: 313–322.
- Wang G, Römheld V, Li C, Bangerth F. 2006.** Involvement of auxin and CKs in boron deficiency induced changes in apical dominance of pea plants (*Pisum sativum* L.). *Journal of Plant Physiology* **163**: 591–600.
- Ward SP, Leyser O. 2004.** Shoot branching. *Current Opinion in Plant Biology* **7**: 73–78.
- Watson MA, Casper BB. 1984.** Morphogenetic constraints on patterns of carbon distribution in plants. *Annual Review of Ecology and Systematics*. **15**: 233–258.
- White, J. 1979.** The plant as a metapopulation. *Annual Review of Ecology and Systematics* **10**: 109–145.
- Wilcox JC. 1944.** Some factors affecting apple yields in the Okanagan Valley, tree size, tree vigor, biennial bearing and distance of planting. *Scientific Agriculture* **25**: 189.
- Wilkie JD, Sedgley M, Olesen T. 2008.** Regulation of floral initiation in horticultural trees. *Journal of Experimental Botany* **59**: 3215–3228.

- Wilkinson S, Davies WJ. 2002.** ABA-based chemical signalling: the co-ordination of responses to stress in plants. *Plant, Cell & Environment* **25**: 195–210.
- Willaume M, Lauri PÉ, Sinoquet H. 2004.** Light interception in apple trees influenced by canopy architecture manipulation. *Trees-Structure and Function* **18**: 705–713.
- Wilson RN, Heckman JW, Somerville CR. 1992.** Gibberellin Is Required for Flowering in *Arabidopsis thaliana* under Short Days. *Plant Physiology* **100**: 403–408.
- Wolters, H, Jürgens, G. 2009.** Survival of the flexible: hormonal growth control and adaptation in plant development. *Nature Reviews Genetics*. **10**(5): 305-317.
- Wünsche JN, Ferguson IB. 2005.** Crop load interactions in apple. *Horticultural Reviews*. **31**: 231-290.
- Wunsche JN, Palmer JW, Greer DH. 2000.** Effects of crop load on fruiting and gas-exchange characteristics of 'Braeburn'/M.26 apple trees at full canopy. *Journal of the American Society for Horticultural Science* **125**: 93–99.
- Xing L-B, Zhang D, Li Y-M, Shen Y-W, Zhao C-P, Ma J-J, An N, Han M-Y. 2015.** Transcription Profiles Reveal Sugar and Hormone Signaling Pathways Mediating Flower Induction in Apple (*Malus domestica* Borkh.). *Plant and Cell Physiology* **56**: 2052–2068.
- Yan H-Pi, Kang MZ, De Reffeye P, Dingkuhn M. 2004.** A Dynamic, Architectural Plant Model Simulating Resource-dependent Growth. *Annals of Botany* **93**: 591-602.

Abstract

Alternate bearing is a common phenomenon for different perennial species. While it can have dramatic economic effects, its causes are still unclear. Alternate bearing results from irregularities in floral induction (FI) between successive years. In apple trees (*Malus x domestica*), large variability in bearing patterns between genotypes have been observed that are partially affected by architectural characteristics. Moreover, large within tree variability in FI also exists since FI occurs each year in a set of buds, only. Different hypotheses exist to explain between years and within tree variability in FI including the involvement of hormones (mainly gibberellins, GA), other signaling molecules (FT protein) and the carbon balance at different scales of plant organization. This thesis aimed at analyzing and modeling the physiological and architectural determinisms of the within tree and between year variability in floral induction in context of genotypic variability in apple tree. First, physiological analyses (photosynthesis, nonstructural carbohydrates and GA concentration) were performed during 2 years on adult 'Golden Delicious' apple trees subjected to different leaf and fruit removal practices in order to modify the leaf/fruit ratio and the distances between the sources of inhibiting and activating signals and shoot apical meristems (SAM). Results showed that effects of fruit and leaves could affect FI in SAM at short distances, only. Moreover, experimental results showed that carbohydrates appeared as not directly implicated in FI but that GA could inhibit FI in SAM. The dataset generated from this experiment was used in a modelling approach aiming at simulating the effects of leaf, fruit, and their distances to SAM on FI. The model simulated FI variability with 3D tree structures by considering the transport of inhibit and activating signal produced by fruit and leaves respectively. Signal transport was simulated considering a signal 'attenuation' parameter, whereas SAM fate was determined by probability functions depending on signal amounts. Model parameter estimations suggested a cumulative effect of activating and inhibiting signals on FI, with SAM being more sensitive to the inhibiting signal. Simulations results also proposed that the activating signal was transported at shorter distances than the inhibiting one. Other experiments performed on a set of genotypes issued from an apple collection, showed that the establishment of plant architecture is under the dependency of hormonal signaling (AIA and ABA) and plays a key role in the onset of biennial bearing between the different genotypes. Results also confirm the poor implication of carbohydrates on FI and showed that gibberellins and cytokinins may be implicated in FI variability between genotypes. At the end of this work, new perspectives are proposed for the identification of the signals controlling FI and for integrating genotypic variability in the modeling approach in order to simulate between-year variability in FI and the resulting bearing patterns.

Key words: apple tree, architecture, floral induction, functional-structural plant models, carbon balance, hormone signaling, genotypic variability.

Résumé

L'alternance de production est un phénomène commun pour différentes espèces pérennes. Bien qu'elle puisse engendrer des effets économiques dramatiques, ses causes sont toujours mal comprises. L'alternance de production résulte d'irrégularités dans l'induction florale (IF) entre les années successives. Chez le pommier (*Malus x domestica*), une grande variabilité des rythmes de production entre les génotypes a été observée, et cette variabilité est en partie reliée aux caractéristiques architecturales des génotypes. Il existe également une grande variabilité intra-arbre dans l'IF, qui ne se produit que sur un nombre variable de bourgeons chaque année. Différentes hypothèses existent pour expliquer la variabilité intra-arbre et interannuelle de l'IF, notamment l'implication des hormones (principalement les gibbérellines, GA), d'autres molécules de signalisation (protéine FT) et du bilan carboné à différentes échelles d'organisation de la plante. Cette thèse vise à analyser et modéliser les déterminismes physiologiques et architecturaux de la variabilité intra-arbre et interannuelle de l'IF dans un contexte de variabilité génotypique chez le pommier. Tout d'abord, des analyses physiologiques (photosynthèse, carbohydrates non structuraux et concentrations en GA) ont été réalisées pendant 2 ans sur des pommiers 'Golden Delicious' adultes soumis à des pratiques de suppression des feuilles et des fruits afin de modifier le rapport feuille/fruit et les distances entre les sources des signaux activateurs et inhibiteurs et les méristèmes apicaux (SAM). Les résultats ont montré que les effets des fruits et des feuilles pouvaient affecter l'IF dans les SAM sur de courtes distances uniquement. De plus, les carbohydrates n'apparaissent pas directement impliqués dans l'IF alors que les GA pouvaient inhiber l'IF dans les SAM. L'ensemble de données générées à partir de cette expérience a été utilisé dans une approche de modélisation visant à simuler les effets des feuilles, des fruits et leurs distances par rapport aux SAM sur l'IF. Le modèle a permis de simuler la variabilité de l'IF sur des structures d'arbres en 3D, en considérant le transport des signaux activateur et inhibiteur produits respectivement par les feuilles et les fruits. Le transport de ces signaux a été simulé en considérant un paramètre d'atténuation du signal, tandis que le devenir des SAM était déterminé par des fonctions de probabilité en fonction des quantités de signaux. Les estimations des paramètres du modèle ont suggéré un effet cumulatif des signaux activateur et inhibiteur sur l'IF, les SAM étant plus sensibles au signal inhibiteur. Les résultats des simulations ont également proposé que le signal activateur était transporté à des distances plus courtes que le signal inhibiteur. D'autres expériences réalisées sur un ensemble de génotypes issus d'une collection de pommiers ont montré que la mise en place de l'architecture végétale est sous la dépendance de la signalisation hormonale (AIA et ABA) et que la dynamique de mise en place de l'architecture joue un rôle clé dans le début de l'alternance de production entre les différents génotypes. Les résultats confirment également la faible implication des carbohydrates dans l'IF et ont montré que les gibbérellines et les cytokinines pourraient être impliquées dans la variabilité de l'IF entre les génotypes. Au terme de ces travaux, de nouvelles perspectives sont proposées pour l'identification précise des signaux contrôlant l'IF et pour intégrer la variabilité génotypique dans l'approche de modélisation afin de simuler la variabilité interannuelle de l'IF et des rythmes de productions qui en résultent.

Mots clefs : pommier, architecture, induction florale, modélisation structure-fonction, bilan carboné, signalétique hormonale, variabilité génotypique.